Nisin resistance in *Streptococcus agalactiae*

Inaugural-Dissertation

For the attainment of the title of doctor
in the Faculty of Mathematics and Natural Sciences
at the Heinrich Heine University Duesseldorf

Presented by

Sakshi Khosa
from New Delhi

Duesseldorf, January 2016

From the Institute of Biochemistry
At the Heinrich Heine University Duesseldorf

Published by permission of the
Faculty of Mathematics and Natural Sciences at
Heinrich Heine University Duesseldorf

Supervisor: Prof. Dr. Lutz Schmitt
Co-supervisor: Prof. Dr. Holger Gohlke

Date of the oral examination: 15/01/2016

There is no substitute for hard work.

(Thomas A. Edison)

Abstract

Nisin is a post-translationally modified, 34-residue antibacterial peptide produced by some strains of *Lactococcus lactis* that is effective against various Gram-positive bacteria. It is widely used in the food industry as a preservative. However, some nisin non-producing strains of bacteria are intrinsically resistant to nisin because of the presence of *nsr* gene, which encodes the 35-kDa nisin resistance protein (NSR). NSR-mediated nisin resistance results from the proteolytic degradation of nisin by this serine protease. Within this thesis, the mechanism of nisin resistance in *Streptococcus agalactiae* was studied on a molecular level.

An operon encoding NSR was discovered in *S. agalactiae* and various other human pathogenic bacteria (nisin non-producers). In addition to NSR, this conserved operon consists of an ATP-binding cassette transporter (NsrFP) and a two-component system comprising of NsrR and NsrK. Furthermore, NSR from *S. agalactiae* (*Sa*NSR) was shown to confer 20-fold resistance against nisin.

In this thesis, *in vitro* studies on the nisin resistance protein from *S. agalactiae* were performed. The structure of NSR was solved using X-ray crystallography at a resolution of 2.1Å. The structure revealed that NSR consists of three structural domains: an N-terminal helical bundle, the protease cap and protease core, which together form a hydrophobic tunnel. The protease core harbors a highly conserved TASSAEM region. A model of *Sa*NSR and nisin was generated through molecular modeling and MD simulations. The *Sa*NSR/ nisin complex and mutagenesis studies revealed that *Sa*NSR is specifically interacting with the N-terminus of nisin, especially the last C-terminally located lanthionine ring.

Furthermore, this thesis also dealt with the molecular characterization of the response regulator NsrR involved in nisin resistance. The structure of NsrR was solved using X-ray crystallography and revealed that NsrR consists of two domains: a N-terminal receiver domain and a C-terminal effector domain.

Finally, the last part of this thesis is dedicated to the cytoplasmic loop, NsrP loop of the ABC transporter NsrFP. An interaction event between NsrP loop and nisin was demonstrated using pull down assays and further confirmed via agar diffusion assays. A binding affinity was also determined by microscale thermophoresis.

Zusammenfassung

Nisin ist ein posttranslational modifiziertes, 34 Aminosäuren langes antimikrobielles Peptid. Es wird von einigen *Lactococcus lactis* Stämmen produziert und weist überwiegend gegen Gram-positive Bakterien eine antimikrobielle Aktivität auf. Seit Jahrzehnten wird es in der Lebensmittelindustrie als Konservierungsmittel eingesetzt und fast keine Resistenzen gegenüber Nisin wurden bisher dokumentiert.

Jedoch besitzen einige bakterielle Stämme, die selbst kein Nisin produzieren, eine intrisische Nisin-Resistenz vermittelt durch das nsr Gen. Dieses Gen codiert für das 35 kDa große Nisin Resistenz Protein (NSR). Die Serin-Protease NSR vermittelte eine Resistenz, bei der Nisin proteolytisch degradiert wird. In der vorliegenden Dissertation wurde der molekulare Mechanismus der NSR-vermittelten Nisin Resistenz in *Streptoccocus agalactiae* untersucht.

In *S. agalactiae* und weiteren humanpathogenen Bakterien, die selbst kein Nisin produzieren, wurde ein NSR-kodierendes Operon entdeckt. Zusätzlich zum NSR, kodiert dieses konservierte Operon für einen ATP-binding-cassette Transporter (NsrFP) und für ein Zwei-Komponenten System bestehend aus NsrR and NsrK. Des weiteren konnte gezeigt werden, das NSR von *S. agalactiae* (*Sa*NSR) eine 20-fach erhöhte Resistenz gegenüber Nisin vermittelt.

In der vorliegenden Thesis wurden *in vitro* Studien zum Nisin Resistenz Protein aus *S. agalactiae* durchgeführt. Die Struktur von NSR konnte mittel Röntgen-Kristallographie gelöst werden. Dabei konnte gezeigt werden, dass NSR aus drei strukturellen Domänen besteht: aus einem N-terminalen α-Helixbündel, einer Deckel-Domäne und einer Kern-Domäne. Dabei formen die zwei zuletzt genannten Domänen einen hydrophoben Tunnel. Außerdem besitzt die Kern-Domäne der Protease ein hoch-konserviertes TASSAEM-Motiv.

Mit Hilfe eines generierten Modells von *Sa*NSR und Nisin konnte der *Sa*NSR/Nisin-Komplex untersucht werden. Das Model des Komplexes und Mutagenesestudien zeigten, dass *Sa*NSR spezifisch mit den N-terminus und im Besonderen mit den letzten C-terminalen Lanthioninring von Nisin interagiert

Des Weiteren behandelt diese Thesis die molekulare Charakterisierung des Antwort-Regulartors NsrR. Der Struktur von NsrR wurde mittels Röntgen-Kristallographie gelöst

und ein Model der Struktur zeigt, dass das Protein aus zwei Domänen besteht. Nämlich aus einer N-terminale Empfänger-Domäne und eine C-terminale Effektor Domäne.
Abschließend ist der letzte Teil der Thesis der extrazellulären Schleife des Proteins NsrP des ABC-Transporters NsrFP gewidmet. Mittels pull-down und Agar-Diffusion Assays konnte die Interaktion zwischen der NsrP-Schleife und Nisin bestätigt werden. Weiterhin konnte durch MicroScale Thermophorese Bindungsaffinitätskonstanten bestimmt werden.

Table of Contents

List of figures

List of tables

Abbreviations

3D	three-dimensional
Å	Ångstrom
ABC	ATP-binding cassette
ADP	adenosine-5-diphosphate
AMP	antimicrobial peptide
ATP	adenosine-5-triphosphate
B. subtilis	*Bacillus subtilis*
C. difficile	*Clostridium difficile*
CTPs	C-terminal processing peptidase
Dha	dehydroalanine
Dhb	dehydroaminobutyric acid
DNA	deoxyribonucleic acid
D-PG	di-phosphatidylglycerol
ED	effector domain
EDTA	ethylenediaminetetraacetic acid
E. faecium	*Enterococcus faecium*
HK	histidine kinase
IMSK	intramembrane-sensing kinase
K_D	dissociation constant
kDa	kilo Dalton
Lan	lanthionine
L. lactis	*Lactococcus lactis*
L. monocytogenes	*Listeria monocytogenes*
LPS	lipopolysaccharide
LTA	lipoteichnoic acid
MacAB	macrolide-specific ABC-type efflux carrier
MALS	multi-angle light scattering
MeLan	methyl-lanthionine
mg	milligram
MprF	multipeptide resistance factor protein
MRSA	methicillin-resistant *Staphylococcus aureus*
NBD	nucleotide binding domain
Ni	nickel
NICE	nisin controlled gene expression

nm	nano meter
nM	nano molar
NMR	nuclear magnetic resonance
NTA	mitrilotriacetic acid
PBP	penicillin-binding protein
PG	phosphatidylglycerol
RD	receiver domain
RR	response regulator
RNA	ribonucleic acid
S. agalactiae	*Streptococcus agalactiae*
S. aureus	*Staphylococcus aureus*
SEC	size exclusion chromatography
S. mutans	*Streptococcus mutans*
TCSs	two-component signaling systems
TMD	transmembrane domain
TSP	tail specific protease
wHTH	winged helix-turn-helix
WTA	wall teichnoic acid
μM	micro molar

Amino acid	Three letter code	One letter code
Alanine	Ala	A
Arginine	Arg	R
Aspargine	Asn	N
Aspartic Acid	Asp	D
Cysteine	Cys	C
Glutamic Acid	Glu	E
Glutamine	Gln	Q
Glycine	Gly	G
Histidine	His	H
Isoleucine	Ile	I
Leucine	Leu	L
Lysine	Lys	K
Methionine	Met	M
Phenylalanine	Phe	F
Proline	Pro	P
Serine	Ser	S
Threonine	Thr	T
Tryptophan	Trp	W
Tyrosine	Tyr	Y
Valine	Val	V

1. Introduction

1.1 Antimicrobial Peptides

Antimicrobial peptides (AMPs) traditionally refer to peptides that can inhibit the growth of microbes and are produced virtually by all organisms. They are also known as the first and important line of defense [1, 2]. Since the early discovery of nisin from *Lactococcus lactis* in 1928 [3, 4] to the discovery of sonorensin from *Bacillus sonorensis* in 2014 [5], hundreds of AMPs have been isolated so far. According to the modern definition, AMPs are relatively short (<60 amino acids), positively charged (net charge of +2 to +9), amphipathic molecules with broad spectrum of antimicrobial activity and multiple modes of action [6-8].

AMPs possess a broad spectrum of antimicrobial activity against various Gram-positive and Gram-negative bacteria, fungi and viruses. Most AMPs interact with microbial membranes or cell surfaces, leading to the loss of cellular integrity [9]. Here, the AMPs can be either membrane-disruptive resulting in cell lysis, or membrane-interactive leading to pore formation and subsequent cell death. Furthermore, AMPs can have diverse intracellular targets including DNA, RNA and protein and also have the capability of inhibiting both cell wall and protein synthesis [10, 11].

AMPs have been expressed by bacteria for millions of years and during the course of evolution, AMPs have retained their antimicrobial activity and are still effective [12]. Compared to the traditionally used antibiotics, AMPs have a broad spectrum of activity with multiple cellular targets and kill bacterial very rapidly [13, 14]. Furthermore, AMPs have the potential of neutralizing endotoxins and bypass the classical antibiotic resistance mechanisms [15-17]. In addition to the antimicrobial activity of AMPs, various other alternate functions of AMPs have been recently identified including immunomodulatory activities and neutralization of wound-healing and anti-neoplastic properties [18-22]. These diverse biological functions of AMPs make them ideal for the development of new therapeutic agents with wide applications involving cancer therapy and anti-inflammation.

AMPs can generally be classified based on their distinct structural features like size, charge, amino acids and physical structure. Numerous classification schemes are currently available for grouping AMPs based on their biological source (amphibian, bacterial, insect, mammalian, plant and viral), biological functions (antibacterial, antiviral, antiparasital,

antifungal, etc.), peptide properties (net charge: cationic, neutral and anionic; hydrophobicity: hydrophobic, amphipathic and hydrophilic; based on size: ultra small, small, medium and large) and molecular targets (cell surface targeting or intracellular targeting), based on three-dimensional structure (linear, β -sheet, loop and with predominance of one or more amino acids) [7, 23]. Likewise, for example, human defensins (Figure 1a) can be grouped as mammalian AMPs that function preliminarily as antibacterial. They are small (around 5kDa), cationic peptides and have β-sheet structure [24].

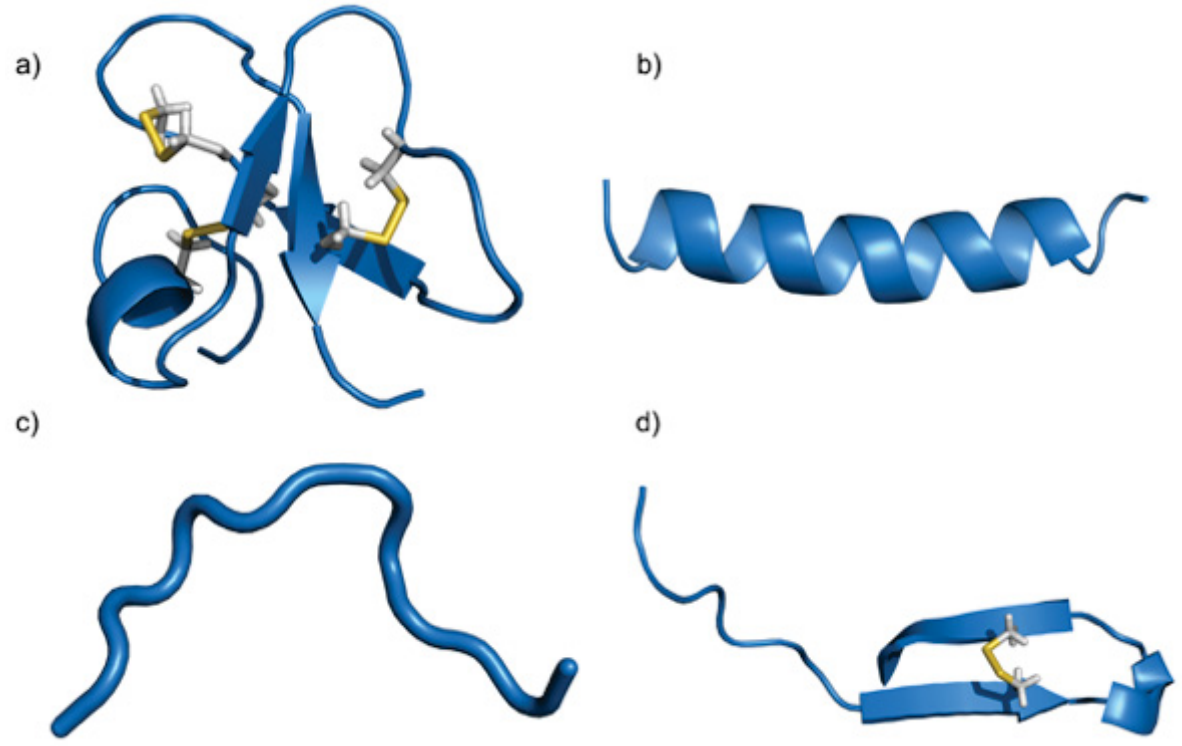

Figure 1: Structural classes of different antimicrobial peptides. (a) β-sheeted human defensin-2 (PDB code: 1FQQ), (b) α-helical magainin (PDB code: 2MAG), (c) the extended boat-shaped structure of bovine indolicidin (PDB code: 1G89), and (d) looped thanatin (PDB code: 8TFV). Based on [25]. Created with MacPymol.

However, the most prominently used classification scheme is based on the three-dimensional structure of the AMPs [26, 27]. Linear peptides possess a α-helical structure and constitute 27% of all the AMPs. Common examples are silk moth's cecropin [28] and magainin from the African clawed frog (shown in Figure 1b) [29]. β-sheet peptides usually have cyclic structures that are stabilized by disulphide bonds and include defensins (Figure 1a) [30]. There are also peptides with predominance of one or more amino acids like tryptophan-rich indolicidin of cow neutrophil (Figure 1c) [31] and proline-rich apidaecins

[32] which represent an extended conformation. Peptides with loop structures are highly stable due to the presence of hairpin structure that is stabilized via disulphide bonds in between the β-strands. The examples include tachyplesins [33] and bactenecin [34] (shown in Figure 1d).

1.2 Bacterial AMPs: Bacteriocins

AMPs produced by bacteria are also referred to as bacteriocins. Bacteriocins are proteinaceous and heterogeneous group of peptides produced by bacteria that are lethal towards other bacteria, either within the same bacterial genus (narrow spectrum) or across genera (broad spectrum) to which the producer has a specific immunity mechanism (Klaenhammer, 1993).

Bacteriocins were the first among the AMPs to be isolated and characterized [35-37]. Colicins from *E. coli* were discovered as early as 1925 [38]. The most extensively studied bacteriocin is nisin, produced by *L. lactis,* it has been commonly used for the past 50 years in the food industry [39, 40]. Mersacidin is produced by *Bacillus spp.* and displays bactericidal activity against Methicillin-resistant *Staphylococcus aureus* (MRSA) [41].

1.2.1 Classification of Bacteriocins

Bacteriocins are divided into three distinct classes: lantibiotics (class I), non-lantibiotics (class II) and bacteriolysins (class III) [42]. Lantibiotics are small peptides of 19-38 amino acids, which undergo various post-translational modifications yielding thioether-based ring structures like lanthionine or methyl-lanthionine rings and various unusual amino acids [43-45]. Some examples of bacteriocins are nisin, mersacidin and lacticin 3147. Detailed description is in section 1.3. Class II bacteriocins are non-lanthionine containing and comprise of small (<10kDa) thermostable peptides, which do not undergo post-translational modifications. These peptides are also active in nanomolar range. Their activity is a result of their insertion into the membranes, promoting membrane depolization and cell death. Examples include pediocin PA1, enterocin AS48, lacticin F and lactococcin A. Class III includes large thermolabile bacteriocins (>30kDa) with complex activity. These are also called bacteriolysins and are non-bacteriocin lytic proteins. Their mode of action is different

from the other classes as they function through cell lysis via hydrolysis of cell-wall [46]. Some examples are lysostaphin and enterolysin A.

There are numerous applications of bacteriocins. Colicins are used in the treatment of urinogenital infection and haemolytic uremic syndrome and have been shown to inhibit the growth of tumour cells [47]. Enterocin CRL35 has potent antilisterial activity [48]. Some studies have also indicated that bacteriocins are active against tumour cells and thus, are potential candidates for anti-tumour drug [49]. Bacteriocins have also huge potential in the biopreservation of packaged food, dairy products, canned foods etc. [50].

1.3 Lantibiotics

The term lantibiotics literally means lanthionine-containing antibiotics [51] which are produced by Gram-positive bacteria. Lantibiotics are ribosomally synthesized peptides of approximately 19-38 amino acids. They are characterized by the extensive post-translational modifications they undergo to be in their biologically active form and the presence of unusual amino acids [52, 53, 45, 54]. The dehydration of the serine and threonine residues in the prepeptide results in the formation of 2,3-didehydroalanine (Dha) and 2,3-didehydrobutyrine (Dhb), which are covalently linked to the free cysteine residues to form the lanthionine (Lan) or 3-methlylanthionine (MeLan) rings [55, 56].

1.3.1 Classification of Lantibiotics

Lantibiotics are classified in three distinct classes according to their size, properties and modification pathway: class I, class II and class III [57]. Class I lantibiotic peptides are less than 5kDa in size and are post-translationally modified by two enzymes, dehydratase LanB and the cyclase LanC [58, 59, 57]. The ABC transporter LanT exports the fully modified prepeptide into the extracellular space where the protease LanP cleaves off the leader peptide resulting in fully modified active peptide. This class of lantibiotics possesses antimicrobial activity in nanomolar range against various Gram-positive bacteria [59, 57]. The common examples are nisin, subtilin and epidermin (Figure 2).

On the contrary, Class II lantibiotics are 5-10kDa in size and are post-translationally modified by a single enzyme, LanM containing N-terminal dehydratase and C-terminal LanC-like cyclase domains, that performs both dehydration and cyclization [57, 60].

Although, LanM bears no homology with LanB proteins, it displays low sequence identity to the cyclase LanC, including the three zinc-binding amino acids. Furthermore, LanT exports the modified prepeptide and cleaves off the leader peptide [61]. Prominent members of this class are lacticin 481 and mersacidin (Figure 2). This class also has antimicrobial activity against Gram-positive bacteria.

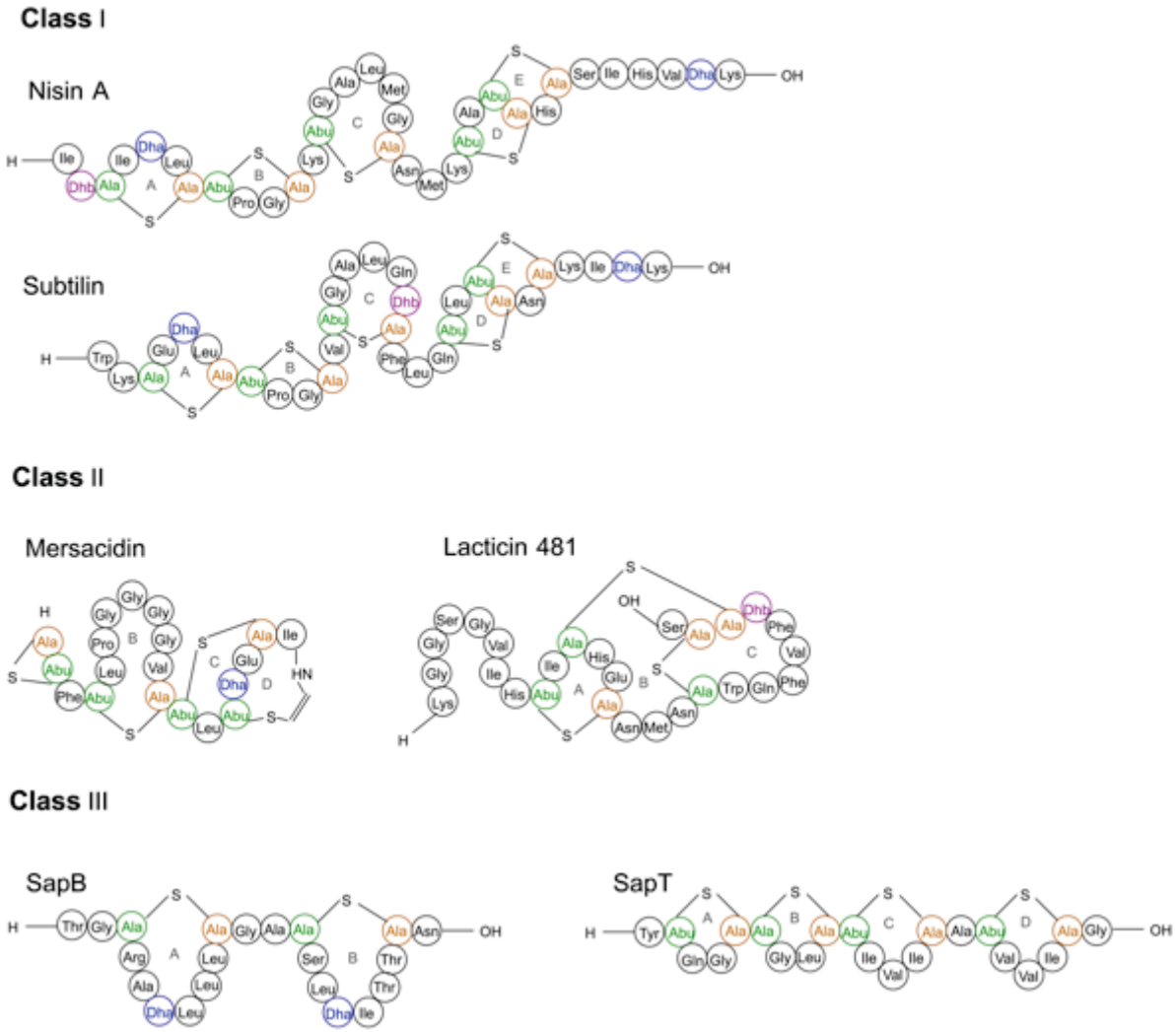

Figure 2: Schematic representation of the structure of various lantibiotics depicting the unusual amino acids. The representatives of various classes of lantibiotics are shown: Class I – nisin and subtilin, Class II - lacticin 481 and mersacidin, and Class III – sapB and sapT. Based on [57] and created using Chem BioDraw 13.0.

Class III lantibiotics, like SapB and SapT (Figure 2), do not possess any antimicrobial activity. Instead, they perform morphogenesis functions. The corresponding modification enzyme is a tri-functional synthetase that comprises of an N-terminal lyase domain, a central kinase domain and a putative C-terminal cyclase domain that lacks the active site residues found in LanC/LanM enzymes [62, 60].

1.3.2 Gene Cluster of Lantibiotics

The genes for the biosynthesis of lantibiotics are generally found on chromosomes as clusters [57]. *lanA* is the structural gene that encodes the prepeptide and comprises of the N-terminal leader sequence (composed of 23 to 59 amino acids) and the C-terminal (core) sequence that forms the mature peptide [63, 59]. *lanB* and *lanC* (class I) or *lanM* (class II) are the modification enzymes. *lanT* is an ABC transporter that transports the fully modified prepeptide. The protease *lanP* cleaves the leader peptide forming the mature active peptide [63].

The biosynthesis of the lantibiotics is auto-regulated via a two-component system consisting of a histidine kinase (*lanK*) and a response regulator (*lanR*) [63]. In order to protect itself from the bactericidal effect of the lantibiotic, the producer strain has a self-protection immunity system comprising of a lipoprotein *lanI* and/or an ABC transporter encoded by *lanFEG* [63, 57]. The gene clusters of various lantibiotic classes are shown in Figure 3.

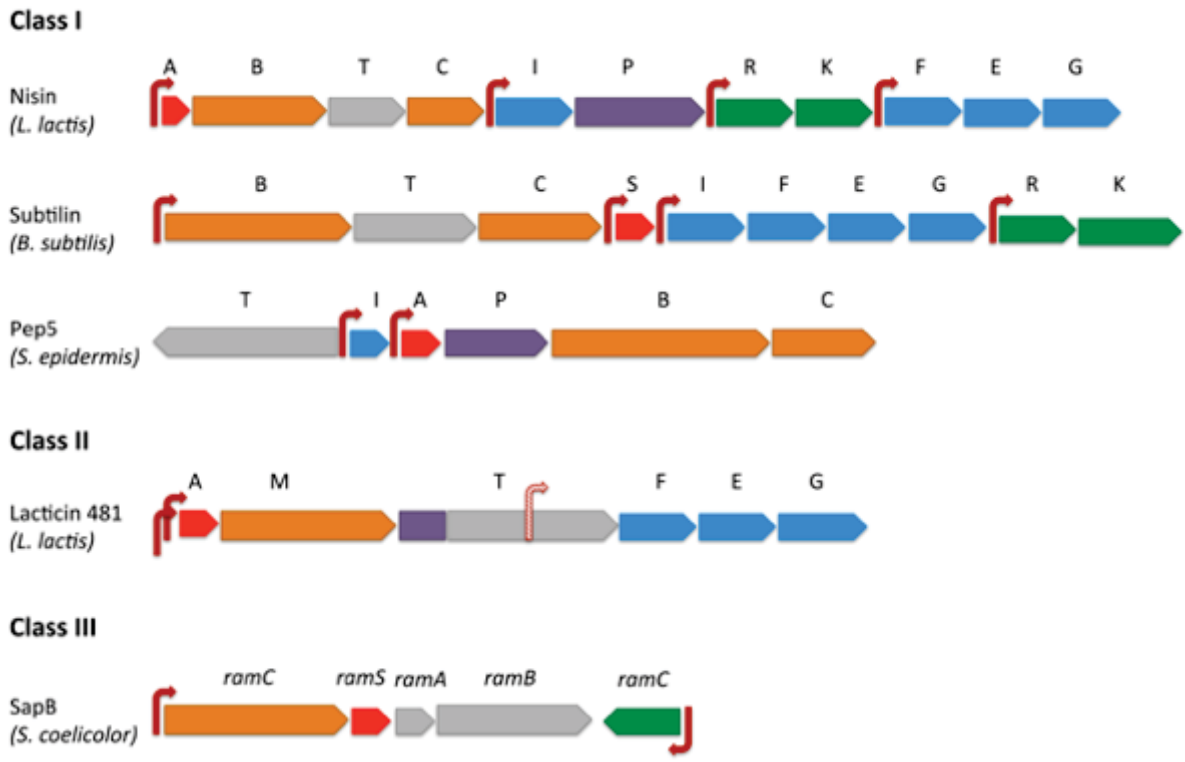

Figure 3: Gene clusters of various lantibiotics from different classes. Shown are the operon for nisin, subtilin, epidermin, Pep5, lacticin 481 and SapB. The structural gene (red), genes for modification (orange), transport (grey), leader cleavage (purple), regulation (green) and immunity (blue) are shown for different lantibiotics. The respective promoters are depicted in red arrows. Based on [64].

1.3.3 Applications of Lantibiotics

With the increasing number of incidences of antibiotic resistance, there is an immense pressure to develop alternative therapeutic agents. Lantibiotics are the most promising candidates [65] due to their capability to inhibit various multidrug-resistant pathogenic bacteria like staphylococci, enterococci, streptococci and clostridia [66]. Some lantibiotics are also effective against Gram-negative bacteria like *Neisseria* and *Helicobacter* [67]. Their mode of action involves multiple targets, which might help in overcoming the pre-existing mechanisms of antibiotic resistance.

Lantibiotics are also of great use in the food industry [68-70, 50, 42]. The lantibiotic nisin has been used for the past 50 years as a food additive. Lantibiotics are also effective in the bio-preservation of meat, dairy products, canned food, fish, alcoholic beverages, salads, egg products, high-moisture bakery products, and fermented vegetables [40].

The pharmaceutical potential of lantibiotics has also been extensively studied and some are already in the preclinical and clinical phases of development [71]. The lantibiotic derivative NVB333 (NovactaBiosystems Limited) was used in the treatment of nosocomial infections [72]. The antimicrobial activity of nisin against *Staphylococcus mastitis* has been utilized in a commercial intramammary product (Mast Out®, ImmuCell) for the treatment of mastitis in cows [73]. It is also effective in the treatment of MRSA, peptic ulcers and enterocolitis [74]. Gallidermin and lacticin 3147 are active against acne causing bacterium *Propionibacterium acnes*, thus, have the potential of being used in cosmetics and personal care products [75]. Mutacin 1140 is active against *Streptococcus mutans* that causes dental cavity [76]. Duramycin is effective against bronchial epithelia and is a potential drug candidate for the treatment of cystic fibrosis and inflammation. It is already in phase II of clinical trials [77]. Cinnamycin is active against retroviruses such as herpes simplex and is also an inhibitor of angiotension converting enzyme. It can probably be used in regulation of blood pressure and in the treatment of virus infections and inflammation. Mersacidin and actagardine are effective against staphylococci and streptococci and therefore, can be used in the treatment of MRSA and streptococcal infections [78, 79].

1.4 Nisin

Nisin is produced by some *L. lactis* and *Streptococcus uberis* strains and was first discovered in 1928 [3, 4]. Nisin is the most studied and best characterized lantibiotic [78]. It has a broad antimicrobial spectrum against a wide range of Gram-positive genera, including staphylococci, streptococci, *Listeria* spp., bacilli, and enterococci.

Nisin is an amphipathic molecule with a hydrophobic N-terminal and hydrophilic C-terminal part. The three-dimensional solution structure of nisin was solved via NMR spectroscopy in 1991 [80] (Figure 4). The structure of active nisin comprises of three parts: an N-terminal region formed by rings A, B and C (first three rings); a flexible hinge region; and a C-terminal region consisting of intertwined rings D and E followed by six amino acids (last two rings) [81, 82, 80] (Figure 4). The first three rings are important for binding to Lipid II, while the last two rings are important for pore formation. The flexible hinge region is crucial for flipping into the membrane [83-87].

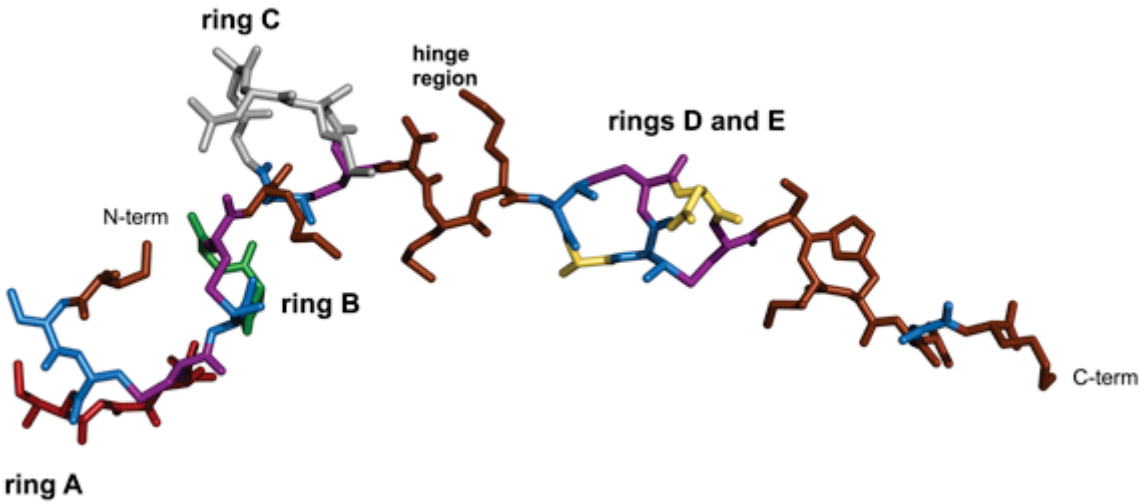

Figure 4: The NMR structure of nisin. The dehydrated amino acids are shown in blue, the cysteine residues are displayed in purple. The lanthionine ring A, methyl-lanthionine rings B and C are displayed in red, green and grey, respectively. In yellow are the methyl-lanthionine rings D and E. Based on PDB code: 1WCO [86] and created with MacPymol.

1.4.1 Mode of Action of Nisin

The target molecule of nisin is a precursor molecule of cell wall synthesis lipid II, which is anchored to the cytoplasmic membrane by an undecaprenyl residue [85]. This anchor is

connected via an ester bridge to a diphosphate moiety that carries a N-acetylmuramic acid molecule and the attachment of a pentapeptide completes the lipid II molecule [57, 88]. Catalyzed by a transglycosylation reaction, more N-acetylmuramic acids molecules fuse to lipid II forming linear polymers that are cross-linked by a transpeptidation reaction to form the mature peptide glycane of Gram-positive bacteria [57, 88] (Figure 5a).

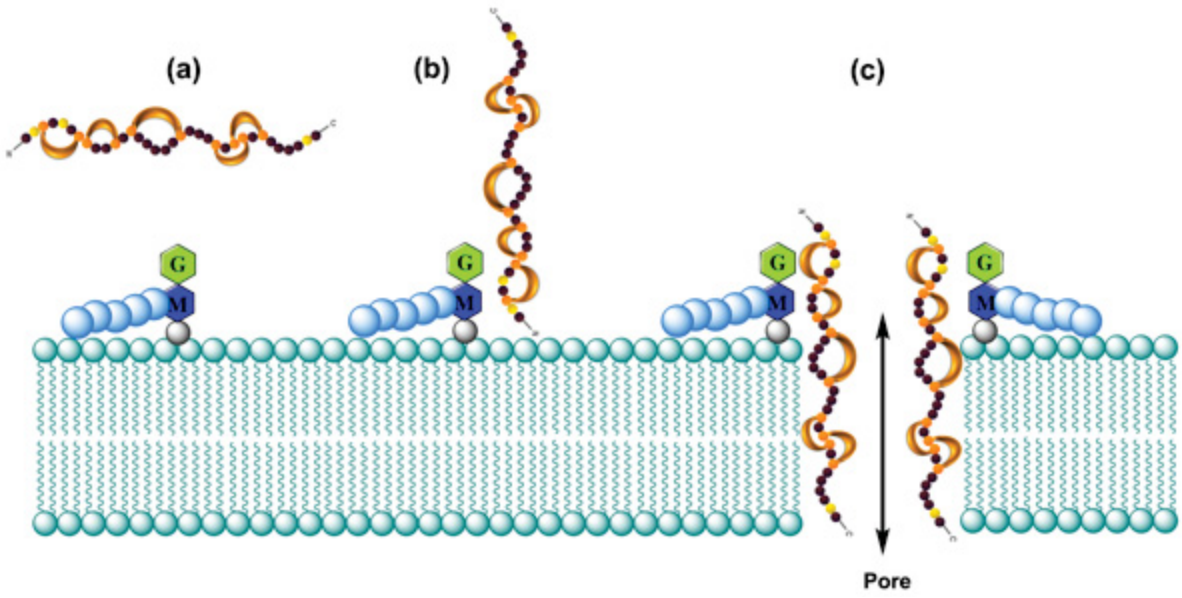

Figure 5: The mode of action of nisin. Nisin comes in contact with the bacterial plasma membrane (a), where it binds to Lipid II via two of its amino-terminal rings (b). This leads to pore formation (c), which involves a stable transmembrane orientation of nisin. The pore complex is formed comprising of four nisin molecules and eight lipid II molecules. Based on [87] and created with Chem BioDraw 13.0.

Nisin binds with the first two (methyl)-lanthionine rings (A and B) to the diphosphate moiety of lipid II [89, 86] and prevents the transglycosylation reaction, thereby inhibiting cell wall synthesis [85] (Figure 5b). When the concentration of nisin-lipid II complexes increases beyond a certain threshold an intermediate complex is formed which induces the insertion of the C-terminus of nisin into the cytoplasmic membrane (Figure 5c). This results in a complex consisting of eight nisin and four lipid II molecules [89], creating a pore (Figure 5c) with a diameter of 2 - 2.5 nm, releasing essential ions and small nutrients, thereby causing a collapse of the membrane potential, subsequently leading to cell death [89]. The threshold concentration for this reaction is in the low nanomolar range [90].

1.4.2 The Nisin System

The nisin gene cluster in *L. lactis* is associated with a conjugative transposon comprising of eleven genes for synthesis, modification, transport, self-immunity and regulation in the order *nis*ABTCIPRKFEG [91-94] (Figure 6). Nisin is synthesized ribosomally as a precursor peptide consisting of 57 amino acids [93]. This precursor peptide NisA is composed of the N-terminal leader peptide (23 amino acids) and the C-terminal core peptide (34 amino acids residues) [95]. The prepeptide is post-translationally modified through two modification enzymes. The dehydratase NisB, dehydrates the serine and threonine residues, while NisC the cyclase, is responsible for the cyclization reaction generating one lanthionine and four methyl-lanthionine rings [96]. For secretion, the ABC transporter NisT exports the peptide across the membrane into the extracellular environment [97, 98], where the protease NisP cleaves off the leader peptide sequence yielding active nisin [92, 99].

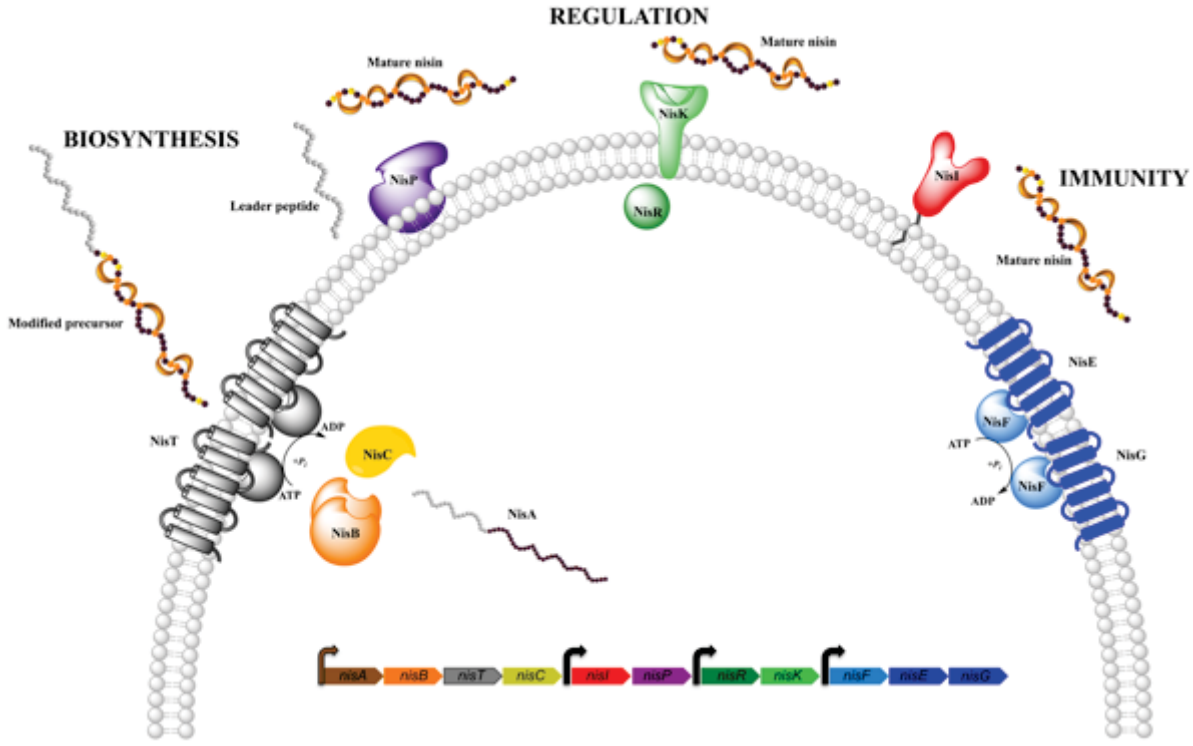

Figure 6: Overview of the nisin operon comprising of genes for biosynthesis, immunity and regulation. The proteins involved in the biosynthesis of nisin are shown comprising NisB (orange), NisC (yellow), NisT (grey) and NisP (purple). The two-component system regulatory proteins: NisR (dark green) and NisK (light green) and the immunity proteins: NisI (red) NisFEG (blue) are also shown. The promoter nisA is shown with brown arrow and the promoters nisF, nisI and nisR are shown in black. Based on [100] and created with Chem BioDraw 13.0.

Since the antimicrobial activity of nisin is targeted specifically against lipid II (precursor molecule for cell wall synthesis), and lipid II is also present in the cytoplasmic membrane of the producer cells; the producer strain has developed a self-immunity mechanism to protect itself from the suicidal effect of the produced nisin. Here, the lipoprotein NisI and the ABC transporter NisFEG provide immunity against nisin [101, 94, 102]. Furthermore, full immunity is achieved only when both NisI and NisFEG are expressed [103].

Nisin acts as a quorum sensor and auto-regulates its own biosynthesis which is controlled by a two-component system comprising of NisRK [104, 105]. Presence of nisin in the extracellular medium of *L. lactis* induces an auto-regulation mechanism, activating NisR and NisK. External nisin acts as a signal, which is recognized by NisK, the histidine-kinase. NisK is attached to the cytoplasmic membrane, which binds to the active mature nisin, activating a signal transduction cascade [105]. After the binding, NisK is auto-phosphorylated at a conserved histidine residue. This high energetic potential of the phosphoryl group is transferred to a conserved aspartate residue of the transcriptional response regulator NisR [104]. Upon activation, NisR binds to the *nisA* promoter on the nisin operon, stimulating the expression of the genes of the nisin operon [105]. Studies have shown that the first two rings of nisin are essential for this regulation mechanism, while the ring C of nisin is important for induction of the expression, whereas the last two rings have no specific influence on the expression [106, 104].

1.4.3 Applications of Nisin

Nisin shows antimicrobial activity against a wide range of Gram-positive bacteria. The major application of nisin to date remains in the food industry as a food preservative and an additive in dairy products [40], canned vegetables [40], bakery products [107], meat [108] and alcoholic beverages [109, 110]. The therapeutic potential of nisin has also been extensively studied. Nisin is effective in the treatment of atopic dermatitis [111], stomach ulcers [112], colon infections [113], respiratory tract infections [114], staphylococcal mastitis [73] and sexually-transmitted infections [115]. In veterinary, nisin is currently used as a sanitizer against mastitis pathogens (*Staphylococcus* and *Streptococcus* species) [116, 117].

1.5 Lantibiotic Resistance

Lantibiotics are effective against numerous bacteria where the bacterial cell wall and membrane comprise the major target for the bactericidal efficiency of lantibiotics. However, bacteria can become resistant to lantibiotics by different mechanisms: (i) modifications in the cell membrane, (ii) changes in cell wall, (iii) two-component system regulation, (iv) ATP-mediated efflux pumps, and (v) lantibiotic degradation [118, 119, 9, 120, 121]. Interestingly, some resistant bacteria counter the effects of the lantibiotics by relying on more than one of the above said mechanisms in form of a gene cluster.

1.6 Cell Wall Modifications

The precursor of cell wall biosynthesis Lipid II is found at the outer leaflet of the bacterial membrane. The cell wall of Gram-positive bacteria is formed by a thick peptidoglycan fabric and by polymers of alternating phosphate and alditol groups called teichoic acids. These polymer chains are either covalently connected via phosphodiester linkage to the peptidoglycan (wall teichoic acids, WTA) or to membrane glycolipids (lipoteichoic acids, LTA). The net negative charge of the bacterial cell surface is generated by anionic components of the cell wall, such as phospholipids and teichoic acids which attracts the positively charged lantibiotics [122]. Therefore, one of the strategies for repelling the lantibiotics is to alter the cell wall components to decrease the overall net charge, thereby hindering the electrostatic attraction of the lantibiotics (Figure 7).

D-alanylation of teichoic acids and lipoteichoic acids of the cell wall by the *dlt* operon (Figure 7a) of various Gram-positive bacteria like *Staphylococcus*, *Listeria*, *Enterococcus*, *Bacillus*, *Clostridium*, *Streptococcus*, *Lactobacillus* and *Lactococcus* [123-128] reduces the negative charge of the cell envelope, thereby influencing the binding and interaction of various lantibiotics.

Penicillin-binding protein (PBP) is a bi-functional enzyme which catalyzes the polymerization of the sugar units (glycosyltransfer) as well as peptide cross-linking (transpeptidation), utilizing lipid II as the substrate [129]. An increased expression of PBP has been observed in various lantibiotic resistant species of *Listeria monocytogenes* [130] and *L. lactis* IL1403 [131].

Furthermore, *irpT* is another gene that is involved in lantibiotic resistance through gene regulation and whose disruption results in increased levels of resistance in *L. lactis* MG1363 [132].

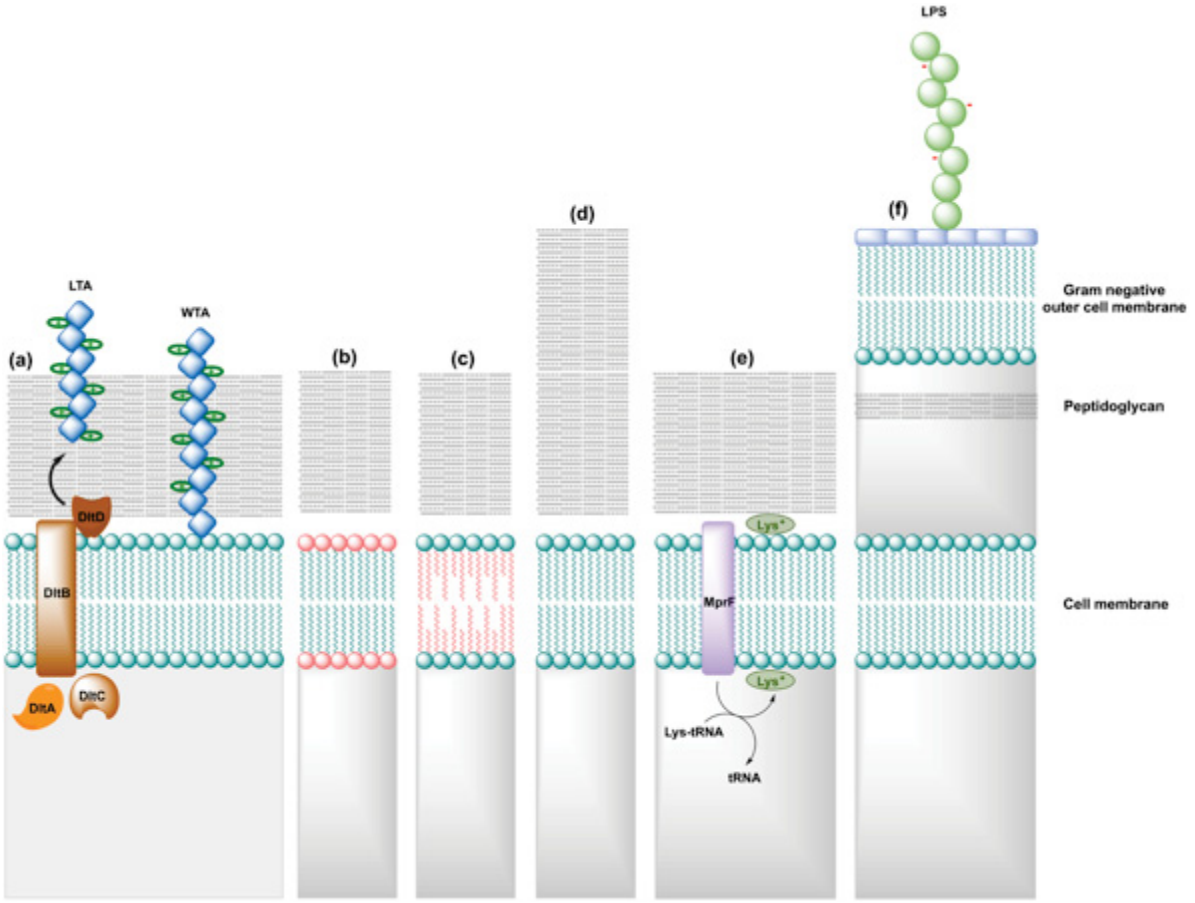

Figure 7: The various mechanisms involving modifications in cell wall and membrane that are associated with lantibiotic resistance. (a) D-Alanylation of lipoteichoic acids (LTA) and wall teichoic acids (WTA) by the *dltABCD* operon, which confers a positive charge. (b) Changes in phospholipid composition. (c) Changes in membrane fatty acid composition. (d) Cell wall thickening. (e) Lysine esterification of one of the two hydroxyl groups of phosphatidylglycerol (PG) by MprF. (f) Gram-negative outer cell membrane containing lipopolysaccharide (LPS). Based on [121]. Created with Chem BioDraw 13.0.

1.7 Cell Membrane Modifications

Other than lantibiotic repulsion, changes in the composition of the bacterial membrane (Figure 7) also contribute to lantibiotic resistance.

Although, lantibiotics are active against Gram-positive bacteria, the Gram-negative bacteria are usually resistant towards them. This is solely because of the presence of the outer membrane that prevents the penetration of lantibiotics. Furthermore, the cell wall of Gram-

negative bacteria comprises only of a few Lipid II molecules [133, 134]. The outer layer forms a site of attachment for Lipid A (a negatively charged dimer of glucosamine linked to fatty acid chains and polar phosphate groups) [135]. A complex called LPS is formed by the covalent attachment of Lipid A to a chain of oligosaccharide units and a core polysaccharide [136]. However, application of chelating agents such as EDTA [137], citrate [138] or stress [139, 140] can disrupt this barrier.

Membranes of Gram-positive bacteria contain phospholipids that vary in composition. However, the most common bacterial phospholipids are phosphatidylglycerol (PG) and di-phosphatidylglycerol (D-PG), whose head groups are negatively charged.

An increase [141] or decrease [142] in the levels of PG in the membrane of *L. monocytogenes* has been associated with lantibiotic resistance [143] (Figure 7b). Furthermore, analysis of the cell membrane components revealed that resistant cells contain a higher proportion of saturated (straight chain) fatty acids versus unsaturated (branched chain) fatty acids [144-146] (Figure 7c). All these modifications result in a decrease in cell membrane fluidity leading to a more rigid membrane conformation, thereby, making it difficult for the lantibiotics to access the membrane.

Additionally, some Gram-positive bacteria have the capability of modifying the net negative charge of the PG via addition of a positively charged amino acid by the multipeptide resistance factor protein, MprF (Figure 7e). MprF is an integral lysyl-phosphatidylglycerol synthetase that synthesizes and translocates aminoacylated-phosphatidylglycerol to the external membrane layer of the bacterial cell. MprF incorporates a positively charged lysine into phosphatidylglycerol to produce lysyl-phosphatidylglycerol (L-PG), decreasing the net negative charge on the bacterial membrane [147, 148] (Figure 8). This MprF-mediated resistance has been observed in various Gram-positive bacteria like *Staphylococcus aureus* [149], *L. monocytogenes* [150], *Bacillus subtilis* [151], *Enterococcus faecalis* [152], *Enterococcus faecium* [153], *Bacillus anthracis* [154] and *Mycobacterium tuberculosis* [155].

Moreover, a fabDG1G2Z1Z2 operon is present in some Gram-positive bacteria, which is involved in membrane synthesis via saturation and elongation of phospholipids [156]. A decreased expression of this operon has also been associated with lantibiotic resistance in *L. lactis* cells [131].

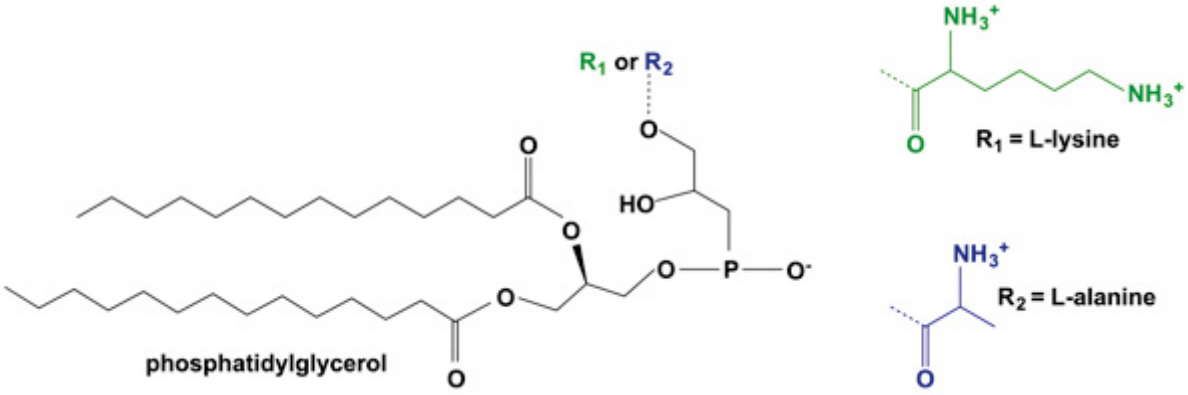

Figure 8: Modification of the membrane net charge by the addition of L-lysine and L-alanine to phosphatidylglycerol. Dashed bonds indicate modifications of phosphatidylglycerol. The lysyl-phosphatidylglycerol synthase (L-PGS) and alanyl phosphatidylglycerol synthase (A-PGS), respectively, regulate the addition of L-lysine (R1, red) and L-alanine (R2, blue) to phosphatidylglycerol (black). Based on [157]. Created by Chem BioDraw 13.0.

1.8 Two-Component System: Regulatory Networks

Bacteria have the ability to sense and survive various environmental stimuli through adaptive responses, which are regulated by two-component signaling systems (TCSs) [158]. TCSs control a wide variety of processes including drug resistance, quorum-sensing, phosphate uptake, sporulation and osmoregulation [159, 160].

TCSs comprise of two genes: a membrane-bound histidine kinase (HK) that acts as a sensor and a response regulator (RR) that mediates the cellular response [159-161].

Many TCSs have been identified which are associated with lantibiotic resistance in various pathogenic bacteria and are encoded on gene clusters [121]: BceRS in *Bacillus spp.* (actagardine and mersacidin resistance) [162], LcrRS in *S. mutans* (nukacin-ISK-1 and lacticin 481) [163], LisRK of *L. monocytogenes* (nisin resistance) [164], GraRS (nisin and nukacin-ISK-1 resistance) [165-167], WalKR , BraRS (bacitracin, nisin and nukacin-ISK-1 resistance) [168] and VraRS (resistance against nisin, mersacidin and nukacin ISK-I) [167] of *S. aureus*, CprRK of *Clostridium difficile* (nisin, gallidermin, subtilin, mutacin 1140 and cinnamycin resistance) [169].

1.8.1 Lantibiotic Resistance Associated Two-Component Systems

Two main classes of TCSs can be identified that are linked with lantibiotic resistance: BceRS-like TCSs and LiaRS-type TCSs. Interestingly, the main differentiating characteristic between them is the sensor kinase.

The BceRS-type of TCSs were first identified in *B. subtilis* where it conferred resistance against actagardine and mersacidin [162]. Since then, several Bce-type TCSs have been identified in *S. aureus* [168, 170], *S. mutans* [171] and *E. faecalis* [172].

Interestingly, the associated histidine kinases of these groups possess two transmembrane helices but lack the characteristic extracellular sensory domain are thus, classified as intramembrane-sensing kinases (IMSK) [173, 174]. Because of their incapability in recognizing the stimulus, these types of kinases are functionally linked with ABC transporters of the BceAB family (described in section 1.9). These kinases rely on them for recognizing the presence of the lantibiotic involving a direct synchronization [174, 170] between sensing of the lantibiotic and signal transduction.

On the contrary, the LiaRS-type form the so-called three-component systems that respond to cell stress signals and were named after LiaRS of *B. subtilis* [175]. This group in addition to the response regulator (LiaR) and the kinase (LiaS), are characterized by the presence of a third component (LiaF) that acts a negative regulator of the gene expression mediated by LiaR [175]. VraRS [167] of *S. aureus*, CesRS of *L. lactis* (nisin, plantaricin C, bacitracin and vancomycin resistance) [176, 177], and LiaRS of *L. monocytogenes* [178] belong to this group of TCSs. This TCSs system acts as a damage sensing and signal transduction system. It operates in an indirect manner via upregulation of the expression of genes involved in cell wall synthesis, thereby altering the composition of the cell wall and cell membrane.

1.9 ABC Transporter-Mediated Lantibiotic Efflux Mechanisms

Another common mechanism used by Gram-positive bacteria for the resistance against lantibiotics is through their transport, or efflux from the cells. The majority of lantibiotic-resistant transport mechanisms consist of multi-protein ABC (ATP-binding cassette) transporter systems, which use ATP to drive the transport of substrates across the cell membrane. All ABC-transporters are composed of two distinct domains: the transmembrane

domain (permease) and the nucleotide-binding domain (NBD), which facilitates ATP-binding [179].

Two types of lantibiotic-associated ABC transporters are present in Gram-positive bacteria: three-component and two-component transporter systems. Three-component ABC transporters are members of the ABC-type 2 sub-family of transporters that consist of one nucleotide-binding domain and two distinct transmembrane permeases [179]. Generally, these types of transporters are present in the lantibiotic producing strains such as NisFEG in *L. lactis* [93, 103] and SpaFEG in *B. subtilis* [180], conferring immunity against their cognate lantibiotic [180, 94]. On the contrary, the two-component ABC transporters are often associated with lantibiotic resistance in Gram-positive bacteria. The canonical two-component ABC-transporter consists of one nucleotide-binding protein and a separate membrane-spanning permease [181]. However, the only known exception to the best of our knowledge is the three-component CprABC transporter of *C. difficile* which provides resistance against lantibiotics such as nisin and gallidermin [182, 169].

The lantibiotic resistance-associated two-component ABC transporters are called BceAB-type transporters and contain an archetypal ATP-binding protein of about 225–300 amino acids and a larger permease component that ranges in size from 620–670 amino acids with a characteristic cytoplasmic loop [183, 181, 184, 185]. Various BceAB-type ABC transporters have been identified such as BceAB in *B. subtilis* [186], BraAB [167], VraDE [187, 167] in *S. aureus* [168], PsdAB in *B. subtilis* [188], MbrAB [189] and BceAB in *S. mutans* [171], SP0812-SP0813 [190] and SP0912-SP0913 [191] *Streptococcus pneumoniae* and NsrFP in various bacteria of corynebacterium, enterococcus, leuconostoc, streptococci genera [184]. Although the members of this group have demonstrated resistance to a wide-range of lantibiotics such as nisin, gallidermin, mersacidin, actagardine and subtilin, antimicrobial peptides like mammalian and fungal defensins, and other antimicrobial compounds; the exact roles of these transporters in conferring resistance is still not known.

1.10 Lantibiotic Degrading Mechanisms

In addition to the above-mentioned resistance mechanisms, some Gram-positive bacteria possess resistance mechanisms that are highly specific for lantibiotics. In some nisin-resistant *Bacillus* spp. strains, a nisin inactivating enzyme, named nisinase was found [192, 193]. Nisinase was shown to be produced by several spp. of bacillus [192], lactobacillus

[194], lactococcus, enterococcus, leuconostoc [39], streptococci [39, 195] and staphylococcus genera [196]. This non-proteolytic enzymatic inactivation of nisin was later identified as a dehydroalanine (Dha) reductase that reduces the carboxyl Dha to Ala (*i.e.,* it breaks the C-terminal lanthionine ring), lowering the antimicrobial potency of nisin [193, 197]. However, in addition to nisin, this enzyme could also inactivate subtilin [192].

Another different mechanism of nisin resistance observed in some nisin-non producing strains involves the presence of a nisin resistance protein NSR (serine protease) that proteolytically cleaves nisin by removing the C-terminal tail of nisin [198]. Similarly, a sublancin degrading protease YqeZ is involved in resistance against sublancin 168 in bacilli [199].

1.11 Lantibiotic Resistance Associated Operons

As described in section 1.5, various lantibiotics non-producing strains including many human pathogenic bacteria are resistant towards lantibiotics because of the presence of a lantibiotic resistance-associated gene operon [184] comprising of four-five genes [170, 184, 169] encoding a two-component system (response regulator and histidine kinase), an ABC transporter and/or a serine protease (or a protein of unknown function) [170, 184]. The encoded proteins utilize a combination of the previously mentioned mechanisms of resistance (section 1.8 and 1.9), thereby providing efficient resistance. Similar to the lantibiotic immunity operons, these lantibiotic resistant operons are also found as gene clusters on the chromosomes of various bacteria [184].

The *gra*XSR/*vra*FG locus in *S. aureus* (Figure 9) provides resistance against various AMPs including lantibiotics [200, 170] and this resistance is regulated by the presence of AMPs in the extracellular environment. *gra*SR together encode for a two-component system while *vra*FG encodes for a BceAB-type ABC transporter (explained in section 1.9) [170]. Furthermore, the fifth component *graX* encodes a cytosolic protein that acts as an accessory protein to the TCS and assists in signalling [170].

A five genes operon *cpr*ABCK-R (Figure 9) has also been identified in *C. difficile* which confers resistance against lantibiotics nisin, gallidermin, subtilin, mutacin 1140, and cinnamycin [169] where *cpr*ABC encodes for an ABC transporter and *cpr*K-R form a two-component system [182, 169].

In *S. mutans*, *lct*GEF*lcr*XRS (Figure 9) and *nsr*XRS form two distinct gene systems which confer resistance against nisin, nukacin ISK-1 and lacticin 481 [163]. *lcr*RS and *nsr*RS form two-component systems, while *lcr*GEF encode for an ABC transporter. LcrX is a hypothetical protein of unknown function while NsrX is homologous to acetyl transferase and binds to nisin, preventing its interaction with lipid II [163].

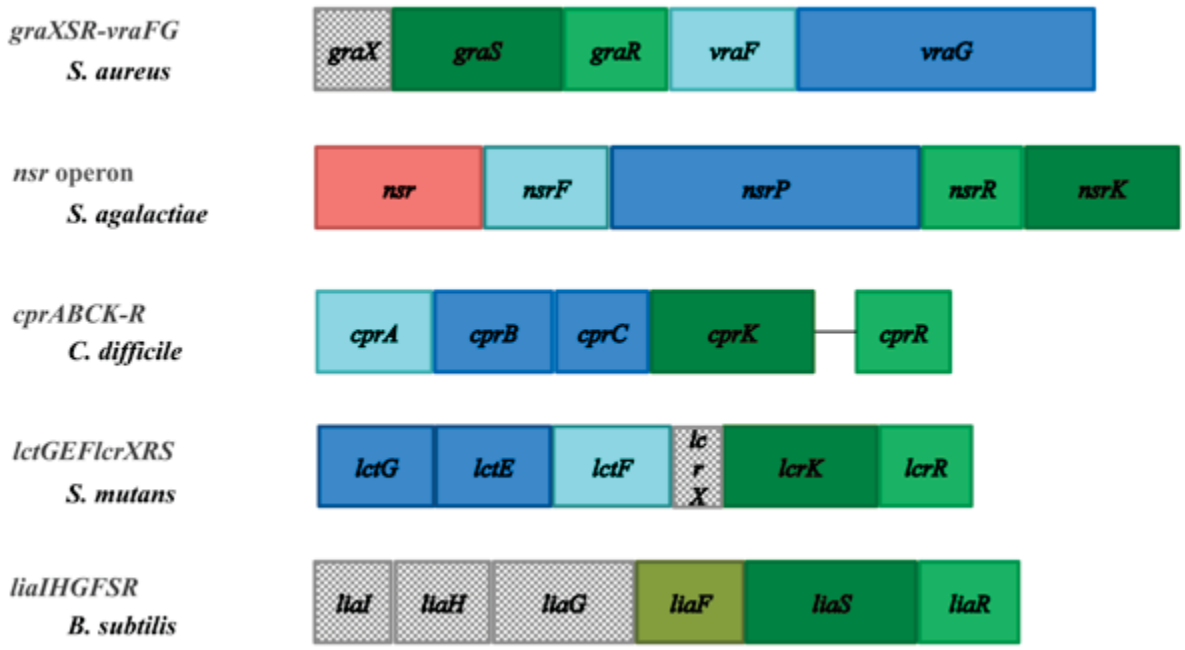

Figure 9: A schematic representation of distinct gene clusters conferring lantibiotic resistance. Shown are the resistance-associated operons *gra*XSR/*vra*FG in *S. aureus*, nisin resistance operon in *S. agalactiae*, *cpr*ABCK-R in *C. difficile*, *lct*GEF*lcr*XRS in *S. mutans* and *lia*IHGFSR in *Bacillus* spp. The genes with similar functions are color-coded identically. The response regulator, histidine kinase (in shade of green); ATP-binding domain and the permease domain of ABC transporter (depicted in blue), the genes with unknown functions (colored in grey) and gene encoding for serine protease (pink) are shown.

Similarly, a multicomponent operon system *lia*IHGFSR is present in *Bacillus* spp. (Figure 9) that is induced with the presence of bacitracin, ramoplanin, vancomycin and nisin [177, 175]. Here, LisFSR form a three-component system, while LiaH is a homologue of *E. coli* phage shock protein A. *liaI* and *liaG* encode for proteins with unknown functions, however, they harbor transmembrane domains, indicating membrane localization [175].

A five gene cluster, *van*RSHAX was also identified in Tn*1546* from *E. faecium* BM4147 which confers resistance against teicoplanin and vancomycin [201].

A sublancin resistance *yqeZyqf*AB operon is identified in *Bacillus subtilis* where *yqeZ* encodes a serine protease and *yqfAB* encode for membrane-anchored proteins of unknown functions [199]. Similar sublancin resistance operon systems are also present in various

species of Bacillus genera such as *Bacillus licheniformis*, *Oceanobacillus iheyensis*, *Symbiobacterium thermophilum*, *S. aureus*, and *Staphylococcus epidermis* [199].

In *S. agalactiae*, a multicomponent operon system (Figure 9), *nsr*FPRK comprising of five genes is involved in nisin resistance [184]. The *nsr* gene encodes for a serine protease, namely nisin resistance protein that proteolytically degrades nisin, reducing its bactericidal activity (explained below in section 1.12) [198, 184]. NsrRK and NsrFP form a two-component system and an ABC transporter, respectively (refer to sections 1.13-15) [184]. Similar homologous operon systems have also been identified in various genera of Gram-positive bacteria including human pathogens like streptococci, streptococcus, staphylococcus, enterococci and listeria [184].

1.12 Nisin resistance protein- the serine protease

A *nsr* gene is present in some species of Gram-positive bacteria that is associated with nisin resistance. Originally, this nisin resistance determinant in non-nisin producer *Streptococcus lactis* subsp. *diacetylactis* DRC3 was found to be associated with a 40-megadalton plasmid pNP40 [202]. However, subsequently various plasmids were identified in different strains that conferred nisin resistance [203-205]. The nisin resistance in non-producing strain DRC3 is 1/10 of the immunity in producing strains [206].

nsr encodes for a 35 kDa nisin resistance protein (NSR) which is strongly hydrophobic and membrane-associated via the N-terminus [206]. Homology modelling revealed that the mechanism by which NSR confers resistance is via a tail specific protease (TSP) domain at its C-terminal [87, 198, 207].

TSPs are present in various species and usually cleave substrates that have non-polar residues and a free alpha-carboxylate at the C-terminus [208]. Such proteases usually contain a conserved PDZ domain adjacent to the TSP domain, which is indispensable for binding of the TSP domain to non-polar C-termini of the peptide substrates and thus important for the catalytic activity [209, 210]. However, NSR differs from other TSP-containing proteins as it harbours charged and polar residues (Lys, His, and Ser) at the C-terminus [209] and does not possess a PDZ domain. Recent *in silico* studies revealed that NSR belongs specifically to the S41 family of peptidases, specifically the CTPs (C-terminal processing peptidase). Furthermore, the active site of these proteases usually consists of a catalytic dyad formed by Ser and Lys or Ser and His [211].

Experimental studies showed that the presence of NSR reduces the bactericidal efficiency of nisin [207] in *L. lactis* MG1363. NSR-mediated nisin resistance is conferred via proteolytic degradation of nisin where NSR cleaves/hydrolyses the peptide bond between MeLan28 and Ser29 of nisin [198] (Figure 10). Interestingly, the predicted N-terminal signal sequence has no effect on the activity of NSR, as both the full-length and the smaller variant were able to inactivate nisin in vitro. The cleaved nisin fragment ($nisin^{1-28}$) (Figure 10), still having the five characteristic lanthionine rings, displays a reduced affinity for the cell membrane, decreased affectivity in pore formation and a 100-fold less bactericidal activity [198], implicating towards the importance of the C-terminus of nisin in its bactericidal efficiency [207].

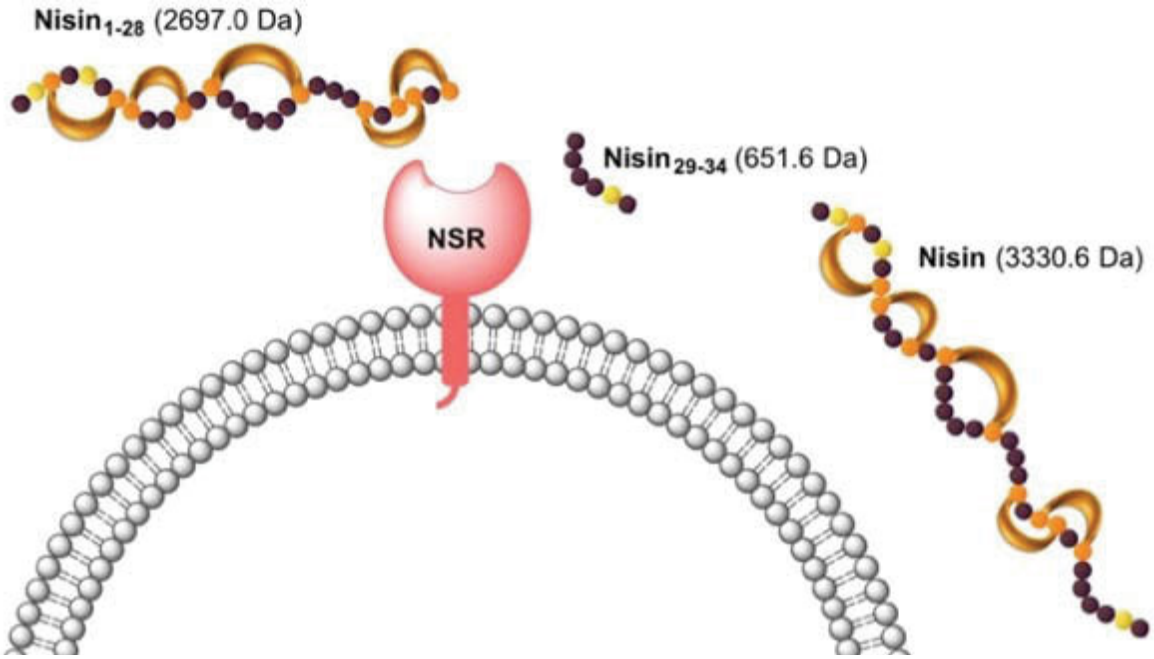

Figure 10: Proteolysis of nisin catalyzed by NSR. Post-translationally modified residues are indicated in orange color. Molecular masses of intact and NSR-cleaved nisin are indicated in parentheses to the right of the corresponding peptides. Based on [198] and created with Chem BioDraw 13.0.

Interestingly, this protein is found within an operon that contains other genes encoding an ABC transporter NsrFP, and a TCS named NsrRK which confers nisin resistance in these strains [184] (Figure 11). Furthermore, these operons were identified in various strains of different genera of corynebacterium, enterococcus, leuconostoc, staphylococcus and streptococcus bacteria.

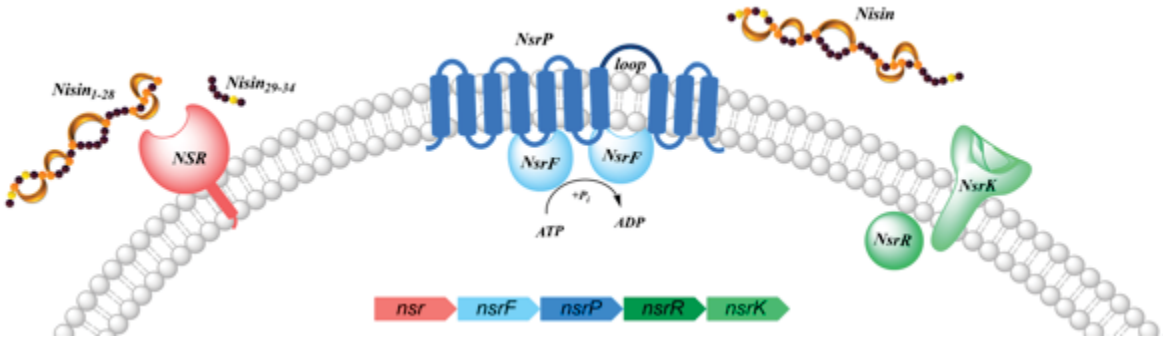

Figure 11: Overview of the nisin resistance operon. The nisin resistance protein (Nsr) is shown in shade of pink. The two-component system regulatory proteins: NsrR (dark green) and NsrK (light green) and the ABC transporter proteins: NsrF (sky blue) NsrP (blue) are also shown with the extracellular domain (loop) highlighted in dark blue. Adapted from chapter I and created with Chem BioDraw 13.0.

1.12.1 Other resistance-associated serine protease

Sublancin is a S-linked glycopeptide [212] encoded by the *sunA* gene located on the SPβ prophage [213] and is produced by *B. subtilis* 168 [214]. Various species of Gram-positive bacteria are found to be intrinsically resistant to sublancin due to the presence of *yqeZyqf*AB operon [199].

YqeZ is a member of the NfeD family of membrane-bound serine proteases (ClpP class; COG1030). Although, the exact molecular mechanism of YqeZ is not known yet, its N-terminal region is similar to SppA (signal peptide peptidase) with conserved catalytic serine and lysine residues [199]. Furthermore, a NfeD homologue (PH1510) from *Pyrococcus horikoshii* is known to cleave within the C-terminal region of the downstream stomatin (PH1511) [215]. Furthermore, it is postulated that the membrane-integrated protease YqeZ might provide resistance by degrading peptides inserted into the membrane [199], indicating towards a similar mode of resistance involving cleavage of lantibiotics.

1.13 The histidine kinases

Histidine kinases (HKs) form integral part of TCS that act as sensors and monitor the external stimuli. ATP-dependent autophosphorylation of HK at a conserved histidine residue results in the dimerization of the kinase. Furthermore, phosphotransfer from the HK to the

RR results in activation of the RR and leads to generation of the output response of the signaling pathway [161].

Histidine kinases vary in size from 40kDa to 200kDa [160] and are cytoplasmic membrane-associated, usually via one or two membrane-spanning sequences which are crucial for substrate binding. They typically contain extracellular sensory input modules fused to the conserved protein kinase catalytic core [159] and their overall activity is dependent on the input signals mediated by the sensory domains.

The sensor domains are responsible for detection of the external signal, while the 350 amino acids long kinase catalytic core is composed of a dimerization domain and an ATP/ADP-binding phosphotransfer (catalytic) domain which is responsible for ATP-binding and directing phosphorylation [160].

1.13.1 NsrK – the histidine kinase

As previously mentioned, most of the known lantibiotic resistance-associated kinases belong to the so-called "intramembrane-sensing kinase" (IMSK) subfamily of histidine kinases which are characterized with a short N-terminal sensing domain, composed of two transmembrane helices separated by a short loop of only a few amino acids (less than 25 amino acids) [173, 216]. Thus, these kinases are buried almost entirely in the cytoplasmic membrane and are conserved in low GC Gram-positive bacteria. These kinases are usually small of about 400 amino acids (Figure 12).

Since they lack a typical HK extracellular sensing domain, it has been suggested that the signal detection involves a process [173] in response to the lantibiotic leading to increased synthesis of the ABC transporter encoded by the neighbouring genes. The ABC transporter then facilitates the removal of the corresponding lantibiotic [173, 216, 121].

In silico studies revealed that NsrK also belongs to the IMSK family of kinases and comprises of the typical short sensory domain and the characteristic kinase domains (HisKA and HATPase_c) [217] and lacks any additional domains that would allow signal detection within the cytoplasm (Figure 12). Therefore, the presence of the ABC transporter NsrFP in the neighborhood is inevitable for providing the full resistance against nisin [184].

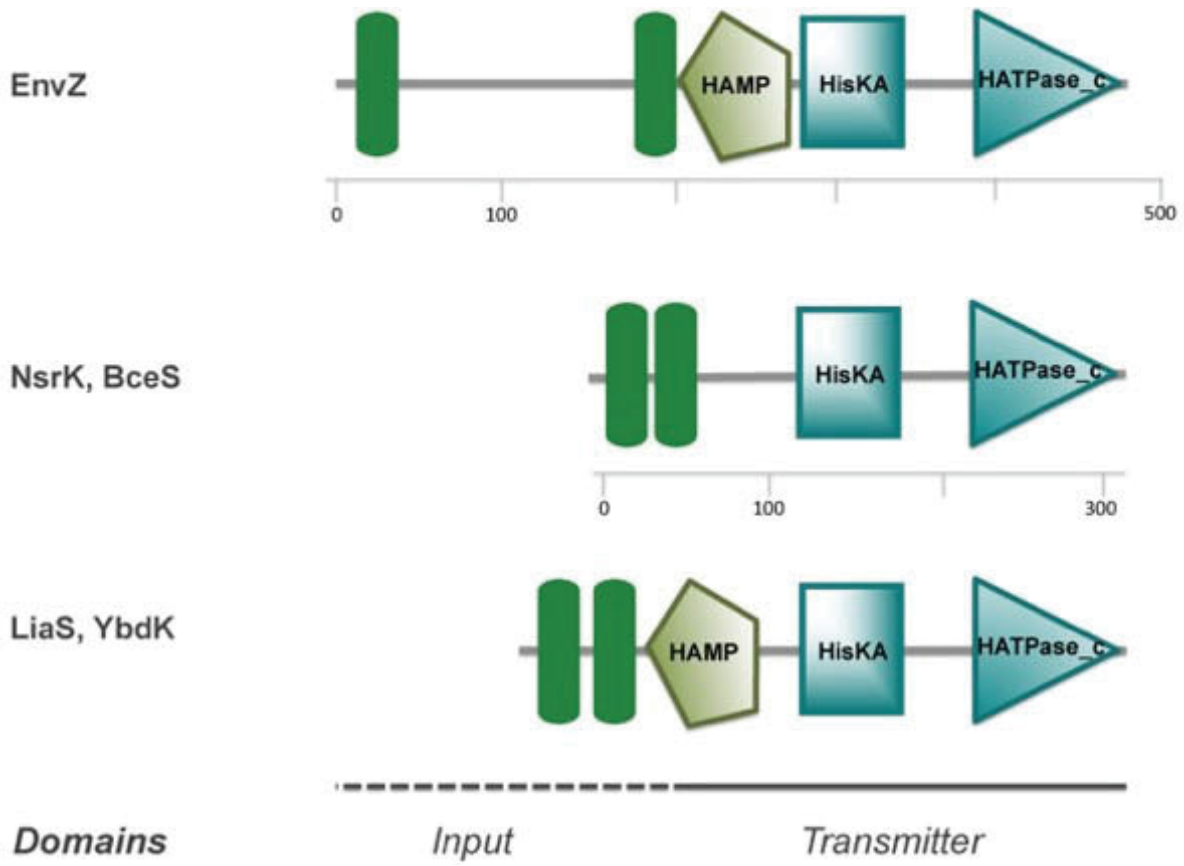

Figure 12: Domain organization of intramembrane-sensing histidine kinases. The structural domains of different lantibiotic resistance associated (IMSK family) kinases are shown in comparison to EnvZ histidine kinase from *E. coli*. NsrK and BceS are associated with ABC transporter while LiaS and YbdK are ABC transporter independent kinases. The figure on based on the graphical output of the SMART interface [217] and [173].

1.14 The response regulator - NsrR

Response regulators of the TCS function as phosphorylation-activated switches that regulate the output responses [161] such as upregulation of genes. Generally, response regulators (RRs) consist of two distinct structural domains, a receiver domain (RD) and an effector domain (ED), that are separated from each other by a flexible linker [159, 160]. RDs contain a highly conserved aspartate residue, which acts as a phosphoacceptor and is phosphorylated by the kinase domain of the histidine kinase upon reception of the external signal. The ED is thereby activated and binds to the designated promoters, initiating transcription of the genes [159, 218].

Lantibiotics serve as a signal for CprRK in *C. difficile* [169] and GraSR in *S. aureus* [170] and upon activation, the corresponding response regulators CprR and GraR promote the

transcription of the *cpr* locus comprising of *cpr*ABCRK, and g*ra*XSR and *vra*FG genes [170, 169], respectively.

A similar function for NsrR has been postulated wherein upon phosphorylation, it induces the expression of all the corresponding genes present in the nisin resistance operon *nsr* and *nsr*RKFP [184].

1.15 The ABC transporter NsrFP

Within the *nsr* operon, the protein encoded by *nsrF*, designated NsrF represents the nucleotide-binding domain (NBD), and NsrP encoded by *nsrP* is the transmembrane domain (TMD), which forms the transport pore within the membrane [184]. The proteins NsrF and NsrP together encode a functional ABC transporter.

NsrFP is a BceAB-type ABC transporter and is closely related to the ABC transporter MbrAB from *S. mutans* (45% sequence similarity). MbrAB, a homologue of BceAB in *B. subtilis*, is an exporter of bacitracin involved in bacitracin resistance [189] and functions together with BreSR, a two-component system to regulate its own gene expression [183]. Various similar ABC transporters associated with lantibiotic resistance have been characterized in *S. pneumoniae* (bacitracin and vancoresmycin resistance) [190], YsaBC in *L. lactis* IL140 (exporter and is involved in nisin resistance) [131], ABC09 and ABC12 of *Lactobacillus casei* BL23 (nisin, bacitracin, subtilin and plectasin resistance) [219], ABC multidrug-resistance efflux pump AnrAB in *L. monocytogenes* (exports nisin, gallidermin, bacitracin and β-lactam antibiotics) [220], BceAB in *B. subtilis* [162, 221, 222] and VraDE and BraDE in *S. aureus* (nisin and bacitracin resistance) [168].

Since NsrFP is an ABC transporter, it should either export or import the substrate. Based on the known ABC transporters from the lantibiotic immunity and resistance systems, the putative function of NsrFP can be postulated. The immunity ABC transporters, NisFEG and SpaFEG in the producer systems, are known to act as an exporter, transporting the nisin/subtilin molecules into the external environment [103, 223]. Thus, NsrFP probably acts as a second-line of defense exporting the nisin molecules out of the cell, thereby providing resistance [184].

2. Aims

The elucidation of the mechanism of nisin resistance as present in *S. agalactiae* on a molecular level and its *in vitro* characterization was the overall aim of this thesis. Although various modifications in cell wall and membrane are responsible for nisin resistance in various nisin non-producing strains [123, 142, 143, 126, 132, 148, 128, 157, 9, 121], a distinct mechanism of nisin resistance in nisin non-producers involving a nisin resistance protein (NSR) was identified in 1957 [196, 192].

This nisin resistant determinant was observed in various non- producing strains of *L. lactis* [202, 203, 206, 204, 205]. However, it was not until 2009 that the underlying mechanism of NSR-mediated nisin resistance was identified [198]. NSR confers nisin resistance by proteolytically degrading nisin by cleaving the six amino acids from the carboxyl tail of nisin [198]. The resulting nisin fragments showed 100-fold less bactericidal activity and reduced affinity for membrane.

These results provide only limited insights into the functioning of this serine protease. Furthermore, biochemical characterizations of NSR including its substrate specificity are still lacking. Additionally, analogous to the immunity system in nisin producing strains [93, 94, 224], involvement of any additional genes in nisin resistance is still ambiguous.

In order to establish the possible involvement of additional genes in this resistance phenomenon, the first aim of the thesis was to characterize the operon involving *nsr* gene and subsequently identify other associated genes.

After successful identification of the five-component operon involving NSR, NsrFP (ABC transporter) and NsrRK (two-component system), the second aim was to solve the crystal structure of NSR from *S. agalactiae*, determine the binding site and the substrate specificity in order to absolve the enigma behind the unusual proteolytic degradation of nisin.

Finally, the third aim was to identify the contribution of NsrFP and NsrRK in nisin resistance in *S. agalactiae*, through biochemical characterization of the proteins on a structural level.

3. Publications

Chapter I Nisin Resistance and Its Gene Cluster

NSR from *Streptococcus agalactiae* confers resistance against nisin and is encoded by a conserved *nsr* operon

Biological Chemistry

Chapter II Nisin Resistance Protein

Overexpression, purification, crystallization and preliminary X-ray diffraction of the nisin resistance protein from *Streptococcus agalactiae*

Acta Crystallographica Section F

Chapter III The Structure of the Nisin Resistance Protein

Structural basis of lantibiotic recognition by the nisin resistance protein from *Streptococcus agalactiae*

Nature Scientific Reports

Chapter IV Response Regulator NsrR

Over-expression, Purification and Crystallization of the Response Regulator NsrR Involved in Nisin Resistance

Acta Crystallographica Section F

Chapter V The Structure of Response Regulator NsrR

Structure of the response regulator NsrR from *Streptococcus agalactiae* which is involved in lantibiotic resistance

Plos One

Chapter VI NsrP Loop

Molecular characterization of the extracellular domain from NsrFP of *S. agalactiae*

In preparation

3.1 Chapter I – Nisin Resistance and its Gene Cluster

Published in: BIOLOGICAL CHEMISTRY
Impact Factor: 3.268
Own work: 60%
Bioinformatics Analyses
Writing the Manuscript

NSR from *Streptococcus agalactiae* confers resistance against nisin and is encoded by a conserved *nsr* operon

Sakshi Khosa, Zainab AlKhatib, and Sander H.J. Smits

DE GRUYTER DOI 10.1515/hsz-2013-0167 — Biol. Chem. 2013; 394(11): 1543–1549

Short Communication

Sakshi Khosa, Zainab AlKhatib and Sander H.J. Smits*

NSR from *Streptococcus agalactiae* confers resistance against nisin and is encoded by a conserved *nsr* operon

Abstract: Nisin is a lantibiotic produced by *Lactococcus lactis* (*L. lactis*), which is active against many Gram-positive bacteria. However, in various pathogenic and non-pathogenic bacteria, the presence of a nisin resistance protein (NSR) confers resistance against nisin. Here, we show that NSR from *Streptococcus agalactiae* (*Sa*NSR) confers 20-fold resistance when expressed in *L. lactis*. We also show that *Sa*NSR is encoded by an operon structure comprising of a lipoprotein and an ATP-binding cassette transporter as well as a two-component system that is putatively involved in expression and regulation. This organization of the operon is conserved in several (non) pathogenic strains that do not produce nisin themselves.

Keywords: ABC transporter; immunity; lantibiotic; lipoprotein; nisin resistance protein; regulation.

***Corresponding author: Sander H.J. Smits,** Institute of Biochemistry, Heinrich Heine University Düsseldorf, D-40225 Düsseldorf, Germany, e-mail: sander.smits@hhu.de
Sakshi Khosa and Zainab AlKhatib: Institute of Biochemistry, Heinrich Heine University Düsseldorf, D-40225 Düsseldorf, Germany

Lantibiotics are ribosomally synthesized peptides that are characterized by the extensive post-translational modifications they undergo and are approximately 19–38 amino acids in length (Sahl and Bierbaum, 1998). The dehydration of serine and threonine residues in the prepeptide forms dehydroalanine and dehydrobutyrine amino acids (Chatterjee et al., 2005a), which then covalently link to the free cysteine thiols to form (methyl) lanthionine rings (Ingram, 1969). These lanthionine rings are important for the activity because they stabilize the peptide and protect it from proteolytic degradation (Bierbaum et al., 1996). Lantibiotics have a broad antimicrobial spectrum against various Gram-positive bacteria and thus are interesting candidates for pharmaceutical applications (Willey and van der Donk, 2007).

One of the best-characterized lantibiotic is nisin, a type I lantibiotic. It is an amphiphilic, cationic peptide of 34 amino acids. It is produced by *Lactococcus lactis* and was first discovered in 1928 (Rogers, 1928). Nisin contains one lanthionine ring and four methyl-lanthionine rings (Chatterjee et al., 2005b) and has bactericidal activity against many Gram-positive bacteria including *Streptococcus pneumonia*. It also prevents the outgrowth of many *Clostridium* and *Bacillus* spp. (Harris et al., 1992). The bactericidal efficiency of nisin is due to its capability to inhibit the cell wall biosynthesis (Reisinger et al., 1980) and its pore-forming ability (Wiedemann et al., 2001; van Heusden et al., 2002), where it uses the cell wall precursor lipid II as a docking molecule (Hasper et al., 2006). This activity can be quantitatively measured by growth inhibition of the target bacteria either on agar plates [minimum inhibitory concentration (MIC)] (Wiedemann et al., 2001) or in liquid medium [the concentration of lantibiotic that inhibits cell growth by 50% (IC_{50})] (Oman and van der Donk, 2009). Because nisin is bactericidal in nature (low nanomolar concentrations of nisin are enough to permeabilize the target membrane), there is a mechanism in nisin-producing strains conferring immunity against their own harmful lantibiotic and thus preventing a suicidal effect. A specific lipoprotein, NisI, and an ATP-binding cassette (ABC) transporter, NisFEG, together fulfill this role (Siegers and Entian, 1995). Interestingly, both these proteins act cooperatively, and only 20% of the total immunity is conferred in the absence of either of the two (Ra et al., 1999).

However, there are some Gram-positive human pathogenic bacteria such as *Staphylococcus aureus* (Carlson and Bauer, 1957) and *Streptococcus agalactiae* (Hirsch, 1950) that display substantial resistance against nisin (Harris et al., 1992). Interestingly, these strains themselves do not produce nisin.

In non-nisin-producer *L. lactis* subsp. *diacetylactis* DRC3, the nisin resistance determinant was found to be associated with the nisin resistance gene, *nsr* (Froseth and McKay, 1991). Sequencing of this *nsr* gene revealed an open

reading frame of 318 codons. The encoded 35-kDa protein nisin resistance protein (NSR) was recently characterized and was found to be membrane-associated, which is likely due to its hydrophobic N-terminus (Froseth and McKay, 1991). It has been shown that NSR from *L. lactis* TS1640 degrades nisin proteolytically by cleaving the peptide bond between MeLan28 and Ser29, thus resulting in the reduced bactericidal efficiency of nisin (Sun et al., 2009). The cleaved nisin, still having the five characteristic lanthionine rings, was found to have a reduced affinity for the cell membrane and showed 100-fold less activity (Sun et al., 2009). NSR belongs to the S41 family of peptidases, also known as the C-terminal processing peptidase (CTP). CTPs are characterized by an active site consisting of a catalytic dyad made up of serine and lysine and an N-terminal signal peptide (Keiler and Sauer, 1995; Rawlings et al., 2012). Based on homology modeling, it was later identified that NSR contains a tail-specific protease domain at its C-terminus (Silber et al., 1992) that is responsible for the C-terminal specific cleavage of its substrate.

By sequence homology studies, we identified an *nsr* gene in *S. agalactiae* ATCC 13813 (Gene Accession No.: HMPREF9171_1170). The gene product, here referred to as *Sa*NSR, shows to confer resistance when expressed in a nisin-sensitive *L. lactis* strain (Figure 1). A shift in IC_{50} toward higher nisin concentrations indicates that *Sa*NSR confers resistance. Comparing the IC_{50} values of nisin incubated with the sensitive strain harboring the empty plasmid (IC_{50}=3.8±0.4 nM) and the *Sa*NSR-expressing strain (IC_{50} of 69±1.2 nM) highlighted the fact that NSR from *S. agalactiae* confers a 20-fold resistance. As previously shown, NSR proteins act as serine proteases and the catalytic serine is conserved among the NSR homologues. When mutating this serine to alanine (gene product annotated as *Sa*NSR-S236A), the resistance against nisin drops to merely 8±1.1 nM. This slight increase when compared with the sensitive strain containing the empty plasmid is likely due to the fact that although catalytically deficient, the expressed *Sa*NSR-S236A protein still binds to the nisin molecules, resulting in a slightly higher number of nisin molecules, which are needed to inhibit the cell growth.

Additionally, through genomic data and comparative sequence analysis and using the *nsr* gene from *S. agalactiae* ATCC 13813 as the query sequence, we found that this gene is localized in a specific operon within the genome, termed here as *nsr* operon encoding six different proteins. Similar to the immunity system present in the producer strains (Alkhatib et al., 2012), the *nsr* operon consists of a lipoprotein, NSR, and an ABC transporter, termed here as NsrFP (NsrF is named after LanF found in the producer strains and P stands for the permease). Furthermore, a two-component system is also present, consisting of the response regulator and the histidine kinase (designated as NsrR and NsrK, respectively). Likely, this nisin resistance mechanism (schematically shown in Figure 2) is similar to the process of immunity in nisin-producing strains because of the high similarity between the genes present in both the systems.

This *nsr* operon is found to be present in some nonpathogenic species *Corynebacterium casei* and *Corynebacterium ammoniagenes*; in various pathogenic strains of *Leuconostoc mesenteroides*, *Leuconostoc carnosum*, *Enterococcus faecium*, *Staphylococcus epidermis*, *Streptococcus ictaluri*, *Streptococcus sanguinis*; and in different strains of *Streptococcus dysgalactiae* and *S. agalactiae*.

Further analysis showed variation in the orientation and the order of the genes in the *nsr* operon, which can be categorized in four different groups (Figure 3). The first group (I) comprises the nonpathogenic strains *C. casei* and *C. ammoniagenes*, which contain *nsrR*, *nsrK*, *nsrFP*, and *nsr* in their operon. However, here, the translational direction of *nsrFP* and *nsr* genes is opposite of *nsrR* and *nsrK* genes. The second group (IIa and IIb) comprises the

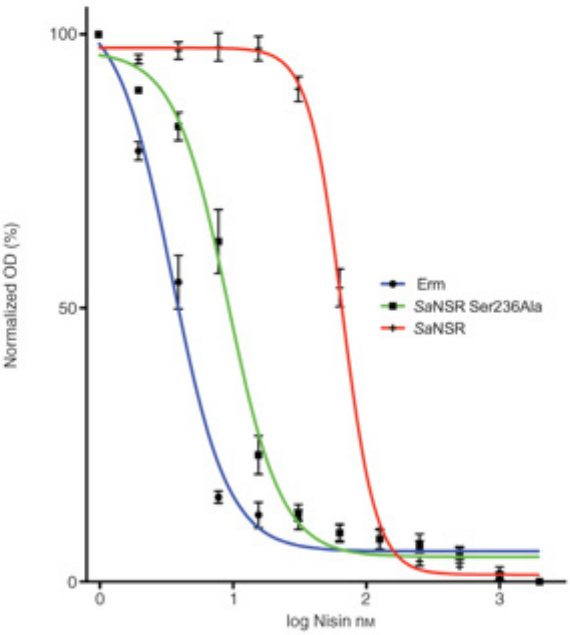

Figure 1 IC_{50} determination of nisin incubated with strains expressing *Sa*NSR and *Sa*NSR-S236A. Shown are the inhibition curves for strains expressing *Sa*NSR (red), *Sa*NSR-S236A (green), and the nisin-sensitive *L. lactis* strain NZ9000 (blue). The IC_{50} measurements were performed according to the protocol mentioned by Abts et al. (2011).

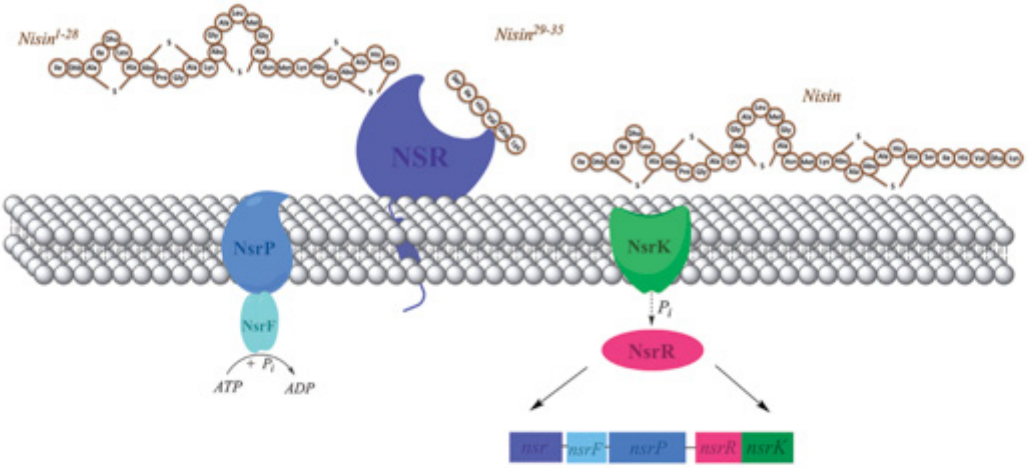

Figure 2 Mechanism of nisin resistance. The nisin resistance system consists of membrane-associated NSR, histidine kinase NsrK, transcriptional regulator NsrR and an ABC-transporter NsrFP. NSR cleaves the nisin molecule into nisin$^{1-28}$ and nisin$^{29-35}$ fragments, which show reduced activity.

pathogenic *Streptococcus* species where the gene order is different, encoding *nsr* and *nsrFP* genes first and then the two-component system genes, *nsrR* and *nsrK*. *S. ictaluri* also belongs to this group, however, here the *nsrP* gene is much smaller than that observed in the other operons (see below) and is therefore classified separately into group IIb. One interesting observation is that the *nsr* operon found in *S. sanguinis* encodes two additional *nsrFP* ABC transporters, suggesting that it might be resistant against different lantibiotic peptides, where every ABC transporter might be responsible for resistance against a specific antimicrobial peptide (group III, Figure 3), which is also reflected by its large operon size. However, the members of group IV do not have the complete operon and in *L. carnosum*, *E. casseliflavus*, and *E. faecium*, only the *nsr* gene is present, whereas the putative genes for regulation and transportation could not be identified. In contrast, the operons of *S. epidermis* and *L. mesenteroides* have *nsr* and *nsrFP*, whereas *nsrR* and *nsrK* genes were not identified. (Note: The genomes of the species of group IV are not fully sequenced or completely assembled, and only DNA contigs could be found, which might be the reason for the missing genes.) Recently, a similar operon structure has also been found, which is associated with nisin resistance in *Streptococcus mutans* UA159 (Kawada-Matsuo et al., 2013). Despite the variation in the operon structures, the same set of genes putatively involved in resistance, regulation, and transport remain present in these groups.

The proteins NsrF and NsrP together encode a functional ABC transporter (Figure 2). ABC transporters comprise one of the largest families of membrane proteins that are present in all kingdoms of life and are subdivided into two major classes, the exporters and the importers (Davidson et al., 2008). Generally, an ABC transporter consists of two hydrophobic transmembrane domains (TMDs) and two hydrophilic cytosolic nucleotide-binding domains (NBDs). Within the *nsr* operon, the protein encoded by *nsrF*, designated NsrF, represents the NBD, and NsrP encoded by *nsrP* is the TMD, which forms the transport pore within the membrane. Sequence analysis of NsrF protein reveals that it contains all the ABC transporter sequence motifs. These are the Walker A, the Walker B, the H-loop, and the two hallmarks of ABC transporters, the C-loop (or ABC signature motif, LSGGQ) (Schmitt and Tampé, 2002) and the D-loop (Higgins and Linton, 2004; Van Der Does and Tampe, 2004; Zaitseva et al., 2006). These sequence motifs are important for ATP binding and hydrolysis and are needed to energize the transport of the substrate *via* the TMDs.

NsrFP belongs to the ISVH family of ABC transporters that comprises a macrolide-specific ABC-type efflux carrier (MacAB), which confers resistance to macrolides, and proteins involved in cell division (FtsE), and lipoproteins released from the cytoplasmic membrane (LolCDE) (Holland et al., 2003). Furthermore, the ABC transporter present in the genus *Enterococcus*, which has been proven to confer resistance against the antimicrobial peptide bacitracin, also belongs to this ABC transporter family (Matos et al., 2009).

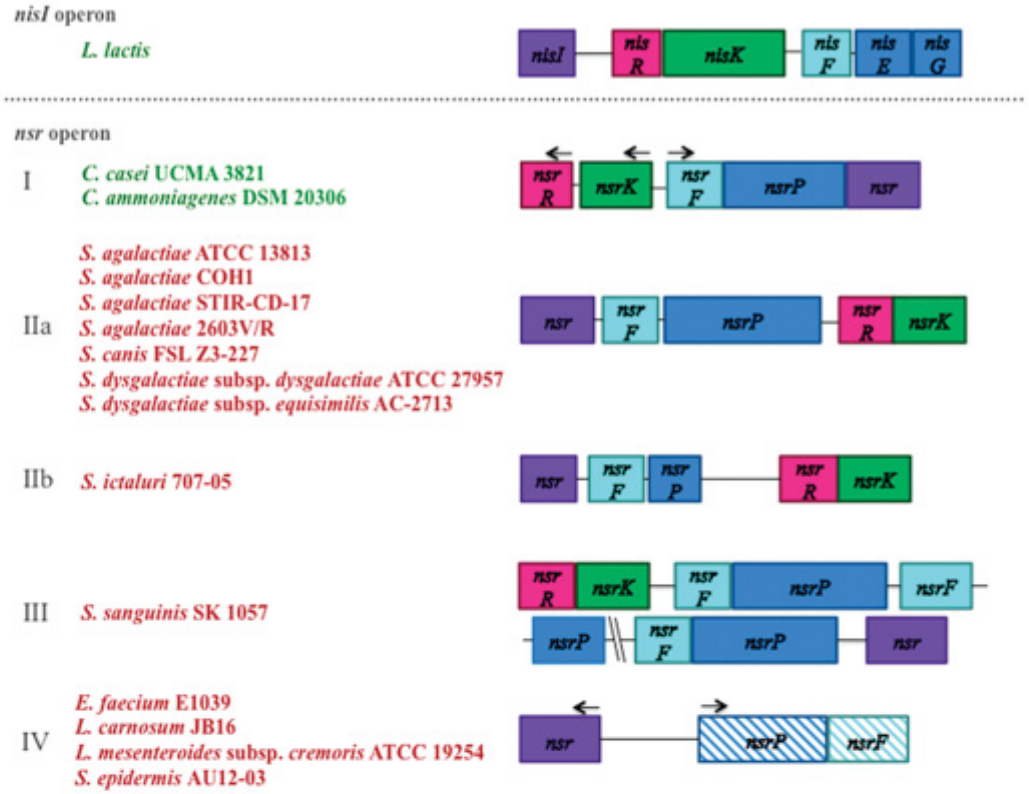

Figure 3 Structure of the nisin resistance operon. The operon structure of *nisI* in producer strain and *nsr* in different nonproducer strains has been shown. Genes performing similar functions are color-coded identically. Nonpathogenic strains are indicated in green, whereas the pathogenic strains are represented in red. Homologues of NSR from *S. agalactiae* ATCC 13813 (GI: 319745028) were manually retrieved from NCBI using a BLAST search (Altschul et al., 1990). Sequences having an E-value <1e-10 and percentage identical amino acids >30 were retained; partial sequences were excluded. Using UniProt (Magrane, 2011) and NCBI (Sayers et al., 2010), the genome of the selected microorganisms were searched for the *nsr* gene, and subsequently, other genes were also identified. *The genome and gene accession numbers are provided in Table 2 of the Supplementary Information.

Generally, the TMDs of ABC transporters display a low sequence similarity, reflecting the large variety of substrates they transport, ranging from small ions to large proteins of up to 900 kDa. A noteworthy feature of the *nsrP* gene is its size (around 2000 bp, encoding 630 amino acids), which is relatively large for a single TMD of an ABC transporter. Analysis of the membrane helical content of NsrP showed that it contains 10–12 transmembrane helices (Bernsel et al., 2009) (Figure 4), indicating that it might be harboring both the TMDs needed for a functional ABC transporter, which would result in the stoichiometry of a monomer of NsrP and a dimeric NsrF. One exception here is the NsrP of *S. ictaluri*, which might be forming a homodimer in the membrane, as it is predicted to contain only six helices (Bernsel et al., 2009) (group IIb, Figure 3).

Interestingly, in the NsrP proteins, a large extracellular loop of 200–250 amino acids (18–24 kDa) is present between helices 7 and 8, representing an extra domain (highlighted in red, Figure 4). The *nsrP* gene of *S. ictaluri* is smaller; consequently, the extracellular loop present in its NsrP (between helices 5 and 6) is also smaller than that present in other NsrP proteins.

Analysis of the loop sequence of NsrFP using BLAST searches (Altschul et al., 1990) did not reveal any sequence similarities to other proteins, except the NsrP-like ABC transporters that are involved in lantibiotic resistance. Furthermore, sequence comparison and structure prediction programs such as PDB-BLAST (Altschul et al., 1990) and Phyre II (Söding, 2005), yielded no significant structural homology with the known crystal structures, suggesting that this extracellular loop is an exclusive characteristic of the lantibiotic resistance-associated family of ABC transporters. Extra domains fused to ABC transporters are not unusual and perform some specific functions. In

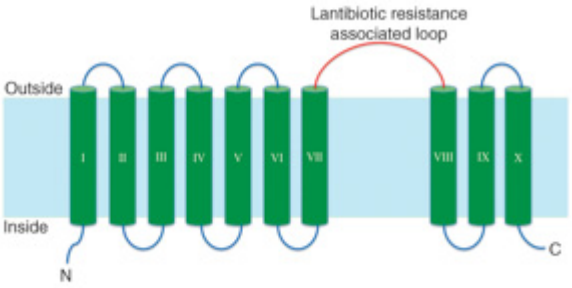

Figure 4 Predicted secondary structure of NsrP. NsrP is composed of 10 transmembrane helices (Bernsel et al., 2009) shown in green. Between helices 7 and 8, an extra loop domain (red) thought to be associated with lantibiotic resistance is present.

the glycine betaine ABC transporter, OpuA from *L. lactis*, an extra domain [identified as substrate-binding protein (SBP)] is fused to the membrane permease. Located at the C-terminus, the main purpose of this SBP is to bind to the substrate in the extracellular space and deliver it to the transporter (van der Heide and Poolman, 2002). A peptidase domain localized at the N-terminal is present in the ABC exporter NukT that transports Nukacin ISK-1 (a class II lantibiotic produced by *Staphylococcus warneri* ISK-1), which cleaves off the signal sequence prior to the transport of the lantibiotic into the external environment (Nishie et al., 2011). Similar to the presence of an extra domain between the helices in NsrP, an extra domain is also localized between transmembrane helices 2 and 3 in $MalFGK_2$ (the maltose uptake ABC transporter system of *Escherichia coli*). The membrane protein MalF contains a large extracellular loop (called P2-loop), which folds into an Ig-like domain, extending 30 Å away from the membrane surface and interacts with MalE (SBP) (Oldham et al., 2007) for regulatory purposes.

Because NsrFP is an ABC transporter, it should either export or import the substrate. Using the lantibiotic immunity system as a model, we hypothesize the function of NsrFP. The immunity ABC transporter SpaFEG in the subtilin-producing systems is known to act as an exporter, transporting the subtilin molecules into the external environment (Stein et al., 2005). Similarly, in the nisin-producing strains, NisFEG has also been shown to function as an exporter, expelling the nisin molecules out of the membrane into the extracellular space (Stein et al., 2003). Studies involving the expression of NisIFEG in *B. subtilis* showed that all the nisin molecules could be recovered from the media and the strain became resistant (Stein et al., 2003). Thus, LanFEG builds a so-called second line of defense in the lantibiotic-producing strains.

It is known that the lipoprotein NSR captures the nisin molecules and cleaves off the last six C-terminal residues, thereby lowering its activity (Sun et al., 2009). However, at higher nisin concentrations, it is likely that NSR is not cleaving all the nisin molecules. We propose that NsrFP would have a similar activity as the NisFEG, rescuing the microorganism from the nisin molecules that escape the first line of defense provided by NSR.

In nisin-producing *L. lactis* strain, the expression of NisI and NisFEG is regulated by the two-component system, NisR and NisK. The presence of *nsrR* and *nsrK* genes, together encoding a two-component regulatory system in the operon, suggests that the expression of NSR and NsrFP is also tightly regulated. In the producer strains, the genes for biosynthesis and immunity are regulated *via* signal transduction involving a two-component regulatory system composed of a receptor NsrK, *nisK*, and a transcriptional NsrR, *nisR* (Kuipers et al., 1995). The transcription of the immunity genes is controlled by *nisR* and *nisK*, based on the concentration of extracellular nisin (Kleerebezem, 2004). Thus, nisin acts as a pheromone and regulates its own biosynthesis and expression (Kuipers et al., 1995). Recently, the involvement of the two-component system NsrRS of *S. mutans* UA159 was confirmed in nisin resistance, which also regulates the expression of other genes found in the operon (Kawada-Matsuo et al., 2013). Thus, we postulate a similar function for NsrR and NsrK, which might also be induced by the amount of external nisin.

In conclusion, the *nsr* gene found in the genome of *S. agalactiae* confers resistance to nisin when expressed in *L. lactis*. *Sa*NSR is encoded by an operon consisting of *nsr*, *nsrR*, *nsrK*, and *nsrFP* genes, which are found in other nisin-nonproducing strains as well. The observed operon structure resembles the one found in nisin-producing strains. However, the exact underlying mechanism of the correlated functioning of these genes is still unknown, and some extensive studies on the encoded proteins are required for proper understanding. An in-depth knowledge about this resistance would open new avenues for the treatment of bacterial infections using lantibiotics.

Acknowledgments: The authors would like to thank André Abts and Ulrich Schulte for their helpful suggestions and valuable comments and all the laboratory members for their support. We sincerely thank Dr. Diana Kleinschrodt and Iris Fey, at the Protein Production Facility, Heinrich-Heine-University Düsseldorf, for cloning the plasmids. We gratefully acknowledge the support (and training) from the International NRW Research School BioStruct and the grants from the Ministry of Innovation, Science and

Research of the State North Rhine-Westphalia, the Heinrich-Heine-University of Düsseldorf, the Entrepreneur Foundation at the Heinrich-Heine-University of Düsseldorf. We are highly indebted to the scholarships provided by CLIB Graduate Cluster Industrial Biotechnology to Z.A. and Heinrich Heine International Graduate School of Protein Science and Technology (iGRASP*seed*) to S.K.

Received May 3, 2013; accepted July 17, 2013; previously published online July 22, 2013

References

Abts, A., Mavaro, A., Stindt, J., Bakkes, P.J., Metzger, S., Driessen, A.J., Smits, S.H., and Schmitt, L. (2011). Easy and rapid purification of highly active nisin. Int. J. Pept. *2011*, 175145.

Alkhatib, Z., Abts, A., Mavaro, A., Schmitt, L., and Smits, S.H. (2012). Lantibiotics: how do producers become self-protected? J. Biotechnol. *159*, 145–154.

Altschul, S.F., Gish, W., Miller, W., Myers, E.W., and Lipman, D.J. (1990). Basic local alignment search tool. J. Mol. Biol. *215*, 403–410.

Bernsel, A., Viklund, H., Hennerdal, A., and Elofsson, A. (2009). TOPCONS: consensus prediction of membrane protein topology. Nucl. Acids Res. *37*, W465–W468.

Bierbaum, G., Szekat, C., Josten, M., Heidrich, C., Kempter, C., Jung, G., and Sahl, H.-G. (1996). Engineering of a novel thioether bridge and role of modified residues in the lantibiotic Pep5. Appl. Environ. Microbiol. *62*, 385–392.

Carlson, S. and Bauer, H. (1957). A study of problems associated with resistance to nisin. Arch. Hyg. Bakteriol. *141*, 445–460.

Chatterjee, C., Miller, L.M., Leung, Y.L., Xie, L., Yi, M., Kelleher, N.L., and van der Donk, W.A. (2005a). Lacticin 481 synthetase phosphorylates its substrate during lantibiotic production. J. Am. Chem. Soc. *127*, 15332–15333.

Chatterjee, C., Paul, M., Xie, L., and van der Donk, W.A. (2005b). Biosynthesis and mode of action of lantibiotics. Chem. Rev. *105*, 633–684.

Davidson, A.L., Dassa, E., Orelle, C., and Chen, J. (2008). Structure, function, and evolution of bacterial ATP-binding cassette systems. Microbiol. Mol. Biol. Rev. *72*, 317–364.

Froseth, B.R. and McKay, L.L. (1991). Molecular characterization of the nisin resistance region of *Lactococcus lactis* subsp. *lactis* biovar diacetylactis DRC3. Appl. Environ. Microbiol. *57*, 804–811.

Harris, L.J., Fleming, H.P., and Klaenhammer, T.R. (1992). Developments in nisin research. Food Res. Int. *25*, 57–66.

Hasper, H.E., Kramer, N.E., Smith, J.L., Hillman, J., Zachariah, C., Kuipers, O.P., De Kruijff, B., and Breukink, E. (2006). An alternative bactericidal mechanism of action for lantibiotic peptides that target lipid II. Science *313*, 1636–1637.

Higgins, C.F. and Linton, K.J. (2004). The ATP switch model for ABC transporters. Nat. Struct. Mol. Biol. *11*, 918–926.

Hirsch, A. (1950). The assay of the antibiotic nisin. J. Gen. Microbiol. *4*, 70–83.

Holland, I.B., Cole, S.P., Kuchler, K., and Higgins, C.F. (2003). ABC Proteins: From Bacteria to Man (Academic Press) Access Online via Elsevier.

Ingram, L.C. (1969). Synthesis of the antibiotic nisin: formation of lanthionine and beta-methyl-lanthionine. Biochim. Biophys. Acta *184*, 216–219.

Kawada-Matsuo, M., Oogai, Y., Zendo, T., Nagao, J., Shibata, Y., Yamashita, Y., Ogura, Y., Hayashi, T., Sonomoto, K., and Komatsuzawa, H. (2013). Involvement of the novel two-component NsrRS and LcrRS systems in distinct resistance pathways against nisin A and nukacin ISK-1 in *Streptococcus mutans*. Appl. Environ. Microbiol. *79*, 4751–4755.

Keiler, K.C., and Sauer, R.T. (1995). Identification of active site residues of the Tsp protease. J. Biol. Chem. *270*, 28864–28868.

Kleerebezem, M. (2004). Quorum sensing control of lantibiotic production; nisin and subtilin autoregulate their own biosynthesis. Peptides *25*, 1405–1414.

Kuipers, O.P., Beerthuyzen, M.M., de Ruyter, P.G., Luesink, E.J., and de Vos, W.M. (1995). Autoregulation of nisin biosynthesis in *Lactococcus lactis* by signal transduction. J. Biol. Chem. *270*, 27299–27304.

Magrane, M. (2011). UniProt Knowledgebase: a hub of integrated protein data. Database: (Oxford) *2011*, bar009.

Matos, R., Pinto, V.V., Ruivo, M., and Lopes, M.D.F.S. (2009). Study on the dissemination of the *bcrABDR* cluster in *Enterococcus* spp. reveals that the BcrAB transporter is sufficient to confer high-level bacitracin resistance. Int. J. Antimicrob. Agents *34*, 142–147.

Nishie, M., Sasaki, M., Nagao, J., Zendo, T., Nakayama, J., and Sonomoto, K. (2011). Lantibiotic transporter requires cooperative functioning of the peptidase domain and the ATP binding domain. J. Biol. Chem. *286*, 11163–11169.

Oldham, M.L., Khare, D., Quiocho, F.A., Davidson, A.L., and Chen, J. (2007). Crystal structure of a catalytic intermediate of the maltose transporter. Nature *450*, 515–521.

Oman, T.J. and van der Donk, W.A. (2009). Insights into the mode of action of the two-peptide lantibiotic haloduracin. ACS Chem. Biol. *4*, 865–874.

Ra, R., Beerthuyzen, M.M., de Vos, W.M., Saris, P.E., and Kuipers, O.P. (1999). Effects of gene disruptions in the nisin gene cluster of *Lactococcus lactis* on nisin production and producer immunity. Microbiology *145*, 1227–1233.

Rawlings, N.D., Barrett, A.J., and Bateman, A. (2012). MEROPS: the database of proteolytic enzymes, their substrates and inhibitors. Nucl. Acid Res. *40*, D343–D350.

Reisinger, P., Seidel, H., Tschesche, H., and Hammes, W.P. (1980). The effect of nisin on murein synthesis. Arch. Microbiol. *127*, 187–193.

Rogers, L. (1928). The inhibiting effect of *Streptococcus lactis* on *Lactobacillus bulgaricus*. J. Bacteriol. *16*, 321–325.

Sahl, H.-G. and Bierbaum, G. (1998). Lantibiotics: biosynthesis and biological activities of uniquely modified peptides from Gram-positive bacteria. Annu. Rev. Microbiol. *52*, 41–79.

Sayers, E.W., Barrett, T., Benson, D.A., Bolton, E., Bryant, S.H., Canese, K., Chetvernin, V., Church, D.M., DiCuccio, M., and Federhen, S. (2010). Database resources of the National Center for Biotechnology Information. Nucl. Acids Res. *38*, D5–D16.

Schmitt, L. and Tampé, R. (2002). Structure and mechanism of ABC transporters. Curr. Opin. Struct. Biol. *12*, 754–760.

Siegers, K. and Entian, K. (1995). Genes involved in immunity to the lantibiotic nisin produced by *Lactococcus lactis* 6F3. Appl. Environ. Microbiol. *61*, 1082–1089.

Silber, K.R., Keiler, K.C., and Sauer, R.T. (1992). Tsp: a tail-specific protease that selectively degrades proteins with nonpolar C termini. Proc. Natl. Acad. Sci. USA *89*, 295–299.

Söding, J. (2005). Protein homology detection by HMM-HMM comparison. Bioinformatics *21*, 951–960.

Stein, T., Heinzmann, S., Solovieva, I., and Entian, K.D. (2003). Function of *Lactococcus lactis* nisin immunity genes nisI and nisFEG after coordinated expression in the surrogate host *Bacillus subtilis*. J. Biol. Chem. *278*, 89–94.

Stein, T., Heinzmann, S., Düsterhus, S., Borchert, S., and Entian, K.-D. (2005). Expression and functional analysis of the subtilin immunity genes spaIFEG in the subtilin-sensitive host *Bacillus subtilis* MO1099. J. Bacteriol. *187*, 822–828.

Sun, Z., Zhong, J., Liang, X., Liu, J., Chen, X., and Huan, L. (2009). Novel mechanism for nisin resistance via proteolytic degradation of nisin by the nisin resistance protein NSR. Antimicrob. Agents Chemother. *53*, 1964–1973.

Van Der Does, C. and Tampe, R. (2004). How do ABC transporters drive transport? Biol. Chem. *385*, 927–933.

van der Heide, T. and Poolman, B. (2002). ABC transporters: one, two or four extracytoplasmic substrate-binding sites? EMBO Rep. *3*, 938–943.

van Heusden, H.E., de Kruijff, B., and Breukink, E. (2002). Lipid II induces a transmembrane orientation of the pore-forming peptide lantibiotic nisin. Biochemistry *41*, 12171–12178.

Wiedemann, I., Breukink, E., van Kraaij, C., Kuipers, O.P., Bierbaum, G., de Kruijff, B., and Sahl, H.-G. (2001). Specific binding of nisin to the peptidoglycan precursor lipid II combines pore formation and inhibition of cell wall biosynthesis for potent antibiotic activity. J. Biol. Chem. *276*, 1772–1779.

Willey, J.M. and van der Donk, W.A. (2007). Lantibiotics: peptides of diverse structure and function. Annu. Rev. Microbiol. *61*, 477–501.

Zaitseva, J., Oswald, C., Jumpertz, T., Jenewein, S., Wiedenmann, A., Holland, I.B., and Schmitt, L. (2006). A structural analysis of asymmetry required for catalytic activity of an ABC-ATPase domain dimer. EMBO J. *25*, 3432–3443.

Supplement Information:

NSR from *Streptococcus agalactiae* confers resistance against nisin and is encoded by a conserved *nsr* operon

Sakshi Khosa, Zainab AlKhatib and Sander H. J. Smits*

Institute of Biochemistry, Heinrich-Heine-University Duesseldorf, 40225 Duesseldorf, Germany

*Corresponding author

Institute of Biochemistry,

Heinrich-Heine-University Duesseldorf,

Universitaetstrasse 1,

40225 Duesseldorf.

Tel.: +49 211 81-12647

Fax: +49 211 81-15310

Email: Sander.Smits@hhu.de

SUPPLEMENT INFORMATION:

Cloning of plasmids:

The plasmid pNZ-SV-Nsr(N-His) was cloned with the In-Fusion HD PCR Cloning Kit (Clontech) according to the manufacturer's protocol. The vector pNZ-SV was linearized by PCR with the primer pair pNZ-SV-for and pNZ-SV-rev. The *nsr* gene was amplified by PCR applying pET28b-Nsr with the primers Inf_pET_Nsr_for and Inf_pET_Nsr_for, both primers with a 15bp homology to the vector for the In-Fusion reaction. Restriction analyses and partial sequencing confirmed the resulting plasmid, whose protein is referred to as *Sa*NSR.

The amino acid residue Ser-236 was replaced by Ala using site-directed mutagenesis and primer pair Nsr-S236A-for and Nsr-S236A-rev (product mentioned as *Sa*NSR-S236A).

Table 1: Sequences of the primers used for cloning.

Primer name	**Primer sequence**
pNZ-SV-for	GCTTTCTTTGAACCAAAATTAG
pNZ-SV-rev	GGTGAGTGCCTCCTTATAAT
Inf_pET_Nsr_for	AAGGAGGCACTCACCTACCATGGGCAGCAGCCATC
Inf_pET_Nsr_rev	TGGTTCAAAGAAAGCTCGACGGAGCTCGAATTCGGATC
Nsr-S236A-for	CTAATCATAAAACTGCTGCGTCGGCAGAAATGAC
Nsr-S236A-rev	GTCATTTCTGCCGACGCAGCAGTTTTATGATTAG

Table 2: Genome and Gene IDs of the various genomes and genes.

Microorganism Strains	Genome/Gene Accession No.
Corynebacterium casei UCMA 3821 (Putative nisin-resistance protein)	CAFW01000086 CAFW01000000/ CCAS_11245
Corynebacterium ammoniagenes DSM 20306 (Peptidase, S41 family)	ADNS01000015 ADNS01000000/ HMPREF0281_01689
Streptococcus agalactiae ATCC 13813 (Nisin-resistance protein)	AEQQ01000060 AEQQ01000000/ HMPREF9171_1170
Streptococcus agalactiae COH1 (Nisin-resistance protein, putative)	AAJR01000021 AAJR01000000/ SAN_1085
Streptococcus agalactiae STIR-CD-17 (Nisin resistance protein Nsr)	ALXB01000029 ALXB01000000/ M3M_06594
Streptococcus agalactiae 2603V/R (Nisin-resistance protein, putative)	AE009948 AE014191-AE014290/ SAG0973
Streptococcus canis FSL Z3-227 (Nisin resistance protein Nsr, putative)	AIDX01000001 AIDX01000000 AIDX01000002 AIDX01000003/ SCAZ3_06155
Streptococcus dysgalactiae subsp. *dysgalactiae* ATCC 27957 (Nisin resistance protein Nsr, putative)	AEGO01000002 AEGO01000000/ SDD27957_04970
Streptococcus dysgalactiae subsp. *equisimilis* AC-2713 (Nisin-resistance protein)	HE858529/ SDSE_1008
Streptococcus ictaluri 707-05 (Peptidase, S41 family)	AEUX02000006 AEUX02000000/ STRIC_1250
Streptococcus sanguinis SK1057 (Nisin resistance protein)	AFBA01000006 AFBA01000000/ HMPREF9394_0793

Enterococcus faecium E1039 (Nisin-resistance protein)	ACOS01000004 ACOS01000000/ EfmE1039_0093
Leuconostoc carnosum JB16 (NisR)	CP003851/ C270_03870
Leuconostoc mesenteroides subsp. *cremoris* ATCC 19254 (Nisin-resistance protein)	ACKV01000021 ACKV01000000/ HMPREF0555_0508
Staphylococcus epidermidis AU12-03 (NisR)	AMCS01000047 AMCS01000000/ B440_10980

* Gene IDs are from GenBank NCBI (Benson et al., 2013).

3.2 Chapter II – Nisin Resistance Protein

Published in: ACTA CRYSTALLOGRAPHICA SECTION F

Impact Factor: 0.527

Own work: 60%

Establishing and Optimization of Expression and Purification Protocols

Crystal Screening and Optimization

Diffraction Experiments and their Analyses

Writing the Manuscript

Overexpression, purification, crystallization and preliminary X-ray diffraction of the nisin resistance protein from *Streptococcus agalactiae*

Sakshi Khosa, Astrid Hoeppner, Diana Kleinschrodt, and Sander H.J. Smits

STRUCTURAL BIOLOGY COMMUNICATIONS

ISSN 2053-230X

Overexpression, purification, crystallization and preliminary X-ray diffraction of the nisin resistance protein from *Streptococcus agalactiae*

Sakshi Khosa,[a] Astrid Hoeppner,[b] Diana Kleinschrodt[c] and Sander H. J. Smits[a]*

[a]Institute of Biochemistry, Heinrich-Heine-University, 40225 Düsseldorf, Germany, [b]Crystal Farm and X-ray Facility, Heinrich-Heine-University, 40225 Düsseldorf, Germany, and [c]Protein Production Facility, Heinrich-Heine-University, 40225 Düsseldorf, Germany. *Correspondence e-mail: sander.smits@hhu.de

Received 9 February 2015
Accepted 26 March 2015

Edited by R. L. Stanfield, The Scripps Research Institute, USA

Keywords: lantibiotic; nisin; resistance; immunity; lipoprotein; *Lactococcus lactis*.

Supporting information: this article has supporting information at journals.iucr.org/f

Nisin is a 34-amino-acid antimicrobial peptide produced by *Lactococcus lactis* belonging to the class of lantibiotics. Nisin displays a high bactericidal activity against various Gram-positive bacteria, including some human-pathogenic strains. However, there are some nisin-non-producing strains that are naturally resistant owing to the presence of the *nsr* gene within their genome. The encoded protein, NSR, cleaves off the last six amino acids of nisin, thereby reducing its bactericidal efficacy. An expression and purification protocol has been established for the NSR protein from *Streptococcus agalactiae* COH1. The protein was successfully crystallized using the vapour-diffusion method in hanging and sitting drops, resulting in crystals that diffracted X-rays to 2.8 and 2.2 Å, respectively.

1. Introduction

The widespread use of antibiotics has led to the emergence of resistant pathogenic bacteria. Thus, there is an urgent need to develop new alternatives in order to fight infectious diseases. Promising candidates are antimicrobial peptides such as lantibiotics produced by some Gram-positive bacteria. Lantibiotics are ribosomally synthesized peptides that are characterized by the extensive modifications that they undergo and normally consist of dehydrated amino acids and (methyl)-lanthionine rings (Chatterjee *et al.*, 2005; Lubelski *et al.*, 2008). Lantibiotics target lipid II, an essential cell-membrane precursor, and form pores within the membrane, causing cell leakage and subsequently cell death (Breukink & de Kruijff, 2006). More than 50 lantibiotics have been discovered to date (Donaghy, 2010) and many of them have already entered the preclinical phase.

Nisin is the most studied and widely used lantibiotic. It is produced by *Lactococcus lactis* and has the characteristic one lanthionine and four methyl-lanthionine rings. Interestingly, nisin has been shown to be insensitive to proteolytic digestion owing to the presence of the five lanthionine rings. Nisin has a wide bactericidal activity spectrum against many Gram-positive bacteria, including *L. lactis* subsp. *lactis* and subsp. *cremoris*, *L. bulgaricus*, *Staphylococcus aureus*, *Clostridium difficile*, *Streptococcus pneumoniae*, MRSA, enterococci and *Listeria monocytogenes*. Nisin also prevents the outgrowth of many *Clostridium* and *Bacillus* species (Harris *et al.*, 1992). The germicidal efficiency of nisin is owing to its capability to inhibit cell-wall biosynthesis and pore-forming ability, where it uses the cell-wall precursor lipid II as a docking molecule (Willey & van der Donk, 2007). Nisin has been found to be

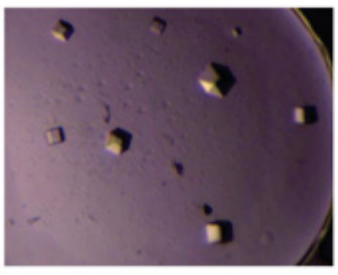

Table 1
Macromolecule-production information.

Source organism	*S. agalactiae*
DNA source	Genomic DNA
Forward primer	TTAAATATTTATCTATTACCTCCTAGTAGCGAAC-GTTATGG
Reverse primer	ATGGCTGCCGCGCGGCACCAG
Cloning vector	pET-28b
Expression vector	pET-28b
Expression host	*E. coli* BL21 (DE3)
Complete amino-acid sequence of the construct produced	MGSSHHHHHHHHSSGLVPRGSHLNIYLLPPSSER-YGRVILDRVEQRGLYSQGRQWQIIRQRSEKKL-KTSKSYQESRNIVQEAVRYGGGKHSQILSKET-VRRDTLDSRYPEYRRLNEDILLITIPSISKLD-KRSISHYSGKLQNILMEKSYKGLILDLSNNTG-GNMIPMIGGLASILPNDTLFHYTDKYGNKKTI-TMKNIPLEALKISRKTINTKHVPIAIITNHKT-ASSAEMTFLSFKGLPNVKSFGQATAGYTTVNE-TFMLYDGARLALTTGIVSDRQGYKYENTPILP-DQVTSLPLQESQSWLKSRINQN

effective against *S. pneumoniae*, *Mycobacterium tuberculosis* and other multi-resistant Gram-positive pathogenic bacteria (Carroll *et al.*, 2010; Cotter *et al.*, 2005). Nisin also has potential for the treatment of various enterococcal infections, atopic dermatitis, peptic ulcers and bacterial mastitis (Cotter *et al.*, 2005; de Arauz *et al.*, 2009). However, there are some non-nisin-producing strains, including various pathogenic bacteria such as *Streptococcus agalactiae* and *S. aureus*, which are resistant against nisin (Harris *et al.*, 1992). This resistance is owing to the presence of the *nsr* gene, which encodes the nisin resistance protein (referred to as NSR). It has been shown that NSR cleaves off the last six amino acids of nisin, thereby degrading nisin proteolytically. The cleaved nisin was found to have reduced affinity for the cell membrane and showed 100-fold less antibacterial efficiency (Sun *et al.*, 2009). NSR is strongly hydrophobic at the N-terminus and was thus postulated to be membrane-associated (Froseth & McKay, 1991). Interestingly, there is a whole operon associated with the mechanism of nisin resistance, consisting of the *nsr* gene, a two-component regulatory system and an ABC transporter. This operon can be found in various species of Gram-positive human-pathogenic bacteria (Khosa *et al.*, 2013).

Thus, the structure of NSR would lead to a deeper understanding of the overall mechanism of nisin resistance.

Here, we present the overexpression, purification and crystallization of the nisin resistance protein.

2. Materials and methods

2.1. Macromolecule production

2.1.1. Cloning and expression. The *nsr* gene from *S. agalactiae* COH1 was amplified using the genomic DNA into pET-28b in a similar manner as described previously (Khosa *et al.*, 2013). Since the encoded protein has an N-terminal transmembrane region, the first 30 amino acids were removed (referred to as NSR30) and an 8×His tag was introduced at the N-terminus. The resulting plasmid (Table 1) was verified by sequencing and transformed into *Escherichia coli* BL21 (DE3) for expression. A single transformed colony was inoculated into 20 ml LB medium containing 30 µg ml^{-1} kanamycin. The culture was grown for 14 h at 310 K with shaking at 200 rev min^{-1}. 2 l LB medium with 30 µg ml^{-1} kanamycin was inoculated with the overnight culture at an OD_{600} of 0.05 and grown at 310 K with shaking at 170 rev min^{-1} until an OD_{600} of 0.3 was reached. The temperature was lowered to 291 K and the cells were further grown to an OD_{600} of 0.8 before induction with 1 m*M* IPTG. The cells were grown for a further 15 h.

The cells were harvested by centrifugation at 8000 rev min^{-1} for 20 min at 277 K. The harvested cell pellet was stored at 253 K until further use.

2.1.2. Purification. All steps were performed at 277 K. The stored cell pellet was thawed and resuspended in 10 ml buffer *A* (50 m*M* Tris pH 8.0, 50 m*M* NaCl, 10% glycerol), and 10 mg DNase (deoxyribonuclease I from bovine pancreas, Sigma–Aldrich) was added. The cells were lysed five times using a cell disruptor (Constant Cell Disruption Systems, United Kingdom) at 260 MPa. The lysate was centrifuged at 42 000 rev min^{-1} for 60 min using a Ti60 rotor to remove unlysed cells and debris.

Histidine was added to the cleared lysate to a final concentration of 1 m*M*. The lysate was then applied onto an Ni^{2+}-loaded HiTrap HP Chelating column (GE Healthcare) pre-equilibrated with buffer *B* (20 m*M* Tris pH 8.0, 250 m*M* NaCl, 1 m*M* histidine) at a flow rate of 1 ml min^{-1}. The column was washed with six column volumes of buffer *B*. The protein was then eluted with increasing concentrations of histidine from 1 to 120 m*M* in the form of a linear gradient spanning 60 min at a flow rate of 2 ml min^{-1}. The fractions containing the protein of interest were pooled and concentrated to 12 mg ml^{-1} in an Amicon centrifugal filter concentrator with a 10 kDa cutoff membrane (Millipore). The concentrated protein was then further purified by size-exclusion chromatography using a Superose 12 GL 10/300 column (GE Healthcare) equilibrated with buffer *C* (25 m*M* MES pH 6.0, 150 m*M* NaCl). The protein eluted as a single homogeneous peak and the concerned fractions were pooled and concentrated to 8.6 mg ml^{-1} as described above. The purity of the protein was analyzed with SDS–PAGE and colloidal Coomassie stain (Dyballa & Metzger, 2009). The purified protein was directly used for crystallization.

2.2. Crystallization

Crystallization screening was performed at 285 K using an NT8 robot (Formulatrix) and the sitting-drop vapour-diffusion method in Corning 3553 sitting-drop plates. For initial screening, various commercial crystallization screens were used (The JCSG Core Suite I, Classics Suite, PEGs Suite and MPD Suite from Qiagen, Germany and MIDAS from Molecular Dimensions, England). Nanodrops consisting of 0.1 µl each of protein and reservoir solution were mixed and equilibrated against 50 µl reservoir solution. The screening yielded some initial rod-shaped crystals after 3 d in the condition 0.5 *M* lithium sulfate, 15%(*w*/*v*) PEG 8000 (The Classics I Suite condition F5). The initial crystals were optimized by

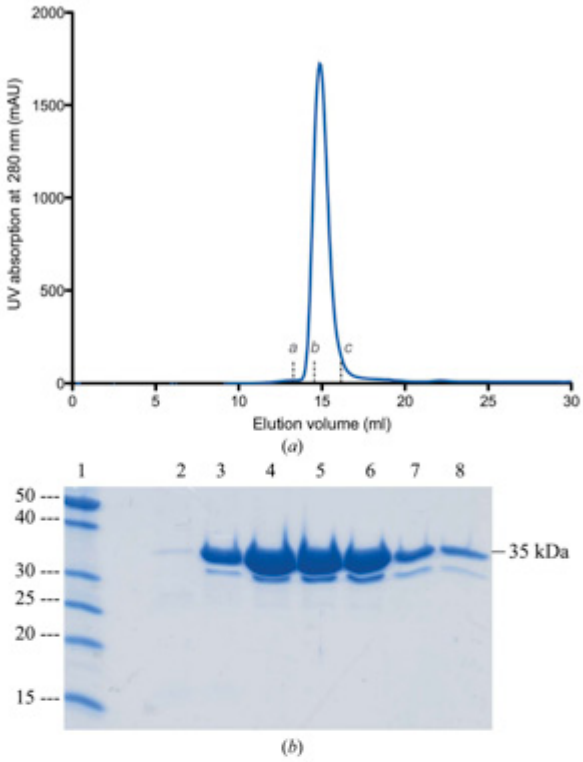

Figure 1
Purification of NSR30. (*a*) Chromatogram representing the purification of NSR30 by size-exclusion chromatography. (*b*) 15% SDS–PAGE showing the purified NSR30 fractions. Lane 1 contains PageRuler Unstained Protein Ladder (labelled in kDa) and lanes 2–8 contain the purified NSR30 fractions at 35 kDa. The lower 30 kDa band also arises from NSR30, as verified by mass spectrometry, and is likely to be a degradation product. *a*, *b* and *c* refer to the protein standards BSA (molecular weight 67 kDa), *β*-lactoalbumin (35 kDa) and cytochrome *c* (12.7 kDa), respectively.

Table 2
Crystallization.

Method	Vapour diffusion
Plate type	Hanging/sitting drop
Temperature (K)	297/285
Protein concentration (mg ml^{-1})	9
Buffer composition of protein solution	25 m*M* MES pH 6.0, 150 m*M* NaCl
Composition of reservoir solution	0.5 *M* lithium sulfate, 15%(*w*/*v*) PEG 8000
Ratio of drop	1:1
Volume of reservoir (µl)	500

varying the concentration of PEG [5, 10, 15, 20, 25 and 30%(*w*/*v*)] and lithium sulfate (0.4, 0.5, 0.6 and 0.7 *M*) using hanging and sitting-drop vapour-diffusion methods at 297 and 285 K, respectively. Each drop consisted of 1 µl protein solution (concentration of 9 mg ml^{-1}) mixed with 1 µl reservoir solution and was equilibrated against a reservoir volume of 500 µl. Crystals were obtained after 1 d and grew to their maximum dimensions within 5 d. Crystallization information is summarized in Table 2.

2.3. Data collection and processing

Drops containing the optimized crystals were overlaid with 2 µl mineral oil before the crystals were harvested and flash-cooled in liquid nitrogen. X-ray diffraction data were collected on the ID23-EH2 beamline at the European Synchrotron Radiation Facility (ESRF; Flot *et al.*, 2010), Grenoble using a Pilatus detector. After the initial diffraction tests, a data-collection strategy was calculated using the *EDNA* software available at the beamline (Incardona *et al.*, 2009) and the data subsequently collected were processed and scaled using *XDS* and *XSCALE* (Kabsch, 2010).

3. Results and discussion

NSR30 was successfully cloned and overexpressed in a soluble form in *E. coli* BL21 (DE3) cells. The protein was purified *via*

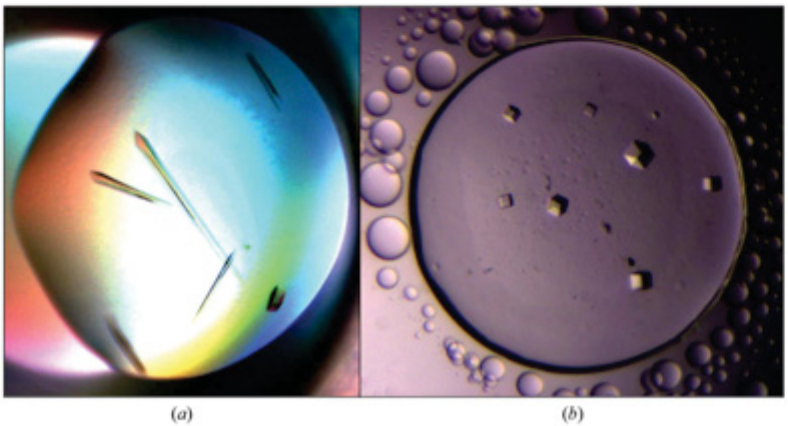

Figure 2
Crystals of NSR30. (*a*) Rod-shaped crystals obtained by the sitting-drop vapour-diffusion method at 285 K. (*b*) Cubic crystals obtained by the hanging-drop vapour-diffusion method at 297 K.

a two-step purification protocol. Nickel-affinity chromatography was performed first, followed by size-exclusion chromatography (Fig. 1*a*). NSR30 eluted from the size-exclusion chromatogram at 14.8 ml, which corresponds to a molecular mass of 30–40 kDa, indicating that NSR30 is a monomer in solution. The yield of the protein was around 5 mg per litre of cell culture. Protein homogeneity and purity was assessed by SDS–PAGE (Fig. 1*b*). The molecular mass of the purified protein was comparable to the theoretically calculated molecular weight of 35.3 kDa (Gasteiger *et al.*, 2005).

Initial crystals of NSR30 appeared after 3 d in The Classics Screen I condition F5 [0.5 *M* lithium sulfate, 15%(*w*/*v*) PEG 8000] with a sitting-drop setup. Optimizations were performed by varying the concentrations of lithium sulfate and PEG. Hanging-drop and sitting-drop vapour-diffusion methods were also tried. Crystals were obtained with 5–30%(*w*/*v*) PEG 8000 and 0.4–0.7 *M* lithium sulfate after 1 d (Fig. 2). Sitting-drop vapour diffusion at 285 K yielded rod-shaped crystals (Fig. 2*a*) with maximum dimensions of 560 × 45 × 30 µm, whereas cubic-shaped crystals with dimensions of 125 × 125 × 40 µm were obtained using the hanging-drop vapour-diffusion method at 297 K (Fig. 2*b*). The crystals obtained were dissolved and analysed by mass spectrometry, revealing the presence of the NSR30 protein (Supporting Information).

The initial rod-shaped crystals diffracted to 2.2 Å resolution using synchrotron X-rays (Fig. 3*a*). The crystals belonged to space group $P2_12_12_1$, with unit-cell parameters a = 58.8, b = 137.2, c = 164.0 Å, $\alpha = \beta = \gamma = 90^\circ$ (Table 3). Matthews coefficient calculations resulted in a V_M of 2.34 Å^3 Da^{-1} and a solvent content of 47.34%, corresponding to four molecules in the asymmetric unit (Matthews, 1968; Kantardjieff & Rupp, 2003). However, the cubic crystals diffracted to 2.8 Å resolution using synchrotron X-rays (Fig. 3*b*). The crystals belonged to space group *P*432, with unit-cell parameters $a = b = c$ = 186.4 Å, $\alpha = \beta = \gamma = 90^\circ$ (Table 3). Interestingly,

Table 3
Data collection and processing.

Values in parentheses are for the outer shell.

	Rod-shaped crystal	Cubic crystal
Diffraction source	ID23-EH2, ESRF	ID23-EH2, ESRF
Wavelength (Å)	0.87260	0.87260
Temperature (K)	100	100
Detector	Pilatus3 2M	Pilatus3 2M
Crystal-to-detector distance (mm)	273.31	359.15
Rotation range per image (°)	0.05	0.05
Total rotation range (°)	120	40
Exposure time per image (s)	0.02	0.04
Space group	$P2_12_12_1$	*P*432
a, b, c (Å)	58.8, 137.2, 164.0	186.4, 186.4, 186.4
α, β, γ (°)	90, 90, 90	90, 90, 90
Mosaicity (°)	0.05	0.05
Resolution range (Å)	100.0–2.21 (2.29–2.21)	100.0–2.87 (2.97–2.87)
Total No. of reflections	303210 (28341)	208348 (19523)
No. of unique reflections	67177 (6695)	25913 (2471)
Completeness (%)	99.6 (99.3)	99.8 (100.0)
Multiplicity	4.5 (4.2)	8.03 (7.9)
$\langle I/\sigma(I)\rangle$	8.67 (1.79)	9.69 (1.71)
$R_{p.i.m.}$ (%)	6.0 (33.5)	7.4 (41.1)
Overall *B* factor from Wilson plot (Å^2)	28.4	33.4

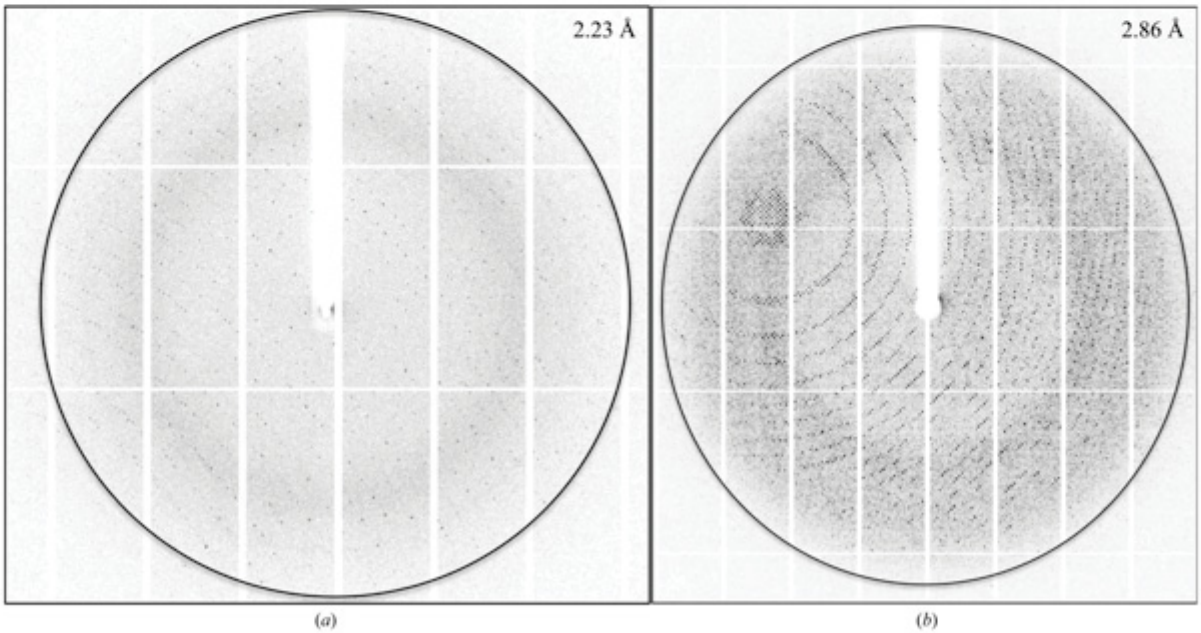

Figure 3
X-ray diffraction pattern of NSR30. Diffraction images of rod-shaped (*a*) and cubic (*b*) NSR30 crystals with an oscillation width of 1.0°. The images were used to calculate a data-collection strategy using *EDNA* (Incardona *et al.*, 2009).

Matthews coefficient calculations resulted in a V_M of 3.81 or 2.54 Å^3 Da^{-1} and a solvent content of 68 or 52%, corresponding to two or three molecules in the asymmetric unit (Matthews, 1968; Kantardjieff & Rupp, 2003). The exact number of molecules in the asymmetric unit will be determined when the structure has been solved. The self-rotation function revealed a noncrystallographic twofold axis for the *P*432 crystal form and a noncrystallographic fourfold axis for the crystal form displaying $P2_12_12_1$ symmetry. Furthermore, no large peaks were seen in the native Patterson function for either of the crystal forms. Since there are no template structures which can be used for molecular replacement in the PDB that display a sequence identity of higher than 22%, the structure will be solved by using experimental phase determination, *i.e.* selenomethionine incorporation or heavy-atom derivatization, which is currently in progress.

The nisin resistance protein could be a model for other lantibiotic resistance proteins observed in the genome of a wide variety of human pathogens. Initial experiments show that NSR cleaves the nisin peptide *in vitro* as observed *in vivo*, where it has been shown that NSR confers a 20-fold resistance towards nisin (Khosa *et al.*, 2013). The structure of the nisin resistance protein would thus lead to a deeper understanding of its function and also pave the way for the development of new therapeutic agents with the potential of substituting for antibiotics.

Acknowledgements

The authors are indebted to Lutz Schmitt for his kind support, advice and invaluable suggestions. This work was initiated by Philipp Ellinger. We also thank André Abts for fruitful scientific discussions and advice. We are grateful to the staff of ESRF ID23-2, especially Christoph Mueller-Dieckmann, for assistance and support during crystal screening and data collection. We are thankful to Heinrich Heine International Graduate School of Protein Science and Technology (iGRASPseed) for providing a scholarship to SK.

References

Arauz, L. J. de, Jozala, A. F., Mazzola, P. G. & Vessoni Penna, T. C. (2009). *Trends Food Sci. Technol.* **20**, 146–154.
Breukink, E. & de Kruijff, B. (2006). *Nature Rev. Drug Discov.* **5**, 321–323.
Carroll, J., Draper, L. A., O'Connor, P. M., Coffey, A., Hill, C., Ross, R. P., Cotter, P. D. & O'Mahony, J. (2010). *Int. J. Antimicrob. Agents*, **36**, 132–136.
Chatterjee, C., Paul, M., Xie, L. & van der Donk, W. A. (2005). *Chem. Rev.* **105**, 633–684.
Cotter, P. D., Hill, C. & Ross, R. P. (2005). *Curr. Protein Pept. Sci.* **6**, 61–75.
Donaghy, J. (2010). *Bioeng. Bugs*, **1**, 437–439.
Dyballa, N. & Metzger, S. (2009). *J. Vis. Exp.*, **2009**, 1431.
Flot, D., Mairs, T., Giraud, T., Guijarro, M., Lesourd, M., Rey, V., van Brussel, D., Morawe, C., Borel, C., Hignette, O., Chavanne, J., Nurizzo, D., McSweeney, S. & Mitchell, E. (2010). *J. Synchrotron Rad.* **17**, 107–118.
Froseth, B. R. & McKay, L. L. (1991). *Appl. Environ. Microbiol.* **57**, 804–811.
Gasteiger, E., Hoogland, C., Gattiker, A., Wilkins, M. R., Appel, R. D. & Bairoch, A. (2005). *The Proteomics Protocols Handbook*, edited by J. M. Walker, pp. 571–607. Totowa: Humana Press.
Harris, L. J., Fleming, H. P. & Klaenhammer, T. R. (1992). *Food. Res. Int.* **25**, 57–66.
Incardona, M.-F., Bourenkov, G. P., Levik, K., Pieritz, R. A., Popov, A. N. & Svensson, O. (2009). *J. Synchrotron Rad.* **16**, 872–879.
Kabsch, W. (2010). *Acta Cryst.* D**66**, 125–132.
Kantardjieff, K. A. & Rupp, B. (2003). *Protein Sci.* **12**, 1865–1871.
Khosa, S., AlKhatib, Z. & Smits, S. H. (2013). *Biol. Chem.* **394**, 1543–1549.
Lubelski, J., Rink, R., Khusainov, R., Moll, G. & Kuipers, O. (2008). *Cell. Mol. Life Sci.* **65**, 455–476.
Matthews, B. W. (1968). *J. Mol. Biol.* **33**, 491–497.
Sun, Z., Zhong, J., Liang, X., Liu, J., Chen, X. & Huan, L. (2009). *Antimicrob. Agents Chemother.* **53**, 1964–1973.
Willey, J. M. & van der Donk, W. A. (2007). *Annu. Rev. Microbiol.* **61**, 477–501.

STRUCTURAL BIOLOGY COMMUNICATIONS

Volume 71 (2015)

Supporting information for article:

Overexpression, purification, crystallization and preliminary X-ray diffraction of the nisin-resistance protein from *Streptococcus agalactiae*

Sakshi Khosa, Astrid Hoeppner, Diana Kleinschrodt and Sander Smits

Mass Spectrometry Analysis

Lanes 1 and 2: NSR30 protein crystals.

	30kDa Semitryptic	30kDa Tryptic	35kDa Semitryptic	35kDa Tryptic
Accession	P0000X	P0000X	P0000X	P0000X
Description	NSR30 OS=S agalactiae GN=NSR30 PE=1 SV=1 - [NSR30_S_AGALACTIAE]	NSR30 OS=S agalactiae GN=NSR30 PE=1 SV=1 - [NSR30_S_AGALACTIAE]	NSR30 OS=S agalactiae GN=NSR30 PE=1 SV=1 - [NSR30_S_AGALACTIAE]	NSR30 OS=S agalactiae GN=NSR30 PE=1 SV=1 - [NSR30_S_AGALACTIAE]
Score	2985.39	2619.54	3427.80	3160.60
Coverage	49.68	49.36	59.29	46.15
#Proteins	1	1	1	1
#Unique Peptides	22	11	36	13
#Peptides	22	11	36	13
#PSMs	75	58	94	78
#AAs	312	312	312	312
MW (kDa)	35.4	35.4	35.4	35.4
Calc. pI	9.91	9.91	9.91	9.91

Sequence Coverage 30kDa band with Semitrypsin:

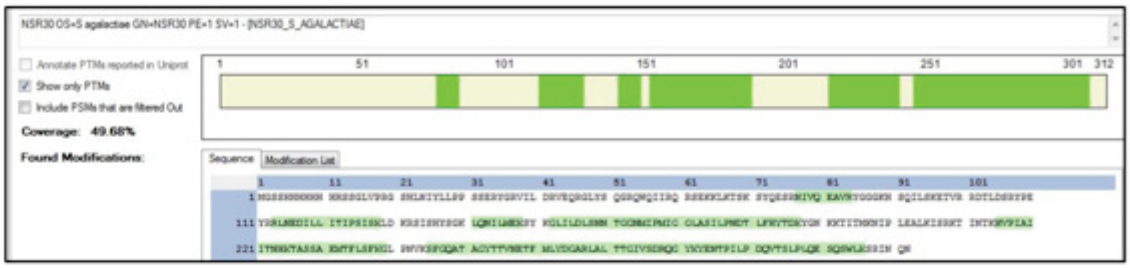

Sequence Coverage 30kDa band with Trypsin:

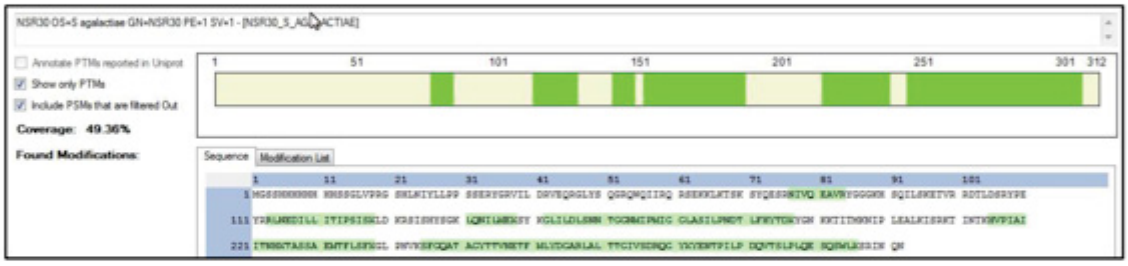

Sequence Coverage 35kDa band with Semitrypsin:

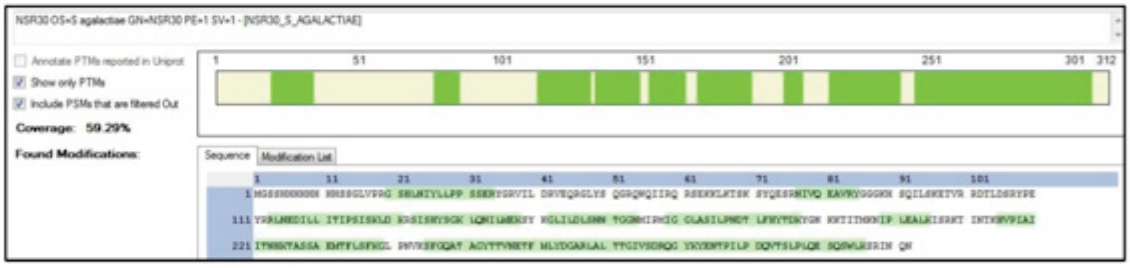

Sequence Coverage 35kDa band with Trypsin:

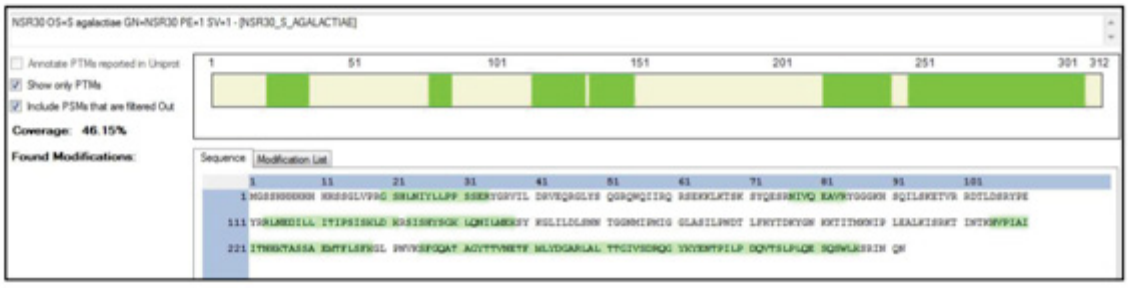

3.3 Chapter III – The Structure of the Nisin Resistance Protein

Published in: NATURE SCIENTIFIC REPORTS

Impact Factor: 5.578

Own work: 30%

Purification and Crystallization

Establishing and Optimization Strategies for Experimental Phases

Structural Determination and Refinement

Establishing Functional Assay of *Sa*NSR

Measuring Functional Data of Wildtype and Variants of *Sa*NSR

Performing MALS-SEC

Writing the manuscript

Structural basis of lantibiotic recognition by the nisin resistance protein from *Streptococcus agalactiae*

Sakshi Khosa[#], Benedikt Frieg[#], Daniel Mulnaes, Diana Kleinschrodt, Astrid Hoeppner, Holger Gohlke, and Sander H.J. Smits

[#]Both authors contributed equally

Accepted on 23.11.2015

Structural basis of lantibiotic recognition by the nisin resistance protein from *Streptococcus agalactiae*

Sakshi Khosa[a#], Benedikt Frieg[b#], Daniel Mulnaes[b] Diana Kleinschrodt[c], Astrid Hoeppner[d], Holger Gohlke[b] and Sander H.J. Smits[a]*

[a]Institute of Biochemistry, Heinrich Heine University, Universitätsstr. 1, 40225 Düsseldorf, Germany

[b]Institute of Pharmaceutical and Medicinal Chemistry, Heinrich Heine University, Universitätsstr. 1, 40225 Düsseldorf, Germany

[c]Protein Production Facility, Heinrich Heine University, Universitätsstr. 1, 40225 Düsseldorf, Germany

[d]Crystal and X-ray Facility, Heinrich Heine University, Universitätsstr. 1, 40225 Düsseldorf, Germany

[#]Both authors contributed equally.

*Corresponding author

Phone: +49-211-81-12647

Fax: +49-211-81-15310

E-Mail: sander.smits@hhu.de

Running title: Lantibiotic recognition by the nisin resistance protein

Keywords: Nisin, lantibiotic, resistance, antimicrobial peptide

ABSTRACT

Lantibiotics are potent antimicrobial peptides. Nisin is the most prominent member and contains five crucial lanthionine rings. Some clinically relevant bacteria express membrane-associated resistance proteins that proteolytically inactivate nisin. However, substrate recognition and specificity of these proteins is unknown. Here, we report the first three-dimensional structure of a nisin resistance protein from *Streptococcus agalactiae* (*Sa*NSR) at 2.2 Å resolution. It contains an N-terminal helical bundle, and protease cap and core domains. The latter harbors the highly conserved TASSAEM region, which lies in a hydrophobic tunnel formed by all domains. By integrative modeling, mutagenesis studies, and genetic engineering of nisin variants, a model of the *Sa*NSR/nisin complex is generated, revealing that *Sa*NSR recognizes the last C-terminally located lanthionine ring of nisin. This determines the substrate specificity of *Sa*NSR and ensures the exact coordination of the nisin cleavage site at the TASSAEM region.

INTRODUCTION

Antibiotics provide a great advantage in the treatment of infections caused by bacteria such as *Streptococcus pneumoniae* and *Streptococcus agalactiae*. However, due to their widespread use, the number of resistant bacterial strains is increasing [1], leading to an urgent need for the development of new antibiotics. Several approaches have been taken to identify new antibiotics where naturally occurring compounds are found to be the most promising ones [2]. Here, small antimicrobial peptides such as lantibiotics are excellent candidates because they exhibit high effectivity against various Gram-positive human pathogenic bacteria including *Streptococcus pneumoniae* and several methicillin-resistant *Staphylococcus aureus* (MRSA) strains [3].

Lantibiotics display antimicrobial activities in the very low nanomolar range [4,5]. The anti-infective potency of lantibiotics such as nisin, mutacin, mersacidin and others has been recognized, and several are in the preclinical stages of medical application [6,7]. After translation, lantibiotics are modified and contain unusual amino acids such as dehydroalanine (Dha) and dehydrobutyrine (Dhb), which are covalently linked to the side chain of cysteine residues forming the so-called lanthionine rings [8,9]. The number as well as the exact location of the lanthionine rings vary within lantibiotics [10]. Lantibiotics have multiple modes of action, of which binding to lipid II, thereby inhibiting cell wall synthesis, and pore formation are the most predominant ones [8,11]. Nisin produced by *Lactococcus lactis* (*L. lactis*) is one of more than 50 lantibiotics discovered so far [12] and is considered to be the role model. Active nisin consists of 34 amino acids and contains five lanthionine-based rings (Supplementary Fig. 1). The first three rings (A-C) are separated from the other two intertwined rings (D-E) by a flexible hinge region. The first two rings are able to bind lipid II [13], the hinge region and the last two intertwined rings are able to flip into the membrane and create a pore [14-16].

Due to their multiple modes of action, hardly any resistance against lantibiotics has developed over the past decades. However, some bacterial strains have been reported to be congenitally resistant against nisin [17] via various mechanisms such as cell wall modifications, biofilm formation or the expression of resistance proteins [18]. For the latter case, a *nsr* gene was identified in the *Streptococcus lactis* subspecies *diacetylactis* (DRC3) that encodes the nisin resistance protein, NSR [17,19]. Similar genes were identified in other species [17,20,21], including several human pathogenic strains [22,23]. NSR is a member of the S41 protease family, specifically the C-terminal processing peptidases (CTPs). NSR from *L. lactis* TS1640 has been shown to degrade nisin by cleaving the peptide bond between $MeLan_{28}$ in ring E and Ser_{29}. The resulting $nisin_{1-28}$ fragment displays a significantly lower bactericidal efficacy and reduced affinity towards cellular membranes [24].

Furthermore, the NSR protein from *S. agalactiae* ATCC 13813 induced a 20-fold increased resistance towards nisin when expressed in *L. lactis* [22].

NSR is localized within an operon comprising five genes, which encode for NSR, a two-component signaling system (NsrRK), and an ABC transporter (NsrFP). When expressed together, these proteins deliver full nisin resistance [22]. Interestingly, similar operon structures were also found to be associated with resistance against other lantibiotics [18,23]. These operons resemble (auto)-immunity systems found in lantibiotic producer [10] strains. Structures of SpaI from *B. subtilis* [25] conferring resistance against subtilin and MlbQ from the actinomycete *Microbispora* ATCC PTA-5024 conferring resistance against NAI-107 [26] were resolved by NMR. However, no significant sequence identity is found between NSR and SpaI or MlbQ, suggesting a different mechanism for the defense against lantibiotics. Furthermore, most (auto)-immunity proteins do not cleave or manipulate the lantibiotic but rather shield the host's membrane from being harmed by its lantibiotic [10,27].

The ability of NSR to cleave nisin is impressive because it has been shown for several lantibiotics that they are not easily accessible for protease cleavage [14]. Here, the lanthionine rings are likely causing steric hindrance within the active site of proteases, thereby inhibiting proteolysis. Thus, notwithstanding the recent advances in this field, we still structurally know relatively little about lantibiotic resistance. In particular, the lantibiotic binding site in NSR and the mechanism how substrate specificity is conferred remains elusive. In this study, we report the first structure of a nisin resistance protein, NSR from *S. agalactiae* COH1 (*Sa*NSR). Mutagenesis studies guided by molecular dynamics (MD) simulations reveal that *Sa*NSR recognizes the lanthionine ring closest to the C- terminus of nisin and that this ring binds at one end of the catalytic tunnel, thereby determining the substrate specificity and ensuring the exact coordination of the nisin cleavage site at the catalytic site region.

RESULTS

Crystal structure of *Sa*NSR

Nisin has been shown to be quite resistant against proteolytic digestion in general [14], supposedly due to the presence of lanthionine rings. Therefore, it is intriguing to understand the proteolytic resistance mechanism mediated by NSRs. To obtain a molecular view on this mechanism, we solved the structure of *Sa*NSR by X-ray crystallography.

Through sequence analyses, it was predicted that the first 30 amino acids encode for a transmembrane helix [28]. We deleted this N-terminal transmembrane helix and included a His_8-tag for purification purposes, resulting in soluble expression of *Sa*NSR. After over-expression, two-step purification yielded 5 mg of pure *Sa*NSR protein per liter of cell culture (Supplementary Fig. 2a). *Sa*NSR is a monomer in solution as determined by multiple angle light scattering (MALS) (Supplementary Fig. 2b). *Sa*NSR protein was crystallized and cubic crystals were obtained that diffracted up to 2.2 Å resolution [29]. We solved the structure by Single Anomalous Dispersion (SAD) phasing, using crystals of selenomethionine-substituted protein (data and refinement statistics are shown in Table 1).

The asymmetric unit (Supplementary Fig. 2c) contained four copies of *Sa*NSR that were virtually identical (root mean square deviation (RMSD) between the monomers = 0.15-0.5 Å over 300 amino acids). Therefore, the overall structure is described only for monomer A. The entire sequence of *Sa*NSR could be fitted into the electron density, with the exception of the N-terminal His_8-tag that was disordered. The R_{work} and R_{free} values after refinement were 0.19 and 0.24, respectively.

A *Sa*NSR monomer (Fig. 1) consists of eleven helices (α_1-α_{11}) and eleven β-strands (β_a-β_k), which form three domains: an N-terminal helical bundle and two protease subdomains. Altogether, these domains form a hydrophobic tunnel of ~10 Å width (Fig. 1b), which could very well harbor the nisin molecule. The N-terminal helical bundle (Fig. 1b, represented in green) comprises 65 amino acid residues (Lys_{31}-Gly_{96}), which form helices α_1-α_3. This domain ends in a triple glycine motif ($_{94}GGG_{96}$) before entering the protease cap domain (Fig. 1b, represented in red). The protease cap domain consists of helix α_4 and a β-hairpin structure formed by strands $\beta_{i\text{-}j}$. The protease cap forms a lid-like structure above the tunnel. The third domain is the so-called protease core domain (Fig. 1b, represented in grey), which adopts a 'protease fold' domain as observed in other S41 peptidases [30-32]. The protease core domain is formed by six strands β_b-β_g and five helices α_5-α_9. It contains the highly conserved TASSAEM region that harbors the previously identified catalytically active serine at position 236 [22] (Fig. 1, represented in blue; Supplementary Fig. 3). The TASSAEM region lies in the tunnel between the two protease subdomains (Fig. 2a).

N-terminal helical bundle

A comparison of the N-terminal helical bundle with all available entries in the Protein Data Bank was performed using the Dali server [33]. The Dali server identifies similarities in 3D structures irrespective of sequence similarities. A structurally similar helical bundle has been identified in the human Factor H (Z-score of 5.2), which is responsible for tight binding of the pneumococcal protein virulence factor CbpA (choline-binding protein A) [34]. Furthermore, a similar helical bundle is present at the C-terminus of the 70 kDa human heat shock protein (HSP70) (Z-score of 5.0). This region is responsible for causing a structural switch of HSP70 allosteric activation, which is important for maintaining a proper conformation of the protein for binding to the J-domain and ATPase activity purposes [35]. Finally, a dynamic helical region is present at the N-termini of staphylococcal complement inhibitors (SCINs) (Z-score of 4.7), which is responsible for binding to the substrate C3b and is also necessary for the formation of higher order complexes of C3b, which blocks phagocytosis [36]. While these findings suggest that a certain degree of mobility of the found helical bundles is required for function, in three replicates of molecular dynamics (MD) simulations of a monomer of *Sa*NSR (termed NSR_{Apo}; see online methods for details), each of 500 ns length, the N-terminal helical bundle is rather immobile with respect to the protease core and cap domain (backbone root mean square fluctuations (RMSF) < 2.5 Å; Supplementary Fig. 4a).

N-pep bound to *Sa*NSR

In the crystal structure, the hydrophobic tunnel is filled with the N-terminal residues $_{31}$KNIYLLPP$_{38}$ of a neighboring *Sa*NSR molecule (termed N-pep; Fig. 2b; shown in light green in Fig. 1). N-pep is predominantly bound to *Sa*NSR via direct backbone interactions to amino acids $_{167}$NNTGGN$_{172}$ of β-strand β_d, which is part of the protease core domain and is structurally located on the opposite site of the TASSAEM sequence motif (Fig. 2c). In addition, N-pep is stabilized via water-mediated hydrogen bonds between backbone atoms of Asn_{32}, Tyr_{34}, Leu_{35} and residues Asn_{265} and Thr_{267} of the protease cap domain (Fig. 2c). The presence of N-pep within the tunnel is clearly an induced artifact of the crystallization procedure, since in the full-length *Sa*NSR protein, another 30 amino acids are attached at the N-terminus of the N-pep sequence that form a transmembrane helix. Yet, during MD simulations of 500 ns length of a *Sa*NSR monomer complexed with N-pep (termed NSR_{Tail}; see online methods for details), N-pep remains stably bound within the hydrophobic tunnel (mean backbone RMSD < 1.6 Å; Supplementary Fig. 4b). The predominance of backbone interactions of N-pep with the protease core and cap domains could explain why N-pep binds into the putative binding region of nisin despite its sequence being very dissimilar to the one of nisin.

Substructures of nisin determining its molecular recognition

To investigate the substrate specificity of *Sa*NSR and determine substructures of nisin important for its recognition by the protein, we used different nisin variants. In order to test the influence of rings D and E located next to the cleavage site of nisin, we genetically replaced the last or the last two cysteine(s) in nisin by alanine, resulting in the expression of active nisin containing only rings A-D (termed CCCCA) or A-C (termed CCCAA), respectively [27]. Similarly, we removed the last six amino acids of nisin (termed $nisin_{1-28}$), resulting in the product of the proteolysis reaction mediated by *Sa*NSR. Furthermore, a truncated variant ($nisin_{1-22}$) was expressed, which contained the rings A-C but lacked the rest of the C-terminus of nisin [27]. Since all variants show a different activity against the nisin sensitive *L. lactis* NZ9000Erm strain (Supplementary Table 1a), we analyzed them with respect to the fold of resistance mediated by the expression of the *Sa*NSR protein in the NZ9000*Sa*NSR strain. From current and previous work, it is known that *Sa*NSR confers a 20-fold increased resistance against wildtype nisin (Fig. 3a) [22].

For CCCCA as well as CCCAA, the resistance mediated by *Sa*NSR decreased to roughly 1.4-1.7 fold when comparing the IC_{50} values of the different strains (Fig. 3b; Supplementary Table 1a). For the truncated variants, $nisin_{1-22}$ and $nisin_{1-28}$, no resistance was observed anymore as the IC_{50} values dropped to the levels observed for the NZ9000Erm strain. Thus, the lanthionine ring E is clearly important for the recognition by *Sa*NSR.

Structural model of nisin binding to *Sa*NSR

Despite intensive trials, we were not successful in obtaining a crystal structure of a *Sa*NSR/nisin complex. Thus, we resorted to generating a structural model by integrative modeling and validating it by mutagenesis studies. Initially, we structurally aligned the backbone of residues 31-36 of nisin to the backbone of N-pep such that the nisin cleavage site between ring E and Ser_{29} was oriented towards the catalytically active Ser_{236} in *Sa*NSR. Rings D and E were then manually placed in three orientations at the tunnel entrances such that they showed good complementarity with the *Sa*NSR surface. This resulted in three structural models of *Sa*NSR/nisin complexes, two (termed $NSR_{Nisin,1}$, $NSR_{Nisin,2}$) where rings D and E are located close to Asn_{172}, Met_{173}, and Ile_{174}, and one (termed $NSR_{Nisin,3}$) where nisin is oriented oppositely with respect to the tunnel axis such that Tyr_{261} stacks onto rings D and E (Supplementary Fig. 5a). The three models were subjected to MD simulations [37] of 500 ns length, with three replicate simulations each.

The average distances between the side chain oxygen of Ser_{236}, previously identified as the catalytically active serine [22], and the carbonyl carbon of Ser_{29} at the nisin cleavage site [24] are 3.71 Å, 4.13 Å, and 7.74 Å for $NSR_{Nisin,1}$, $NSR_{Nisin,2}$ and $NSR_{Nisin,3}$, respectively (Fig. 4a). This strongly indicates that a nucleophilic attack of the side chain of Ser_{236} at the nisin cleavage site as a first step in the catalytic mechanism [24] is possible for the first two models but not for the third, suggesting

that $NSR_{Nisin,1}$ and $NSR_{Nisin,2}$ represent the most likely orientation of nisin within the *Sa*NSR tunnel. Thus, we focused further analyses on the $NSR_{Nisin,1}$ and $NSR_{Nisin,2}$ models.

Visual inspection of the MD trajectories and computations of the backbone RMSF identified residues Lys_{22}, His_{31}, Val_{32}, Dha_{33}, and Lys_{34} of nisin as highly mobile (RMSF values up to 6.39 Å ± 0.49 Å) (Fig. 4b). In contrast, the core region ($Nisin_{Core}$) composed of the rings D and E, and residues Ser_{29} and Ile_{30} revealed RMSF values < 1.85 Å ± 0.24 Å (Fig. 4b) suggesting a tightly bound $Nisin_{Core}$ region. This was corroborated by a per-residue decomposition of effective binding energies computed by the MM-PBSA approach [38]. Here, rings D and E (treated as one residue in the energy decomposition) and Ile_{30} are identified as essential for nisin binding (residue-wise effective binding energies in the range from -4.26 kcal mol^{-1} to -8.63 kcal mol^{-1}) (Fig. 4c). In contrast, for Ser_{29}, a smaller contribution to the effective binding energy of -1.64 kcal mol^{-1} (-0.70 kcal mol^{-1}) for *Sa*$NSR_{Nisin,1}$ (*Sa*$NSR_{Nisin,2}$) was found (Fig. 4c). Overall, this suggests that the rings D and E as well as Ile_{30} form a binding motive, that way ensuring that also Ser_{29} at the nisin cleavage site is correctly positioned within the catalytic site.

In Figure 4d, a representative set of six nisin structures within the *Sa*NSR tunnel is shown. For this, the structure with the smallest backbone RMSD to the average structure was extracted from each of the $NSR_{Nisin,1}$ and $NSR_{Nisin,2}$ MD trajectories. The set shows that the location and orientation of rings D and E, Ser_{29}, and Ile_{30} agree well in all cases, with RMSD values with respect to the average structure for the $Nisin_{Core}$ ranging from 0.80 Å to 2.27 Å (Supplementary Fig. 5b). Thus, both $NSR_{Nisin,1}$ and $NSR_{Nisin,2}$ models were considered equivalent and used to identify residues in *Sa*NSR important for catalysis and nisin binding for mutagenesis studies. The remaining residues of nisin show large structural deviations, in agreement with the above analyses (Supplementary Fig. 5b, Fig. 4b, c).

The TASSAEM region and His_{98} form the active site

The NSR superfamily contains a highly conserved sequence motif "TASSAEM" (Supplementary Fig. 3) located at the rear end of the protease core domain. Within this TASSAEM region, Ser_{236} has been previously identified as the catalytically active serine [22]. This serine is in close proximity to the strictly conserved His_{98} residue, which is localized at the end of the N-terminal helical bundle directly next to the $_{94}GGG_{96}$ motif (Fig. 1) and is in hydrogen bonds distance with the side chain of Ser_{236}. In the $NSR_{Nisin,1}$ and $NSR_{Nisin,2}$ MD simulations, hydrogen bonds were found in up to ~23% of all conformations (Supplementary Fig. 6a), which indicates that both residues likely interact also in the nisin-bound state. Based on the interactions of Ser_{236} and His_{98} and the absence of any other lysine or aspartate residue localized nearby, we presume that *Sa*NSR acts via a catalytic dyad mechanism as observed for some other serine proteases [39,40]. The NZ9000*Sa*NSR-Ser_{236}Ala strain

displayed a low background activity as observed by an IC_{50} value of 12.6±0.7 nM (Supplementary Table 1b), which relates to a *Sa*NSR residual activity of 14% (Fig. 3c). The His_{98}Ala mutation displayed a similar IC_{50} value of 12.3±1.5 nM and a residual activity of 14% (Fig. 3c, Supplementary Table 1a). The residual activity displayed by both variants is likely due to the binding of nisin to that particular *Sa*NSR variant such that a higher concentration of nisin is required to kill the corresponding nisin sensitive NZ9000Erm *L. lactis* strain.

Within the TASSAEM sequence, a second serine residue, Ser_{237}, is present. In the $NSR_{Nisin,1}$ and $NSR_{Nisin,2}$ MD simulations, the mean distance between the side chain oxygen and the carbonyl carbon of ring E is < 5.7 Å (Supplementary Fig. 6b). However, the distance to the δ-nitrogen of His_{98} is > 9 Å (Supplementary Fig. 6c), and no hydrogen bonds were detected between both residues, making a proton shift between Ser_{237} and His_{98} unlikely. Instead, we observed hydrogen bond formation between the side chain of Ser_{237} and the backbone of Gly_{171} of the protease core in at least 46% of the conformations that may be relevant for nisin recognition (see section "Residues involved in nisin recognition and *Sa*NSR specificity") but not for catalytic activity. Thus, Ser_{237} is not expected to be involved in the catalytic mechanism. In accordance, a Ser_{237}Ala mutation does not have a pronounced effect on the activity of *Sa*NSR (residual activity 74%; see Fig. 3c, Supplementary Table 1b).

The next residue in the TASSAEM motif is Glu_{239}, which is pointing away from the active site. In the crystal structure, the Glu_{239} side chain interacts with backbone atoms of Gly_{260} and Tyr_{261} via hydrogen bonds, and during the $NSR_{Nisin,1}$ and $NSR_{Nisin,2}$ MD simulations this interaction is present in at least 82% of all conformations (Supplementary Fig. 6a). Additionally, we found hydrogen bond interactions between Glu_{239} and Ser_{236} in at least 25% of the cases (Supplementary Fig. 6a). These interactions are likely important for the correct positioning of the TASSAEM region. This is in line with the drastically lowered activity of the Glu_{239}Ala mutant (IC_{50} value of 17.1±0.7 nM; residual activity of 22%; Fig. 3c, Supplementary Table 1b). Furthermore, we found stabilizing hydrogen bonds between Thr_{263} and His_{98} in up to ~28%, and between Asn_{265} and His_{98} in up to ~20% of all cases (Supplementary Fig. 6a). These interactions likely ensure a correct orientation of His_{98} as the mutations Thr_{263}Ala and Asn_{265}Ala decreased the residual activities of *Sa*NSR to 20% and 30%, respectively, (Fig. 3c) with associated IC_{50} values of 16.0±0.3 and 22.1±1.1 nM (Supplementary Table 1b). Taken together, the TASSAEM sequence is crucial for the activity of *Sa*NSR and contains the catalytically active serine as well as a glutamic acid residue, which is likely responsible for a correct positioning of the TASSAEM helix.

Residues involved in nisin recognition and *Sa*NSR specificity

Next, we investigated nisin recognition by *Sa*NSR. Residue-wise effective binding energies were computed for both the $NSR_{Nisin,1}$ and $NSR_{Nisin,2}$ MD trajectories to identify *Sa*NSR residues likely to be important for nisin binding (Supplementary Fig. 7a). Considering energies < -0.8 kcal mol^{-1} resulted in seven candidates (Leu_{102}, Leu_{137}, Asn_{172}, Met_{173}, Ile_{174}, Glu_{266}, Ala_{277}). Our model (Fig. 4d) suggests that the hydrophobic residues Leu_{102}, Leu_{137}, Met_{173}, Ile_{174}, Ala_{277} and the polar/charged ones Asn_{172} and Glu_{266} bind to rings D and E in nisin. Asn_{172}, Met_{173}, and Ile_{174} form a pocket that harbors rings D and E in our model (Fig. 4e). The Asn_{172}Ala mutant displayed an activity of 47% (IC_{50} value of 33.5±2.9 nM) (Fig. 3c, Supplementary Table 1b). Furthermore, when mutating the strictly conserved Met_{173} residue (Supplementary Fig. 3), a reduced activity of 42% compared to the wild type value was observed (IC_{50} value of 30.3±1.4 nM). Additionally, the Ile_{174}Ala mutant exhibited an activity of 33% (IC_{50} value of 24.1±2.2 nM) (Fig. 3c, Supplementary Table 1b).

Moreover, we found hydrogen bonds between backbone atoms of Thr_{169} and Gly_{171} with the $Nisin_{Core}$ residues (Supplementary Fig. 7b). These interactions are reminiscent to those found for N-pep (Fig. 2c) and likely ensure a proper placement of the $Nisin_{Core}$ within the binding site. Additional stabilizing hydrogen bonds were observed between Asn_{168} and Gly_{170} (Supplementary Fig. 7b), which could contribute to nisin binding indirectly. A similar indirect effect was found for Glu_{266}, for which we observed salt-bridge formation with Arg_{54} from the N-terminal helical bundle (Supplementary Fig. 7c; mean distance < 3.4 Å). We also found water-mediated hydrogen bonds between backbone atoms of rings D and E, and Asn_{265} and Thr_{267}, respectively (Supplementary Fig. 7d), again mimicking what was observed for the bound N-pep (Fig. 2c). Accordingly, the mutations Asn_{265}Ala (see above) and Thr_{267}Ala decreased the residual activity of *Sa*NSR to 30% and 71%, respectively, (Fig. 3c) with associated IC_{50} values of 22.1±1.1 and 48.5±0.6 nM (Supplementary Table 1b).

Role of the protease cap domain in *Sa*NSR

Other S41 peptidases also contain a protease cap domain comprising a helix and a β-hairpin structure, where the helix appears to open and close depending on the presence of the peptide substrate: once a peptide is bound, the cap closes and seals the active site. As such, the protease CtpB from *Bacillus subtilis* has been crystallized in an open and closed state with the helix of the protease cap moving by 10-15 Å towards the active site once the peptide was bound[30]. In *Sa*NSR, helix α_4 ($_{103}$SKETVRRDTLDS$_{114}$) was identified as the protease cap helix, localized directly after the N-terminal helical bundle. Out of all residues of this helix, only the side chain of Asp_{110} is intruding into the tunnel, which neither forms an interaction to N-pep in the crystal structure nor in the NSR_{Tail} MD simulations. This suggests that the protease cap is not adopting a fully closed state,

rather an intermediate state. MD simulations show a salt-bridge formation between Asp_{110} and Arg_{275} of the protease cap domain for both $NSR_{Nisin1,2}$ models (Supplementary Fig. 8a). In those cases where the salt-bridge formation is weak (mean distance is > 10 Å), a loss of the secondary structures of helix α_4 is observed (Supplementary Fig. 8b). The Asp_{110}Ala mutant of *Sa*NSR is still active although with a lower IC_{50} value of 32.8±2.1 nM (residual activity of 46%; Fig. 3c, Supplementary Table 1b). The Arg_{275}Ala mutant revealed an identical IC_{50} value of 33.6±2.3 nM (residual activity of 48%). Taken together, this suggests that a proper secondary structure of helix α_4 is required for *Sa*NSR function, and that Asp_{110} contributes to the stability of the secondary structure.

DISCUSSION

The present study reveals that the lanthionine ring E of nisin determines substrate specificity of the nisin resistance protein (NSR) and contributes to the coordination of the nisin cleavage site at the catalytic center. These results are based on the first structure of a nisin resistance protein from *S. agalactiae* COH1 (*Sa*NSR) at 2.2 Å resolution and subsequent integrative modeling and mutagenesis studies. The *Sa*NSR structure consists of an N-terminal helical bundle, a protease cap domain, and a protease core domain (Fig. 1). The core domain harbors the highly conserved TASSAEM motif, which contains the catalytically important Ser_{236} residue, in a hydrophobic tunnel formed by all three domains. In this tunnel, an N-terminal peptide from another *Sa*NSR protomer (N-pep) in the asymmetric unit is bound predominantly by direct and water-mediated backbone hydrogen bonds (Fig. 2). A very similar binding pattern is found for the C-terminal lanthionine rings D and E, and residues Ser_{29}, and Ile_{30} of nisin in our model of the *Sa*NSR/nisin complex (Fig. 5a, b; Supplementary Fig. 7d). According to this model, lanthionine ring E binds at one end of the hydrophobic tunnel (Fig. 5a, b) and ensures the exact coordination of the nisin cleavage site at the highly conserved TASSAEM region (Fig. 5a, b).

In contrast to some other C-terminal processing proteases [30,32], the active center of *Sa*NSR consists of a catalytic dyad formed by residues Ser_{236} [22], which is part of the TASSAEM motif, and His_{98} as determined by mutational analysis and also described for some other proteases [41] (Fig. 5c). Mutational analysis and geometric parameters in the crystal structure and during MD simulations exclude that the neighboring Ser_{237} participates in the catalytic step. Residues Glu_{239}, Gly_{260}, Tyr_{261} and Thr_{263}, form hydrogen bonds with either Ser_{236} or His_{98} during all-atom MD simulations of the *Sa*NSR/nisin complexes (Supplementary Fig. 6a, Fig 5b) and, thus, likely stabilize the catalytic residues, as also indicated by alanine mutations of these residues that lead to a decrease in *Sa*NSR activity (Fig. 3c).

Since all our efforts to obtain crystals of *Sa*NSR with bound nisin were unsuccessful, we generated a model (Fig. 5a – c) of the *Sa*NSR/nisin complex by integrative modeling and subsequent site-directed mutagenesis studies and activity measurements for validation. The modeling step was guided by exploiting the knowledge on the location of N-pep in the *Sa*NSR crystal structure as well as on the substructures of nisin determining its molecular recognition. As to the latter, we focused on the C-terminus of nisin ($nisin_{22-34}$) where NSR from *L. lactis* TS1640 has been shown to cleave [24]. As a result, nisin variants in which the bulky lanthionine rings D and E, or only E, were replaced by a linear sequence (CCCCA, CCCAA) showed a large drop in the fold of resistance comparable to those exhibited when the last 12 or 6 residues of nisin ($nisin_{1-22}$, $nisin_{1-28}$) were missing (Fig. 3b). These results demonstrated that ring E is essential for nisin recognition by *Sa*NSR.

Initial models of *Sa*NSR/nisin complexes were generated in which the linear, C-terminal sequence (sequence Lys_{22} - Lys_{34}) were placed at the location of the backbone trace of N-pep and where rings D and E showed a good complementarity with the *Sa*NSR surface at the tunnel entrance. We considered that no *a priori* knowledge on the direction of nisin with respect to the tunnel axis was available by generating models with both possible directions. By subsequent all-atom MD simulations, we could exclude one of the possibilities ($NSR_{Nisin,3}$) as in this case the distance between Ser_{236} and the nisin cleavage site was too large as to allow for a nucleophilic attack of the serine side chain (Fig. 4a). In contrast, for the other direction ($NSR_{Nisin,1}$, $NSR_{Nisin,2}$), such an attack is very likely according to distances that are only slightly larger than the sum of van der Waals radii of oxygen and carbon. This model of a *Sa*NSR/nisin complex is further supported by rather immobile residues of the core region of nisin (rings D and E, Ser_{29} and Ile_{30}), which is considered to facilitate a nucleophilic attack, in contrast to the more mobile C-terminal residues 31-34 (Fig. 4b), and by a residue-wise decomposition of the effective binding energy, which identified rings D and E as well as Ile_{30} as major contributors to the binding affinity (Fig. 4c).

The model (Fig. 5a – c) reveals that *Sa*NSR binding to rings D and E of nisin is dominated by hydrophobic interactions (Fig. 5b, c). Within the protease core Asn_{172}, Met_{173}, and Ile_{174} form a pocket that harbors both rings D and E (Fig. 4e, Fig. 5b). In agreement with this model, mutation of these residues reduces the activity of *Sa*NSR. Furthermore, water-mediated hydrogen bonds between backbone atoms of rings D and E and side chains of Asn_{265} and Thr_{267}, respectively, were identified, mimicking interactions with N-pep. Asn_{265}Ala and Thr_{267}Ala mutations decreased the residual activity of *Sa*NSR (Fig. 3c). Finally, along the tunnel, hydrogen bonds between backbone atoms of Thr_{169} and Gly_{171} of *Sa*NSR with Ser_{29} and Ile_{30} of nisin were found (Fig 5b, c; Supplementary Fig. 7b), which likely contribute towards the correct orientation of the nisin cleavage site at the catalytic center and are again reminiscent of interactions observed for N-pep in the crystal structure.

N-pep and the C-terminus of nisin are not similar on the amino acid level. Together with the above findings of similar interactions along the tunnel between backbone atoms of *Sa*NSR and the two peptides, respectively, suggest that the tunnel's role in peptide binding is not to confer substrate specificity but rather to "rope in" the peptide while establishing these interactions. In the case of nisin, this "roping in" is stopped when the lanthionine ring E starts interacting with *Sa*NSR, thereby acting as a plug on the tunnel (Fig. 5c). These interactions are highly relevant for the molecular recognition of nisin and the substrate specificity of *Sa*NSR, as shown by a decrease in the fold of resistance for the nisin variants CCCCA and CCCAA (Fig. 3b) and a decrease in the activity of *Sa*NSR mutants Asn_{172}Ala, Met_{173}Ala, and Ile_{174}Ala (Fig. 3c). In addition, rings D and E are highly likely relevant for a proper placement of the nisin cleavage site with respect to the catalytic Ser_{236},

as only with nisin a distance to this residue compatible with a nucleophilic attack and, simultaneously, hydrogen bonds with His_{98} are found in the MD simulations. In contrast, during MD simulations of NSR_{Tail}, no hydrogen bond formation between Ser_{236} and His_{98} was detected. This may explain why N-pep binds to *Sa*NSR but is not cleaved.

Previously, an "inhibiting role" of lanthionine rings has been recognized in that they protect lantibiotics from degradation by standard proteases [42], likely because of their bulky 3D structure which prevents a proper placement in the substrate binding regions of proteases evolved to cleave linear peptides. In turn, the findings in this study for the first time reveal a significant "fostering role" of the lanthionine rings D and E in nisin for the highly specific cleavage of this lantibiotic by *Sa*NSR. These findings and our structural model of the *Sa*NSR/nisin complex open up a new avenue in the understanding of lantibiotic resistance by human pathogens. They may also facilitate the development of therapeutics to overcome nisin resistance.

METHODS

Cloning, expression and purification of *Sa*NSR

The *nsr* gene from *Streptococcus agalactiae* COH1 was cloned into pET28b and purified as previously described. For details see Supplementary Information.

Multiple angle light scattering

For HPLC-MALS analysis, a Bio SEC-5 HPLC column (Agilent Technologies Deutschland GmbH, Böblingen, Germany) with a pore size of 300 Å was equilibrated with 25 mM MES pH 6.0, 150 mM NaCl for HPLC using a system from Agilent Technologies connected to a triple-angle light-scattering detector (miniDAWN TREOS, Wyatt Technology Europe GmbH, Dernbach, Germany) followed by a differential refractive index detector (OPTILab T-rEX, Wyatt Technology). Typically, 100 µl of purified *Sa*NSR (2.0 mg/ml) was loaded onto the Bio SEC-5 HPLC column, and the obtained data were analyzed with the ASTRA software package (Wyatt Technology).

Crystallization, data collection and structure determination of SaNSR

Crystals were obtained and optimized as described in the Supplementary Information. X-ray diffraction data were collected at the ID23eh2 or ID29 beamlines of the European Synchrotron Radiation Facility (ESRF), Grenoble. All the data sets were processed and scaled using XDS and XSCALE software package [43]. Data sets from native crystals were collected at a wavelength of 0.872 Å at 100 K. For selenomethionine-substituted crystals, the ID29 beamline (ESRF Synchrotron, Grenoble) [44] was used for anomalous diffraction data collection, done at 100 K. The structure was solved by single-wavelength anomalous dispersion (SAD) from a single selenomethionine derivative crystal measured at 0.976 Å, which diffracted up to 2.7 Å. The Auto-Rickshaw program [45] was then used to phase the protein and build an initial model, which was further manually build and refined using COOT [46] and phenix.refine from the Phenix package [47]. This model was then used to phase the native data set at a resolution of 2.2 Å. After molecular replacement, automatic model building was performed with the program ARP/wARP [48], followed by manual iterative cycles of model refinement using the program phenix.refine [47]. Manual adjustments between the refinement cycles were done with the program Coot [46] and Ramachandran validation was done using MolProbity [49]. Almost all residues (96.3%) were in the preferred regions of the Ramachandran plot, and the remaining 3.7% were in the additionally allowed regions. The data collection and refinement statistics are listed in Table 1. The images of the models were prepared using MacPyMOL [50].

IC_{50} determination of nisin and its variants

Cells from the different expressing strains were grown overnight in GM17 media supplemented with 5 $\mu g ml^{-1}$ erythromycin in the presence of 1 $ng ml^{-1}$ nisin. The diluted cells (final OD_{600} of 0.1) were incubated with a serial dilution of nisin or its variants in a 96-well plate. The total volume in each well was 200 µl, consisting of 50 µl nisin or its variants and 150 µl GM17 containing the corresponding *L. lactis* strain. The plate was then incubated at 30°C and after 5 hours, the optical density was measured at 600 nm *via* 96-well plate reader BMG. The IC_{50} value was determined as previously described [51].

Molecular dynamics simulations

In order to investigate nisin recognition by *Sa*NSR we performed molecular dynamics (MD) simulations of an unbound *Sa*NSR monomer (NSR_{Apo}), a *Sa*NSR monomer bound to the N-terminal part of *Sa*NSR (residues 31 – 36; in the following named "Tail") from an adjacent subunit (NSR_{Tail}) in the crystal structure (see Fig. 1), and a *Sa*NSR monomer bound to the C-terminal part (residues 22 – 34; Supplementary Fig. 2c) of nisin (NSR_{Nisin}). Initial coordinates for NSR_{Apo} and NSR_{Tail} were taken from the crystal structure described here. Since no structural information is available for nisin bound to *Sa*NSR, we generated models as starting structures for MD simulations by structurally aligning the nisin part to the Tail using the program Moloc. The nisin cleavage site between ring E and Ser_{29} was oriented towards the catalytically active Ser_{236} in *Sa*NSR [22]. Rings D and E were manually placed in three orientations within the binding site such that they showed good complementarity with the *Sa*NSR surface, resulting in three different models of *Sa*NSR/nisin complexes ($NSR_{Nisin,1}$, $NSR_{Nisin,2}$, and $NSR_{Nisin,3}$, Supplementary Fig. 4a).

For the MD simulations, structures of NSR_{Apo}, NSR_{Tail}, and $NSR_{Nisin,1-3}$ were prepared, relaxed, and thermalized as described in detail in the Supporting Information. Three independent production runs of MD simulations of 500 ns length in the canonical (NVT) ensemble at 300 K were then conducted for each of the five systems, leading to a total simulation time of 5 x 3 x 500 ns = 7.5 µs; see Supporting Information for details.

The trajectories were analyzed with respect to distances, root mean square fluctuations (RMSF) and deviations (RMSD) as a measure for mobility and structural similarity, respectively, and hydrogen bonds defined by a distance between the two donor and acceptor atoms < 3.2 Å and an angle (donor atom, H, acceptor atom) between 120° and 180° using *cpptraj* [52]. Salt-bridge interaction are defined by a distance < 4.0 Å between the center of mass of both charged groups. The set of structural models binding to *Sa*NSR (see section "Structural model of nisin binding to *Sa*NSR) was generated by structurally aligning *Sa*NSR and subsequent RMSD calculations for the nisin peptide.

Calculation of the effective binding energy

In order to identify amino acids in *Sa*NSR that contribute most to nisin binding, we computed the residue-wise contribution to binding effective energies by the "single trajectory" molecular mechanics Poisson-Boltzman area (MM-PBSA) approach [53-55]. To determine the per-residue contribution, the decomposition scheme [56] as implemented in the mm_pbsa.pl script in Amber 14 [37] was applied. The calculations were performed with the ff99SB force field [57,58]. The polar part of the solvation free energy was determined by applying the PBSA solver using a dielectric constant of 1 (solute) and 80 (solvent) together with Parse radii [59]. The conformational ensemble consists of 10,000 snapshots and was extracted from the 1 – 200 ns interval of each of the $NSR_{Nisin,1-2}$ trajectories. Prior to the MM-PBSA computations, counter ions and water molecules were stripped from the snapshots. For the computations, we considered the *Sa*NSR protein the receptor, whereas the nisin C-terminus was considered the ligand. All residues in *Sa*NSR and nisin were considered for per-residue decomposition. Rings D and E in nisin were treated as one residue.

PDB DEPOSITION:

The final model has been deposited in the PDB database under the accession code: 4Y68.

ACKNOWLEDGEMENTS

We thank Lutz Schmitt for fruitful discussions, encouragement, support and invaluable advice. We are grateful to Philipp Ellinger for initiating the project, André Abts for stimulating discussions, Michael Lenders and Iris Fey for technical assistance. We acknowledge the European Synchrotron Radiation Facility for provision of synchrotron radiation facilities and are grateful to the staff of ESRF ID23-2 and ID29 for support during crystal screening and data collection, especially Christoph Mueller-Dieckmann for his enormous patience, assistance and support. We are thankful to Heinrich Heine International Graduate School of Protein Science and Technology (iGRASPseed) for providing a scholarship to S.K and to the International NRW Research School BioStruct, granted by the Ministry of Innovation, Science and Research of the State North Rhine-Westphalia, the Heinrich Heine University Düsseldorf, and the Entrepreneur Foundation at the Heinrich Heine University Düsseldorf for a scholarship to B.F. We are also grateful to the "Zentrum für Informations- und Medientechnologie" (ZIM) at the Heinrich-Heine-University Düsseldorf for providing computational support.

AUTHOR CONTRIBUTION STATEMENT

SK, AH, DK performed the biochemical and structural experiments. BF, DM performed molecular modeling and MD simulations. SK, BF, HG, SS designed the experiments, evaluated the data, and wrote the manuscript. All authors reviewed the manuscript.

ADDITIONAL INFORMATION

Competing financial interests: the authors declare to have no competing financial interests.

Literature

1. Levy, S.B. Antibiotic Resistance: Consequences of Inaction. *Clin. Infect. Dis.* **33**, S124-S129 (2001).
2. Ling, L.L. et al. A new antibiotic kills pathogens without detectable resistance. *Natur* **517**, 455-459 (2015).
3. Sahl, H.-G. & Bierbaum, G. Lantibiotics: biosynthesis and biological activities of uniquely modified peptides from gram-positive bacteria. *Annual Reviews in Microbiology* **52**, 41-79 (1998).
4. Willey, J.M. & van der Donk, W.A. Lantibiotics: peptides of diverse structure and function. *Annu. Rev. Microbiol.* **61**, 477-501 (2007).
5. Breukink, E. et al. Use of the cell wall precursor lipid II by a pore-forming peptide antibiotic. *Sci* **286**, 2361-2364 (1999).
6. Breukink, E. & de Kruijff, B. Lipid II as a target for antibiotics. *Nature Reviews Drug Discovery* **5**, 321-323 (2006).
7. Hancock, R.E. & Sahl, H.-G. Antimicrobial and host-defense peptides as new anti-infective therapeutic strategies. *Nat. Biotechnol.* **24**, 1551-1557 (2006).
8. Bierbaum, G. & Sahl, H.G. Lantibiotics: Mode of Action, Biosynthesis and Bioengineering. *Current Pharmaceutical Biotechnology* **10**, 2-18 (2009).
9. Xie, L. & Van Der Donk, W.A. Post-translational modifications during lantibiotic biosynthesis. *Curr. Opin. Chem. Biol.* **8**, 498-507 (2004).
10. Chatterjee, C., Paul, M., Xie, L.L. & van der Donk, W.A. Biosynthesis and mode of action of lantibiotics. *Chem Rev* **105**, 633-683 (2005).
11. Héchard, Y. & Sahl, H.-G. Mode of action of modified and unmodified bacteriocins from Gram-positive bacteria. *Biochimie* **84**, 545-557 (2002).
12. Dischinger, J., Basi Chipalu, S. & Bierbaum, G. Lantibiotics: promising candidates for future applications in health care. *Int. J. Med. Microbiol.* **304**, 51-62 (2014).
13. Hsu, S.T. et al. The nisin-lipid II complex reveals a pyrophosphate cage that provides a blueprint for novel antibiotics. *Nature structural & molecular biology* **11**, 963-7 (2004).
14. Wiedemann, I. et al. Specific Binding of Nisin to the Peptidoglycan Precursor Lipid II Combines Pore Formation and Inhibition of Cell Wall Biosynthesis for Potent Antibiotic Activity. *J. Biol. Chem.* **276**, 1772-1779 (2001).
15. van Heusden, H.E., de Kruijff, B. & Breukink, E. Lipid II induces a transmembrane orientation of the pore-forming peptide lantibiotic nisin. *Biochemistry* **41**, 12171-12178 (2002).

16. Hasper, H.E., de Kruijff, B. & Breukink, E. Assembly and stability of nisin-lipid II pores. *Biochemistry* **43**, 11567-75 (2004).
17. Froseth, B.R. & Mckay, L.L. Molecular characterization of the nisin resistance region of Lactococcus lactis subsp. lactis biovar diacetylactis DRC3. *Appl. Environ. Microbiol.* **57**, 804-811 (1991).
18. Draper, L.A., Cotter, P.D., Hill, C. & Ross, R.P. Lantibiotic Resistance. *Microbiol. Mol. Biol. Rev.* **79**, 171-191 (2015).
19. McKay, L.L. & Baldwin, K.A. Conjugative 40-megadalton plasmid in *Streptococcus lactis* subsp. *diacetylactis* DRC3 is associated with resistance to nisin and bacteriophage. *Applied and Environmental Microbiology* **47**, 68-74 (1984).
20. Duan, K., Harvey, M., Liu, C.Q. & Dunn, N. Identification and characterization of a mobilizing plasmid, pND300, in Lactococcus lactis M189 and its encoded nisin resistance determinant. *J. Appl. Bacteriol.* **81**, 493-500 (1996).
21. Klaenhammer, T.R. & Sanozky, R.B. Conjugal transfer from Streptococcus lactis ME2 of plasmids encoding phage resistance, nisin resistance and lactose-fermenting ability: evidence for a high-frequency conjugative plasmid responsible for abortive infection of virulent bacteriophage. *J. Gen. Microbiol.* **131**, 1531-1541 (1985).
22. Khosa, S., Alkhatib, Z. & Smits, S.H. NSR from Streptococcus agalactiae confers resistance against nisin and is encoded by a conserved nsr operon. *Biol. Chem.* **394**, 1543-1549 (2013).
23. Kawada-Matsuo, M. et al. Three distinct two-component systems are involved in resistance to the class I bacteriocins, nukacin ISK-1 and nisin A, in Staphylococcus aureus. *PLoS One* **8**, e69455 (2013).
24. Sun, Z. et al. Novel mechanism for nisin resistance via proteolytic degradation of nisin by the nisin resistance protein NSR. *Antimicrob. Agents Chemother.* **53**, 1964-1973 (2009).
25. Christ, N.A. et al. The First structure of a lantibiotic immunity protein, SpaI from Bacillus subtilis, reveals a novel fold. *The Journal of biological chemistry* **287**, 35286-98 (2012).
26. Pozzi, R. et al. Distinct mechanisms contribute to immunity in the lantibiotic NAI-107 producer strain Microbispora ATCC PTA-5024. *Environmental microbiology* (2015).
27. Alkhatib, Z. et al. The C‐terminus of nisin is important for the ABC transporter NisFEG to confer immunity in Lactococcus lactis. *MicrobiologyOpen* **3**, 752-763 (2014).
28. Bernsel, A., Viklund, H., Hennerdal, A. & Elofsson, A. TOPCONS: consensus prediction of membrane protein topology. *Nucleic Acids Res.*, gkp363 (2009).
29. Khosa, S., Hoeppner, A., Kleinschrodt, D. & Smits, S. Overexpression, purification, crystallization and preliminary X-ray diffraction of the nisin resistance protein from

Streptococcus agalactiae. *Acta Crystallographica Section F: Structural Biology Communications* **71**, 0-0 (2015).

30. Mastny, M. et al. CtpB assembles a gated protease tunnel regulating cell-cell signaling during spore formation in Bacillus subtilis. *Cell* **155**, 647-658 (2013).
31. Kim, J.-S. et al. Navigation inside a protease: substrate selection and product exit in the tricorn protease from Thermoplasma acidophilum. *J. Mol. Biol.* **324**, 1041-1050 (2002).
32. Liao, D.-I., Qian, J., Chisholm, D.A., Jordan, D.B. & Diner, B.A. Crystal structures of the photosystem II D1 C-terminal processing protease. *Nat. Struct. Mol. Biol.* **7**, 749-753 (2000).
33. Holm, L. & Rosenström, P. Dali server: conservation mapping in 3D. *Nucleic Acids Res.* **38**, W545-W549 (2010).
34. David, A. et al. Structural determinants of host specificity of complement Factor H recruitment by Streptococcus pneumoniae. *Biochem. J* **465**, 325-335 (2015).
35. Gao, X.-C. et al. The C-terminal Helices of Heat Shock Protein 70 Are Essential for J-domain Binding and ATPase Activation. *J. Biol. Chem.* **287**, 6044-6052 (2012).
36. Garcia, B.L. et al. A structurally dynamic N-terminal helix is a key functional determinant in staphylococcal complement inhibitor (SCIN) proteins. *J. Biol. Chem.* **288**, 2870-2881 (2013).
37. Case, D.A. et al. AMBER 14. *University of California, San Francisco.* (2014).
38. Metz, A. et al. Hotspots and transient pockets: predicting the determinants of small-molecule binding to a protein-protein interface. *J Chem Inf Model* **52**, 120-133 (2012).
39. Wang, Y., Zhang, Y. & Ha, Y. Crystal structure of a rhomboid family intramembrane protease. *Natur* **444**, 179-180 (2006).
40. Hodel, A.E. et al. The Three-Dimensional Structure of the Autoproteolytic, Nuclear Pore-Targeting Domain of the Human Nucleoporin Nup98. *Mol. Cell* **10**, 347-358 (2002).
41. Page, M. & Di Cera, E. Serine peptidases: classification, structure and function. *Cell. Mol. Life Sci.* **65**, 1220-1236 (2008).
42. Bierbaum, G. et al. Engineering of a novel thioether bridge and role of modified residues in the lantibiotic Pep5. *Appl. Environ. Microbiol.* **62**, 385-392 (1996).
43. Kabsch, W. Xds. *Acta Crystallogr. D Biol. Crystallogr.* **66**, 125-132 (2010).
44. de Sanctis, D. et al. ID29: a high-intensity highly automated ESRF beamline for macromolecular crystallography experiments exploiting anomalous scattering. *J. Synchrotron Radiat.* **19**, 455-461 (2012).
45. Panjikar, S., Parthasarathy, V., Lamzin, V.S., Weiss, M.S. & Tucker, P.A. On the combination of molecular replacement and single-wavelength anomalous diffraction

phasing for automated structure determination. *Acta Crystallogr. D Biol. Crystallogr.* **65**, 1089-97 (2009).

46. Emsley, P., Lohkamp, B., Scott, W.G. & Cowtan, K. Features and development of Coot. *Acta Crystallogr. D Biol. Crystallogr.* **66**, 486-501 (2010).
47. Adams, P.D. et al. PHENIX: a comprehensive Python-based system for macromolecular structure solution. *Acta Crystallogr. D Biol. Crystallogr.* **66**, 213-221 (2010).
48. Langer, G., Cohen, S.X., Lamzin, V.S. & Perrakis, A. Automated macromolecular model building for X-ray crystallography using ARP/wARP version 7. *Nat. Protoc.* **3**, 1171-1179 (2008).
49. Chen, V.B. et al. MolProbity: all-atom structure validation for macromolecular crystallography. *Acta Crystallogr D Biol Crystallogr* **66**, 12-21 (2010).
50. Delano, W.L. The PyMOL molecular graphics system. (2002).
51. Abts, A. et al. Easy and Rapid Purification of Highly Active Nisin. *International Journal of Peptides* **2011**, 9 (2011).
52. Roe, D.R. & Cheatham, T.E. PTRAJ and CPPTRAJ: software for processing and analysis of molecular dynamics trajectory data. *J. Chem. Theory Comput.* **9**, 3084-3095 (2013).
53. Srinivasan, J., Cheatham, I., T. E., Cieplak, P., Kollman, P.A. & Case, D.A. Continuum solvent studies of the stability of DNA, RNA, and phosphoramidate - DNA helices. *J. Am. Chem. Soc.* **120**, 9401-9409 (1998).
54. Gohlke, H. & Case, D.A. Converging free energy estimates: MM-PB(GB)SA studies on the protein-protein complex Ras-Raf. *J. Comput. Chem.* **25**, 238-50 (2004).
55. Homeyer, N. & Gohlke, H. Free energy calculations by the molecular mechanics Poisson-Boltzmann surface area method. *Molecular Informatics* **31**, 114-122 (2012).
56. Gohlke, H., Kiel, C. & Case, D.A. Insights into protein–protein binding by binding free energy calculation and free energy decomposition for the Ras–Raf and Ras–RalGDS complexes. *J. Mol. Biol.* **330**, 891-913 (2003).
57. Cornell, W.D. et al. A second generation force field for the simulation of proteins, nucleic acids, and organic molecules. *J. Am. Chem. Soc.* **118**, 2309-2309 (1996).
58. Hornak, V. et al. Comparison of multiple Amber force fields and development of improved protein backbone parameters. *Proteins: Struct., Funct., Bioinf.* **65**, 712-725 (2006).
59. Sitkoff, D., Sharp, K.A. & Honig, B. Accurate Calculation of Hydration Free-Energies Using Macroscopic Solvent Models. *J. Phys. Chem.* **98**, 1978-1988 (1994).

Tables

Table 1: Data collection, phasing and refinement statistics for *Sa*NSR

	Native *Sa*NSR	**SeMet *Sa*NSR**
Data collection		
Space group	$P2_12_12_1$	$P4_32$
Cell dimensions		
a, b, c (Å)	58.8, 137.2, 164.0	186.1, 186.1, 186.1
α, β, γ (°)	90, 90, 90	90, 90, 90
Wavelength	0.87260	0.97625
Resolution (Å)	100.0–2.21 (2.29–2.21)	100.0–2.80 (2.9-2.8)
R_{merge}	11.5 (63.8)	29.3 (110.5)
$\langle I / \sigma (I) \rangle$	8.67 (1.79)	20.33 (1.72)
Completeness (%)	99.6 (99.3)	99.8 (98.7)
Redundancy	4.5 (4.2)	75.6 (70.5)
Refinement		
Resolution (Å)	55.36-2.21 (2.28-2.21)	
No. reflections	303208 (27954)	
R_{work} / R_{free}	0.19 (0.27)/ 0.24 (0.31)	
No. of atoms	9588	
Protein	9017	
Ligand/ion	48	
Water	523	
B-factors (Å^3)	40.5	
Protein	40.3	
Ligand/ion	68.1	
Water	41.2	
R.m.s deviations		
Bond lengths (Å)	0.008	
Bond angles (°)	1.09	

*Values in parentheses are for highest-resolution shell.

FIGURE CAPTIONS

Figure 1: Structural architecture of the *Sa*NSR monomer.

(a) Schematic illustration of the domain organization of *Sa*NSR indicating the domain borders and catalytically important residues (His_{98} and Ser_{236}).

(b) The overall structure of *Sa*NSR monomer in a cartoon representation. The N-terminal helical bundle is depicted in green where the light green region represents the N-pep. The protease cap and core domains are highlighted in red and grey, respectively. The catalytically important residues and the highly conserved "TASSAEM" region are depicted in blue.

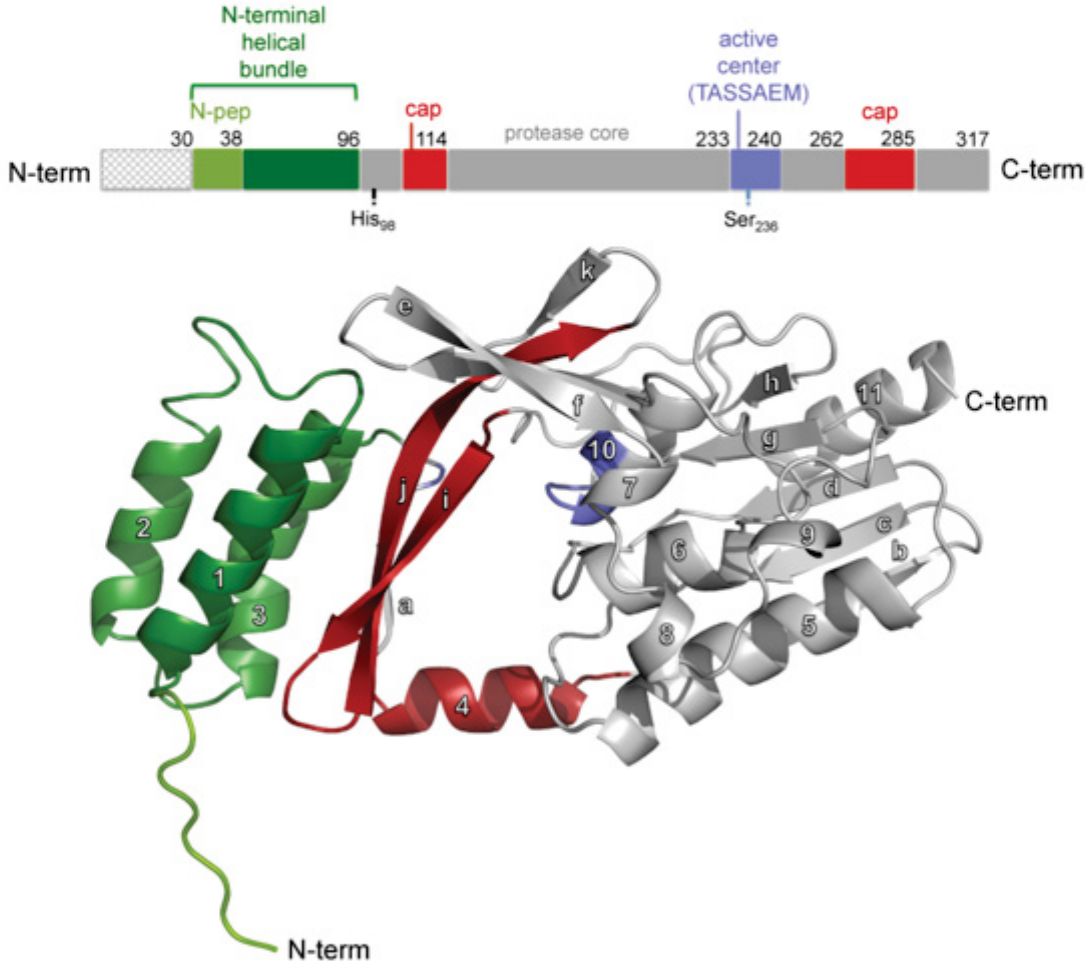

Figure 2: Surface representation of *Sa*NSR.

(a) The surface representation of *Sa*NSR in white, highlighting the tunnel localized in between the protease cap and the core domain. The TASSAEM motif is colored in blue.

(b) Surface representation of *Sa*NSR with bound N-pep (colored in orange).

(c) Stereo view on the active site architecture of *Sa*NSR highlighting the N-pep that is bound within the tunnel as ball and stick representation**.** The corresponding $2F_oF_c$ omit electron density map is calculated at 2.2 Å and contoured at 1.0 σ. The direct interactions of N-pep (colored in orange) with residues of the protease cap (depicted in red) and the water-mediated interactions with the residues of the protease core (grey color) are shown.

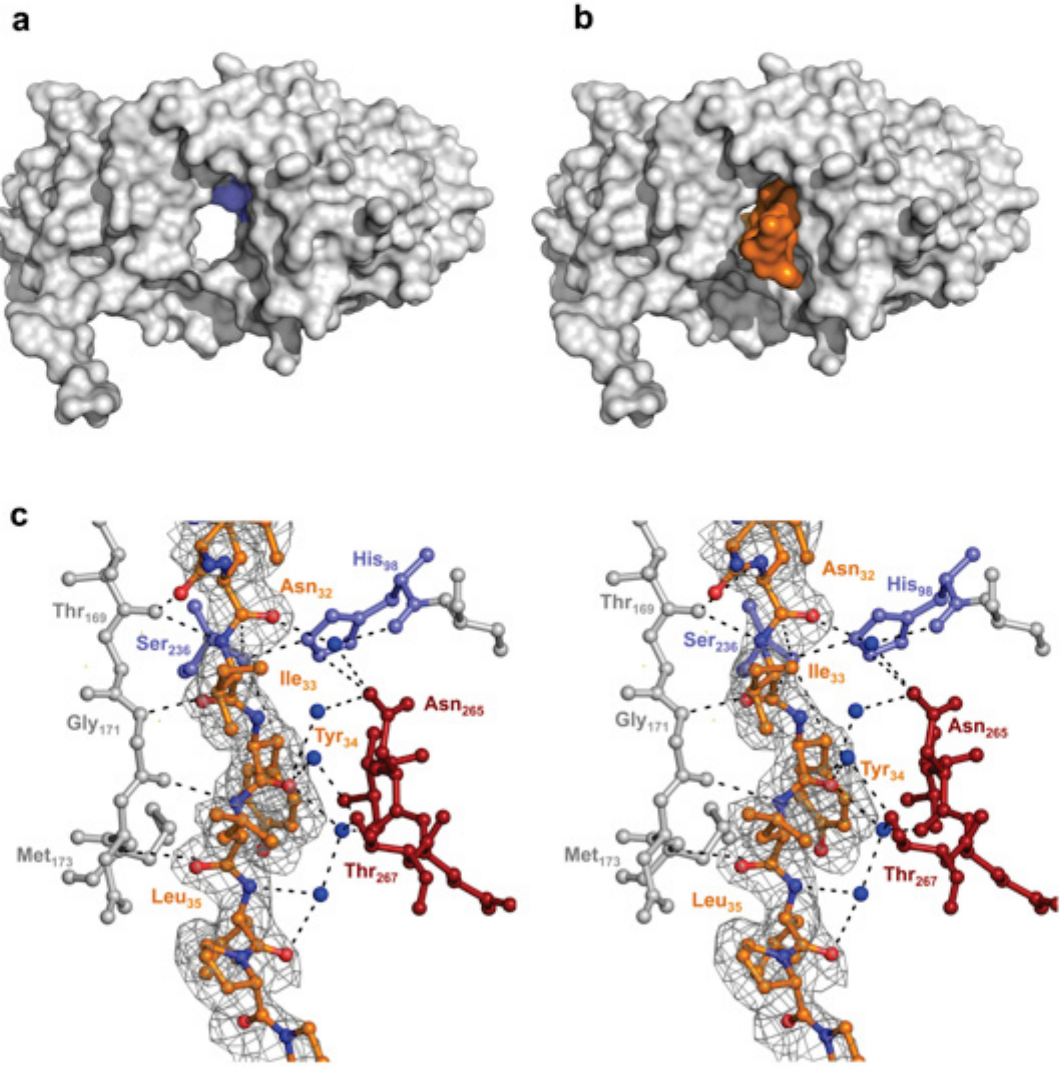

Figure 3: Influence of wild type *Sa*NSR and its mutations against nisin and its variants.

(a) Growth inhibition experiment of *Sa*NSR with nisin. The activity of *Sa*NSR is determined using the *L. lactis* NZ9000 strain, where the plasmid encoding the *Sa*NSR wildtype and the mutations were transformed, and the IC_{50} against nisin was determined. As a control, the empty vector was transformed and used in the IC_{50} study (termed NZ9000Erm). Black lines represent the NZ9000Erm (filled Δ) and NZ9000-*Sa*NSR (◆) strains, respectively. The black dotted lines represent the NZ9000-*Sa*NSR-His_{98}Ala (□) and NZ9000-*Sa*NSR-Ser_{236}Ala (O) strains. The data were fitted and evaluated as described in [51]. The difference in the growth exhibited by the strains was used to calculate the percentage of activity. Each experiment was performed at least in triplicates.

(b) Graphical representation of the fold of resistance exhibited by *Sa*NSR with nisin and different nisin variants (CCCCA, CCCAA, $nisin_{1-22}$ and $nisin_{1-28}$). The NZ9000Erm and NZ9000*Sa*NSR strains were used to determine the activity of all the nisin variants. The error bars indicate the standard error of at least three independent experiments.

(c) The activity of *Sa*NSR and its mutations is determined using the *L. lactis* NZ9000 strain. A normalization of the IC_{50} values were done by setting the values exhibited by the empty vector (NZ9000Erm) and NZ9000*Sa*NSR to 0% and 100%, respectively. The error bars indicate the standard error of at least three independent experiments.

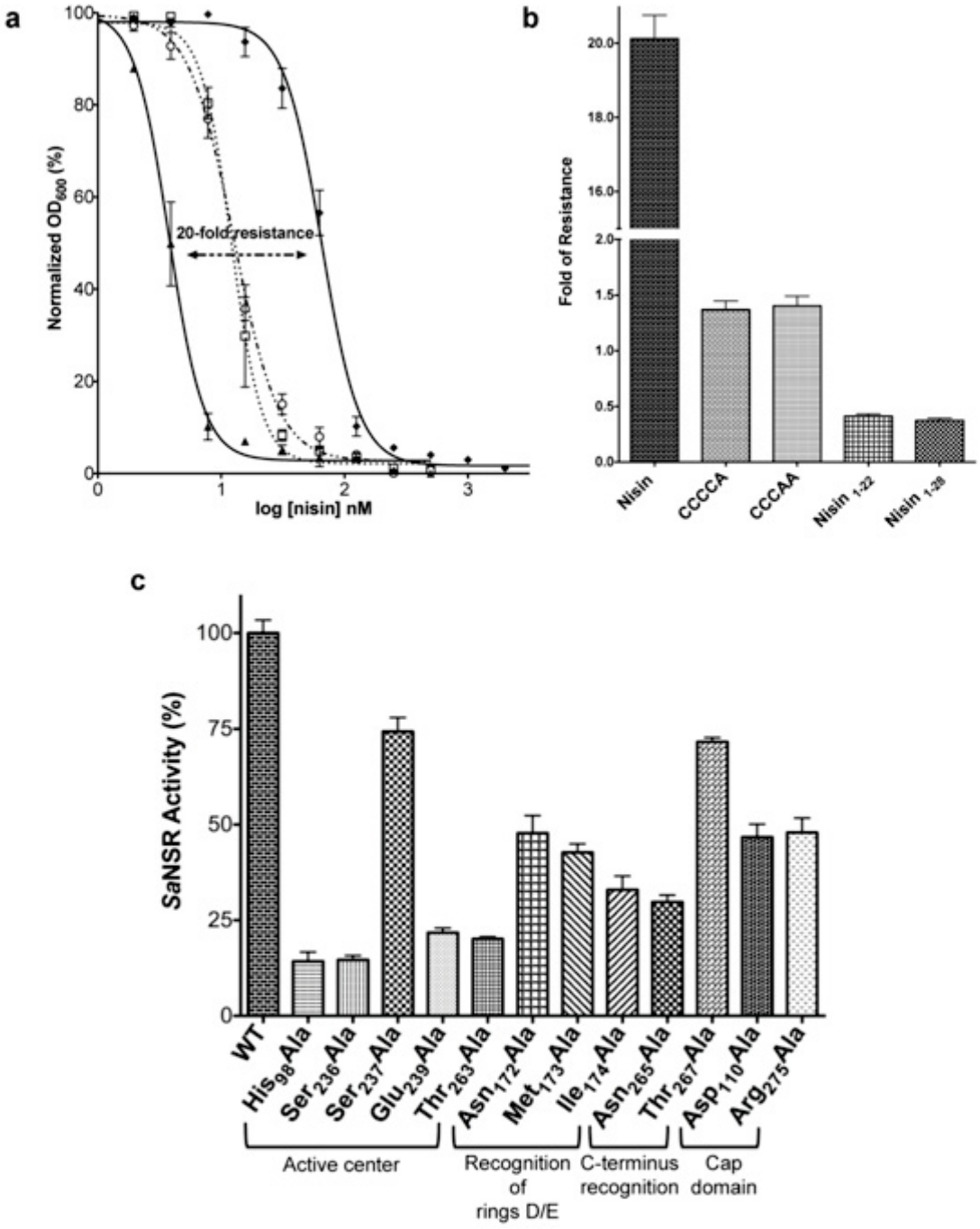
a
Normalized OD600 (%)
20-fold resistance
log [nisin] nM
b
Fold of Resistance
Nisin
CCCCA
CCCAA
Nisin 1-22
Nisin 1-28
c
SaNSR Activity (%)
WT
His98Ala
Ser236Ala
Ser237Ala
Glu239Ala
Thr263Ala
Asn172Ala
Met173Ala
Ile174Ala
Asn265Ala
Thr267Ala
Asp110Ala
Arg275Ala
Active center
Recognition of rings D/E
C-terminus recognition
Cap domain

Figure 4: Structural and energetic analysis of MD simulations of *Sa*NSR/nisin model complexes.

(a) Distance between the side chain oxygen of Ser_{236} and the carbonyl carbon of ring E at the nisin cleavage site (black dotted line in the upper right panel) in $NSR_{Nisin,\{1,2,3\}}$ during 500 ns of MD simulations; lines were smoothed by cubic splines. Mean values and mean standard error (MSE; in parentheses) are shown in the legend. The mean distance over all three MD simulations is shown in the lower right panel (MSE < 0.1 Å and not shown).

(b) Mean backbone RMSF (MSE indicated as error bars) for $NSR_{Nisin,\{1,2\}}$ models over three trajectories each of 500 ns length. Rings D and E, Ser_{29}, and Ile_{30} compose the $Nisin_{Core}$.

(c) Mean effective binding energy per residue for $NSR_{Nisin,\{1,2\}}$ models. Error bars indicate MSE over three trajectories.

(d) Superimposition of six close-to-average structures (based on the backbone RMSD) of nisin (ball-and-stick models each colored differently), extracted from three independent MD simulations each of $NSR_{Nisin,1}$ and $NSR_{Nisin,2}$, within the tunnel of *Sa*NSR (white surface representation). Ser_{236} of the catalytic dyad is colored in blue. For clarity, the N-terminal helical bundle and part of the cap region of *Sa*NSR have been omitted.

(e) Representative nisin model (orange and green ball-and-stick model) within the tunnel of *Sa*NSR (white cartoon representation with transparent surface). Residues Asn_{172}, Met_{173}, and Ile_{174} that bind to rings D and E are colored in magenta.

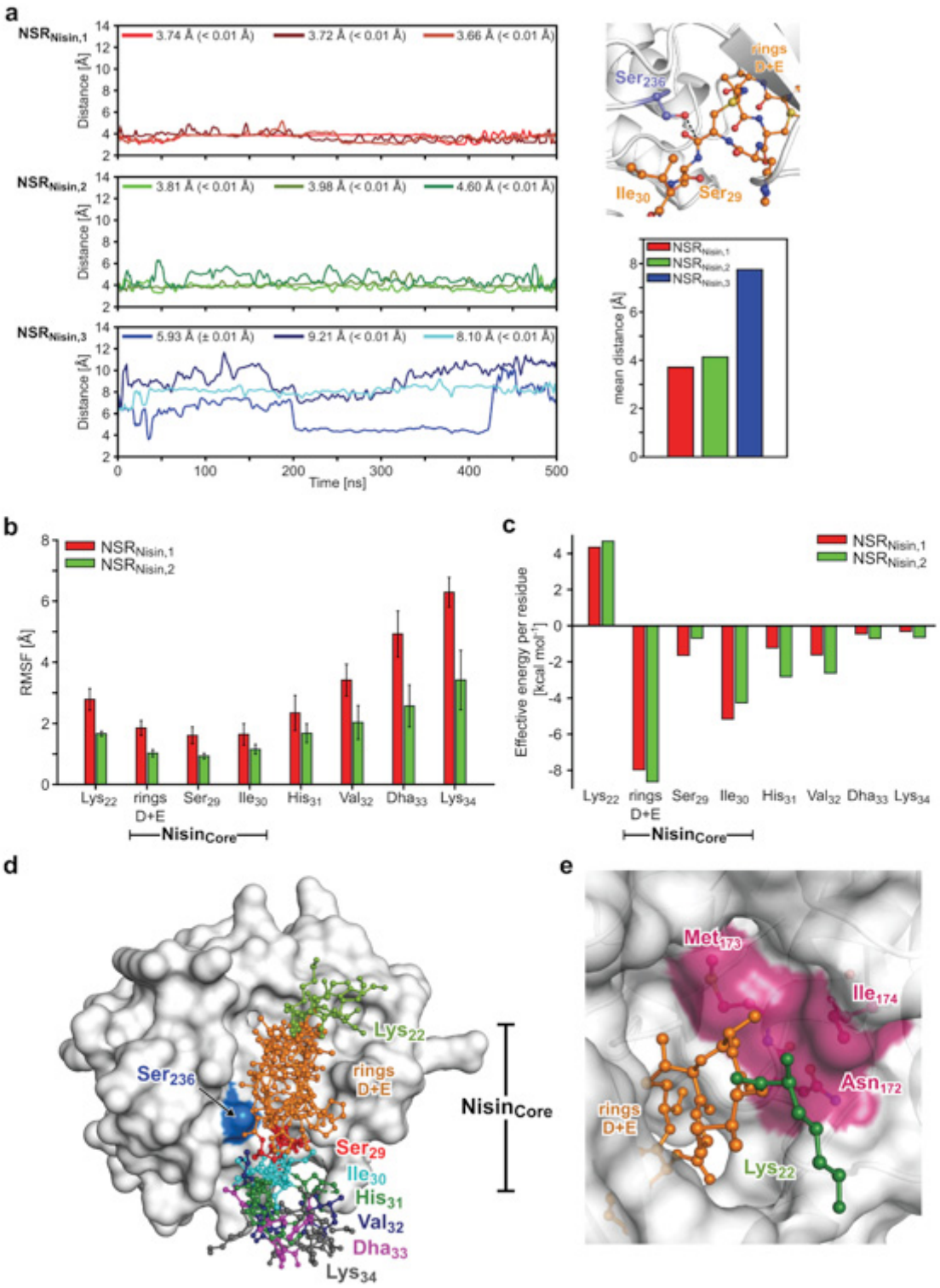
a
NSR Nisin,1
3.74 Å (< 0.01 Å)
3.72 Å (< 0.01 Å)
3.66 Å (< 0.01 Å)
Distance [Å]
NSR Nisin,2
3.81 Å (< 0.01 Å)
3.98 Å (< 0.01 Å)
4.60 Å (< 0.01 Å)
NSR Nisin,3
5.93 Å (± 0.01 Å)
9.21 Å (< 0.01 Å)
8.10 Å (< 0.01 Å)
Time [ns]
rings D+E
Ser236
Ile30
Ser29
mean distance [Å]
b
RMSF [Å]
Lys22
rings D+E
Ser29
Ile30
His31
Val32
Dha33
Lys34
NisinCore
c
Effective energy per residue [kcal mol-1]
d
e
Met173
Ile174
Asn172
Lys22

Figure 5: Nisin/*Sa*NSR binding model.

a) Representative structure of nisin (residues 22-34; extracted from the $NSR_{Nisin,1}$ model) bound to the crystal structure of *Sa*NSR (cartoon representation with transparent surface; each domain is colored differently). Orange spheres with one-letter/three letter amino acid code indicate nisin residues 1-21 not considered for modeling studies (abbreviations: abu = aminobutyric acid; dha = dehydroalanine; dhb = dehydrobutyrine; ala-S-X = lanthionine derivatives).

b) Close up view of nisin binding to *Sa*NSR residues important for nisin recognition (left), residues with catalytic function (middle), and residues with a regulatory function (right). Amino acids of interest are depicted as ball-and-stick model; residues for which experimental data is reported in this study are, additionally, shown in transparent surface representation.

c) Schematic representation of the $Nisin_{core}$ bound to *Sa*NSR residues (residue numbers according to the crystal structure described here). Residues that compose the catalytic site are colored in blue, residues that contribute to nisin binding in magenta, residues that have an indirect effect on binding in black-magenta, and residues with a supposedly regulatory function in *Sa*NSR in red. For residues with colored background, *Sa*NSR activity information for alanine mutants is available (see Fig. 3c). Residues marked with a star form the catalytic dyad.

In panels a, b, and c, the nisin structure is depicted as orange ball-and-stick model.

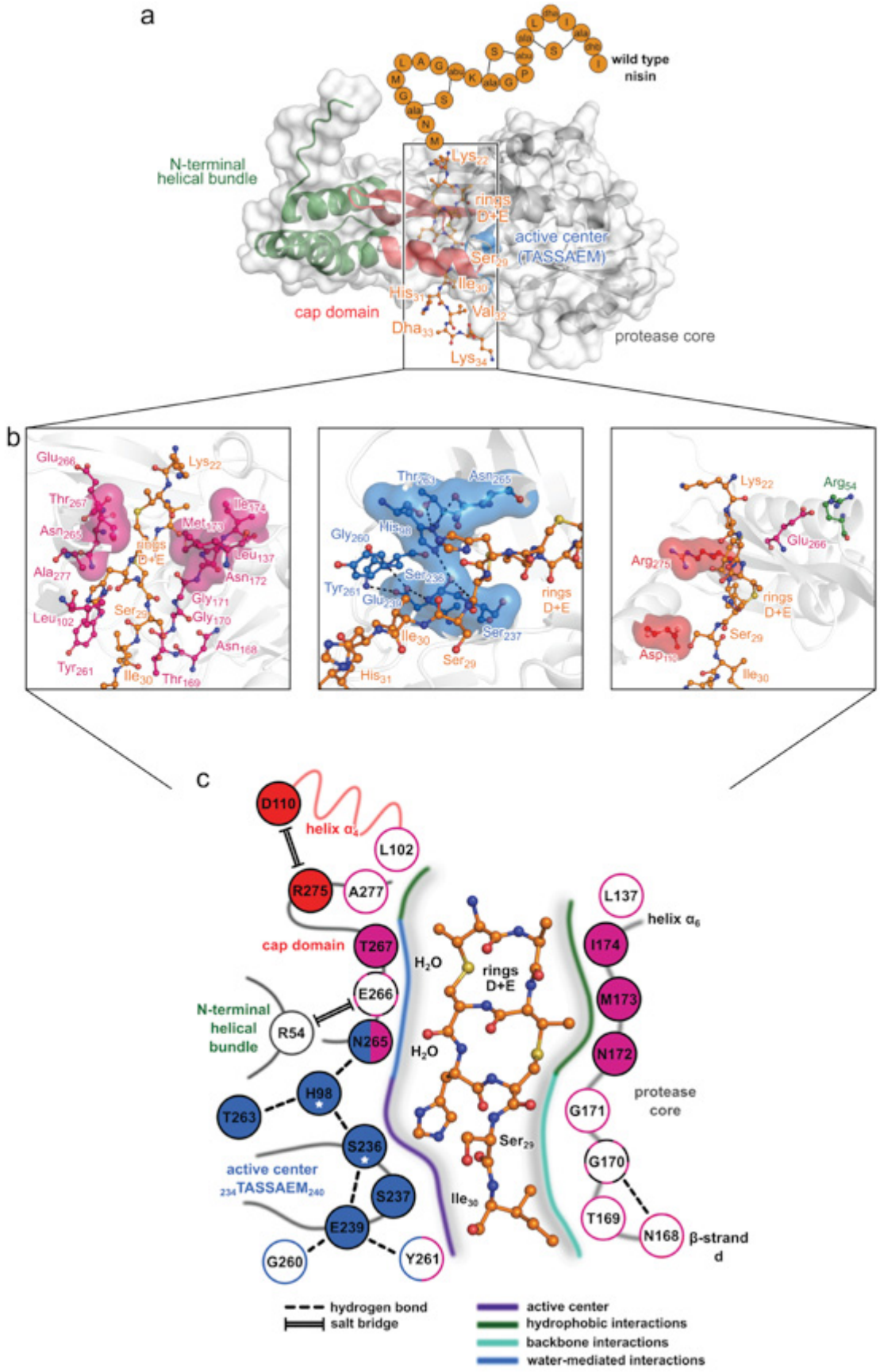
a
wild type nisin
N-terminal helical bundle
Lys22
rings D+E
active center (TASSAEM)
Ser29
Ile30
His31
Val32
Dha33
Lys34
cap domain
protease core
b
Glu266
Lys22
Thr267
Ile174
Asn265
Met173
rings D+E
Leu137
Ala277
Asn172
Gly171
Ser29
Leu102
Gly170
Asn168
Tyr261
Ile30
Thr169
Thr267
Asn265
Gly260
His31
Ser29
Tyr261
Glu278
rings D+E
Ile30
Ser237
Ser29
His31
Lys22
Arg54
Glu266
Arg275
rings D+E
Ser29
Asp116
Ile30
c
D110
helix α4
L102
R275
A277
cap domain
T267
E266
N-terminal helical bundle
R54
N265
H98
T263
S236
active center 234TASSAEM240
S237
E239
G260
Y261
H2O
rings D+E
H2O
Ser29
Ile30
L137
helix α6
I174
M173
N172
protease core
G171
G170
T169
N168
β-strand d
hydrogen bond
salt bridge
active center
hydrophobic interactions
backbone interactions
water-mediated interactions

Supplementary information

Structural basis of lantibiotic recognition by the nisin resistance protein from *Streptococcus agalactiae*

Sakshi Khosa[a#], Benedikt Frieg[b#], Daniel Mulnaes[b] Diana Kleinschrodt[c], Astrid Hoeppner[d], Holger Gohlke[b] and Sander H.J. Smits[a]*

[a]Institute of Biochemistry, Heinrich Heine University, Universitätsstr. 1, 40225 Düsseldorf, Germany
[b]Institute of Pharmaceutical and Medicinal Chemistry, Heinrich Heine University, Universitätsstr. 1, 40225 Düsseldorf, Germany
[c]Protein Production Facility, Heinrich Heine University, Universitätsstr. 1, 40225 Düsseldorf, Germany
[d]Crystal and X-ray Facility, Heinrich Heine University, Universitätsstr. 1, 40225 Düsseldorf, Germany

[#]Both authors contributed equally.
*Corresponding author: Phone: +49-211-81-12647; Fax: +49-211-81-15310; E-Mail: sander.smits@hhu.de

Material and Methods

Cloning, expression and purification of *Sa*NSR

The primers were designed in such a way that the first 30 amino acids encoding for the transmembrane helix were not present in the construct. This allowed soluble expression and included an 8xhis-tag at the N-terminus for purification purposes. *Sa*NSR was expressed and purified via two-step purification protocol. A single transformed colony was inoculated into 20 ml LB media containing 30 µg ml^{-1} kanamycin. The culture was grown for 14 h at 310 K with shaking at 200 rev min^{-1}. 2 L LB media with 30 µg ml^{-1} kanamycin was inoculated with the overnight culture at an OD600 of 0.05 and grown at 310 K with shaking at 170 rev min^{-1} till OD_{600} of 0.3 was reached. The temperature was lowered to 291 K and the cells were further grown till OD_{600} of 0.8 before induction with 1 mM IPTG. The cells were further grown for 15 h.

The cells were harvested by centrifugation at 8000 rev min^{-1} for 20 min at 277 K. The harvested cell pellet was stored at 253 K till further use. The stored cell pellet was thawed and resuspended in 10 ml of buffer A (50 mM Tris pH 8.0, 50 mM NaCl and 10% glycerol) and 10 mg of DNase (Deoxyribonuclease I from bovine pancreas, Sigma Aldrich) was added. The cells were lysed five times using a cell disruptor (Constant Cell Disruption Systems, United Kingdom) at 37709 psi (1kbar = 14.50 psi). The lysate was centrifuged at 42000 rev min^{-1} for 60 min using a Ti60 rotor to remove unlysed cells and debris.

Histidine was added to the cleared lysate at a final concentration of 1 mM. The lysate was then applied to a Ni^{2+} loaded HiTrap HP Chelating column (GE Healthcare) pre-equilibrated with buffer B (20 mM Tris pH 8.0, 250 mM NaCl and 1 mM Histidine) at a flow rate of 1 ml min^{-1}. The column was washed with six column volumes of buffer B. The protein was then eluted with increasing concentrations of Histidine from 1 mM to 120 mM, in form of a linear gradient spanning 60 min with a flow rate of 2 ml min^{-1}. The fractions containing the protein of interest were pooled and concentrated up to 12 mg ml^{-1} in an Amicon centrifugal filter concentrator with a 10 kDa cut-off membrane (Millipore). The concentrated protein was then further purified by size exclusion chromatography using Superose 12 GL 10/300 column (GE Healthcare), equilibrated with buffer C (25 mM MES pH 6.0, 150 mM NaCl). The protein eluted as a single homogeneous peak and the concerned fractions were pooled and concentrated to 8.6 mg ml^{-1} as mentioned before. The purity of the protein was analyzed with SDS-PAGE and colloidal coomassie stain.

To determine the oligomeric state of *Sa*NSR protein in solution, we used conventional size-exclusion chromatography (SEC) and high performance liquid chromatography coupled to multi

angle light scattering detection (HPLC-MALS). SEC was performed as described previously[1] and the size-exclusion column was standardized with a gel filtration markers kit (Sigma).

Crystallization

Crystallization screening was performed at 285 K using NT8 robot (Formulatrix) and sitting-drop vapour diffusion method in Corning 3553 sitting drop plates. For initial screening different commercial crystallization screens were used {Nextal JCSG Core Suites I, Classics Suite, PEGs Suite, MPD Suite (Qiagen, Germany) and MIDAS (Molecular Dimensions, England)}. Nanodrops consisting of 0.1 µl each of protein and reservoir solution were mixed and equilibrated over 50 µl reservoir solution. The screening yielded some initial rod shaped crystals after three days in the condition 0.5 M lithium sulfate and 15% (w/v) PEG 8000 (Classic I suite, condition F5). The initial crystals were optimized by varying the concentration of PEG (5, 10, 15, 20, 25 and 30% (w/v)) and salt (0.4, 0.5, 0.6 and 0.7 M), using hanging and sitting-drop vapour diffusion methods at 297 K and 285 K, respectively. Each drop consisted of 1 µl of protein solution (concentration of 9 mg ml^{-1}) mixed with 1 µl of reservoir solution, equilibrated over a reservoir volume of 500 µl. Crystals were obtained after one day and grew to their maximum dimensions within 5 days. For preliminary analysis of the crystals see [1].

Expression, purification and crystallization of selenomethionine-substituted SaNSR

For selenomethionine substitution, *E. coli* BL834 (DE3) cells were grown according to manufacturer's protocol in M9 minimal media (Molecular Dimensions) supplemented with 50 µg ml^{-1} of L-seleno-methionine. Expression and purification were identical to the native SaNSR [1]. Selenomethionine derivatized *Sa*NSR was crystallized in a similar manner as the native protein, using the hanging drop vapor diffusion method with a protein concentration of 10 mg ml^{-1}.

Cloning of pNZ-SV-*Sa*NSR and variants

The plasmid pNZ-SV-*Sa*NSR (N-His) was cloned with the In-Fusion HD PCR Cloning Kit (Clontech) as previously published [2]. Different mutations were introduced into the pNZ-SV-*Sa*NSR (N-His) using standard site-directed mutagenesis protocol. The used primers are listed in Supplementary Table 1a.

Expression of *Sa*NSR and its variants in *L. lactis* NZ9000

The plasmid encoding pNZ-SV-*Sa*NSR and its variants were transformed into the nisin sensitive *L. lactis* strain NZ9000. As a control the empty vector was also transformed, termed NZ9000Erm. The

strains expressing NZ9000SaNSR and its mutations were grown in GM17 media supplemented with 5 μg ml^{-1} erythromycin to an OD_{600} of 0.8. The expression was induced by the addition of nisin (at a final concentration of 1 $ngml^{-1}$) and the cultures were further grown overnight. The cells were then diluted to an OD_{600} of 0.1 in fresh GM17 media supplemented with 5μg ml^{-1} erythromycin. These cells were then used for the assays described below.

Cloning, Overexpression and purification of nisin and its variants

Nisin was purified from commercially available powder as described [3]. The cloning, overexpression and purification of precursor nisin variants were performed as described previously [3,4], excepting that the elution buffer of the cationic exchange chromatography of the various precursor nisin variants were changed to 50 mM HEPES-NaOH, pH 7.0, 1 M NaCl, and 10% glycerol. The concentrations of nisin and its variants were determined by using RP-HPLC and in order to activate the nisin variants, the leader peptide was cleaved off using the protease NisP as previously described, thereby [5].

Molecular dynamics simulations

Structures of NSR_{Apo}, NSR_{Tail}, and $NSR_{Nisin,1-3}$ were prepared using LEaP[6] of the Amber 14 suite of programs [7]. First, missing hydrogen atoms were added by LEaP [6], and histidine residues were assigned the HIE state. Second, counter ions were added to neutralize each system. Finally, systems were solvated using the TIP3P water model [8]. The obtained systems comprised ~ 60.000 atoms. Atomic partial charges for Dha33 (dehydroalanine) and rings D and E in nisin, which are treated as one "residue" in the Amber scheme, were obtained following the RESP procedure[9] using Gaussian09 [10]. For the non-standard amino acid Dha33, force field parameters were adapted from ref. [11]. All other parameters were taken from the Amber ff99SB force field [12,13]. Structural relaxation, thermalization, and production runs of MD simulations were conducted with pmemd.cuda [14] of Amber 14 [7]. Two steps of energy minimization were performed to relax the systems. First, harmonic restraints with a force constant of 25 $kcalmol^{-1}Å^{-2}$ were applied to all protein atoms while all other atoms were free to move during 50 cycles of steepest descent (SD) and 200 cycles of conjugate gradient (CG) minimization. Second, the force constant of the harmonic restraints was reduced to 5 $kcalmol^{-1}Å^{-2}$, and 50 cycles of SD and 200 cycles of CG minimization were performed. Subsequently, the systems were heated from 100 K to 299.9 K, 300 K, or 300.1 K during canonical (NVT) MD simulations of 50 ps length to setup three independent MD production simulations for NSR_{Apo}, NSR_{Tail}, and $NSR_{Nisin,1-3}$, respectively. Afterwards, the density was adjusted to 1 g·cm-3 during 30 ps of isobaric-isothermal (NPT) MD simulations. During heating and density

adaptation, positional restraints of 5 kcal·mol^{-1}·Å^{-2} were applied to all protein atoms. Finally, these positional restraints were removed by gradually decreasing the force constant from 5 to 0 kcal·mol^{-1}·Å^{-2} in six NVT-MD runs of 10 ps length each. For MD simulations, the particle mesh Ewald (PME) method [15-17] was employed to treat long-range electrostatic interactions. For short-range non-bonded interactions, we set a distance cutoff of 8 Å. The SHAKE algorithm [18] was applied to all bonds involving hydrogens, allowing a 2 fs time step for integrating Newton's equations of motion. Production MD simulations were performed in the NVT ensemble at 300 K for 500 ns. Coordinates were saved every 20 ps and used for analyses. This led to a total simulation time of 5 x 3 x 500 ns = 7.5 µs.

Supplementary Table 1

(a) IC_{50} values of nisin and its variants against the NZ9000Erm and NZ9000-*Sa*NSR strains as well as the calculated "Fold of resistance".

	NZ9000Erm (nM)	NZ9000-*Sa*NSR (nM)	*Fold of resistance*
Nisin	3.3±0.1	66.4±2.1	20.1
CCCCA	42.2±0.7	57.8±3.3	1.7
CCCAA	184.9±9.7	259.5±16.6	1.4
$Nisin_{1-22}$	294.7±9.7	121.1±6.1	0.4
$Nisin_{1-28}$	277.1±14.0	103.5±5.5	0.4

The values reported are the average over minimum triplicates ± SEM.

(b) IC_{50} values of nisin against the NZ9000Erm, NZ9000-*Sa*NSR, and NZ9000-*Sa*NSR variant strains.

	IC_{50} value (nM)	*Activity (%)*
NZ9000Erm	3.3±0.1	0
NZ9000-*Sa*NSR (wildtype)	66.4±2.1	100
NZ9000-*Sa*NSR-His_{98}Ala	12.3±1.5	14.2
NZ9000-*Sa*NSR-Ser_{236}Ala	12.6±0.7	14.6
NZ9000-*Sa*NSR-Ser_{237}Ala	50.2±2.3	74.3
NZ9000-*Sa*NSR-Glu_{239}Ala	17.1±0.7	21.7
NZ9000-*Sa*NSR-Asn_{172}Ala	33.5±2.9	47.7
NZ9000-*Sa*NSR-Met_{173}Ala	30.3±1.4	42.7
NZ9000-*Sa*NSR-Ile_{174}Ala	24.1±2.2	32.9
NZ9000-*Sa*NSR-Thr_{263}Ala	16.0±0.3	20.1
NZ9000-*Sa*NSR-Asn_{265}Ala	22.1±1.1	29.7
NZ9000-*Sa*NSR-Thr_{267}Ala	48.5±0.6	71.6
NZ9000-*Sa*NSR-Asp_{110}Ala	32.8±2.1	46.7
NZ9000-*Sa*NSR-Arg_{275}Ala	33.6±2.3	47.9

The values reported are the average over minimum triplicates ± SEM.

Supplementary Table 2: Primers used in this study.
Shown below are the primers used to create the point mutations within the expression plasmid pNZ-SV-*Sa*NSR-NHis [2] .

Primer Name	*Sequence (5'-3')*
His_{98}Ala-for	CGGTATGGAGGAGGTAAAGCAAGTCAAATATTATCC
His_{98}Ala-rev	GGATAATATTTGACTTGCTTTACCTCCTCCATACCG
Ser_{236}Ala-for	CTAATCATAAAACTGCTGCGTCGGCAGAAATGAC
Ser_{236}Ala-rev	GTCATTTCTGCCGACGCAGCAGTTTTATGATTAG
Ser_{237}Ala-for	CTAATCATAAAACTGCTAGTGCAGCAGAAATGACTTTTTTATC
Ser_{237}Ala-rev	GATAAAAAAGTCATTTCTGCTGCACTAGCAGTTTTATGATTAG
Glu_{239}Ala-for	CTGCTAGTTCGGCAGCAATGACTTTTTTATC
Glu_{239}Ala-rev	GATAAAAAAGTCATTGCTGCCGAACTAGCAG
Asn_{172}Ala-for	CGAATAATACTGGCGGCGCAATGATCCCTATGATTG
Asn_{172}Ala-rev	CAATCATAGGGATCATTGCGCCGCCAGTATTATTCG
Met_{173}Ala-for	GAATAATACTGGCGGCAATGCAATCCCTATGATTGGG
Met_{173}Ala-rev	CCCAATCATAGGGATTGCATTGCCGCCAGTATTATTC
Ile_{174}Ala-for	CTGGCGGCAATATGGCACCTATGATTGGGGG
Ile_{174}Ala-rev	CCCCCAATCATAGGTGCCATATTGCCGCCAG
Thr_{263}Ala-for	CAGCAGGATATACGGCAGTTAATGAAACTTTC
Thr_{263}Ala-rev	GAAAGTTTCATTAACTGCCGTATATCCTGCTG
Asn_{265}Ala-for	GCAGGATATACGACTGTTGCAGAAACTTTCATGCTTTAC
Asn_{265}Ala-rev	GTAAAGCATGAAAGTTTCTGCAACAGTCGTATATCCTGC
Thr_{267}Ala-for	GATATACGACTGTTAATGAAGCATTCATGCTTTACGACG
Thr_{267}Ala-rev	CGTCGTAAAGCATGAATGCTTCATTAACAGTCGTATATC
Asp_{110}Ala-for	GAGACTGTACGAAGAGCAACCCTAGATAGTCG
Asp_{110}Ala-rev	CGACTATCTAGGGTTGCTCTTCGTACAGTCTC
Arg_{275}Ala-for	GCTTTACGACGGTGCTGCATTAGCTTTAACTACAG
Arg_{275}Ala-rev	CTGTAGTTAAAGCTAATGCAGCACCGTCGTAAAGC

Supplementary Figure 1: Schematic representation of the structure of nisin and the different variants used in this study.

Shown are structural representations of wildtype nisin and the variants CCCCA, CCCAA, $nisin_{1-22}$ and $nisin_{1-28}$. Highlighted in yellow are the dehydrated amino acids while the amino acids which are dehydrated as well as cyclized are shown in orange. The lanthionine rings are also shown in orange and are numbered A-E.

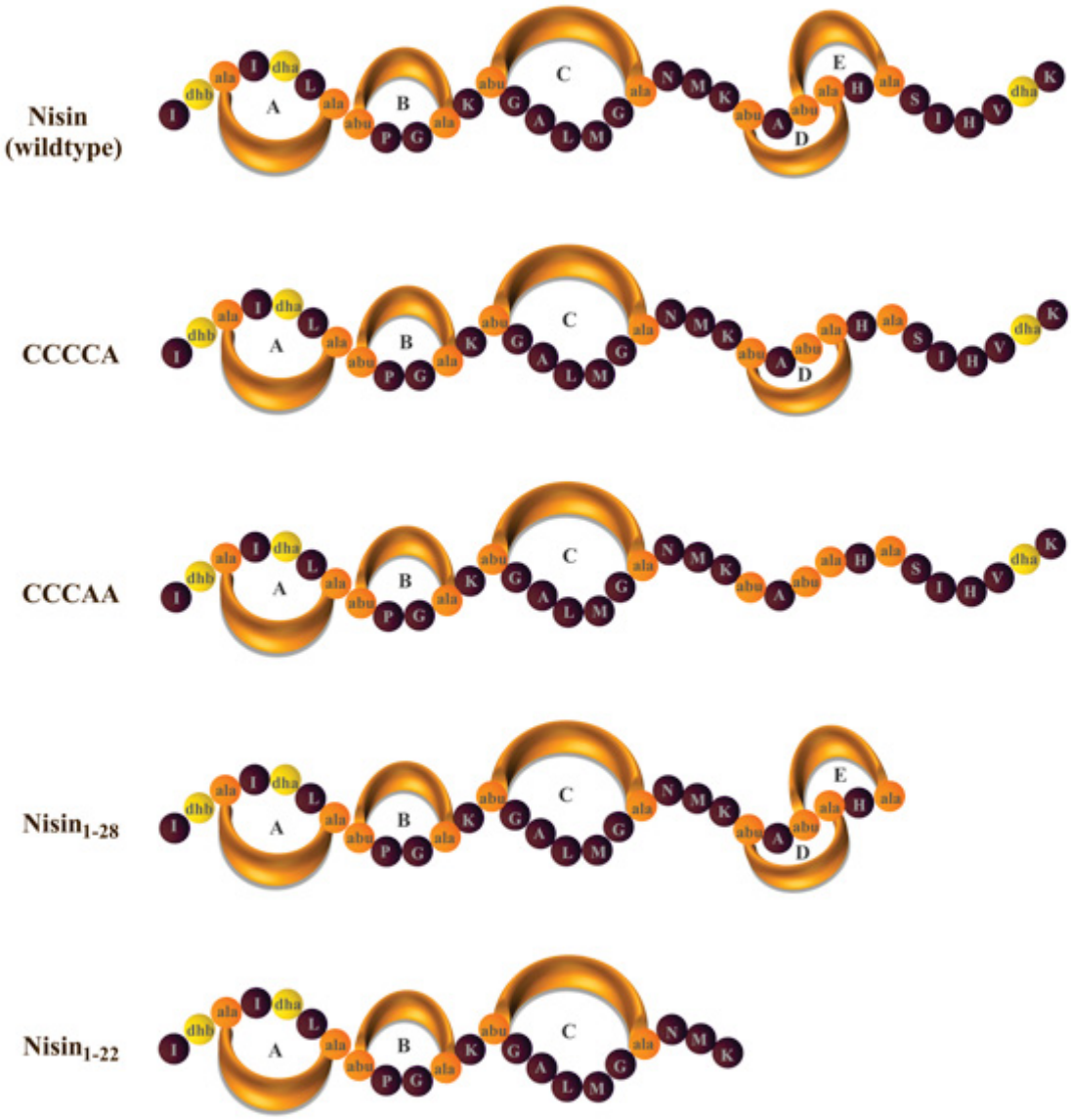

Supplementary Figure 2: Purification, oligomeric state and structure of *Sa*NSR.
(a) 15% SDS gel showing purified *Sa*NSR after the two-step purification involving IMAC and SEC. Lane M represents PageRuler Unstained Protein Ladder; the remaining lanes are the purified *Sa*NSR fractions at 35 kDa. The lower 30 kDa band also arises from *Sa*NSR, as verified by mass spectrometry, and could likely be a degradation product. (b) Determination of the oligomeric state of the purified *Sa*NSR protein using HPLC-MALS. The x-axis represents the time in minutes; the left and right y-axes depict the relative intensity and molecular mass, respectively. The blue line is the differential refractive index signal; the blue dotted line indicates the calculated molar mass. (c) The structure of *Sa*NSR in the asymmetric unit. The four copies of the monomer are colored in green, cyan, pink and yellow for chains A, B, C and D, respectively.

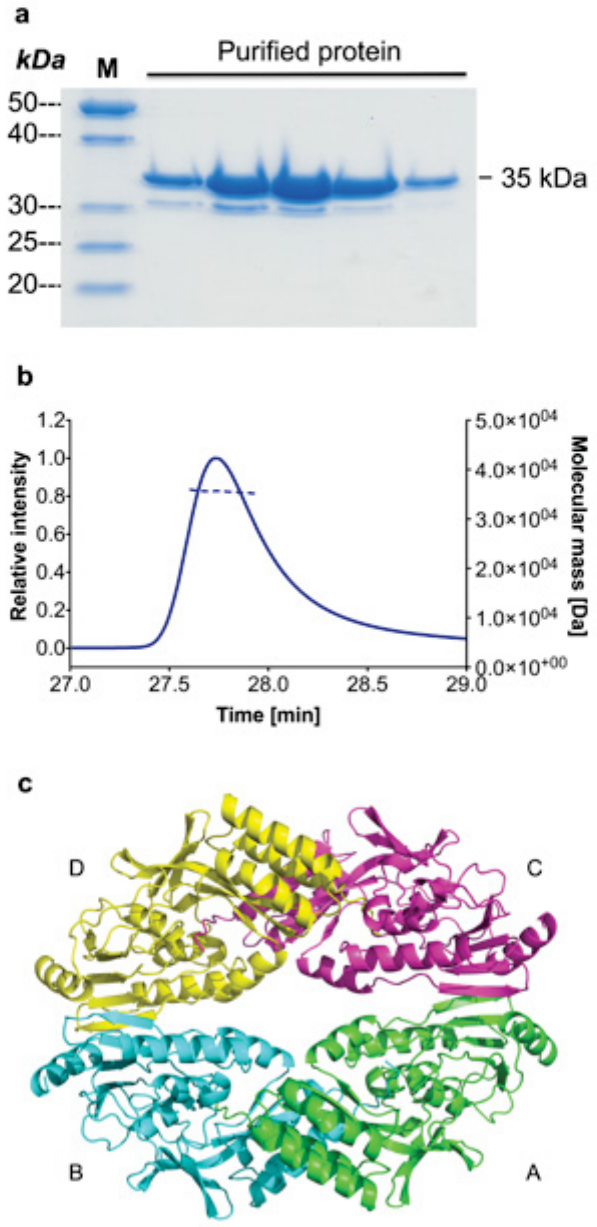

Supplementary Figure 3: Alignment of the nisin resistance proteins.
Homolog sequences of nisin resistance protein were aligned using ClustalW2 [19]. Visualization of the sequence alignment was performed by ESPript [20]. Secondary structure elements were calculated based on the *Sa*NSR structure. The TASSAEM motif is marked by a dotted blue line.

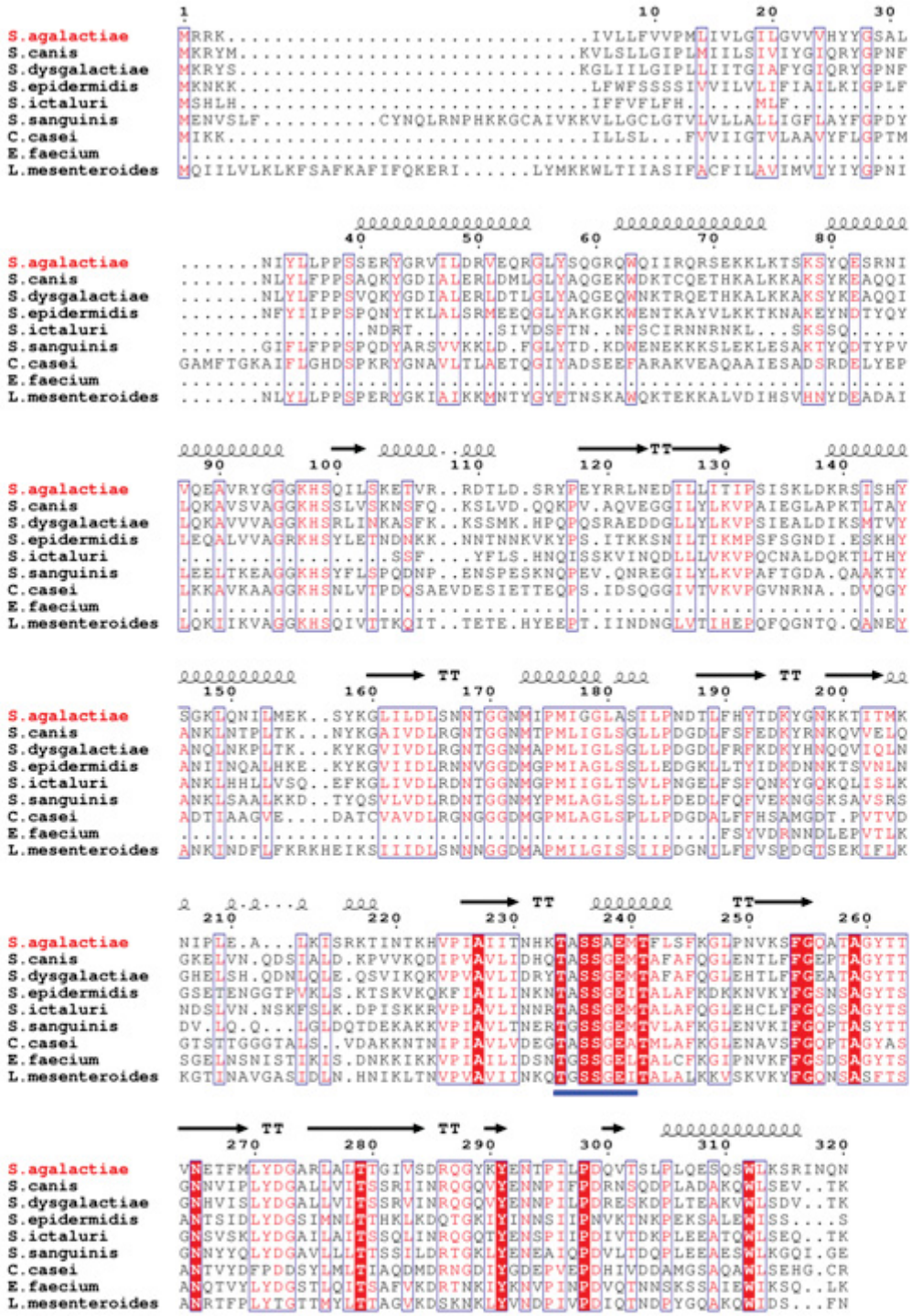
S.agalactiae
S.canis
S.dysgalactiae
S.epidermidis
S.ictaluri
S.sanguinis
C.casei
E.faecium
L.mesenteroides

Supplementary Figure 4: Mobility and structural deviations in MD simulations of NSR_{Apo} and NSR_{Tail}.

(a) Mean backbone RMSF of residues of the N-terminal helical bundle in NSR_{Apo} models after superimposition of the cap domain and the protease core for three trajectories (colored differently) of 500 ns length each. (b) Backbone RMSD for N-pep in the NSR_{Tail} model for three independent MD simulations. Mean values are shown in the legend. Mean standard error < 0.1 Å and not shown.

(b)

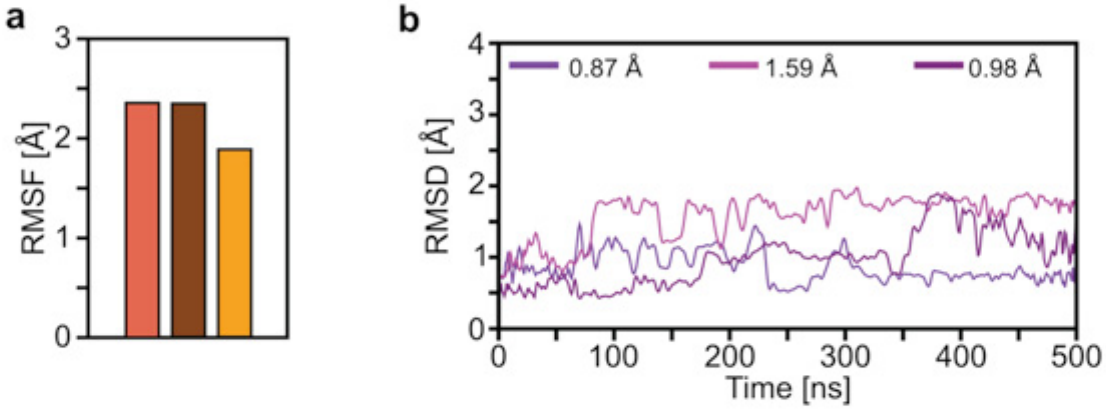

Supplementary Figure 5: Models of *Sa*NSR/nisin complexes used as starting structures for and RMSD analysis of MD simulations.

(a) View into the binding site of *Sa*NSR with Asn_{172}, Met_{173}, and Ile_{174} colored in magenta, Ser_{236} in blue, and Tyr_{261} in orange; for clarity, the N-terminal bundle and protease core domains of *Sa*NSR were omitted. The C-terminus of nisin (residues 22 - 34) is shown in ball and stick representation. The right panels show a close-up view of all initial NSR/nisin complexes used as starting structures for the MD simulations (red: $NSR_{Nisin,1}$; green: $NSR_{Nisin,2}$; blue: $NSR_{Nisin,3}$).

(b) All atom RMSD values, relative to the respective average structures, over 500 ns of MD simulations for the C-terminus of nisin and for the $Nisin_{core}$ (composed of rings D and E, Ser_{29}, and Ile_{30}; see Figure 4b-d). RMSD values are shown for each of the three independent MD trajectories.

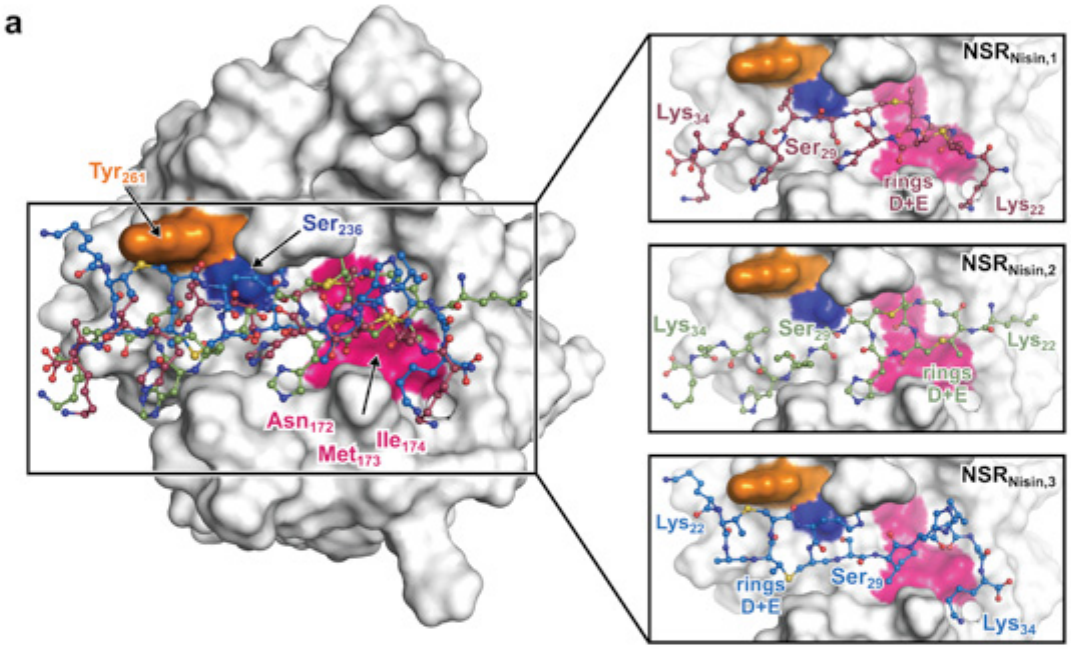

b

Model \ RMSD [Å][a]	mean $Nisin_{C\text{-}terminus}$ [b]	mean $Nisin_{core}$ [b]
$NSR_{Nisin,1}$ (1)	2.75	1.38
$NSR_{Nisin,1}$ (2)	2.60	1.34
$NSR_{Nisin,1}$ (3)	3.19	2.27
$NSR_{Nisin,2}$ (1)	1.44	0.80
$NSR_{Nisin,2}$ (2)	1.80	1.34
$NSR_{Nisin,2}$ (3)	2.16	1.28

[a] relative to average structure
[b] MSE < 0.01 Å

Supplementary Figure 6: Structural analyses of the TASSAEM region over the MD trajectories.

(a) Close-up view of the catalytic site residues in blue and Gly_{171} from the protease core in magenta ball-and-stick representation. Identified hydrogen bonds (1 – 7) are depicted as orange dotted lines. The table shows minimum (min.) and maximum (max.) occupancies of hydrogen bonds 1 to 7 across the six MD trajectories. Distance between the side chain oxygen in Ser_{237} and the carbonyl carbon of ring E from the nisin cleavage site (b), and the side chain oxygen in Ser_{237} and the δ-nitrogen in His_{98} (c) for both $Nsr_{Nisin,1}$ (top panel) and $Nsr_{Nisin,2}$ (bottom panel) models during the three independent MD simulations. Mean values over each trajectory are shown in the legend.

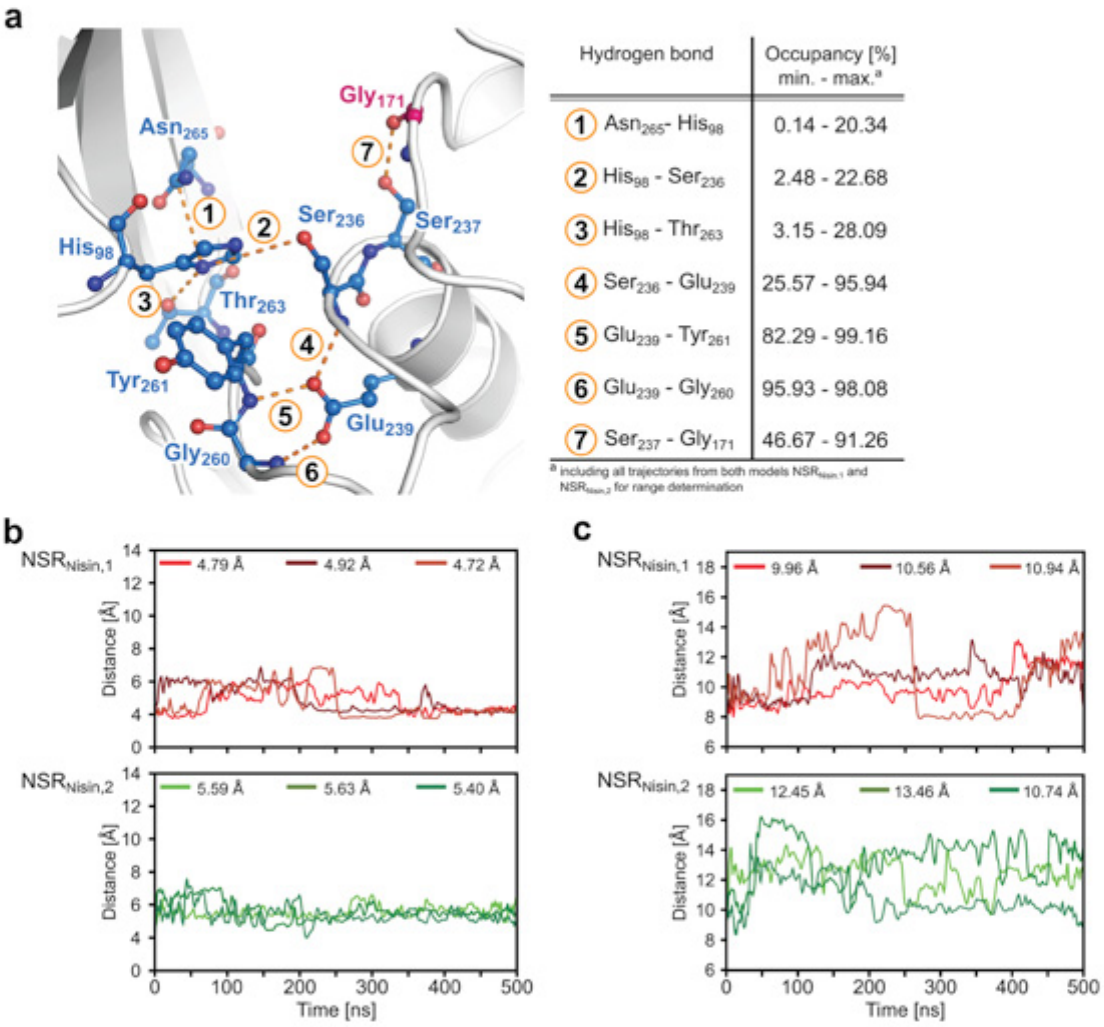

Hydrogen bond	Occupancy [%] min. - max.[a]
1 Asn_{265}- His_{98}	0.14 - 20.34
2 His_{98} - Ser_{236}	2.48 - 22.68
3 His_{98} - Thr_{263}	3.15 - 28.09
4 Ser_{236} - Glu_{239}	25.57 - 95.94
5 Glu_{239} - Tyr_{261}	82.29 - 99.16
6 Glu_{239} - Gly_{260}	95.93 - 98.08
7 Ser_{237} - Gly_{171}	46.67 - 91.26

[a] including all trajectories from both models $NSR_{Nisin,1}$ and $NSR_{Nisin,2}$ for range determination

Supplementary Figure 7: Energetic and structural analyses of nisin binding over the MD trajectories.

(a) Per-residue effective binding energies computed by the MM-PBSA approach for residues within 5 Å of the C-terminus of nisin occupying the catalytic site of *Sa*NSR for model $NSR_{Nisin,1}$ (red) and $NSR_{Nisin,2}$ (green). The gray lines indicate a threshold of ± 0.8 kcal mol^{-1}. (b) Close-up view of the binding site residues (magenta) in the crystal structure bound to nisin (orange). Identified hydrogen bonds (1 – 3) are depicted as orange dotted lines. (c) Distance between the side chain carboxylate of residue Glu_{266} and the guanidino group of Arg_{54} from the N-terminal helical bundle for both $NSR_{Nisin,1}$ (top panel) and $NSR_{Nisin,2}$ (bottom panel) over the course of 500 ns MD simulations. Mean values for each MD trajectory are shown in the legend. (d) Close-up view of the binding site residues (magenta) and nisin (orange). Water-mediated interactions (1 – 2) are indicated by dark blue dotted lines. In (b) and (d), the tables show minimum and maximum occupancies of hydrogen bonds or water-mediated interactions. Hydrogen bonds and water-mediated interactions were determined for each of the $NSR_{Nisin,1}$ and $NSR_{Nisin,2}$ trajectories.

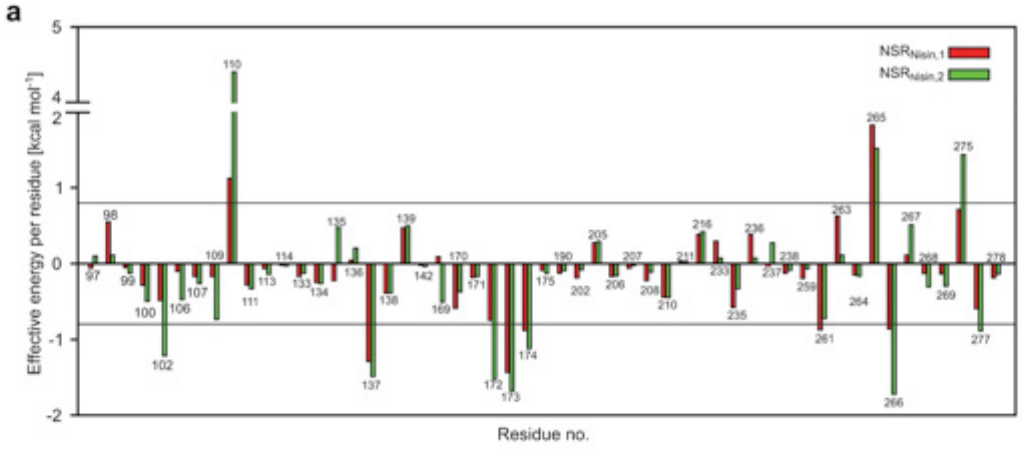

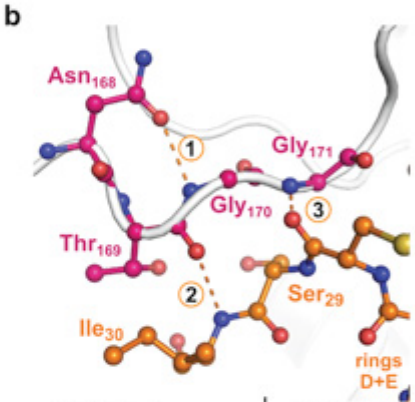

Hydrogen bond	Occupancy [%] min. - max.*
1 Asn_{168} - Gly_{170}	44.46 - 83.00
2 Thr_{169} - Nisin Ile_{30}	0.00 - 68.87
3 Gly_{171} - Nisin rings D+E	0.00 - 75.67

* including all trajectories from both models $NSR_{Nisin,1}$ and $NSR_{Nisin,2}$ for range determination

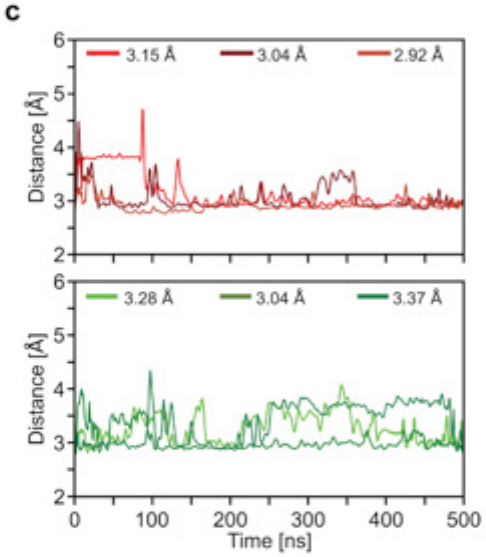

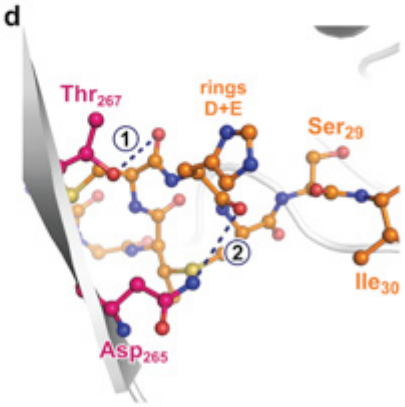

Water-mediated interaction	Occupancy [%] min. - max.*
1 Thr_{267} - Nisin rings D+E	0.18 - 28.26
2 Asn_{265} - Nisin rings D+E	9.92 - 20.46

* including all trajectories from both models $NSR_{Nisin,1}$ and $NSR_{Nisin,2}$ for range determination

Supplementary Figure 8: Structural analysis of helix α4 over the MD trajectories.
(a) For models $NSR_{Nisin,1}$, and $NSR_{Nisin,2}$ distances were measured between the side chain carboxylate of Asp_{110} and the guanidino group of Arg_{275}. (b) Residue-wise α-helix probability for residues that compose helix α4. Mean distances and mean α-helix probabilities over the independent MD trajectories are shown in the legend.

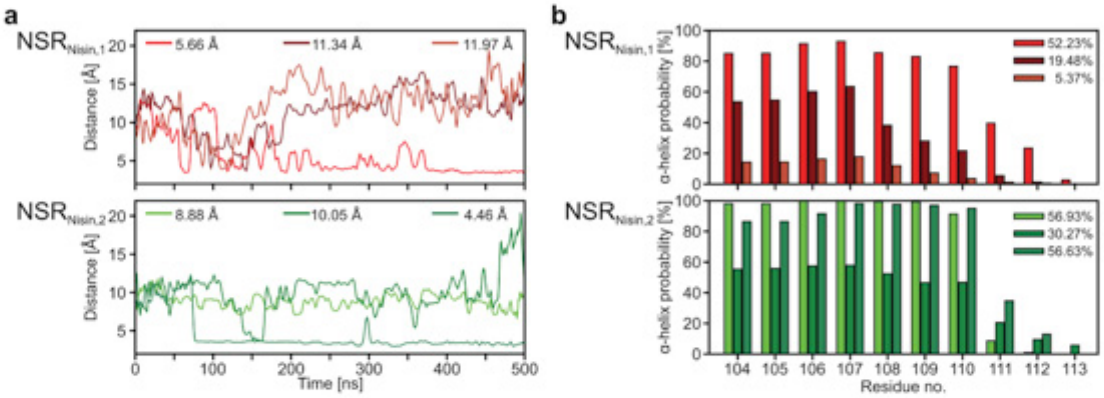

Supplementary References

1. Khosa, S., Hoeppner, A., Kleinschrodt, D. & Smits, S. Overexpression, purification, crystallization and preliminary X-ray diffraction of the nisin resistance protein from Streptococcus agalactiae. *Acta Crystallogr. F Biol. Crystallogr.* **71**, 0-0 (2015).
2. Khosa, S., Alkhatib, Z. & Smits, S.H. NSR from Streptococcus agalactiae confers resistance against nisin and is encoded by a conserved nsr operon. *Biol. Chem.* **394**, 1543-1549 (2013).
3. Abts, A. et al. Easy and Rapid Purification of Highly Active Nisin. *International Journal of Peptides* **2011**, 9 (2011).
4. Mavaro, A. et al. Substrate recognition and specificity of the NisB protein, the lantibiotic dehydratase involved in nisin biosynthesis. *J. Biol. Chem.* **286**, 30552-30560 (2011).
5. Abts, A., Montalban-Lopez, M., Kuipers, O.P., Smits, S.H. & Schmitt, L. NisC binds the FxLx motif of the nisin leader peptide. *Biochemistry* **52**, 5387-5395 (2013).
6. Zhang, W., Hou, T., Schafmeister, C., Ross, W.S. & Case, D.A. LEaP. *University of California, San Francisco* (1995).
7. Case, D.A. et al. AMBER 14. *University of California, San Francisco.* (2014).
8. Jorgensen, W.L., Chandrasekhar, J., Madura, J.D., Impey, R.W. & Klein, M.L. Comparison of simple potential functions for simulating liquid water. *J. Chem. Phys.* **79**, 926-935 (1983).
9. Bayly, C.I., Cieplak, P., Cornell, W.D. & Kollman, P.A. A well-behaved electrostatic potential based method using charge restraints for deriving atomic charges - the RESP Model. *J. Phys. Chem.* **97**, 10269-10280 (1993).
10. Frisch, M.J. et al. Gaussian 09. (Gaussian, Inc., Wallingford, CT, USA, 2009).
11. Alagona, G. & Ghio, C. Force field parameters for molecular mechanical simulation of dehydroamino acid residues. *J. Comput. Chem.* **12**, 934-942 (1991).
12. Cornell, W.D. et al. A second generation force field for the simulation of proteins, nucleic acids, and organic molecules. *J. Am. Chem. Soc.* **118**, 2309-2309 (1996).
13. Hornak, V. et al. Comparison of multiple Amber force fields and development of improved protein backbone parameters. *Proteins: Struct., Funct., Bioinf.* **65**, 712-725 (2006).
14. Salomon-Ferrer, R., Gotz, A.W., Poole, D., Le Grand, S. & Walker, R.C. Routine microsecond molecular dynamics simulations with Amber on GPUs. 2. Explicit solvent particle mesh ewald. *J. Chem. Theory Comput.* **9**, 3878-3888 (2013).
15. York, D.M., Darden, T.A. & Pedersen, L.G. The effect of long-range electrostatic interactions in simulations of macromolecular crystals - a comparison of the ewald and truncated list methods. *J. Chem. Phys.* **99**, 8345-8348 (1993).
16. Darden, T., York, D. & Pedersen, L. Particle mesh Ewald: An N· log (N) method for Ewald sums in large systems. *J. Chem. Phys.* **98**, 10089-10092 (1993).
17. Srinivasan, J., Cheatham, I., T. E., Cieplak, P., Kollman, P.A. & Case, D.A. Continuum solvent studies of the stability of DNA, RNA, and phosphoramidate - DNA helices. *J. Am. Chem. Soc.* **120**, 9401-9409 (1998).
18. Ryckaert, J.P., Ciccotti, G. & Berendsen, H.J.C. Numerical integration of cartesian equations of motion of a system with constraints molecular dynamics of n-alkanes. *J. Comput. Phys.* **23**, 327-341 (1977).
19. Larkin, M.A. et al. Clustal W and Clustal X version 2.0. *Bioinformatics* **23**, 2947-2948 (2007).
20. Robert, X. & Gouet, P. Deciphering key features in protein structures with the new ENDscript server. *Nucleic Acids Res.* **42**, W320-W324 (2014).

3.4 Chapter IV – Response Regulator NsrR

Published in: ACTA CRYSTALLOGRAPHICA SECTION F

Impact Factor: 0.527

Own work: 60%

Establishing and Optimization of Expression and Purification Protocols

Crystal Screening and Optimization

Diffraction Experiments and their Analyses

Writing the Manuscript

Over-expression, Purification and Crystallization of the Response Regulator NsrR Involved in Nisin Resistance

Sakshi Khosa, Astrid Hoeppner, Diana Kleinschrodt, and Sander H.J. Smits

STRUCTURAL BIOLOGY COMMUNICATIONS

ISSN 2053-230X

Overexpression, purification and crystallization of the response regulator NsrR involved in nisin resistance

Sakshi Khosa,[a] Astrid Hoeppner,[b] Diana Kleinschrodt[c] and Sander H. J. Smits[a]*

[a]Institute of Biochemistry, Heinrich-Heine-University, Universitätsstrasse 1, 40225 Düsseldorf, Germany, [b]Crystal Farm and X-ray Facility, Heinrich-Heine-University, Universitätsstrasse 1, 40225 Düsseldorf, Germany, and [c]Protein Production Facility, Heinrich-Heine-University, Universitätsstrasse 1, 40225 Düsseldorf, Germany. *Correspondence e-mail: sander.smits@hhu.de

Received 4 August 2015
Accepted 3 September 2015

Edited by R. L. Stanfield, The Scripps Research Institute, USA

Keywords: response regulator; nisin; lantibiotic; resistance; X-ray analysis.

Supporting information: this article has supporting information at journals.iucr.org/f

A number of Gram-positive bacteria produce a class of bacteriocins called 'lantibiotics'. These lantibiotics are ribosomally synthesized peptides that possess high antimicrobial activity against Gram-positive bacteria, including clinically challenging pathogens, and are therefore potential alternatives to antibiotics. All lantibiotic producer strains and some Gram-positive non-producer strains express protein systems to circumvent a suicidal effect or to become resistant, respectively. Two-component systems consisting of a response regulator and a histidine kinase upregulate the expression of these proteins. One of the best-characterized lantibiotics is nisin, which is produced by *Lactococcus lactis* and possesses bactericidal activity against various Gram-positive bacteria, including some human pathogenic strains. Within many human pathogenic bacterial strains inherently resistant to nisin, a response regulator, NsrR, has been identified which regulates the expression of proteins involved in nisin resistance. In the present study, an expression and purification protocol was established for the NsrR protein from *Streptococcus agalactiae* COH1. The protein was successfully crystallized using the vapour-diffusion method, resulting in crystals that diffracted X-rays to 1.4 Å resolution.

1. Introduction

The increasing incidence of antibiotic resistance has led to an urgent need for alternative therapeutic options. A potential class of alternatives are small ribosomally synthesized antimicrobial peptides called lantibiotics, which are produced by various Gram-positive bacteria. Lantibiotics bind to lipid II, an essential cell-membrane precursor, forming a complex that inhibits cell-wall synthesis and forms pores within the membrane (Breukink & de Kruijff, 2006; Hsu *et al.*, 2004). Lantibiotics have a wide antibacterial efficacy and their therapeutic potential has already been recognized (Hancock & Sahl, 2006; Boakes & Wadman, 2008).

The best-characterized lantibiotic is nisin, which is produced by some *Lactococcus lactis* strains and has a wide bactericidal activity spectrum against human pathogenic strains including *Clostridium difficile* and methicillin-resistant *Staphylococcus aureus* (MRSA) (Bartoloni *et al.*, 2004; Severina *et al.*, 1998; Cotter *et al.*, 2005). Nisin has also been used in the food industry as a food preservative (Delves-Broughton *et al.*, 1996).

All nisin producer strains naturally express an immunity system to avoid a suicidal effect. However, there are also some nisin-nonproducing strains, including various pathogenic bacteria such as *Streptococcus agalactiae* and *S. aureus*, which are naturally resistant to nisin (Harris *et al.*, 1992). There is a

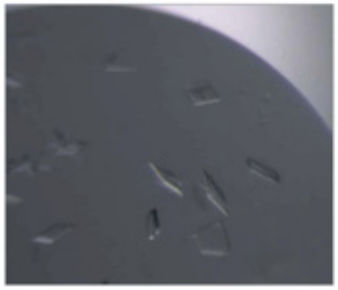

Table 1
Macromolecule-production information.

Source organism	*S. agalactiae*
DNA source	*S. agalactiae*
Forward primer	GGAGGGCATATGTCACAAGAGCAAGG
Reverse primer	GGAATCGGATCCTGTAGTAAATACCCAACTCC
Expression vector	pET-24a
Expression host	*E. coli* BL21 (DE3)
Complete amino-acid sequence of the construct produced	MSQEQGKIYIVEDDMTIVSLLKDHLSASYHVSSV-SNFRDVKQEIIAFQPDLILMDITLPYFNGFYW-TAELRKFLTIPIIFISSSNDEMDMVMALNMGG-DDFISKPFSLAVLDAKLTAILRRSQQFIQQEL-TFGGFTLTREGLLSSQDKEVILSPTENKILSI-LLMHPKQVVSKESLLEKLWENDSFIDQNTLNV-NMTRLRKKIVPIGFDYIHTVRGVGYLLQDPNS-SSVDKLAAALEHHHHHH

whole gene operon associated with the mechanism of nisin resistance, which was recently found in various species of Gram-positive human-pathogenic bacteria. The operon consists of four genes which encode the nisin-resistance protein NSR, a two-component system (TCS) and an ABC transporter (Khosa *et al.*, 2013).

The TCS comprises a sensor histidine kinase (NsrK) localized in the membrane and a response regulator (NsrR). NsrK is autophosphorylated upon external signal (in this case, nisin) and the phosphate is then transferred to an aspartate residue of the response regulator NsrR. This phosphorylation activates the regulator, thereby triggering transcription of the genes (Stock *et al.*, 2000; Khosa *et al.*, 2013).

Various two-component systems have been identified which are involved in lantibiotic resistance (Draper *et al.*, 2015; Kawada-Matsuo, Oogai *et al.*, 2013). The BraRS, GraRS and VraSR TCSs of *S. aureus* are associated with resistance against bacitracin, nisin and nukacin ISK-1 (Kawada-Matsuo, Yoshida *et al.*, 2013). The LiaRS and CprRK TCSs were also shown to be involved in resistance against antimicrobial peptides in *Listeria monocytogenes* and *Clostridium difficile*, respectively (Bergholz *et al.*, 2013; Suárez *et al.*, 2013). The presence of these numerous TCS members emphasizes their importance in lantibiotic resistance. Thus, the structure of the response regulator involved would help to expand our restricted knowledge regarding the underlying mechanism of lantibiotic resistance involving response regulators.

In this study, we present the overexpression, purification and crystallization of the response regulator from *S. agalactiae*, NsrR.

2. Materials and methods

2.1. Macromolecule production

2.1.1. Cloning and expression. The GBSCOH1_0895 gene (accession No. HG939456.1) from *S. agalactiae* COH1 was amplified by PCR using chromosomal DNA as template and the primer pair NsrR-for (GGAGGGCATATGTCACAAGAGCAAGG) and NsrR-rev (GGAATCGGATCCTGTAGTAAATACCCAACTCC). The PCR fragment was digested with NdeI and BamHI and ligated into pET-24a, with a His_6 tag introduced at the C-terminus. The resulting plasmid pET-24a-NsrR (Table 1) was verified by sequencing and subsequently transformed into *Escherichia coli* BL21 (DE3) cells for expression. A single transformed colony was inoculated into 20 ml LB medium containing 30 µg ml^{-1} kanamycin. The culture was grown for 14 h at 310 K with shaking at 200 rev min^{-1}. 4 l LB medium with 30 µg ml^{-1} kanamycin was inoculated with the overnight culture at an OD_{600} of 0.05 and grown at 310 K with shaking at 170*g* until an OD_{600} of 0.3 was reached. The temperature was lowered to 291 K and the cells were further grown to an OD_{600} of 0.8 before induction with 1 m*M* IPTG. The cells were grown for a further 15 h. The cells were harvested by centrifugation at 8000 rev min^{-1} for 20 min at 277 K. The harvested cell pellet was stored at 253 K until further use.

2.1.2. Purification. In the purification of NsrR, all steps were performed at 277 K. The stored cell pellet was thawed and resuspended in 10 ml buffer *A* [50 m*M* Tris pH 8.0, 50 m*M* NaCl, 2 m*M* PMSF, 10%(*v*/*v*) glycerol] and 10 mg DNase (deoxyribonuclease I from bovine pancreas; Sigma–Aldrich) was added. The cells were lysed five times using a cell disruptor (Constant Cell Disruption Systems, UK) at 160 MPa. The lysate was centrifuged at 42 000 rev min^{-1} for 60 min using a Ti-60 rotor to remove unlysed cells and debris.

Imidazole was added to the cleared lysate to a final concentration of 20 m*M*. The lysate was then applied onto an Ni^{2+}-loaded HiTrap HP Chelating column (GE Healthcare) pre-equilibrated with buffer *B* (20 m*M* Tris pH 8.0, 250 m*M* NaCl, 20 m*M* imidazole) at a flow rate of 1 ml min^{-1}. The column was washed with six column volumes of buffer *B*. The protein was then eluted with increasing concentrations of imidazole from 20 to 400 m*M* in form of a linear gradient spanning 60 min with a flow rate of 2 ml min^{-1}. The fractions containing the protein of interest were pooled and concentrated to 8 mg ml^{-1} in an Amicon centrifugal filter concentrator with a 10 kDa cutoff membrane (Millipore). The concentrated protein was then further purified by size-exclusion chromatography using a Superdex 200 GL 10/300 column (GE Healthcare) equilibrated with buffer *C* (25 m*M* Tris pH 9.0, 50 m*M* NaCl, 2 m*M* PMSF). The protein eluted as a single homogeneous peak and the fractions containing the protein were pooled and concentrated to 11 mg ml^{-1} as mentioned before. The purity of the protein was analyzed with 15% SDS–PAGE and colloidal Coomassie stain (Dyballa & Metzger, 2009). The purified protein was directly used for crystallization. Macromolecule-production information is summarized in Table 1.

2.2. Crystallization

Crystallization screening was performed at 285 K using an NT8 robot (Formulatrix) and the sitting-drop vapour-diffusion method in Corning 3553 sitting-drop plates. For initial screening, various commercial crystallization screens were used [NeXtal JCSG Core Suites I, Classics Suite, PEGs Suite and MPD Suite (Qiagen, Germany) and MIDAS (Molecular Dimensions, England)]. Nanodrops consisting of 0.1 µl each of protein solution and reservoir solution were mixed and

Table 2
Crystallization.

Method	Vapour diffusion
Plate type	Sitting-drop vapour diffusion
Temperature (K)	285
Protein concentration (mg ml^{-1})	11
Buffer composition of protein solution	25 m*M* Tris pH 9.0, 50 m*M* NaCl, 2 m*M* PMSF
Composition of reservoir solution	PEG 1500 [21, 23, 25, 28 or 30%(*w*/*v*)] and buffer pH 6.0, 7.0, 8.0 or 9.0
Volume and ratio of drop	1 µl:1 µl
Volume of reservoir (µl)	500

equilibrated against 50 µl reservoir solution. The screening yielded initial rectangular plate-shaped crystals after 2 d in the condition 0.1 *M* SPG buffer (succinic acid:sodium dihydrogen phosphate:glycine in a molar ratio of 2:7:7) pH 8.0, 25%(*w*/*v*) PEG 1500 (PACT suite condition A5). The initial crystals were optimized by varying the concentration of PEG [21, 23, 25, 28 and 30%(*w*/*v*)] and the pH of the buffer (6.0, 7.0, 8.0 and 9.0) using the sitting-drop vapour-diffusion method at 285 K. Crystals of similar quality appeared throughout the conditions. Each drop consisted of 1 µl protein solution (at a concentration of 11 mg ml^{-1}) mixed with 1 µl reservoir solution and was equilibrated against a reservoir volume of 500 µl. Crystals were obtained after 1 d and grew to maximum dimensions of 80 × 40 × 20 µm within 3 d. Crystallization information is summarized in Table 2.

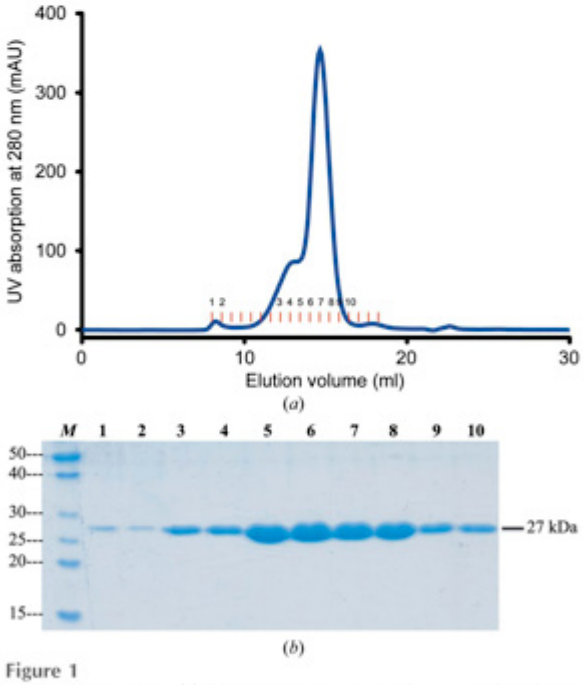

Figure 1
Purification of NsrR. (*a*) Chromatogram representing the purification of NsrR by size-exclusion chromatography. The *y* axis represents the UV absorption of the protein at 280 nm, while the *x* axis represents the elution volume. The red lines indicate the fractions collected. (*b*) 15% SDS–PAGE showing the purified NsrR fractions. Lane *M* contains molecular-mass marker (labelled in kDa); lanes 1–10 contain the corresponding purified NsrR fractions from the size-exclusion chromatogram displayed in (*a*).

Table 3
Data collection and processing.

Values in parentheses are for the outer shell.

Diffraction source	ID30A-3, ESRF
Wavelength (Å)	0.9677
Temperature (K)	100
Detector	Pilatus3 2M
Crystal-to-detector distance (mm)	148.66
Rotation range per image (°)	0.1
Total rotation range (°)	130
Exposure time per image (s)	0.02
Space group	$P2_12_12$ or $P2_12_12_1$
a, *b*, *c* (Å)	56.3, 60.4, 56.8
α, *β*, *γ* (°)	90, 90, 90
Mosaicity (°)	0.047
Resolution range (Å)	100.0–1.4 (1.45–1.40)
Total No. of reflections	183274 (18114)
No. of unique reflections	38706 (3801)
Completeness (%)	99.3 (98.6)
Multiplicity	4.7 (4.8)
$\langle I/\sigma(I)\rangle$	13.2 (1.7)
R_{meas}† (%)	6.3 (91.6)
Overall *B* factor from Wilson plot (Å^2)	24.6
Matthews coefficient V_M (Å^3 Da^{-1})	1.75
Solvent content (%)	29.6

† $R_{meas} = \sum_{hkl}[N(hkl)/[N(hkl)-1]]^{1/2}\sum_i |I_i(hkl) - \langle I(hkl)\rangle|/\sum_{hkl}\sum_i I_i(hkl)$.

2.3. Data collection and processing

Drops containing the optimized crystals were overlaid with 2 µl mineral oil before the crystals were harvested and flash-cooled in liquid nitrogen. X-ray diffraction data were collected at 100 K from a single crystal on the ID30A-3 beamline of the European Synchrotron Radiation Facility (ESRF), Grenoble, France (Theveneau *et al.*, 2013). The data-collection strategy was calculated with *EDNA* (Incardona *et al.*, 2009) using four diffraction images at 0, 90, 180 and 270° with an oscillation

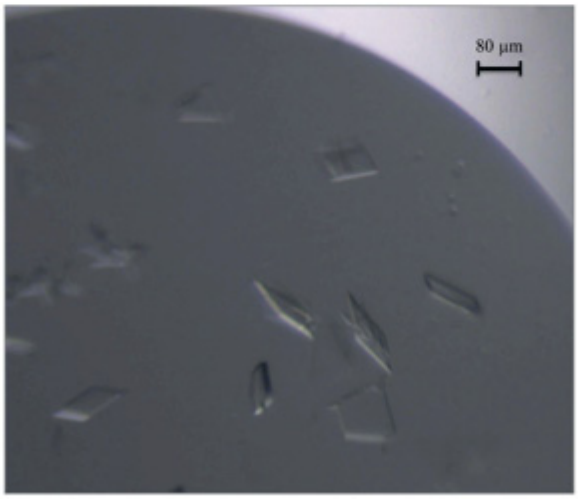

Figure 2
Crystals of NsrR. Rectangular plate-shaped crystals obtained using the sitting-drop vapour-diffusion method at 285 K.

width of 1° each. The subsequently collected data were processed and scaled using *XDS* and *XSCALE* (Kabsch, 2010*a*,*b*). Data-collection and processing statistics are summarized in Table 3.

3. Results and discussion

NsrR was successfully cloned and overexpressed in *E. coli* BL21 (DE3) cells. The protein was purified *via* a two-step purification protocol. Nickel-affinity chromatography was performed first, followed by size-exclusion chromatography (Fig. 1*a*). The yield of the protein was around 2 mg per litre of cell culture. Protein homogeneity and purity were assessed by SDS–PAGE (Fig. 1*b*). The molecular mass of the purified NsrR protein was comparable to the theoretically calculated molecular weight of 27.7 kDa (Gasteiger *et al.*, 2005).

Initial crystals of NsrR appeared after 2 d in PACT suite condition A5 [0.1 *M* SPG buffer pH 8.0, 25%(*w*/*v*) PEG 1500] using a sitting-drop setup. Optimizations were performed by varying the PEG concentration and the pH of the buffer. Rectangular plate-shaped crystals were obtained with 21–30%(*w*/*v*) PEG 1500, 0.1 *M* SPG buffer pH 8.0 after 1 d (Fig. 2), with maximum dimensions of 80 × 40 × 20 µm.

The rectangular plate-shaped crystals diffracted to 1.4 Å resolution using synchrotron X-rays (Fig. 3). The total data-collection time was 26 s. The crystals belonged to space group $P2_12_12$ (or its enantiomorph $P2_12_12_1$), with unit-cell parameters $a = 56.3$, $b = 60.4$, $c = 56.8$ Å, $\alpha = \beta = \gamma = 90°$ (Table 2). Currently, it is not possible to differentiate between space groups $P2_12_12$ or $P2_12_12_1$, as the systematic absences are not conclusive. The calculated Matthews coefficient resulted in a V_M of 1.75 Å^3 Da^{-1} and a solvent content of 29.6% for one monomer in the asymmetric unit (Matthews, 1968; Kantardjieff & Rupp, 2003). Mass-spectrometric analysis revealed 15 peptides covering 49% of the whole NsrR protein. Solving the structure by molecular replacement has so far failed, since all structures deposited in the PDB share a sequence identity at the amino-acid level of less than 34% (the BaeR structure has 33% identity; PDB entry 4b09; Choudhury & Beis, 2013), which therefore might not be sufficient. Reprocessing in space group *P*1 and subsequent molecular replacement also did not yield a satisfying solution. Hence, experimental phase determination is needed and we are currently attempting heavy-atom treatment using the optimized crystals.

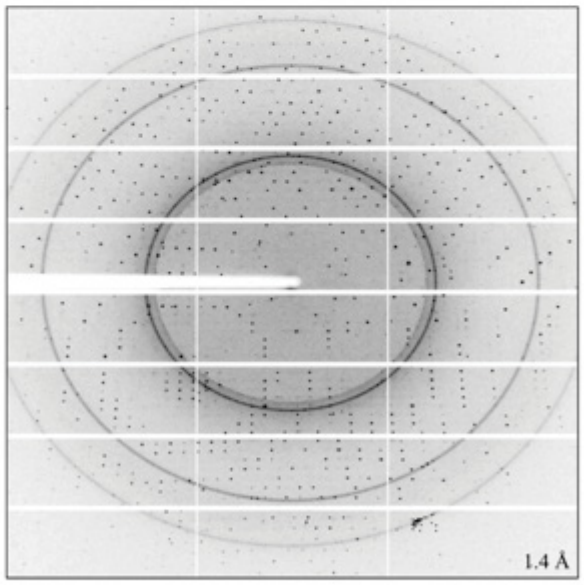

Figure 3
X-ray diffraction pattern of NsrR. Diffraction image of rectangular plate-shaped crystals of NsrR with an oscillation width of 1.0°. Four images at different angles were used to calculate the data-collection strategy using *EDNA* (Incardona *et al.*, 2009). The edge of the detector represents 1.4 Å.

NsrR represents a model for various two-component systems involved in lantibiotic resistance. The structure of NsrR would help us to further understand the mechanism of regulation behind lantibiotic resistance, thereby helping in its prevention.

Acknowledgements

The authors are grateful to Lutz Schmitt for his kind support, advice and invaluable suggestions. We would also like to thank André Abts for fruitful scientific discussions and Iris Fey for technical support. We acknowledge the European Synchrotron Radiation Facility for provision of synchrotron-radiation facilities and we would like to thank Philippe Carpentier for assistance in using beamline ID30A-3. We are also grateful to Heinrich-Heine International Graduate School of Protein Science and Technology (iGRASP$_{seed}$) for providing a scholarship to SK.

References

Bartoloni, A., Mantella, A., Goldstein, B., Dei, R., Benedetti, M., Sbaragli, S. & Paradisi, F. (2004). *J. Chemother.* **16**, 119–121.
Bergholz, T. M., Tang, S., Wiedmann, M. & Boor, K. J. (2013). *Appl. Environ. Microbiol.* **79**, 5682–5688.
Boakes, S. & Wadman, S. (2008). *Innov. Pharm. Technol.* **27**, 22–25.
Breukink, E. & de Kruijff, B. (2006). *Nature Rev. Drug Discov.* **5**, 321–323.
Choudhury, H. G. & Beis, K. (2013). *Protein Sci.* **22**, 1287–1293.
Cotter, P. D., Hill, C. & Ross, R. P. (2005). *Curr. Protein Pept. Sci.* **6**, 61–75.
Delves-Broughton, J., Blackburn, P., Evans, R. & Hugenholtz, J. (1996). *Antonie Van Leeuwenhoek*, **69**, 193–202.
Draper, L. A., Cotter, P. D., Hill, C. & Ross, R. P. (2015). *Microbiol. Mol. Biol. Rev.* **79**, 171–191.
Dyballa, N. & Metzger, S. (2009). *J. Vis. Exp.*, e1431.
Gasteiger, E., Hoogland, C., Gattiker, A., Wilkins, M. R., Appel, R. D. & Bairoch, A. (2005). *The Proteomics Protocols Handbook*, edited by J. M. Walker, pp. 571-607. Totowa: Humana Press.
Hancock, R. E. & Sahl, H.-G. (2006). *Nature Biotechnol.* **24**, 1551–1557.
Harris, L. J., Fleming, H. P. & Klaenhammer, T. R. (1992). *Food. Res. Int.* **25**, 57–66.
Hsu, S.-T. D., Breukink, E., Tischenko, E., Lutters, M. A. G., de Kruijff, B., Kaptein, R., Bonvin, A. M. J. J. & van Nuland, N. A. J. (2004). *Nature Struct. Mol. Biol.* **11**, 963–967.
Incardona, M.-F., Bourenkov, G. P., Levik, K., Pieritz, R. A., Popov, A. N. & Svensson, O. (2009). *J. Synchrotron Rad.* **16**, 872–879.

Kabsch, W. (2010*a*). *Acta Cryst.* D**66**, 125–132.
Kabsch, W. (2010*b*). *Acta Cryst.* D**66**, 133–144.
Kantardjieff, K. A. & Rupp, B. (2003). *Protein Sci.* **12**, 1865–1871.
Kawada-Matsuo, M., Oogai, Y., Zendo, T., Nagao, J., Shibata, Y., Yamashita, Y., Ogura, Y., Hayashi, T., Sonomoto, K. & Komatsuzawa, H. (2013). *Appl. Environ. Microbiol.* **79**, 4751–4755.
Kawada-Matsuo, M., Yoshida, Y., Zendo, T., Nagao, J., Oogai, Y., Nakamura, Y., Sonomoto, K., Nakamura, N. & Komatsuzawa, H. (2013). *PLoS One*, **8**, e69455.
Khosa, S., AlKhatib, Z. & Smits, S. H. J. (2013). *Biol. Chem.* **394**, 1543–1549.
Matthews, B. W. (1968). *J. Mol. Biol.* **33**, 491–497.
Severina, E., Severin, A. & Tomasz, A. (1998). *J. Antimicrob. Chemother.* **41**, 341–347.
Stock, A. M., Robinson, V. L. & Goudreau, P. N. (2000). *Annu. Rev. Biochem.* **69**, 183–215.
Suárez, J. M., Edwards, A. N. & McBride, S. M. (2013). *J. Bacteriol.* **195**, 2621–2631.
Theveneau, P. *et al.* (2013). *J. Phys. Conf. Ser.* **425**, 012001.

3.5 Chapter V – Structure of the Response Regulator NsrR

Published in: PLOS ONE

Impact Factor: 3.234

Own work: 60%

Purification and Crystallization

Establishing and Optimization Strategies for Experimental Phases

Structural Determination and Refinement

Bioinformatical Analyses of the Structure of NsrR

Writing the manuscript

Structure of the response regulator NsrR from *Streptococcus agalactiae*, which is involved in lantibiotic resistance

Sakshi Khosa, Astrid Hoeppner, Holger Gohlke, Lutz Schmitt, and Sander H.J. Smits

Structure of the Response Regulator NsrR From *Streptococcus agalactiae*, which is Involved in Lantibiotic Resistance

Sakshi Khosa[1], Astrid Hoeppner[2], Holger Gohlke[3], Lutz Schmitt[1], and Sander H.J. Smits[1]*

[1]Institute of Biochemistry, Heinrich Heine University Düsseldorf, Universitätsstr. 1, 40225 Düsseldorf, Germany

[2]X-Ray Facility and Crystal Farm, Heinrich Heine University Düsseldorf, Universitätsstr. 1, 40225 Düsseldorf, Germany

[3]Institute of Pharmaceutical and Medicinal Chemistry, Heinrich Heine University Düsseldorf, Universitätsstr. 1, 40225 Düsseldorf, Germany

* Correspondence:

E-Mail: sander.smits@hhu.de

Phone: +49-211-81-12647

Fax: +49-211-81-15310

Running title: Structure of the Lantibiotic Resistance Response Regulator

Keywords: Antimicrobial peptide/ lantibiotic/ nisin/ resistance/ regulation/ two-component system

Abstract

Lantibiotics are antimicrobial peptides produced by Gram-positive bacteria. Interestingly, several clinically relevant and human pathogenic strains are inherently resistant towards lantibiotics. The expression of the genes responsible for lantibiotic resistance is regulated by a specific two-component system consisting of a histidine kinase and a response regulator. Here, we focused on a response regulator involved in lantibiotic resistance, NsrR from *Streptococcus agalactiae,* and determined the crystal structures of its N-terminal receiver domain and its C-terminal DNA-binding effector domain. The C-terminal domain exhibits a fold that classifies NsrR as a member of the OmpR/PhoB subfamily of regulators. Amino acids involved in phosphorylation, dimerization, and DNA-binding were identified and demonstrated to be conserved in lantibiotic resistance regulators. Finally, a model of the full-length NsrR in the active and inactive state provides insights into protein dimerization and DNA-binding.

Introduction

The dramatic rise in antibiotic resistance has posed a major threat to the treatment of infectious diseases. This has led to the search for novel antibiotics that can be used as pharmaceuticals against human pathogenic bacteria. One of the potential antibiotic alternatives are lantibiotics (1). Lantibiotics are small antimicrobial peptides (30-50 amino acids in length), which are produced by several Gram-positive bacterial strains. They are post-translationally modified and contain specific lanthionine/methyl-lanthionine rings, which are crucial for their high antimicrobial activity (2). Lantibiotics are for example highly effective against various Gram-positive, human pathogenic bacteria including *Streptococcus pneumoniae* and several methicillin-resistant *Staphylococcus aureus* (MRSA) strains (3). The high potency of lantibiotics for medical usage has already been noticed, and several lantibiotics are already included in clinical trials (4, 5). Their high potency is highlighted by the fact that, although being extensively used in food industry, resistance has not been described so far (6). Nisin is the most prominent member of the lantibiotic family and is able to inhibit cell growth, penetrates the membranes of various Gram-positive bacteria, and is characterized by five specific (methyl-)lanthionine rings, which are crucial for stability and activity in the nanomolar range (7, 8).

Recently, gene clusters were identified in certain clinically relevant human pathogenic strains such as *Streptococcus agalactiae*, *S. aureus*, and others that confer inherent resistance against specific lantibiotics such as nisin (9-11). Within these resistance operons, genes encoding for a membrane-associated protease and an ABC transporter were identified. Expression of these proteins provides resistance against lantibiotics. Two genes, which by sequence similarity encode a two-component signaling system (TCS) consisting of a sensor histidine kinase (HK) and a response regulator (RR), apparently mediate the expression of the resistance proteins (12): HK senses the external lantibiotic and, upon receiving the stimuli, auto-phosphorylates at a conserved histidine residue within the cytosol; this high-energetic phosphoryl group is then transferred to the associated RR inducing a

conformational change there, which activates the RR to evoke the cellular response. Bacteria have the ability to sense and survive various environmental stimuli through adaptive responses, which are regulated by TCSs (13). These processes include drug resistance, quorum-sensing, phosphate uptake, sporulation, and osmoregulation (14). The absence of TCSs within mammals makes them unique targets for novel antimicrobial drugs (15).

The expression of the lantibiotic-resistance genes via TCS is generally regulated by microorganism-specific lantibiotics, which act via external stimuli. Some examples of TCS are: BraRS in *S. aureus* which is induced by bacitracin, nisin and nukacin-ISK-1 resistance (16), BceRS in *Bacillus spp.* that is induced by actagardine and mersacidin resistance (17), LcrRS in *Streptococcus mutans* induced by nukacin-ISK-1 and lacticin 481 (10) and LisRK of *Listeria monocytogenes* induced by nisin resistance (18). Furthermore, multiple lantibiotics can induce the TCS CprRK from *Clostridium difficile*, leading to the expression of the genes localized on the *cpr* operon, resulting in resistance against several lantibiotics of which nisin, gallidermin, subtilin, and mutacin 1140 are some examples.

The recently discovered *nsr* gene cluster of the human pathogen *S. agalactiae* encodes for the resistance protein NSR and the ABC transporter NsrFP, both conferring resistance against nisin (9). Homologous operons have been identified in various human pathogenic strains such as *Staphylococcus epidermis* and *Streptococcus ictaluri* based on the high sequence identity of NSR and NsrFP. In this gene cluster, the TCS NsrRK is responsible for the expression of the *nsr* and *nsrFP* genes (9). The similarity of the TCS within all the described nisin resistance operons suggests an expression specifically induced by nisin (9). Thus, NsrRK might be a useful target to combat inherently pathogenic lantibiotic-resistant strains.

Generally, RRs consist of two distinct structural domains, a receiver domain (RD) and an effector domain (ED), that are separated from each other by a flexible linker. RDs contain a highly conserved aspartate residue, which acts as a phosphoryl acceptor that becomes phosphorylated by the kinase domain of the histidine kinase upon reception of an external signal. The ED is thereby

activated and binds to the designated promoters, thus initiating transcription of the target genes.

The RRs are classified into different subfamilies depending on the three-dimensional structure of their EDs (14, 19). The OmpR/PhoB subfamily is the largest subgroup of RRs and comprises approximately 40% of all response regulators in bacteria. All their members are characterized by a winged helix-turn-helix (wHTH) motif (20). Although numerous structures of the single domains are known, only a few structures of full-length OmpR/PhoB-type RRs have been determined: RegX3 (PDB code: 2OQR) (21), MtrA (PDB code: 2GWR) (22), PrrA (PDB code: 1YS6) (23) and PhoP (PDB code: 3R0J) (24) from *Mycobacterium tuberculosis*; DrrB (PDB code: 1P2F) (25) and DrrD (PDB code: 1KGS) (26) from *Thermotoga maritima*; and KdpE from *Escherichia coli* (PDB code: 4KNY) (27). The various structures of RRs reveal that in addition to being in either "inactive" or "active" state, the RRs can also exist in two distinct conformations: "open" and "closed". MtrA and PrrA exhibit a very compact, closed structure with the DNA-binding sequence, called recognition helix, of the ED being inaccessible to DNA (22, 23). The structures of DrrD and DrrB exist in an open conformation, here the recognition helix is fully exposed (25, 26), suggesting that RRs are flexible in solution and can adopt multiple conformations.

Here, we describe the crystal structures of the N-terminal RD and the C-terminal ED of the lantibiotic resistance-associated RR NsrR from *S. agalactiae*. NsrR is part of the nisin resistance operon (9). The expression of the genes of this operon is induced by a TCS consisting of the HK NsrK and the RR NsrR. Based on the crystal structures of both the domains, modeling was employed to shed light on the putative DNA-bound state of full-length NsrR.

Materials and Methods

Cloning, expression and purification NsrR

NsrR was constructed, expressed, and purified as described previously (28). In brief, the *nsrR* gene (accession no. HG939456.1) from *S. agalactiae* COH1 was ligated into the expression vector pET24a allowing expression in *E. coli* with a His_6-tag introduced at the C-terminus. The resulting plasmid pET24a-NsrR was transformed into *E. coli* BL21 (*DE3*) for expression. A single transformed colony was inoculated into 20 ml LB media containing 30 µg/ml kanamycin. The culture was grown for 14 h at 310 K with shaking at 200 rpm. 4 l LB media with 30 µg/ml kanamycin were inoculated with the overnight culture at an OD_{600} of 0.05 and grown at 310 K with shaking at 170 rpm until an OD_{600} of 0.3 was reached. Subsequently, temperature was lowered to 291 K, and cells were further grown until an OD_{600} of 0.8 was reached before inducing the expression by addition of 1 mM IPTG. Cells were further grown for 15 h and harvested by centrifugation at 8000 rpm for 20 min at 277 K. The harvested cell pellet was re-suspended in 10 ml of buffer *A* (50 mM Tris pH 8.0, 50 mM NaCl, 2 mM PMSF and 10% (v/v) glycerol) and 10 mg of DNase (Deoxyribonuclease I from bovine pancreas, Sigma Aldrich) was added. Cells were lysed using a cell disruptor (Constant Cell Disruption Systems, United Kingdom) at 2.6×10^5 kPa. The lysate was centrifuged at 42000 rpm for 60 min using a Ti60 rotor to remove non-lysed cells and cell debris.

20 mM imidazole was added to the cleared lysate prior to applying it onto a Ni^{2+} loaded Hi-Trap HP Chelating column (GE Healthcare) pre-equilibrated with buffer *B* (20 mM Tris pH 8.0, 250 mM NaCl and 20 mM imidazole, 2 mM PMSF). The column was washed with six column volumes of buffer *B*. Protein was eluted with a linear gradient of imidazole from 20 mM to 400 mM in buffer *B*. The fractions containing NsrR were pooled and concentrated up to 8 mg/ml in an Amicon centrifugal filter concentrator with a 10 kDa cut-off membrane (Millipore). The concentrated protein was further purified by size exclusion chromatography using a Superdex 200 GL 10/300

column (GE Healthcare), equilibrated with buffer *C* (25 mM Tris pH 9.0, 50 mM NaCl, 2 mM PMSF). The eluted protein fractions were pooled and concentrated to 11 mg/ml as described above. The purity of the protein was analyzed with 15% SDS-PAGE using colloidal Coomassie blue staining (29).

Crystallization of NsrR

Crystals were obtained by using 1 µl of protein solution (concentration of 6.0 mg/ml) mixed with 1 µl of reservoir solution using the hanging-drop vapor diffusion method at 285 K. The reservoir solution contained PEG 20000 (11, 13, 15, 17 and 21% (w/v)) and 0.1 M MES pH (6.0, 6.5, 7.0 and 7.5). Crystals were obtained after three weeks and grew to their maximum dimensions within one month. Two different crystal forms, rectangular plate-shaped crystals and thin plates, were observed in the same drop. Both crystals forms were transferred into a buffer containing the reservoir solution plus 30% (v/v) ethylene glycol for 5 min prior to flash cooling using liquid nitrogen. For phasing, 20 mM tetra-chloro platinate IV (Hampton Research) was added to the crystallization drop, and the rectangular plate-shaped crystals were soaked for 30 min. The crystals with no obvious optical damage were harvested and flash-cooled in liquid nitrogen following the procedure above.

Data collection

Initially crystals were screened for quality at beamline P13 (DESY, EMBL Hamburg). All X-ray diffraction data were collected at beamline ID23eh1 of the European Synchrotron Radiation Facility (ESRF), Grenoble (30). All data sets were processed and scaled using XDS and XSCALE software package (31). Data sets from both native crystal forms were collected at 100 K. A single-wavelength anomalous dispersion (SAD) dataset from a single heavy-atom derivatized crystal (rectangular plate-shaped crystal) was collected at 1.0714 Å at 100 K. Diffraction data up to 1.7 Å was used for heavy atom localization and subsequent phasing.

Structure determination of NsrR

The structure of the thin plate-shaped crystals was solved by molecular replacement using the structure of the receiver domain of PhoB (PDB entry: 1B00) (32) as a model to phase the native data set at 1.8 Å resolution. The model generated was refined manually in COOT followed by iterative cycles of refinement using the program *phenix.refine* (33). Manual adjustments between the refinement cycles were performed with the program COOT (34) and Ramachandran validation was done using MolProbity (35).

The SAD dataset of the rectangular plate-shaped crystal was used for phasing *via* the Auto-Rickshaw server (36). The initial model was further built and refined manually using COOT (34) and *phenix.refine* from the Phenix package (33) with iterative cycles of refinement. This model was used to phase the native data set of the rectangular plate-shaped crystals at a resolution of 1.6 Å.

Data collection and refinement statistics are listed in Table 1 and all images of the models were prepared using PyMOL (37).

Accession numbers

Coordinates and structure factors have been deposited in the PDB with accession numbers 5DCL (NsrR-RD) and 5DCM (NsrR-ED).

Results and Discussion

NsrR was expressed and purified as described (28) with a yield of 2 mg per liter of cell culture. The purified NsrR protein has a theoretical molecular mass of 27.7 kDa and was >98% pure as assessed by SDS-PAGE (Fig. 1a, indicated by *). Surprisingly, over time NsrR degraded into two distinct fragments as visible on SDS-PAGE analysis using the same purified protein sample after one week (Fig. 1b, indicated by ** and ***, respectively). Both bands were subjected to mass spectrometry analysis. The analysis revealed that the larger fragment (**) represents the N-terminal receiver domain (residues 1-119; referred to as NsrR-RD) whereas the smaller fragment (***) contained the C-terminal DNA-binding effector domain of NsrR (residues 129-243 including 21 amino acids derived from the expression tag; referred to as NsrR-ED) (Fig. 1b). Residues 120-128 form the linker connecting the RD and ED. Such a cleavage of the full-length RR into two specific domains is not unusual and has been previously reported for other RRs as well (38). Mass spectrometry analysis did not reveal the presence of any specific protease in the purified NsrR sample. Furthermore, addition of a protease inhibitor, such as PMSF (Phenylmethylsulfonyl fluoride) and AEBSF (4-(2-Aminoethyl) benzenesulfonyl fluoride hydrochloride), even at high concentrations, did not inhibit proteolysis (data not shown).

Since formation of the crystals took around one month, it is not surprising that this cleavage also occurred in the crystallization drop. NsrR was crystallized yielding two crystal forms, which were distinguishable by visual inspection. Initially, we tried to solve the structure of NsrR by molecular replacement, which was not successful. Therefore, we tried heavy atom phasing using a platinum compound. This succeeded for the rectangular plate-shaped crystals. After the structure was solved, it became evident that these crystals contained two monomers of the ED of NsrR in the asymmetric unit.

We also tried to solve the structure of the thin plate-shaped crystals with this template, but the resulting model generated was not sufficient. Therefore, we thought that these crystals contained the

N-terminal domain of NsrR and successfully phased this dataset using molecular replacement with the N-terminal domain of PhoB (PDB code: 1B00; as a template. This approach revealed that this crystal form indeed contained two monomers of the RD of NsrR in the asymmetric unit. Since both crystals forms were obtained in the same drop it is not surprising that, when dissolving several crystals and performing subsequent mass-spectrometry to identify the protein in the crystals, it yielded peptide fragments throughout the NsrR sequence (28).

In summary, the two crystal forms contained one of the two domains, respectively, such that both domains were successfully crystallized. We determined the crystal structures of NsrR-RD and NsrR-ED separately. However, a part of the linker region (residues 120-128; $_{120}$RRSQQFIQQ$_{128}$; underlined are the amino acid residues not visible in either domain) could not be traced in the electron density.

Overall structure of the N-terminal NsrR receiver domain (NsrR-RD)

The structure of the NsrR-RD was determined at a resolution of 1.8 Å (Table 1). The R_{work} and R_{free} values after refinement were 0.17 and 0.22, respectively. Ramachandran validation revealed that all residues (100%, 236 amino acids) were in the preferred or allowed regions (34). Data collection and refinement statistics are listed in Table 1.

The asymmetric unit contains two copies of NsrR-RD. Although the entire N-terminal receiver domain is composed of residues Met1-Leu119, only residues Asn4 to Arg121 of chain A (including residues Arg120 and Arg121 of the linker) and Gln5 to Ser122 of chain B (including residues Arg120 until Ser122 of the linker) could be traced in the electron density of NsrR-RD. For Asn85, Asp86, and Glu87 of chain A, poor electron density was observed for the side chains and, thus, these side chains were deleted during refinement and are not present in the final structure. Since the two monomers of NsrR-RD were virtually identical (rmsd of 0.6 Å over 116 Cα atoms for the two monomers). Therefore, the overall structure is described for monomer A only.

NsrR-RD structurally adopts a αβ doubly-wound fold previously observed in OmpR/PhoB type regulators. Five β-strands (β1-β5) are arranged in a parallel fashion constituting the central core of the structure, which is surrounded by two α-helices (α1 and α5) on one and three helices (α2, α3, α4) on the other side (Fig. 2). The NsrR-RD structure shows a β1-α1-β2-α2-β3-α3-β4-α4-β5-α5 topology as also observed for other RRs (25, 26).

Comparison with structures of other receiver domains

NsrR belongs to the OmpR/PhoB family of RRs. The receiver domain of NsrR was superimposed with other structurally characterized receiver domains from the OmpR/PhoB family, such as DrrB (25), KdpE (27), MtrA (22), and the crystal structure of only the receiver domain of PhoB (39). The rmsd of the overlays and the corresponding PDB codes used are highlighted in Table 2. Superimposition of the structures revealed that helix α4 is slightly rotated outward in NsrR-RD (Fig. 2). In receiver domains of response regulators, helix α4 has been shown to be a crucial part of the dimerization interface (40, 41). Furthermore, helix α4 in NsrR is shorter than in other RRs. The first helical turn is unwound and adopts an unstructured region (see Fig. 2). This outward rotation and unwinding of helix α4 has not been observed in other RRs and is likely due to the circumstance that NsrR-RD is crystallized as an isolated monomer, due to helix α4 is not part of an interface. Inspection of the crystal contacts revealed no major interactions in this region that could have influenced the orientation of helix α4.

Based on the Dali server (42), the NsrR-RD domain is structurally closely related to KdpE (PDB code: 4KNY) from *E. coli*, displaying a sequence identity of 28% (43). This structural homology is also reflected by the low rmsd of 1.9 Å over 117 Cα atoms after superimposition of the receiver domains of NsrR and KdpE (Table 2) (27).

Active site residues and dimerization

All RRs contain a highly conserved aspartate residue in the active site (Fig. 3; shown in red). Phosphorylation of this aspartate residue induces a conformational change leading to the activation of the effector domain that binds DNA and regulates the transcription of target genes. This site of phosphorylation is conserved throughout the family of response regulators, including the lantibiotic resistance-associated RRs such as BraR from *L. monocytogenes* (16), BceR from *Bacillus subtilis* (17), CprR from *C. difficile* (44, 45), GraR from *S. aureus* (46, 47), LcrR from *S. mutans* (10), LisR (18), and VirR from *L. monocytogenes* (48) (Fig. 3).

The putative phosphorylation site of NsrR is Asp55, which is localized at the end of strand β3 (Fig. 3, shown in red; Fig. 4) and lies within an acidic environment composed of the side chains of Glu12 and Asp13 (Fig. 3, highlighted in pink). This pocket is similar to the acidic active site observed within most structures of RRs such as PhoB from *E. coli* (32), PhoP from *M. tuberculosis* (24), and DivK from *Caulobacter crescentus* (49). In NsrR, Glu12, Asp13, and Asp55 are in close proximity of a highly conserved Lys104 residue (highlighted in green in Fig. 3).

A divalent metal ion is usually bound in this acidic environment and is essential for phosphorylation and de-phosphorylation of RRs (50, 51). In some RRs like CheY, Mg^{2+} is observed in the structure, bound near the phosphorylation site (32, 52, 53). In the KdpE regulator from *E. coli* that is involved in osmoregulation, a divalent calcium ion is present. However, the structure of NsrR-RD did not contain any divalent ion. Instead, a water molecule is present, which interacts with Glu12 of the acidic pocket, Lys104, and another water molecule in the vicinity.

Within the β4-α4 loop and in β5 of the RD of RRs, specific amino acids are crucial for signal transduction from the RD to the ED via conformational changes that are a consequence of phosphorylation of the RD. These amino acids are Ser/Thr and Phe/Tyr located at the end of β4 and before β5, respectively, and designated as “signature switch residues”. As seen in the alignment (Fig. 3, highlighted in blue), these signature residues (Ser/Thr and Phe/Tyr) are highly conserved in the lantibiotic resistance-associated RRs. The orientation of the side chains of these residues determines whether the RD is in an active or inactive state (14, 54). In the inactive state, the

phenylalanine or tyrosine residue faces away from the active site, and the corresponding serine or threonine residue adopts an outward-facing conformation as well (54-56) (Fig. 4a). In contrast, the switch residues face towards the active site in the active state conformation (Fig. 4b).

By sequence alignment with other lantibiotic resistance-associated RRs, these "signature switch residues" are identified as Ser82 and Phe101 in NsrR (see above). Although some RRs such as KdpE, BraR, BceR, GraR, and VirR contain a serine residue as the first switch residue, the others possess a threonine instead. Furthermore, the second switch residue is mostly a tyrosine, with NsrR, BraR, and BceR being the only exceptions containing a phenylalanine at that position. A comparison of the NsrR-RD structure with the available structures of PhoB (Fig. 4) in the active (PDB code: 1ZES) and inactive (PDB code: 1B00) states demonstrates that Ser82 (NsrR-RD) is oriented away from the active site Asp55, and that Phe101 is also in an outward conformation suggesting an inactive state of the NsrR-RD (Fig. 4a).

As mentioned above, RRs contain a phosphorylation-activated switch and normally exist in equilibrium between the active and inactive conformations. Phosphorylation shifts the equilibrium towards the active conformation (57) and induces the formation of rotationally symmetric dimers on the α4-β5-α5 interface of RDs (40). It has been suggested that dimerization is crucial for DNA-binding of RRs of the OmpR/PhoB subfamily.

The RD domain of NsrR was crystallized with two separate monomers in the asymmetric unit. Therefore, we performed a DALI search (42) and focused on RD domains that were structurally determined as functional dimers. In this context, the dimer of full-length KdpE from *E. coli* (Z-score 18.8, rmsd 1.9 Å over 117 Cα atoms) (PDB code: 4KNY) (27) and the structure of the functional dimer of the RD of KdpE from *E. coli* (PDB code: 1ZH2) (58) represent the most structurally related structures.

We aligned NsrR-RD on both monomers of the RD of KdpE. Since helix α4 of NsrR-RD is orientated slightly different when compared with other structures of RDs (Fig. 2), helix α4 and the N-terminal loop of one monomer were clashing with the second monomer (Fig. S1a). Therefore,

helix α4 and the N-terminal loop were shifted to the position of KdpE by primarily modifying backbone torsion angles in the region immediately C-terminal to helix α4. Afterwards, helix α4 and the adjacent loops were energy minimized with the MAB force field (59) as implemented in the program Moloc; all other atoms of NsrR-RD were kept fixed. The result is highlighted in Fig. S1b. The energy minimized structure of NsrR-RD was then superimposed on the dimeric structure of KdpE (58).

The putative functional dimer of NsrR-RD is depicted in Fig. 5. The dimeric interface is formed by α4-β5-α5 of RD (Fig. 5a), as previously observed in other RRs (25, 41, 58). In KdpE, a network of salt bridges and other electrostatic interactions stabilize the interface within a single monomer as well as between the monomers. Majority of these interactions involve residues that are highly conserved within the OmpR/PhoB subfamily of RRs. In addition, the dimeric interface of KdpE is characterized by hydrophobic patch formed by residues Ile88 (α4), Leu91 (α4), Ala110 (α5), and Val114 (α5). Structurally, a similar set of residues is also found in NsrR: Leu94 (α4), Val110 (α5) and Ala113 (α5), respectively (depicted as spheres in Fig. 5b), which are conserved to some extent on sequence level (highlighted in yellow; Fig. 3).

Conserved intermolecular electrostatic interactions further stabilize the monomer-monomer interaction of KdpE and are formed between Asp97 (β5) and Arg111 (α5), Asp96 (α4–β5 loop) and Arg118 (α5), and Asp92 (α4) and Arg113 (α5). Some of these interactions can also be identified in the dimeric model of NsrR-RD. Here, Asp100 (β5) and Lys114 (α5) form an interaction within one monomer, and an intermolecular interaction can be observed between Asn95 (α4) of one monomer with Thr116 (α5) of the other monomer (Fig. 3, shown in cyan). Asp99 (α4–β5 loop; Fig. 3, shown in cyan) points toward the side chain of Arg121. This interaction is also observed in KdpE (Asp96 (α4–β5 loop) and Arg118 (α5)). In KdpE, Arg111 is additionally stabilized by another intra-molecular salt bridge with Glu107 (α5). Interestingly, in NsrR-RD this amino acid corresponds to Val110 (highlighted in yellow in Fig. 3). As observed in this alignment, the above-mentioned arginine residue (Arg111 in KdpE) is either an arginine or a lysine residue (Lys114 in NsrR) in all

RRs used in the alignment (Fig. 3, shown in cyan). Interestingly, whenever an arginine is present at this position (Arg111 in KdpE), a glutamate (Glu107 in KdpE) is present as well, presumably stabilizing the arginine side chain. However, when a lysine is present at this position, the glutamate is exchanged to a hydrophobic residue contributing to the hydrophobic patch described above.

Overall Structure of C-terminal DNA-binding effector domain of NsrR

The structure of NsrR-ED from *S. agalactiae* was determined using experimental phases from a single-wavelength anomalous dispersion dataset from the rectangular plate-shaped crystal derivatized with platinum at a resolution of 1.6 Å in space group $P2_12_12$. The R_{work} and R_{free} values after refinement were 0.18 and 0.22, respectively. Ramachandran validation was done using MolProbity (35). Almost all residues (99.48%, 193 amino acids) were in the preferred or allowed regions, while 0.52% (1 amino acid) were localized in the disallowed region. The latter is Glu128 (last residue of the linker region) of chain B that is involved in crystal contacts and, therefore, likely adopts an unfavorable conformation. The structure contained a few ethylene glycol molecules introduced by the cryo-protecting procedure. The data collection and refinement statistics are listed in Table 1.

The C-terminal effector DNA-binding domain of NsrR is about 13 kDa in size and consists of residues 129-243 (including 21 amino acid residues of the expression tag). Monomer A contains residue 129-224 and monomer B contain residues 128-225. For Asp147 of chain A and Glu174 of chain B, poor electron density was observed for the side chains and, thus, these side chains were removed during refinement. The asymmetric unit contains two copies of NsrR-ED related by two-fold rotational symmetry. An overlay revealed that both monomers display high similarity in their overall structure with an rmsd of 0.5 Å over 95 Cα atoms. We therefore describe for the overall structure only monomer A.

The ED domain of NsrR consists of six β-strands and three α-helices in a β6-β7-β8-β9-α6-α7-α8-β10-β11 topology (the secondary structure elements are counted in continuation of those of the

RD). The effector domain starts with a 4-stranded antiparallel β-sheet, followed by three α-helices and eventually ends in a C-terminal β-hairpin (Fig. 6). The two β-sheets sandwich the three α-helices.

The characteristic feature of the OmpR/PhoB subfamily of RRs is a winged helix-turn-helix (wHTH) fold that is adopted by the α7-loop-α8 segment in full-length and single effector domain structures of RRs of this subfamily. The structure of NsrR-ED also contains such a wHTH motif built up by helices α7 and α8 (Fig. 6). The second helix of the wHTH motif is important for DNA-binding and, therefore, is termed "recognition helix" (20) (shown in cyan in Fig. 6). Furthermore, a helix within the HTH motif, named "positioning helix", is important for proper orientation and positioning of the loop between these two helices and is referred to as "transactivation loop" (also called α-loop; Fig. 6) (20, 60). In the structure of NsrR-ED, helix α8 is identified as the recognition helix, α7 as the positioning helix, and the loop region between helices α7-α8 as transactivation loop as observed in other RRs (Fig. 6). The 16-residue long, solvent-exposed recognition helix α8 of NsrR-ED contains four positively charged residues that can potentially interact with DNA. These are Arg198, Arg200, Lys201, and Lys202. When comparing the sequence of NsrR with PhoB, KdpE, and MtrA, the alignment (Fig. 3, colored in blue) emphasizes the variations at these positions, except for Arg200, which is conserved throughout the lantibiotic resistance RRs. Additionally, Lys202 is also highly conserved throughout the family of RRs except PhoB, clearly reflecting differences in the sequences of DNA to be bound.

Comparison with structures of other effector domains

We performed a DALI search (42) to identify structurally related proteins to NsrR-ED. Here the structure of the effector domain of PhoB from *E. coli* (PDB code: 1GXQ) (Z-score of 13.7) (39) is structurally the most closely related. Similar to the PhoB effector domain, a 9-residues long loop (amino acid 182-189) is also present in the structure of NsrR-ED that connects helices α7 and α8. The rmsd between the three helices of the effector domain (including the two helices forming the

wHTH motif) of PhoB (39) and NsrR-ED is 1.6 Å over 47 C α atoms, clearly indicating that NsrR belongs to the OmpR/PhoB family of RRs.

Therefore, we superimposed the Cα traces of the effector domain of NsrR (NsrR-ED) with other previously determined effector domains from the OmpR/PhoB family such as DrrB (25), MtrA (22) and of only the effector domain structure of PhoB (39) from *E. coli*. Overall, the structures are very similar with rmsd's ranging from 1.7 to 2.6 Å (Table 2). The highest variations (Fig. 6) are visible in in the loop regions α7-α8, which corresponds to the transactivation loop. Interestingly, this region also shows low sequence conservation (Fig. 3). In many RRs this transactivation loop along with the recognition helix α8, form inter-domain contacts in the inactive state and are only exposed upon activation of the RRs via a conformational change where the N- and C-terminal domains move away from each other (23).

Linker region

The linkers that connect the RDs and EDs in response regulators are highly variable with respect to both length and sequence. The exact boundaries of these linkers are difficult to predict from sequence alignments in the absence of structural information of the distinct RR. Linker lengths in OmpR/PhoB proteins of unknown structure have been estimated by comparing the number of residues between conserved landmark residues in the regulatory and effector domains to those from structurally characterized family members. Such analysis has indicated that linker lengths vary from 5 to 20 residues (20). Similar to the OmpR/PhoB family, the lantibiotic resistance-associated family of response regulators also displays diverse linker regions, which are recognized in sequence alignments by the introduction of gaps (Fig. 3). Interestingly, two arginine residues (Arg120 and Arg121 in NsrR; Fig. 3, shown in purple) at the end of the RDs seem to be strictly conserved throughout the family of response regulators in both the OmpR/PhoB and lantibiotic resistance-associated RRs, indicating a conserved similarity. As seen in the structures of MtrA and KdpE (22, 58), this arginine residue residing at the end of α5 participates in the active state dimer interface of

the RD through a salt bridge interaction (41) with an aspartate residue. This aspartate residue is identified in NsrR as Asp99 (see above). Arginine 121 of NsrR points towards this Asp99 residue however, the distance for a salt bridge interaction is too large.

Although we aimed at crystallizing full-length NsrR, this endeavor failed due to proteolytic cleavage within the linker region during the time period of crystallization. Nonetheless, the structures of NsrR-RD and NsrR-ED together provide the required structural knowledge to predict the linker region that joins the receiver and effector domains. The linker region of NsrR consists of approximately nine residues (Fig. 3), comprising $_{120}$RRSQQFIQQ$_{128}$ (underlined residues are neither present in the structure of RD nor in ED of NsrR) and contains two positively charged amino acids.

DNA-binding mode of NsrR using a full-length model

Since the structures of both domains of NsrR were determined, we used this structural information together with the available crystal structures of related proteins to create a model of the full-length NsrR in its active and inactive state.

To achieve this, we first carefully analyzed the outcome of the Dali search for each domain and identified structurally highly similar proteins (based on Z-scores and rmsd values) and choose the full-length structures previously reported. This resulted in a list of possible templates for modeling the full-length structure of NsrR (Table 2). In solution, RRs exist in equilibrium between the active and inactive state, which is shifted towards the active state upon phosphorylation of the ED. This results in oligomerization of the RR and a higher affinity towards DNA.

Based on the above-mentioned criteria, the structure of MtrA from *M. tuberculosis*, crystallized in an inactive and non-phosphorylated state (22), seemed best suited for modeling purposes. Furthermore, the linker between the two domains of MtrA contains nine amino acids and is of similar length as the linker of NsrR. We aligned the NsrR-RD and -ED to the corresponding MtrA

domains and evaluated the structure. This mimics the closed inactive conformation of NsrR (Fig. 7a; the missing linker is represented as dotted line).

In MtrA, the two domains interact via the α4-β5-α5 interface of the receiver domain and the end of α7, α7-α8 loop and α8 of the effector domain. Both interfaces have been shown to form functionally important contact areas in the active state within members of the OmpR/PhoB subfamily. In our model of full-length NsrR, a similar orientation between the domains is observed, contributing to the inter-domain interactions. The inactive conformation of MtrA is supported by the orientation of the side chain of Tyr102, which points away from the active Asp56 residue, while the side chain of Tyr102 interacts with Asp190 of the RD of MtrA, thereby stabilizing its closed conformation. In the model of NsrR, similar amino acids are present, Phe101 (switch residue) and Asp188 (Fig. 3, represented by orange boxes) forming a likewise similar network of interaction.

Next, we were interested in the active conformation of the NsrR protein adopting an active "open" conformation in the dimeric state. We compared and aligned the NsrR-RD and ED on the dimeric structure of KdpE that was solved in the DNA-bound state (27, 61) (Fig. 7b). The N-terminal RDs of NsrR form a dimeric interface consisting of α4-β5-α5 of both the monomers (see above). This is a common hallmark of RRs belonging to the OmpR/PhoB subfamily (see above) (41, 58).

The linker region of KdpE is of similar length as of NsrR, which suggests that the distance in the DNA-bound state between the RD and ED of NsrR will be similar to that in the KdpE active dimer. We superimposed the ED of NsrR with the DNA-binding domain of KdpE resulting in a reasonably well-aligned structure (rmsd of 2.6Å over 86 Cα atoms; Table 2). The major differences are the orientation and size of β6-β7-β8-β9 helices, while the remaining part of the ED fits nicely with some small variations in the loops connecting the helices.

We also observed that this orientation creates a major positively charged groove-like surface, which is mainly formed by four positively-charged residues of the "recognition helix". This positively-charged groove would allow the binding of DNA as shown in Fig. 7c.

Conclusion

In numerous pathogenic bacteria such as *S. agalactiae*, *S. aureus*, and *C. difficile* that apparently do not produce a lantibiotic, a gene cluster is present to provide resistance against lantibiotics such as nisin, nukacin ISK-1, lacticin 481 gallidermin, actagardine, or mersacidin (9, 12, 44). The regulation of the expression of these genes is mediated by two-component systems. The structure of the response regulator NsrR from *S. agalactiae* presented in this study is the first structural information available for the subgroup of lantibiotic resistance-associated RRs.

Author contributions

Conceptualization, S.K. and S.H.J.S.; Methodology, S.K., A.H., H.G., L.S. and S.H.J.S.; Investigation, S.K., A.H., H.G. and S.H.J.S.; Writing – Original Draft, S.K., A.H., and S.H.J.S.; Writing – Review & Editing, S.K., A.H., H.G., L.S. and S.H.J.S.; Funding Acquisition, S.H.J.S.; Resources, L.S. and S.H.J.S; Supervision, L.S and S.H.J.S.

Acknowledgments

We are grateful to Diana Kleinschrodt and Iris Fey for technical assistance. We acknowledge the European Synchrotron Radiation Facility (ESRF Grenoble) and EMBL Hamburg for provision of synchrotron radiation facilities and are grateful to the staff of ESRF ID23-2 and ID29 for support during data collection, especially Christoph Mueller-Dieckmann for his enormous patience, assistance, and support. We are also thankful to Heinrich Heine International Graduate School of Protein Science and Technology (*i*GRASP*seed*) for providing a scholarship to S.K.

References

1. Cotter PD, Ross RP, Hill C. Bacteriocins—a viable alternative to antibiotics? Nature Reviews Microbiology. 2012;11(2):95-105.

2. Bierbaum G, Szekat C, Josten M, Heidrich C, Kempter C, Jung G, et al. Engineering of a novel thioether bridge and role of modified residues in the lantibiotic Pep5. Appl Environ Microbiol. 1996;62(2):385-92.

3. Sahl H-G, Bierbaum G. Lantibiotics: biosynthesis and biological activities of uniquely modified peptides from gram-positive bacteria. Annual Reviews in Microbiology. 1998;52(1):41-79.

4. Cotter PD, Hill C, Ross RP. Bacterial lantibiotics: strategies to improve therapeutic potential. Current Protein and Peptide Science. 2005;6(1):61-75.

5. Dischinger J, Basi Chipalu S, Bierbaum G. Lantibiotics: promising candidates for future applications in health care. Int J Med Microbiol. 2014;304(1):51-62.

6. Boakes S, Wadman S. The therapeutic potential of lantibiotics. Innov Pharm Technol. 2008;27:22-5.

7. Alkhatib Z, Lagedroste M, Zaschke J, Wagner M, Abts A, Fey I, et al. The C‐terminus of nisin is important for the ABC transporter NisFEG to confer immunity in *Lactococcus lactis*. MicrobiologyOpen. 2014;3(5):752-63.

8. Wiedemann I, Breukink E, Van Kraaij C, Kuipers OP, Bierbaum G, De Kruijff B, et al. Specific Binding of Nisin to the Peptidoglycan Precursor Lipid II Combines Pore Formation and Inhibition of Cell Wall Biosynthesis for Potent Antibiotic Activity. J Biol Chem. 2001;276(3):1772-9.

9. Khosa S, Alkhatib Z, Smits SH. NSR from *Streptococcus agalactiae* confers resistance against nisin and is encoded by a conserved nsr operon. Biol Chem. 2013;394(11):1543-9.

10. Kawada-Matsuo M, Oogai Y, Zendo T, Nagao J, Shibata Y, Yamashita Y, et al. Involvement of the Novel Two-Component NsrRS and LcrRS Systems in Distinct Resistance Pathways against Nisin A and Nukacin ISK-1 in *Streptococcus mutans*. Appl Environ Microbiol. 2013;79(15):4751-5.

11. Falord M, Karimova G, Hiron A, Msadek T. GraXSR proteins interact with the VraFG ABC transporter to form a five-component system required for cationic antimicrobial peptide sensing and resistance in *Staphylococcus aureus*. Antimicrob Agents Chemother. 2012;56(2):1047-58.

12. Draper LA, Cotter PD, Hill C, Ross RP. Lantibiotic Resistance. Microbiol Mol Biol Rev. 2015;79(2):171-91.

13. Kleerebezem M, Quadri LE, Kuipers OP, De Vos WM. Quorum sensing by peptide pheromones and two‐component signal‐transduction systems in Gram‐positive bacteria. Mol Microbiol. 1997;24(5):895-904.

14. Stock AM, Robinson VL, Goudreau PN. Two-component signal transduction. Annu Rev Biochem. 2000;69(1):183-215.

15. Barrett JF, Hoch JA. Two-component signal transduction as a target for microbial anti-infective therapy. Antimicrob Agents Chemother. 1998;42(7):1529-36.

16. Hiron A, Falord M, Valle J, Débarbouillé M, Msadek T. Bacitracin and nisin resistance in *Staphylococcus aureus*: a novel pathway involving the BraS/BraR two‐component system (SA2417/SA2418) and both the BraD/BraE and VraD/VraE ABC transporters. Mol Microbiol. 2011;81(3):602-22.

17. Ohki R, Giyanto, Tateno K, Masuyama W, Moriya S, Kobayashi K, et al. The BceRS two-component regulatory system induces expression of the bacitracin transporter, BceAB, in *Bacillus subtilis*. Mol Microbiol. 2003;49(4):1135-44.

18. Cotter PD, Emerson N, Gahan CG, Hill C. Identification and disruption of lisRK, a genetic locus encoding a two-component signal transduction system involved in stress tolerance and virulence in *Listeria monocytogenes*. J Bacteriol. 1999;181(21):6840-3.

19. Gao R, Mack TR, Stock AM. Bacterial response regulators: versatile regulatory strategies from common domains. Trends Biochem Sci. 2007;32(5):225-34.

20. Martínez-Hackert E, Stock AM. Structural relationships in the OmpR family of winged-helix transcription factors. J Mol Biol. 1997;269(3):301-12.

21. King-Scott J, Nowak E, Mylonas E, Panjikar S, Roessle M, Svergun DI, et al. The structure of a full-length response regulator from *Mycobacterium tuberculosis* in a stabilized three-dimensional domain-swapped, activated state. J Biol Chem. 2007;282(52):37717-29.

22. Friedland N, Mack TR, Yu M, Hung L-W, Terwilliger TC, Waldo GS, et al. Domain orientation in the inactive response regulator *Mycobacterium tuberculosis* MtrA provides a barrier to activation. Biochemistry. 2007;46(23):6733-43.

23. Nowak E, Panjikar S, Konarev P, Svergun DI, Tucker PA. The structural basis of signal transduction for the response regulator PrrA from *Mycobacterium tuberculosis*. J Biol Chem. 2006;281(14):9659-66.

24. Menon S, Wang S. Structure of the response regulator PhoP from *Mycobacterium tuberculosis* reveals a dimer through the receiver domain. Biochemistry. 2011;50(26):5948-57.

25. Robinson VL, Wu T, Stock AM. Structural analysis of the domain interface in DrrB, a response regulator of the OmpR/PhoB subfamily. J Bacteriol. 2003;185(14):4186-94.

26. Buckler DR, Zhou Y, Stock AM. Evidence of intradomain and interdomain flexibility in an OmpR/PhoB homolog from *Thermotoga maritima*. Structure. 2002;10(2):153-64.

27. Narayanan A, Kumar S, Evrard AN, Paul LN, Yernool DA. An asymmetric heterodomain interface stabilizes a response regulator–DNA complex. Nat Commun. 2014;5.

28. Khosa S, Hoeppner A, Kleinschrodt D, Smits SHJ. Overexpression, purification and crystallization of the response regulator NsrR involved in nisin resistance. Acta Crystallographica Section F. 2015;71(10):1322-6.

29. Dyballa N, Metzger S. Fast and sensitive colloidal coomassie G-250 staining for proteins in polyacrylamide gels. Journal of visualized experiments: JoVE. 2009(30).

30. Nurizzo D, Mairs T, Guijarro M, Rey V, Meyer J, Fajardo P, et al. The ID23-1 structural biology beamline at the ESRF. Journal of synchrotron radiation. 2006;13(3):227-38.

31. Kabsch W. Xds. Acta Crystallogr D Biol Crystallogr. 2010;66(2):125-32.

32. Solà M, Gomis-RuÈth FX, Serrano L, González A, Coll M. Three-dimensional crystal structure of the transcription factor PhoB receiver domain. J Mol Biol. 1999;285(2):675-87.

33. Adams PD, Afonine PV, Bunkóczi G, Chen VB, Davis IW, Echols N, et al. PHENIX: a comprehensive Python-based system for macromolecular structure solution. Acta Crystallogr D Biol Crystallogr. 2010;66(2):213-21.

34. Emsley P, Lohkamp B, Scott WG, Cowtan K. Features and development of Coot. Acta Crystallogr Sect D Biol Crystallogr. 2010;66(4):486-501.

35. Chen VB, Arendall WB, 3rd, Headd JJ, Keedy DA, Immormino RM, Kapral GJ, et al. MolProbity: all-atom structure validation for macromolecular crystallography. Acta Crystallogr D Biol Crystallogr. 2010;66(Pt 1):12-21.

36. Panjikar S, Parthasarathy V, Lamzin VS, Weiss MS, Tucker PA. On the combination of molecular replacement and single-wavelength anomalous diffraction phasing for automated structure determination. Acta Crystallogr D Biol Crystallogr. 2009;65(Pt 10):1089-97.

37. Delano WL. The PyMOL molecular graphics system. 2002.

38. Okajima T, Doi A, Okada A, Gotoh Y, Tanizawa K, Utsumi R. Response regulator YycF essential for bacterial growth: X-ray crystal structure of the DNA-binding domain and its PhoB-like DNA recognition motif. FEBS Lett. 2008;582(23):3434-8.

39. Blanco AG, Sola M, Gomis-Rüth FX, Coll M. Tandem DNA Recognition by PhoB, a Two-Component Signal Transduction Transcriptional Activator. Structure. 2002;10(5):701-13.

40. Toro-Roman A, Mack TR, Stock AM. Structural analysis and solution studies of the activated regulatory domain of the response regulator ArcA: a symmetric dimer mediated by the α4-β5-α5 face. J Mol Biol. 2005;349(1):11-26.

41. Bachhawat P, Swapna G, Montelione GT, Stock AM. Mechanism of activation for transcription factor PhoB suggested by different modes of dimerization in the inactive and active states. Structure. 2005;13(9):1353-63.

42. Holm L, Rosenström P. Dali server: conservation mapping in 3D. Nucleic Acids Res. 2010;38(suppl 2):W545-W9.

43. Altschul SF, Gish W, Miller W, Myers EW, Lipman DJ. Basic local alignment search tool. J Mol Biol. 1990;215(3):403-10.

44. Suárez JM, Edwards AN, McBride SM. The *Clostridium difficile cpr* locus is regulated by a noncontiguous two-component system in response to type A and B lantibiotics. J Bacteriol. 2013;195(11):2621-31.

45. McBride SM, Sonenshein AL. Identification of a genetic locus responsible for antimicrobial peptide resistance in *Clostridium difficile*. Infect Immun. 2011;79(1):167-76.

46. Neoh H-m, Cui L, Yuzawa H, Takeuchi F, Matsuo M, Hiramatsu K. Mutated response regulator graR is responsible for phenotypic conversion of *Staphylococcus aureus* from heterogeneous vancomycin-intermediate resistance to vancomycin-intermediate resistance. Antimicrob Agents Chemother. 2008;52(1):45-53.

47. Meehl M, Herbert S, Götz F, Cheung A. Interaction of the GraRS two-component system with the VraFG ABC transporter to support vancomycin-intermediate resistance in *Staphylococcus aureus*. Antimicrob Agents Chemother. 2007;51(8):2679-89.

48. Mandin P, Fsihi H, Dussurget O, Vergassola M, Milohanic E, Toledo‐Arana A, et al. VirR, a response regulator critical for *Listeria monocytogenes* virulence. Mol Microbiol. 2005;57(5):1367-80.

49. Guillet V, Ohta N, Cabantous S, Newton A, Samama J-P. Crystallographic and biochemical studies of DivK reveal novel features of an essential response regulator in *Caulobacter crescentus*. J Biol Chem. 2002;277(44):42003-10.

50. Lukat GS, Stock JB. Response regulation in bacterial chemotaxis. J Cell Biochem. 1993;51(1):41-6.

51. McCleary WR, Stock JB. Acetyl phosphate and the activation of two-component response regulators. J Biol Chem. 1994;269(50):31567-72.

52. Stock AM, Martinez-Hackert E, Rasmussen BF, West AH, Stock JB, Ringe D, et al. Structure of the magnesium-bound form of CheY and mechanism of phosphoryl transfer in bacterial chemotaxis. Biochemistry. 1993;32(49):13375-80.

53. Bellsolell Ls, Cronet P, Majolero M, Serrano L, Coll M. The three-dimensional structure of two mutants of the signal transduction protein CheY suggest its molecular activation mechanism. J Mol Biol. 1996;257(1):116-28.

54. West AH, Stock AM. Histidine kinases and response regulator proteins in two-component signaling systems. Trends Biochem Sci. 2001;26(6):369-76.

55. Zhu X, Rebello J, Matsumura P, Volz K. Crystal Structures of CheY Mutants Y106W and T87I/Y106W CheY Activation Correlates with Movement of Residue 106. J Biol Chem. 1997;272(8):5000-6.

56. Appleby JL, Bourret RB. Proposed signal transduction role for conserved CheY residue Thr87, a member of the response regulator active-site quintet. J Bacteriol. 1998;180(14):3563-9.

57. Gardino AK, Kern D. [5]-Functional Dynamics of Response Regulators Using NMR Relaxation Techniques. Methods Enzymol. 2007;423:149-65.

58. Toro‐Roman A, Wu T, Stock AM. A common dimerization interface in bacterial response regulators KdpE and TorR. Protein Sci. 2005;14(12):3077-88.

59. Gerber PR, Müller K. MAB, a generally applicable molecular force field for structure modelling in medicinal chemistry. J Comput Aided Mol Des. 1995;9(3):251-68.

60. Martínez-Hackert E, Stock AM. The DNA-binding domain of OmpR: crystal structures of a winged helix transcription factor. Structure. 1997;5(1):109-24.

61. Hasegawa H, Holm L. Advances and pitfalls of protein structural alignment. Curr Opin Struct Biol. 2009;19(3):341-8.

62. Zhao H, Heroux A, Sequeira RD, Tang L. Preliminary crystallographic studies of the regulatory domain of response regulator YycF from an essential two-component signal transduction system. Acta Crystallographica Section F: Structural Biology and Crystallization Communications. 2009;65(7):719-22.

63. Wang S, Engohang-Ndong J, Smith I. Structure of the DNA-binding domain of the response regulator PhoP from *Mycobacterium tuberculosis*. Biochemistry. 2007;46(51):14751-61.

64. Yamane T, Okamura H, Ikeguchi M, Nishimura Y, Kidera A. Water‐mediated interactions between DNA and PhoB DNA‐binding/transactivation domain: NMR‐restrained molecular dynamics in explicit water environment. Proteins: Structure, Function, and Bioinformatics. 2008;71(4):1970-83.

65. Li Y-C, Chang C-k, Chang C-F, Cheng Y-H, Fang P-J, Yu T, et al. Structural dynamics of the two-component response regulator RstA in recognition of promoter DNA element. Nucleic Acids Res. 2014:gku572.

66. Leonard PG, Golemi-Kotra D, Stock AM. Phosphorylation-dependent conformational changes and domain rearrangements in *Staphylococcus aureus* VraR activation. Proceedings of the National Academy of Sciences. 2013;110(21):8525-30.

Figure Legends:

Fig. 1: SDS PAGE analysis of purified NsrR directly and one week after purification.
(a) Freshly purified NsrR protein, and (b) NsrR protein after one week.
Lanes: M represents the PAGE Ruler Unstained Ladder; 1: NsrR after a two-step purification; 2: NsrR one week after purification. * corresponds to full-length NsrR protein at 27 kDa, while ** and *** correspond to the NsrR-RD and NsrR-ED domain at around 13 kDa, respectively.

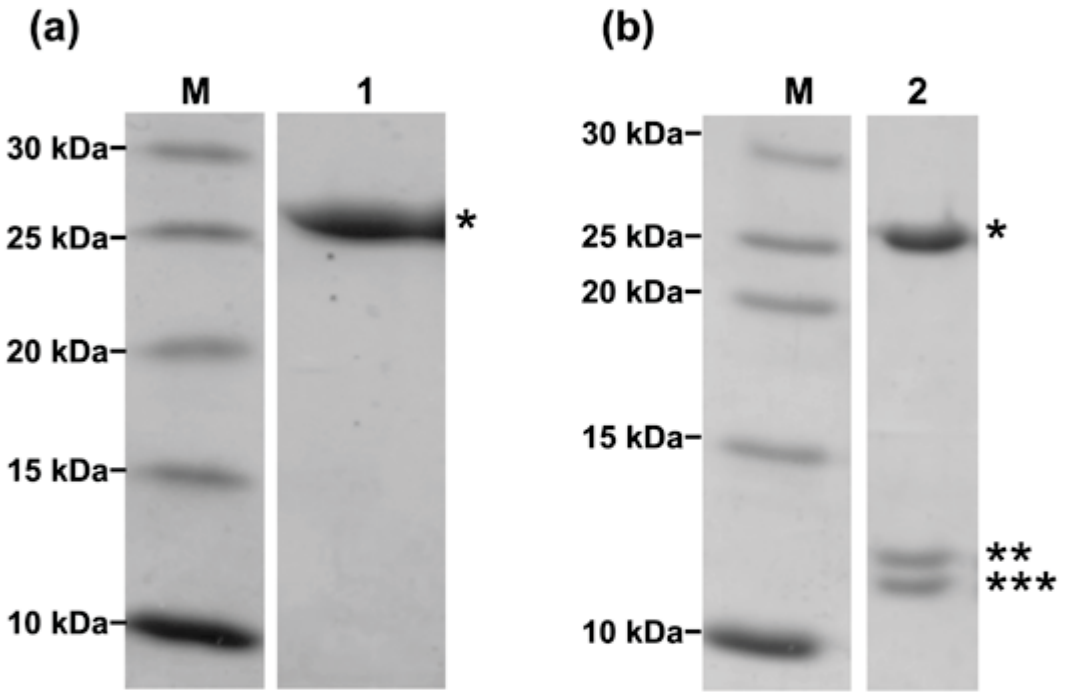

Fig. 2: Structure of NsrR-RD.
Cartoon representation of the helices (α1 – α5) and β-sheets (β1 - β5). Structural areas with the highest variations to the receiver domains of DrrB (pink, 1P2F), MtrA (grey, 2GWR), and PhoB (blue, 1B00) are marked in separate boxes.

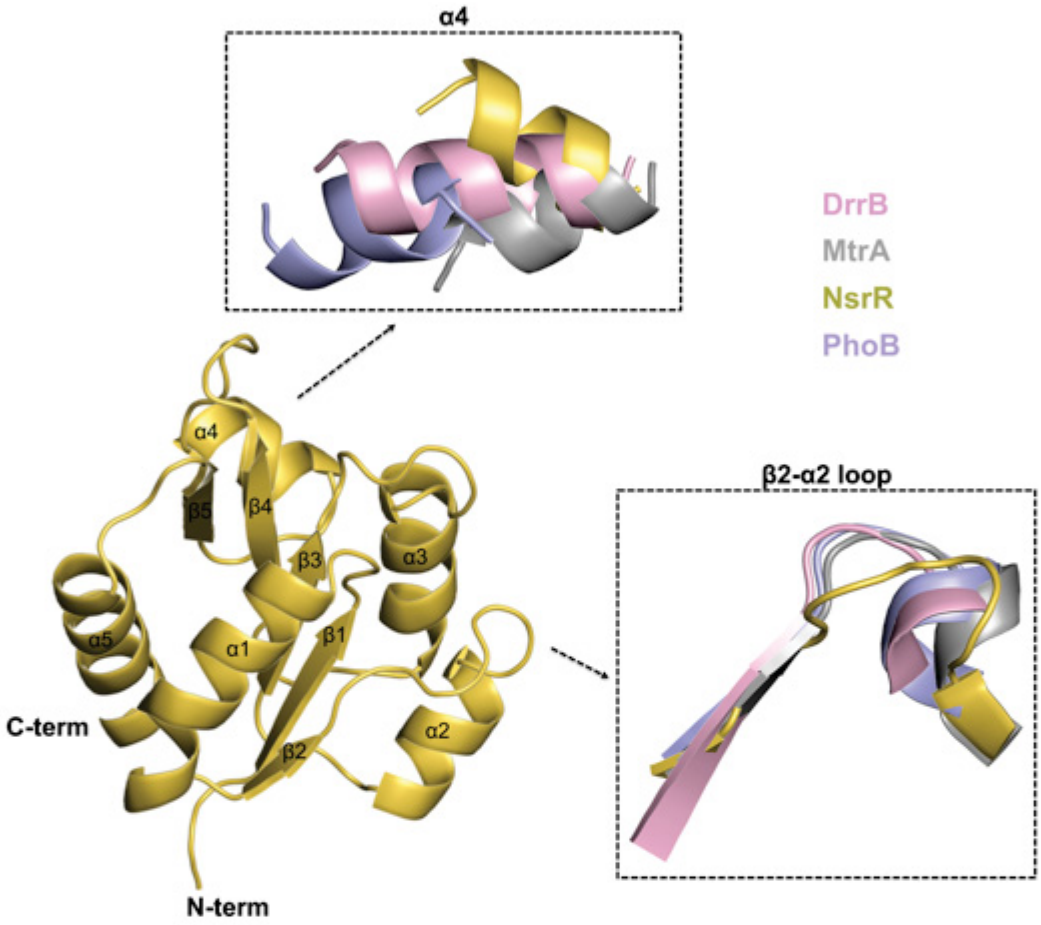

Fig. 3: Sequence alignment of NsrR protein with other response regulators.

A sequence alignment of NsrR with RRs belonging to the OmpR/PhoB subfamily (marked in grey) and RRs involved in lantibiotic resistance (black) is shown.

The active site aspartate residue (highlighted in red), the residues forming the acidic pocket surrounding it (highlighted in pink), the switch residues (highlighted in blue), the conserved lysine residue (highlighted in green), the highly conserved residues of the linker region (colored in purple), the residues involved in dimer interface of receiver domain (highlighted in yellow), residues involved in interdomain interactions (shown in orange boxes and in cyan) and the residues involved in interaction with DNA (colored in blue) are shown. The linker region of the known structures is underlined within the sequence.

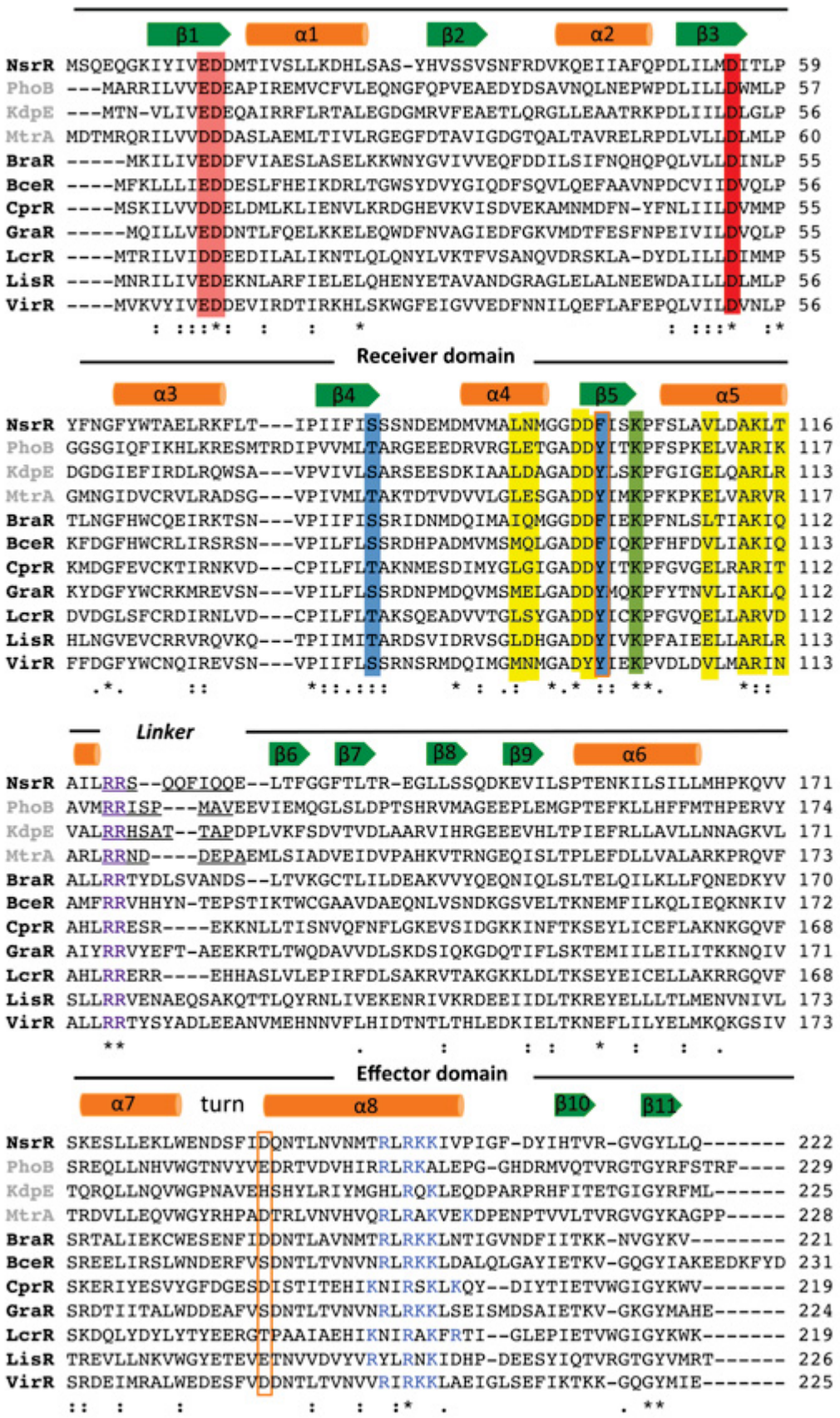
β1 α1 β2 α2 β3
NsrR MSQEQGKIYIVEDDMTIVSLLKDHLSAS-YHVSSVSNFRDVKQEIIAFQPDLILMDITLP 59
PhoB ---MARRILVVEDEAPIREMVCFVLEQNGFQPVEAEDYDSAVNQLNEPWPDLILLDWMLP 57
KdpE ---MTN-VLIVEDEQAIRRFLRTALEGDGMRVFEAETLQRGLLEAATRKPDLIILDLGLP 56
MtrA MDTMRQRILVVDDDASLAEMLTIVLRGEGFDTAVIGDGTQALTAVRELRPDLVLLDLMLP 60
BraR -----MKILIVEDDFVIAESLASELKKWNYGVIVVEQFDDILSIFNQHQPQLVLLDINLP 55
BceR ----MFKLLLIEDDESLFHEIKDRLTGWSYDVYGIQDFSQVLQEFAAVNPDCVIIDVQLP 56
CprR ----MSKILVVDDELDMLKLIENVLKRDGHEVKVISDVEKAMNMDFN-YFNLIILDVMMP 55
GraR -----MQILLVEDDNTLFQELKKELEQWDFNVAGIEDFGKVMDTFESFNPEIVILDVQLP 55
LcrR ----MTRILVIDDEEDILALIKNTLQLQNYLVKTFVSANQVDRSKLA-DYDLILLDIMMP 55
LisR ----MNRILIVEDEKNLARFIELELQHENYETAVANDGRAGLELALNEEWDAILLDLMLP 56
VirR ----MVKVYIVEDDEVIRDTIRKHLSKWGFEIGVVEDFNNILQEFLAFEPQLVILDVNLP 56
Receiver domain
α3 β4 α4 β5 α5
NsrR YFNGFYWTAELRKFLT---IPIIFISSSNDEMDMVMALNMGGDDFISKPFSLAVLDAKLT 116
PhoB GGSGIQFIKHLKRESMTRDIPVVMLTARGEEEDRVRGLETGADDYITKPFSPKELVARIK 117
KdpE DGDGIEFIRDLRQWSA---VPVIVLSARSEESDKIAALDAGADDYLSKPFGIGELQARLR 113
MtrA GMNGIDVCRVLRADSG---VPIVMLTAKTDTVDVVLGLESGADDYIMKPFKPKELVARVR 117
BraR TLNGFHWCQEIRKTSN---VPIIFISSRIDNMDQIMAIQMGGDDFIEKPFNLSLTIAKIQ 112
BceR KFDGFHWCRLIRSRSN---VPILFLSSRDHPADMVMSMQLGADDFIQKPFHFDVLIAKIQ 113
CprR KMDGFEVCKTIRNKVD---CPILFLTAKNMESDIMYGLGIGADDYITKPFGVGELRARIT 112
GraR KYDGFYWCRKMREVSN---VPILFLSSRDNPMDQVMSMELGADDYMQKPFYTNVLIAKLQ 112
LcrR DVDGLSFCRDIRNLVD---CPILFLTAKSQEADVVTGLSYGADDYICKPFGVQELLARVD 112
LisR HLNGVEVCRRVRQVKQ---TPIIMITARDSVIDRVSGLDHGADDYIVKPFAIEELLARLR 113
VirR FFDGFYWCNQIREVSN---VPIIFLSSRNSRMDQIMGMNMGADYYIEKPVDLDVLMARIN 113
Linker
β6 β7 β8 β9 α6
NsrR AILRRS--QQFIQQE--LTFGGFTLTR-EGLLSSQDKEVILSPTENKILSILLMHPKQVV 171
PhoB AVMRRISP---MAVEEVIEMQGLSLDPTSHRVMAGEEPLEMGPTEFKLLHFFMTHPERVY 174
KdpE VALRRHSAT--TAPDPLVKFSDVTVDLAARVIHRGEEEVHLTPIEFRLLAVLLNNAGKVL 171
MtrA ARLRRND----DEPAEMLSIADVEIDVPAHKVTRNGEQISLTPLEFDLLVALARKPRQVF 173
BraR ALLRRTYDLSVANDS--LTVKGCTLILDEAKVVYQEQNIQLSLTELQILKLLFQNEDKYV 170
BceR AMFRRVHHYN-TEPSTIKTWCGAAVDAEQNLVSNDKGSVELTKNEMFILKQLIEQKNKIV 172
CprR AHLRRESR----EKKNLLTISNVQFNFLGKEVSIDGKKINFTKSEYLICEFLAKNKGQVF 168
GraR AIYRRVYEFT-AEEKRTLTWQDAVVDLSKDSIQKGDQTIFLSKTEMIILEILITKKNQIV 171
LcrR AHLRRERR----EHHASLVLEPIRFDLSAKRVTAKGKKLDLTKSEYEICELLAKRRGQVF 168
LisR SLLRRVENAEQSAKQTTLQYRNLIVEKENRIVKRDEEIIDLTKREYELLLTLMENVNIVL 173
VirR ALLRRTYSYADLEEANVMEHNNVFLHIDTNTLTHLEDKIELTKNEFLILYELMKQKGSIV 173
Effector domain
α7 turn α8 β10 β11
NsrR SKESLLEKLWENDSFIDQNTLNVNMTRLRKKIVPIGF-DYIHTVR-GVGYLLQ------- 222
PhoB SREQLLNHVWGTNVYVEDRTVDVHIRRLRKALEPG-GHDRMVQTVRGTGYRFSTRF---- 229
KdpE TQRQLLNQVWGPNAVEHSHYLRIYMGHLRQKLEQDPARPRHFITETGIGYRFML------ 225
MtrA TRDVLLEQVWGYRHPADTRLVNVHVQRLRAKVEKDPENPTVVLTVRGVGYKAGPP----- 228
BraR SRTALIEKCWESENFIDDNTLAVNMTRLRKKLNTIGVNDFIITKK-NVGYKV-------- 221
BceR SREELIRSLWNDERFVSDNTLTVNVNRLRKKLDALQLGAYIETKV-GQGYIAKEEDKFYD 231
CprR SKERIYESVYGFDGESDISTITEHIKNIRSKLKQY--DIYTIETVWGIGYKWV------- 219
GraR SRDTIITALWDDEAFVSDNTLTVNVNRLRKKLSEISMDSAIETKV-GKGYMAHE------ 224
LcrR SKDQLYDYLYTYEERGTPAAIAEHIKNIRAKFRTI--GLEPIETVWGIGYKWK------- 219
LisR TREVLLNKVWGYETEVETNVVDVYVRYLRNKIDHP-DEESYIQTVRGTGYVMRT------ 226
VirR SRDEIMRALWEDESFVDDNTLTVNVVRIRKKLAEIGLSEFIKTKK-GQGYMIE------- 225

Fig. 5: Functional dimer orientation of the RDs of NsrR.

Dimeric structure of the RD of NsrR aligned to the structure of KdpE (PDB code 1ZH2, not shown).

(a) The two monomers of NsrR as functional dimers are represented in a cartoon representation displayed in cyan and yellow colors.

(b) Zoom-in of the dimeric interface mediated by α4-β5-α5. The monomer-monomer interactions are facilitated by hydrophobic residues (displayed as spheres), inter- and intra-domain interactions (displayed as sticks). The layout is adopted from (40).

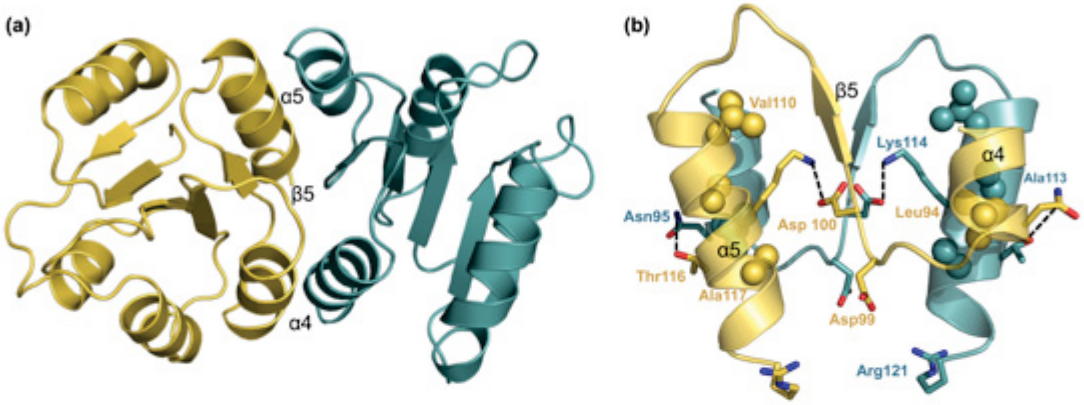

Fig. 6: Structure of the C-terminal effector domain of NsrR.
Cartoon representation of the C-terminal effector domain of NsrR (green; recognition helix in cyan). The structural areas with the highest variations compared to the effector domains of DrrB (pink, 1P2F), MtrA (grey, 2GWR), and PhoB (blue, 1GXQ) are marked.
The transactivation loop of MtrA is missing in the structure, therefore, the two termini are connected by a dashed line.

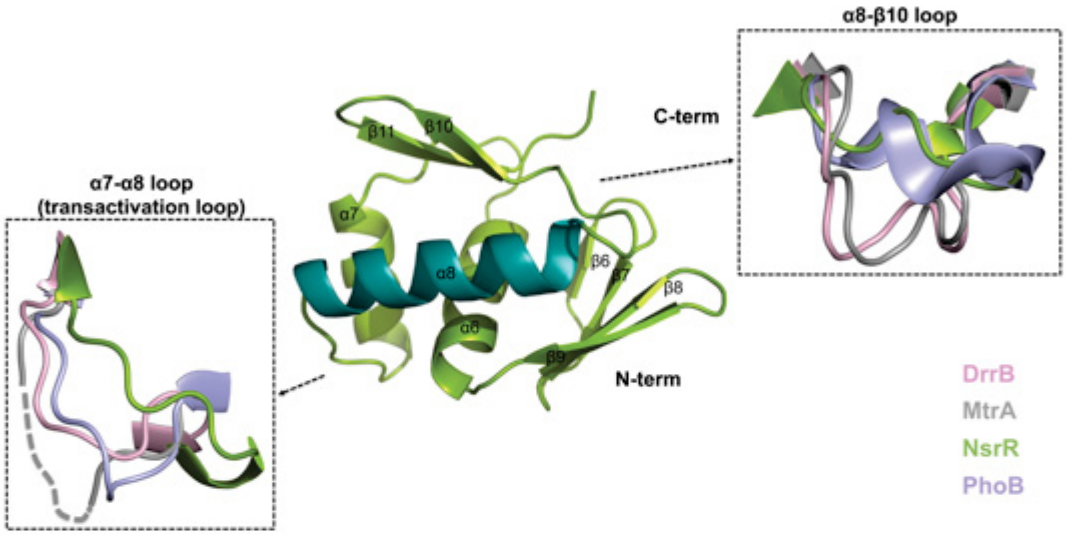

Fig. 7: Model of full-length NsrR in its inactive state and active state

The RD domain of NsrR is highlighted in yellow and the ED domain in green with the "recognition helix" colored in cyan.

(a) Inactive state conformation: Both domains of NsrR were aligned to the structure of MtrA (not shown), which adopts a closed inactive conformation, to obtain a model of full-length NsrR. Phe101 and Asp187 stabilize this closed conformation. The missing linker is represented by a dotted line.

(b) Active state conformation: A model of full-length NsrR in active conformation based on the alignment of both the domains of NsrR to the structure of DNA bound structure of KdpE (PDB code: 4KNY), adopting an active open conformation.

(c) A surface representation is shown highlighting the positively-charged groove of ED of NsrR where the DNA binds.

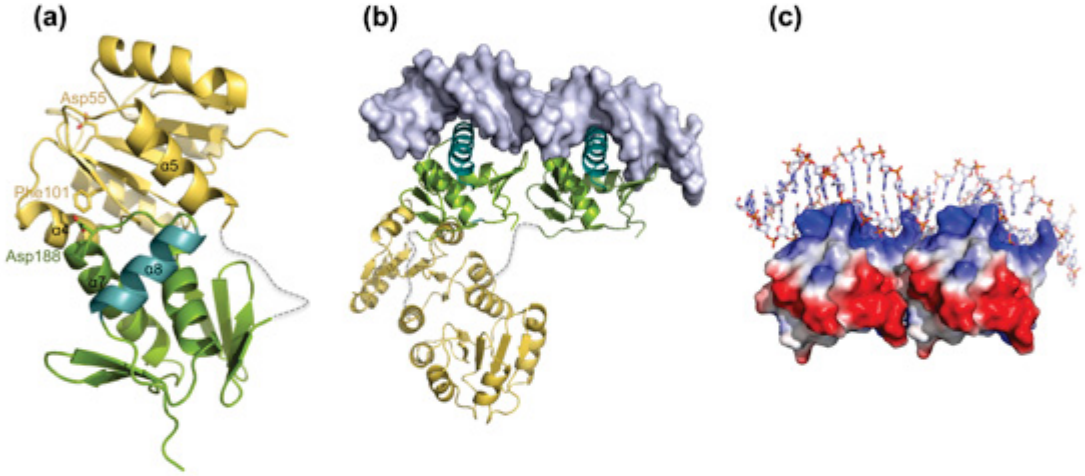

Tables:

Table 1: Data collection, phasing, and refinement statistics for the receiver and effector domains of NsrR.

	NsrR-RD (native)	NsrR-ED (native)	NsrR-ED (SAD dataset)
Data collection			
Space group	P 2_1 2_1 2	P 2_1 2_1 2	P 2_1 2_1 2
Cell dimensions			
a, b, c (Å)	57.0 107.1 39.4	56.3 60.4 56.8	56.3 60.6 56.7
α, β, γ (°)	90.0 90.0 90.0	90.0 90.0 90.0	90.0 90.0 90.0
Wavelength	1.0688	0.9677	1.0714
Resolution (Å)	39.48 - 1.80 (1.86 - 1.80)	56.85 - 1.60 (1.65 - 1.60)	100.00 - 1.70 (1.75 - 1.70)
R_{merge} [a]	3.4 (33.3)	4.8 (30.5)	6.8 (97.0)
I /σ(I)	26.2 (5.1)	18.2 (4.6)	21.6 (1.7)
Completeness (%)	98.8 (98.8)	99.5 (99.7)	98.8 (90.2)
Redundancy	4.8 (4.8)	4.8 (4.9)	11.7 (6.5)
Structure Refinement			
Resolution (Å)	39.48 - 1.80 (1.86 - 1.80)	56.85 – 1.60 (1.65 – 1.60)	
No. of reflections	109201 (10602)	124810 (12438)	
R_{work} [b] / R_{free} [b]	0.17 (0.21)/ 0.22 (0.27)	0.18 (0.21)/ 0.22 (0.27)	
No. of atoms	2019	1838	
Macromolecules	1884	1573	
Ligand/ion	20	8	
Water	115	257	
B-factors (Å^2)	28.1	21.8	
Macromolecules	27.5	20.2	
Ligand/ion	33.2	39.1	
Solvent	36.6	30.7	
R.m.s. deviations			
Bond lengths (Å)	0.011	0.009	
Bond angles (°)	1.12	1.17	
Ramachandran plot (%)			
Favored	99.0	97.0	

Allowed	1.0	2.48
Outliers	0.0	0.52

Values in parentheses are for the highest resolution shell.

[a] R_{merge} is defined as $R_{sym} = \sum_{hkl}\sum_{i}\left|I_i(hkl) - \langle I(hkl)\rangle\right| \Big/ \sum_{hkl}\sum_{i} I_i(hkl)$ and [b] R_F as

$$R_f = \sum_{hkl}\left||F_{obs}| - |F_{calc}|\right| \Big/ \sum_{hkl}|F_{obs}| \quad .$$

Table 2: The structures of the RD and ED domains of NsrR aligned to other response regulators.

The rmsd values of the superimpositions of the structures of NsrR-RD and NsrR-ED with the available structures of members of the OmpR/PhoB subfamily are highlighted. *Seq ID (%) corresponds to the full-length protein sequence.

Protein	*PDB*	*Z-score*	*RMSD (Å)*	*Number of residues (total number of residues)*	*Seq. ID (%)**	*Reference*
Receiver domain						
KdpE	4KNY	18.8	1.9	117 (222)	28	(27)
YycF	2ZWM	18.3	1.7	115 (120)	35	(38)
YycF	3F6P	18.1	1.7	114 (120)	35	(62)
DivK	1M5T	18.1	1.9	116 (123)	27	(49)
KdpE	1ZH2	18.0	1.9	115 (120)	28	(58)
PhoB	1B00	17.0	1.9	113 (122)	30	(32)
Effector domain						
PhoB	1GXQ	13.7	1.7	92 (105)	30	(39)
PhoP	2PMU	13.4	1.7	87 (93)	30	(63)
PhoB	2Z33	13.3	1.8	92 (104)	30	(64)
PhoB (DNA bound)	1GXP	13.3	2.0	92 (101)	30	(39)
SaeR	4IXA	13.0	2.1	94 (102)	29	Not available
RstA	4NHJ	11.8	1.9	85 (101)	29	(65)
KdpE	4KNY	11.5	2.6	86 (222)	28	(27)
Full-length Response Regulators						
	PDB code	*N-terminal rmsd (Å)*	*C-terminal rmsd (Å)*	*DNA bound*		*Reference*
DrrB	1P2F	2.1	2.3	No		(25)
DrrD	1KGS	2.1	1.9	No		(26)
KdpE	4KNY	1.9	2.6	Yes		(27)
MtrA	2GWR	2.1	2.0	No		(22)
PrrA	1YS6	2.0	2.2	No		(23)

RegX3	2OQR	2.3	2.1	No		(21)
VraR	4GVP	2.3	2.6	No		(66)

Supplementary Information:

Fig. S1: The structure of the RD of NsrR is aligned with the corresponding domain of KdpE. Structural comparison of the RD domain of NsrR with the receiver domain of KdpE (colored in silver) is shown.
(a) Comparison of helices α4 clearly indicates its slightly outward orientation in NsrR (shown in yellow).
(b) Alignment after energy minimization of the Cα atoms of helix α4 of NsrR (shown in brown).

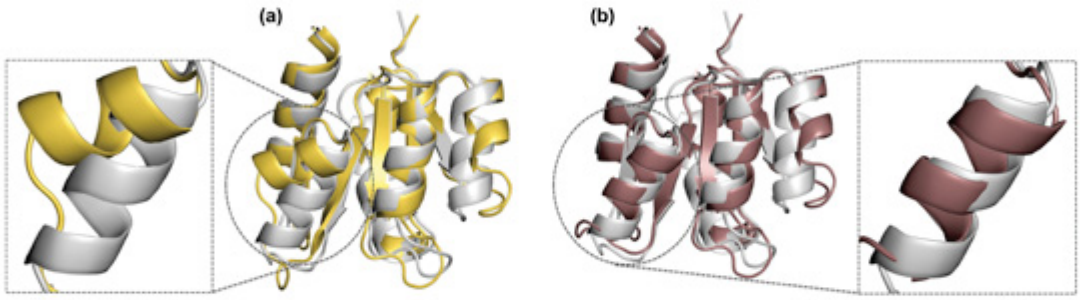

3.6 Chapter VI – NsrP Loop

In Preparation

Own work: 50%
Cloning
Establishing and Optimization of Expression and Purification Strategies
Crystal Screening and Optimization
Functional Studies (MicroScale Thermophoresis)
Writing the Manuscript

Molecular characterization of the extracellular domain from NsrFP of *S. agalactiae*

Sakshi Khosa, Tim Kroll, Jens Reiners and Sander H.J. Smits

Molecular characterization of the extracellular domain from NsrFP of *S. agalactiae*

Sakshi Khosa, Tim Kroll, Jens Reiners, Sander H.J. Smits*
Institute of Biochemistry, Heinrich-Heine-University, 40225 Duesseldorf, Germany
*Corresponding author:
Institute of Biochemistry, Heinrich-Heine-University Duesseldorf, Universitaetstrasse 1,40225. Duesseldorf.
Tel.: +49 211 81-12647 Fax: +49 211 81-15310 Email: Sander.Smits@hhu.de

***Abstract* - Lantibiotics are posttranslationally modified, (methyl-)lanthionine-containing peptides which are produced by Gram-positive bacteria. However, some bacteria develop/ have the presence of innate resistance systems that act against the activity of lantibiotics. Mostly two-component signaling systems and ABC transporters jointly contribute towards resistance. However, in *S. agalactiae*, nisin resistance is conferred by a five-component operon system. The operon comprises of a nisin resistance protein (NSR), a TCS (NsrRK) and a BceAB-type ABC transporter (NsrFP). The exact mechanism of NsrFP is poorly understood. Interestingly NsrFP harbors a large extracellular domain termed "NsrP-loop".**

The present study focused on elucidating the function of this loop by expressing purifying and biochemically characterizing the single domain. It was established that NsrP loop is involved in nisin resistance via binding to nisin which was further confirmed through agar diffusion assay. Furthermore, the dissociation constant for NsrP loop/nisin complex was determined using microscale thermophoresis and it was observed that NsrP loop binds to nisin with a moderate affinity. A model was predicted for NsrP loop and a complex of NsrP loop/nisin was also generated to gain structural insight into the putative complex formation. These data together represent the first example of *in vitro* studies of the extracellular domain of BceAB-type resistance-associated transporters.

Key Words – ABC transporter, extracellular domain, lantibiotic, nisin, resistance

INTRODUCTION

Lantibiotics are ribosomally synthesized peptides of approximately 19-38 amino acids, which are produced by numerous Gram-positive bacteria. They are characterized by the extensive post-translational modifications they undergo to be in their biologically active form and the presence of unusual amino acids (Vos *et al.*, 1995, Sahl *et al.*, 1995, Sahl & Bierbaum, 1998, Guder *et al.*, 2000). Lantibiotics are the most promising candidates as antibiotics alternatives due to their capability to inhibit various multidrug-resistant pathogenic bacteria like staphylococci, enterococci, streptococci and clostridia (Dischinger *et al.*, 2014). Some lantibiotics are also effective against gram-negative bacteria like *Neisseria* and *Helicobacter* (Mota-Meira *et al.*, 2000). Their mode of action involves multiple targets, which might help in overcoming the pre-existing mechanisms of antibiotic resistance. Lantibiotics are of great use in the food industry. The pharmaceutical potential of lantibiotics has also been extensively studied and some are already in the preclinical and clinical phases of development (Yang *et al.*, 2014).

One of the most studied and best characterized lantibiotic is nisin (Jung & Sahl, 1991) which is produced by some *Lactococcus lactis* and *S. uberis* strains. It has a broad antimicrobial spectrum against a wide range of Gram-positive bacteria and has a dual mode of action. Nisin uses lipid II a precursor molecule of cell wall synthesis as a docking molecule and inhibits cell wall synthesis (Wiedemann *et al.*, 2001) and forms pores (Hasper *et al.*, 2004) leading to cell death. Nisin has been widely used in the food industry as a food preservative and an additive in dairy products (Delves-Brougthon, 1990). Nisin is also effective in the treatment of atopic dermatitis (Valenta *et al.*, 1996), stomach ulcers (Dubois, 1995), colon infections (Kim *et al.*, 2003), respiratory tract infections (De Kwaadsteniet *et al.*, 2009) and staphylococcal mastitis (Fernández *et al.*, 2008).

However, some bacteria bypass the lantibiotics by expressing various protein systems that can detect and respond to the presence of lantibiotics (Draper *et al.*, 2015). These broad range resistance systems can either be less specific such as changes in bacterial cell wall and membrane (Draper *et al.*, 2015, de Freire Bastos *et al.*, 2015, Nawrocki *et al.*, 2014) or specific involving proteolytic degradation of the lantibiotic (Sun *et al.*, 2009).

Another mechanism involving lantibiotic resistance is by (ATP)-binding cassette (ABC) transporters, which are putatively involved in lantibiotic removal from the membrane (Draper *et al.*, 2015, Gebhard, 2012, Revilla-Guarinos *et al.*, 2014). Various resistance-associated ABC transporters have been identified such as BceAB in *B. subtilis* (Rietkötter *et al.*, 2008, Ohki *et al.*, 2003), BraAB (Kawada-Matsuo *et al.*, 2013), VraDE (Yoshida *et al.*, 2011, Kawada-Matsuo *et al.*, 2013) in *S. aureus* (Hiron *et al.*,

2011), PsdAB in *B. subtilis* (Staroń *et al.*, 2011), MbrAB (Tsuda *et al.*, 2002) and BceAB in *S. mutans* (Ouyang *et al.*, 2010), SP0812-SP0813 (Becker *et al.*, 2009) and SP0912-SP0913 (Majchrzykiewicz *et al.*, 2010) in *S. pneumoniae* and NsrFP in various bacterial strains of *corynebacterium, enterococcus, leuconostoc, streptococcus and staphylococcus* genera (Khosa *et al.*, 2013). Since BceAB was the first one to be characterized, these transporters are known as BceAB-type transporters.

Although these transporters are known to identify a broad range of substrates, however, they can often differentiate between structurally similar substrates (Gebhard, 2012). For example, PsdAB of *B. subtilis* can transport actagardine but not the structurally similar mersacidin (Staroń *et al.*, 2011).

These transporters are usually encoded next to a TCS where the histidine kinase contains two-transmembrane helices without any extracellular sensory domain, also known as the 'intramembrane-sensing' histidine kinases (Dintner *et al.*, 2011, Mascher, 2006). In *B. subtilis*, BceAB is encoded next to TCS BceRS (Falord *et al.*, 2012, Hiron *et al.*, 2011), VraFG in *S. aureus* acts together with TCS GraRS (Falord *et al.*, 2012, Falord *et al.*, 2011), NsrFP in *S. agalactiae* in encoded next to TCS NsrRK (Khosa *et al.*, 2013). Thus, in addition to conferring resistance, these transporters assist in signalling as confirmed from experimental evidence from various homologous systems (Rietkötter *et al.*, 2008, Falord *et al.*, 2012, Hiron *et al.*, 2011, Staroń *et al.*, 2011, Ouyang *et al.*, 2010). Furthermore, these transporters are known to have co-evolved with the associated TCS (Dintner *et al.*, 2011).

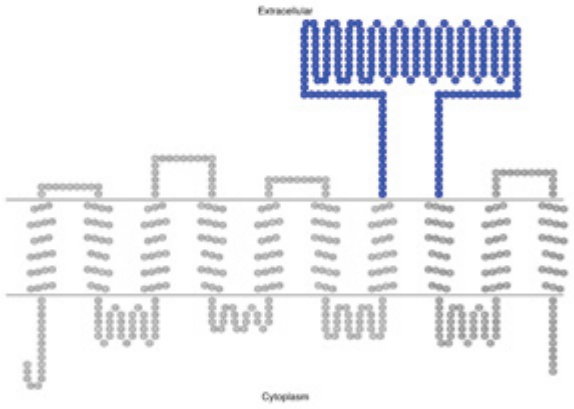

Fig. 1: Schematic representation of NsrP loop.
The amino acid sequence of NsrP is shown. 221 residues comprising NsrP loop are highlighted in blue while the rest residues are colored in grey. The figure is the output of TOPO2 server (Johns & Speth, 2010).

The most distinct feature of these resistance-associated ABC transporters is the presence of a large external domain (ECD) of approximately 200-250 amino acids in between helices VII and VIII of the permease (Ohki *et al.*, 2003, Rietkötter *et al.*, 2008, Khosa *et al.*, 2013) (Fig 1). They are localized on the outside of the cell. ECDs (or loops) have been identified in the permease domains of bacitracin resistance-associated ABC transporter BceAB in Bacillus species (Rietkötter *et al.*, 2008); bacitracin and nisin resistance-associated VraDE in *S. aureus* (Hiron *et al.*, 2011), nisin resistance-associated NsrFP in *S. agalactiae* (Khosa *et al.*, 2013).

These loops are found to be crucial for function and are the resistant determinants as they recognize the extracellular lantibiotic and upon ATP-dependent transport, subsequently induce the TCS-dependent signal transduction (Rietkötter *et al.*, 2008, Hiron *et al.*, 2011). Furthermore, substrate binding usually occurs *via* these ECDs.

In *S. agalactiae*, nisin resistance occurs due to the presence of a five-component resistance system comprising of NSR (nisin resistance protein; a serine protease), an ABC transporter (NsrFP) and a TCS (NsrRK) (Khosa *et al.*, 2013) (Fig. 2). The most distinguishing feature of this operon is the presence of NSR which proteolytically degrades nisin (Sun *et al.*, 2009) and is known to confer 20-fold resistance (Khosa *et al.*, 2013). Interestingly, the histidine kinase NsrK belongs to the IM-SK subfamily (Schultz *et al.*, 1998) and the permease NsrP harbours a large extracellular domain (named NsrP loop) of 221 amino acids (25.1 kDa) in between helices VII and VIII (Khosa *et al.*, 2013) (Fig. 1). However, there are no studies yet determining the possible substrates of NsrP loop.

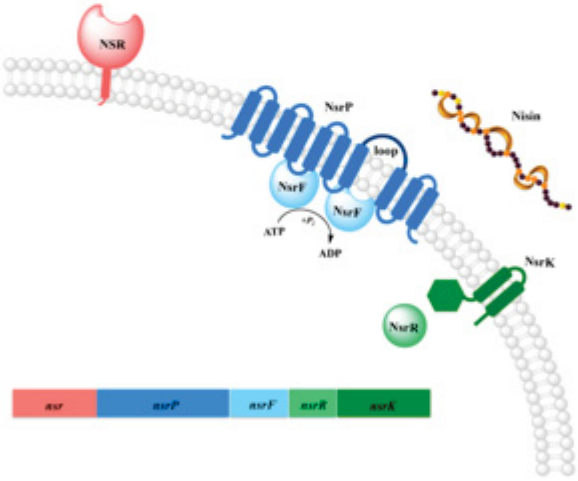

Fig. 2: Schematic representation the nisin resistance system of *S. agalactiae*.
The nisin resistance protein (Nsr) is shown in shade of pink. The two-component system regulatory proteins: NsrR (light green) and NsrK (dark green) and the ABC transporter proteins: NsrF (sky blue) NsrP (blue) are also shown with the extracellular domain (loop) highlighted in dark blue. Adapted from Khosa *et al.* (2013).

In this study, we sought to determine the exact role of NsrP-loop in conferring resistance in *S. agalactiae*. We demonstrated and further confirmed that NsrP-loop interacts with nisin. Additionally, structural model of NsrP-loop/nisin

complex was also predicted. Based on these observations, we conclude that the Nsr ABC transporter is the replica of the BceAB-type ABC transporter system and are required for nisin sensing and detoxification in addition to the nisin resistance protein (NSR) in the nisin resistant strains.

MATERIALS AND METHODS

Cloning and Expression

The *nsrP-loop* from *Streptococcus agalactiae* COH1 was amplified using the chromosomal DNA into pET28b and His_6-tag was introduced at the N-terminus. The resulting plasmid (Table 1) was verified by sequencing and transformed into *E. coli* BL21 (DE3) for expression. A single transformed colony was inoculated into 20 ml LB media containing 30 µg ml^{-1} kanamycin. The culture was grown for 14 h at 310 K with shaking at 200 rev min^{-1}. 2 L LB media with 30 µg ml^{-1} kanamycin was inoculated with the overnight culture at an OD_{600} of 0.05 and grown at 310 K with shaking at 170 rev min^{-1} till OD_{600} of 0.3 was reached. The temperature was lowered to 291 K and the cells were further grown till OD_{600} of 0.8 before induction with 1m*M* IPTG. The cells were further grown for 15 h.
The cells were harvested by centrifugation at 8000 rev min^{-1} for 20 min at 277 K. The harvested cell pellet was stored at 253 K till further use.

Table 1: Primers used for this study and the sequence of the expressed construct

Source organism	*Streptococcus agalactiae* COH1
Forward primer	CGGCAGCCATATGTCAAATACACAAAATGTTGTTAC CGGACTATTTC
Reverse primer	GTGGTGCTCGAGTTACATTTGATAACCTTCTTTTAGA AAACTCTGTTTAGTGCTAATATTTC
Complete amino acid sequence of NsrP loop	M G S S H H H H H H S S G L V P R G S H M S N T Q N V V T G L F P K S V S L S I D N S K G D A K N I F E E K I L K K L G K S S K E A I T Y N Q T M I S M P V S Q S S E L N I T S K N V K H V D I T K T G F M Y L I T Q N D F R R L G H Q L P K L K D N Q V A Y F V Q K G D S R L K K I N L L G N K F D V V K N L K E A Y V P E T T N T Y N P G L I I F A N N K Q I D N I R K A Y L P Y T K N I N T F P K T F K A Y L D L N S Q E I N S I S K N D I I E V D G K Y V G N I S T K Q S F L K E G Y Q M

Purification

All steps were performed at 277 K. The stored cell pellet was thawed and resuspended in 10 ml of buffer *A* (50 m*M* TRIS pH 8.0, 50 m*M* NaCl and 10% glycerol), 10 mg ml^{-1} of RNase and 10 mg of DNase (Deoxyribonuclease I from bovine pancreas, Sigma Aldrich) was added. The cells were lysed five times using a cell disruptor (Constant Cell Disruption Systems, United Kingdom) at 37709 psi (1kbar = 14.50 psi). The lysate was centrifuged at 42000 rev min^{-1} for 60 min using a Ti60 rotor to remove unlysed cells and debris. Imidazole was added to the cleared lysate at a final concentration of 1m*M*. The lysate was then applied to a Ni^{2+} loaded HiTrap HP Chelating column (GE Healthcare) pre-equilibrated with buffer *B* (20 m*M* Tris pH 8.0, 250 m*M* NaCl and 20 m*M* Imidazole) at a flow rate of 1 ml min^{-1}. The column was washed with six column volumes of buffer *B*. The column was further washed using buffer C (20 m*M* Tris pH 8.0, 250 m*M* NaCl and 96 m*M* Imidazole). The protein was then eluted with buffer *D* (25 m*M* sodium citrate pH 4, 250 m*M* NaCl) with a flow rate of 2 ml min^{-1} and instantly mixed with buffer *E* (1.5 M Tris pH 8, 250 m*M* sodium chloride) in a 1:1 ratio. The fractions containing the protein of interest were pooled and concentrated up to 5 mg ml^{-1} in an Amicon centrifugal filter concentrator with a 10 kDa cut-off membrane (Millipore). The concentrated protein was then further purified by size exclusion chromatography using Superdex 75 GL 10/300 column (GE Healthcare), equilibrated with buffer *F* (25 m*M* Tris pH 7.0, 500 m*M* NaCl). The protein eluted as a single homogeneous peak and the concerned fractions were pooled and concentrated to 5 mg ml^{-1} as mentioned before. The purity of the protein was analyzed with SDS-PAGE and colloidal coomassie stain (Dyballa & Metzger, 2009).

Nisin preparation

Commercially available nisin powder (Sigma Aldrich) was dissolved in 50 mM lactic acid at a concentration of 40 mg ml^{-1} and filtered through a 0.2 µm filter. The buffer was exchanged to buffer *F* (see above) using PD-10 mini column (GE Healthcare) and the concentration of nisin was determined by using RP-HPLC (Abts *et al.*, 2011).

Ni-NTA binding analyses

100 µl of Ni-NTA agarose resin (Qiagen, Germany) was prepared according to manufacturer's protocol. 100 µl of purified NsrP loop at a concentration of 50 µ*M* was loaded onto the resin pre-equilibrated with buffer *B* (section 3.2). The resin was washed two times with buffer *B*. 100 µl of purified nisin (concentration of 409.26 µ*M*) was added to the resin and allowed to incubate for 1 hr at 4°C using a roller. The resin was washed again three times with buffer *B* and the complex was eluted using buffer *F* (20 m*M* Tris pH 8.0, 250 m*M* NaCl and 400 m*M* Imidazole). Control reactions under the same conditions with only nisin and only purified NsrP loop was also performed. The eluted samples were analyzed for complex formation using SDS-PAGE (Dyballa & Metzger, 2009) and HPLC for detection of nisin in the elution samples.

Agar diffusion assay

The presence of complex formation was also further confirmed by detecting nisin by the solid agar medium test (Li *et al.*, 2006). A GM17 agar plate was seeded with the test strain *L. lactis* NZ9000 by inoculating liquid GM17 agar at 50°C with an overnight culture at a final O.D. of 0.05. After agar solidification, sterilized antimicrobial assay discs (6mm diameter) were placed onto the medium and seeded with 20 µl of the samples from pull-down assays. The GM17 agar plates were incubated at 30°C for 15 hr. The presence of nisin in the fractions was correlated with

the inhibition zone obtained. Here the size of the inhibition zone correlates with the concentration of nisin present.

Microscale Thermophoresis binding analyses

NsrP loop was fluorescently labeled with an amine-reactive blue dye (NT-495) following the manufacturer's protocol (NanoTemper, Germany) using labeling buffer (0.1M potassium phosphate, 500 mM sodium chloride). Labeled protein was mixed with serial dilutions of unlabeled nisin in buffer containing 25 m*M* Tris pH 7.0, 500 m*M* NaCl. After incubation for 1hr at room temperature, the mixed samples were loaded into premium-coated capillaries and measured on a NanoTemper Monolith NT.115 (20% LED, 20% MST power). The data were analyzed using NanoTemper analysis software (version 2.0.1334).

Crystallization

Crystallization screening was performed at 285 K using NT8 robot (Formulatrix) and sitting-drop vapour diffusion method in Corning 3553 sitting drop plates using the purified protein at a concentration of 7.5 mg ml^{-1}. For initial screening different commercial crystallization screens were used (Nextal JCSG Core Suites I, Classics Suite, PEGs Suite, MPD Suite (Qiagen, Germany) and MIDAS (Molecular Dimensions, England)). Nanodrops consisting of 0.1 µl each of protein and reservoir solution were mixed and equilibrated over 50 µl reservoir solution. The screening yielded some initial diamond-shaped crystals in condition 0.2 M Sodium fluoride, 0.1 M Bis-Tris propane pH 8.5, 20% w/v PEG 3350 (PACT suite, condition H1) after 1 month.

Prediction of the structure of NsrP loop

A model of NsrP loop was generated by comparative modeling using the in-house workflow TopModel (D. Mulnaes and H. Gohlke, unpublished results), which is based on the Modeler program (Šali & Blundell, 1993). A model of NsrP loop/nisin complex was generated using the online ZDOCK server (Pierce *et al.*, 2014).

RESULTS

Cloning, Expression and Purification of NsrP loop

NsrP loop was successfully cloned and overexpressed in a soluble form in *E. coli* BL21 (DE3) cells. The protein was purified *via* two-step purification protocol. A nickel affinity chromatography was performed first, followed by a size exclusion chromatography (Fig. 3A).

NsrP loop protein eluted in a single peak from the size exclusion column. The yield of the protein was around 2 mg L^{-1} of cell culture. Protein homogeneity and purity was assessed by SDS-PAGE (Fig. 3B). The molecular mass of the purified protein was comparable to the theoretically calculated molecular weight, of 27.2 kDa (Gasteiger *et al.*, 2005).

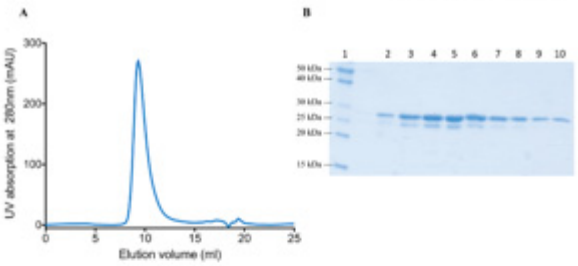

Fig. 3: Purification of NsrP loop.
A) Chromatogram representing the purification of NsrP loop by size exclusion chromatography using Superdex 75 10/300 GL column.
B) 15% SDS-PAGE showing the purified NsrP loop fractions. Lane 1 represents PageRuler Unstained Protein Ladder and lanes 2-10 display the purified NsrP loop fractions at 27kDa.

Binding of nisin to immobilized NsrP loop

Previous studies have indicated towards a probable interaction between the extracytoplasmic loop of the ABC transporter and the corresponding lantibiotic (Gebhard *et al.*, 2014, Staroń *et al.*, 2011, Falord *et al.*, 2012, Draper *et al.*, 2015). However, no studies for NsrFP were conducted yet.

An interaction between NsrP loop and nisin was established by a simple Ni-NTA based experiment. Nisin bound to the His-tagged NsrP loop immobilized on Ni-NTA resin. At high imidazole concentrations, this complex of NsrP loop and nisin eluted as seen from a SDS-PAGE analysis (Fig. 4A).

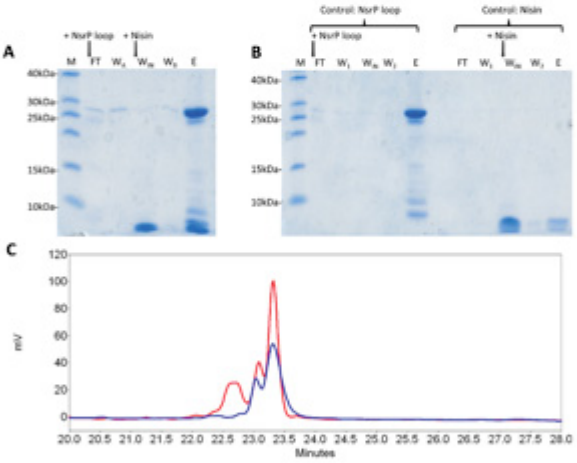

Fig. 4: Interaction between nisin and NsrP loop
A) and B) 15% SDS-PAGE gel representing the fractions from the pull-down assays. Lane M represents the Page Ruler unstained ladder. Lane FT: Flow-through of the resin after addition of NsrP loop (in control: nisin, only the buffer was added), Lane W_A: wash fraction, Lane W_{IN}: Flow-through of the resin after addition nisin (in control: NsrP loop, only the buffer was added), Lane W_B: wash fraction, Lane E: elution fraction.
C) Detection of nisin in the elution fraction. Nisin (red) and the eluted fraction (blue) from NsrP loop + nisin pull-down assay were analyzed by RP-HPLC. Elution times of both the samples are identical and all the experiments were performed at least in triplicate.

The NsrP loop/nisin complex separated under reducing conditions of SDS-PAGE where NsrP loop corresponds to 27 kDa band while the lower band is nisin. Furthermore, in the nisin control, most of the nisin didn't bind to the resin, while only a small amount of nisin was detected in the elution fraction (Fig. 4B). Additionally, the eluted fractions were also run on HPLC that confirmed the presence of nisin in the eluted fractions (Fig. 4C).

Agar diffusion assay for quantification of nisin

The agar diffusion test is a common method to examine the antimicrobial activity of nisin (Beach, 1952, Rogers & Montville, 1991). Low nanomolar concentrations of nisin are enough to permeabilize the bacterial membranes, inhibiting their growth (Abts *et al.*, 2011). As nisin diffuses through the agar to inhibit the growth of nisin-sensitive microorganism, there is formation of an inhibition zone whose size is directly related to the concentration of nisin. The greater the nisin concentration, the greater is the inhibition zone diameter (Linton, 1958).

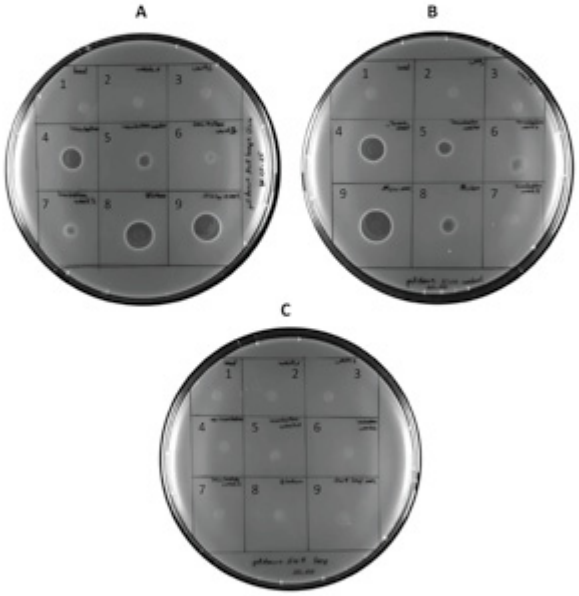

Fig. 5: Agar diffusion assay for detection of nisin
(A) Samples from the pull down assay with NsrP loop and nisin, (B) Control samples from the pull down assay with only nisin, (C) Control samples from the pull down assay with only purified NsrP loop.
Lanes 1: loading of protein (not in case of B), lanes 2: wash 1, lanes 3: wash 2, lanes 4: addition of nisin with incubation (not in C), lanes 5: incubation wash 1, lanes 6: incubation wash 2, lanes 7: incubation wash 3, lanes 8: elution, lane 9A and 9B: control nisin stock, lane 9C: control NsrP loop stock.

The presence of nisin in the fractions from section 4.4 was readily detected using this simple and sensitive method. An inhibition zone was formed with the elution fraction of the NsrP loop/nisin complex, clearly indicating the presence of nisin (Fig. 5A). A small inhibition zone can also be seen from the nisin molecules that don't bind to the resin. Fig. 5B shows the inhibition zones formed from the control run with only nisin. However, in contrast, here is formation of a bigger inhibition zone in the wash fraction and only a small inhibition zone in the elution fraction confirming that most of the nisin molecules don't bind to the resin. Additionally, the control NsrP loop did not show any inhibitory effect on the nisin sensitive *L. lactis* NZ000 strain.

Determination of the affinity between NsrP loop and nisin

We employed microscale thermophoresis (MST) to further determine the dissociation constant of the interaction between NsrP loop and nisin. MST measures the intrinsic property of biomolecules to align along a laser-induced temperature gradient of only a few degrees Celsius. This property (thermophoresis) depends specifically upon the size, shape and charge of molecules and thus, binding affinities can be calculated by measuring the changes in thermophoresis of a specific protein (molecule) as a function of increased ligand concentration (in this case, nisin).

Nisin (concentrations ranging from 500 to 15.25 µM) was titrated against 455 nM of NT-495 labeled NsrP loop. After one hour of incubation time, the samples were loaded into glass capillaries and a thermophoretic analysis was performed on the Monolith.NT115 using 20% LED-power. A normalized fluorescence F_{norm} (Fraction bound) was plotted for different concentrations of nisin (Fig. 6). An apparent K_d value of 1.60±0.13 µM was calculated for this interaction.

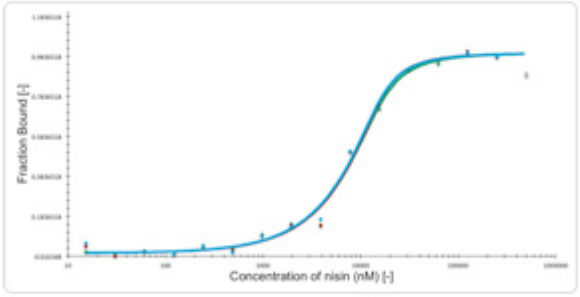

Fig. 6: Microscale thermophoresis analysis of binding of NsrP loop to nisin.
Fluorescence binding curve acquired by titrating non-labeled nisin into labeled NsrP loop. A 1:1 dilution series was applied, with the highest nisin concentration being 500 µM, whereas the concentration of labeled NsrP loop was kept constant at 455 nM. The fitted MST data yielded apparent K_d value of 1.60±0.13 µM.

Crystallization of NsrP loop

Initial diamond- shaped crystal of NsrP loop appeared after 1 month under the PACT H1 condition (0.2M Sodium fluoride, 0.1M Bis-Tris propane pH 8.5, 20% w/v PEG

3350) in a sitting drop setup with maximum dimensions 80 × 80 × 15 μm^3 (Fig. 7).

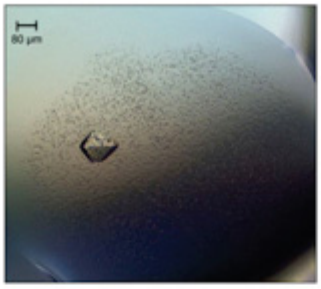

Fig. 7: Crystal of NsrP loop. The initial diamond-shaped crystal obtained from sitting drop-vapour diffusion method at 285 K.

Model of NsrP loop

The difficulties obtained in optimizing the crystals for diffraction purposes, led to the use of TopModel (D. Mulnaes and H. Gohlke, unpublished results) to predict the structure of NsrP loop. The obtained model showed that NsrP loop is composed of two main components: N- and C-terminal regions and a mixed αβ region, which are arranged in a sickle-shaped orientation (Fig. 8A).

To gain further structural insight into the putative complex of NsrP loop/nisin, a model was generated using ZDOCK server (Pierce *et al.*, 2014) (Fig. 8B). The model revealed revealed the probable orientation of the nisin molecule in the NsrP loop structure. According to the predicted model, the C-terminus of nisin is responsible for interacting with NsrP loop. Furthermore, the last two lanthionine rings of nisin (rings D and E) are laying in the centre of the structure (Fig. 8B).

DISCUSSION

Lantibiotics are produced by Gram-positive bacteria and possess antimicrobial activity against various bacteria including MRSA strains. However, various bacteria are inherently resistant against lantibiotics. ATP-driven ABC transporters play a major role in effluxing the lantibiotic, thereby conferring resistance (Gebhard, 2012). In contrast to the three-component ABC transporters (three genes which encode for one nucleotide-binding domain and two transmembrane domains) present in lantibiotic producing strains, these resistance-associated ABC transporters are composed of only two-components (BceAB-type transporters; one gene each for NBD and TMD, respectively) and are characterized by the presence of a large extracellular domain. The only exception known so far is CprABC from *C. difficile*, that is composed of three components (McBride & Sonenshein, 2011). Although, various BceAB-type transporters have been identified in various homologous systems (Falord *et al.*, 2012, Meehl *et al.*, 2007, Kallenberg *et al.*, 2013) with conserved sequence motifs, the extracellular domain is the least conserved domain among these resistance-associated ABC transporters (Fig. S1). Despite the variation, these domains are known to be specific for their own ABC transporters (Coumes-Florens *et al.*, 2011). A hybrid of the permease BceB from *B. subtilis* and the extracellular domain from another related Bce-AB type transporter did not restore bacitracin resistance in the BceAB transporter (Coumes-Florens *et al.*, 2011). Furthermore, these transporters are usually found in conjunction with an adjoining TCS. Since in various lantibiotic resistant systems, the histidine kinases of the associated TCSs lack the sensory domain, these loops function as an additional co-sensor for the regulation of the transcription of the associated genes (Coumes-Florens *et al.*, 2011, Rietkötter *et al.*, 2008) which includes binding to the antimicrobial peptide or lantibiotic and somehow passes on the signal to the TCSs for upregulation and sensing.

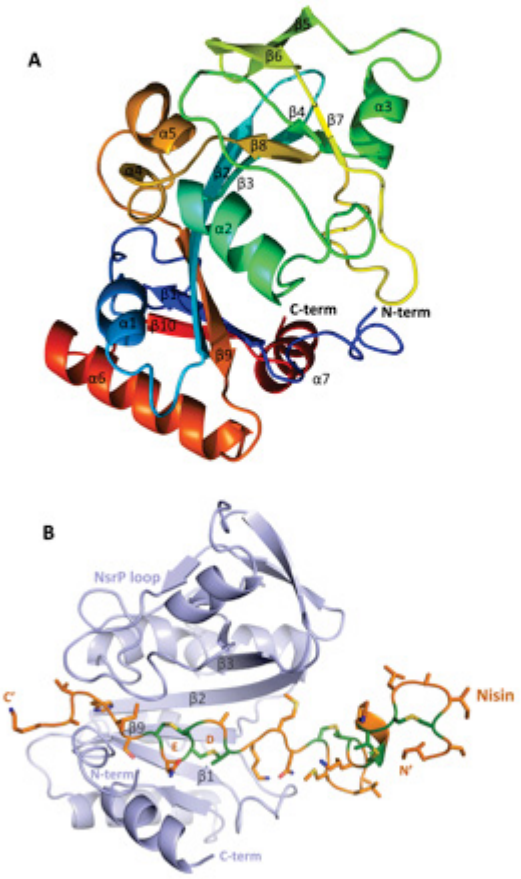

Fig. 8: Structural model of NsrP loop
A) Cartoon representation of the predicted model of NsrP loop using TopModel based comparative modeling.
B) The NsrP loop/nisin complex model as generated using XX server. NsrP loop is represented in light blue color while nisin molecule is in orange. The (methyl-) lanthionine rings of nisin are shown in green, while the last two rings are labeled D-E.

The present study investigated the role of NsrP loop in nisin resistance in *S. agalactiae*. We heterologously expressed and purified the extracellular domain NsrP loop (Fig. 3) of the ABC transporter NsrFP. We were thus able to characterize in detail the molecular properties of NsrP loop and obtain an insight into the structure.

Previous studies in homologous systems (Kallenberg *et al.*, 2013) and similarity of NsrK to IMSK kinases (lacking sensory domains) have indicated towards a probable binding event between these domains and the cognate lantibiotic, in this case nisin. Subsequently, an interaction event between NsrP loop and nisin could be established (Fig. 4,5) based on the results of the pull-down assays which were further supported by an agar diffusion assay (Fig. 5) and confirmed via HPLC (Fig. 4C). It was observed that most nisin molecules do not bind to the Ni-NTA resin and are eluted directly after the first washing step. However, a small fraction of nisin molecules still binds the column and can be eluted from the resin as seen from a smaller inhibition zone formed in the diffusion test (Fig. 5B). In contrast, when NsrP loop is immobilized on the resin, only a small fraction of nisin molecules don't bind the resin (Fig. 5A), while majority of the nisin molecules are still bound to the resin and can be eluted successfully with higher imidazole concentrations.

Furthermore, NsrP loop displays a weak affinity for nisin as indicated from the obtained value for the equilibrium dissociation constant K_D for NsrP loop and nisin interaction in the micromolar range (around 1.60±0.13 µM) (Fig. 6). This rather low affinity of NsrP loop for nisin is unexpected since nanomolar concentrations of nisin are already enough to affect cell growth. Thus, if NsrP loop provides resistance against nisin through binding, it should have a higher affinity towards nisin.

One important factor affecting this measurement could be the purity of nisin. Since, powdered nisin was used for determining the K_D, it could very well be that this high value is a result of the possible impurities present in the nisin sample. Thereby, it is worthwhile to repeat the measurement using purified nisin to rule out the effect of any possible impurities on the assay.

However, this high value of dissociation constant is supported by a similar weak affinity for nisin (K_D of 0.6-2 µM) displayed by the nisin immunity protein NisI of lantibiotic producing strains (Hacker *et al.*, 2015, Takala *et al.*, 2004) which also functions primarily by specifically binding to nisin (Stein *et al.*, 2003, Takala *et al.*, 2004). Thus, this weak affinity could probably hint towards possible additional roles for the loop, other than just binding nisin. In *B. subtilis*, the BceB-loop is required for bacitracin induced expression of *bce*AB genes and for proper folding of BceAB (Coumes-Florens *et al.*, 2011).

After predicting the substrate for NsrP loop, the next question was to have insight into the structure of NsrP loop and consequently, into the NsrP loop/nisin complex.

Although, diamond-shaped crystals (Fig. 7) were obtained for NsrP loop, further optimizations are still required for future experiments. Meanwhile, a model was predicted using TopModel server to visualize the putative structure of NsrP loop. The tip regions of permeases are usually characterized by presence of a α-helix and a β-hairpin (Xu *et al.*, 2009) as seen in the tip of the periplasmic regions of macrolide antibiotic-specific transporter MacB (Xu *et al.*, 2009) and multidrug exporter AcrB (Sennhauser *et al.*, 2007) of *E. coli*. In NsrP loop, the tip region is formed by α3 and β5-β6 for NsrP loop (Fig. 8A).

Using the model of NsrP loop and the structure of nisin, a model of NsrP loop/nisin model was predicted via ZDOCK server (Pierce *et al.*, 2014) (Fig. 8B). While the N-terminus of nisin is available freely in the predicted complex, the C-terminal region of nisin is embedded in the central core of the protein. Furthermore, the center of NsrP loop has sufficient space to accommodate the C-terminally located last two rings of nisin. This hints towards the substrate specificity of NsrP loop where the C-terminus of nisin might be important for the binding of NsrP loop with nisin. The fact that the first two rings of nisin are important for binding to lipid II while the last two rings are responsible for pore formation (Hsu *et al.*, 2004, Wiedemann *et al.*, 2001, Hasper *et al.*, 2004), further supports this finding. Thus, as nisin starts binding lipid II via the N-terminus, NsrP loop binds the nisin molecule through its C-terminus and probably passes onto NsrK. However, these finding needs to be confirmed through additional studies involving mutagenesis of nisin.

Interestingly, these resistance-associated ABC transporters are not specific against a single lantibiotic, but are known to identify multiple substrates. The expression of CprABC from *C. difficile* is induced by nisin, gallidermin, subtilin, mutacin 1140, actagardine and cinnamycin (Suárez *et al.*, 2013). However, further studies are required to confirm whether NsrP loop is only specific for nisin or has the ability to identify a broad range of substrates.

In conclusion, the data obtained here, along with those available in the literature, suggest the involvement of a common mechanism of action for these BceAB-type extra cellular domains (loop). Although, the *nsr* system is structurally different from the others (due to the presence of an additional serine protease), these ABC transporters unifying require the extracellular domain structurally as well as functionally. Furthermore, an insight was gained into the substrate specificity revealing the importance of the C-terminus of nisin. However, better knowledge and further studies are required that might provide interesting clues towards possible ways of overcoming resistance.

REFERENCES

Abts, A., Mavaro, A., Stindt, J., Bakkes, P. J., Metzger, S., Driessen, A. J., Smits, S. H. & Schmitt, L. (2011). *International journal of peptides* **2011**.

Beach, A. (1952). *J. Gen. Microbiol.* **6**, 60-63.

Becker, P., Hakenbeck, R. & Henrich, B. (2009). *Antimicrob. Agents Chemother.* **53**, 2034-2041.

Coumes-Florens, S., Brochier-Armanet, C., Guiseppi, A., Denizot, F. & Foglino, M. (2011). *PLoS One* **6**.

de Freire Bastos, M. d. C., Coelho, M. L. V. & da Silva Santos, O. C. (2015). *Microbiology* **161**, 683-700.

De Kwaadsteniet, M., Doeschate, K. & Dicks, L. (2009). *Lett. Appl. Microbiol.* **48**, 65-70.

Delves-Brougthon, J. (1990). *Food Technol.* **44**, 100-117.

Dintner, S., Staroń, A., Berchtold, E., Petri, T., Mascher, T. & Gebhard, S. (2011). *J. Bacteriol.* **193**, 3851-3862.

Dischinger, J., Chipalu, S. B. & Bierbaum, G. (2014). *Int. J. Med. Microbiol.* **304**, 51-62.

Draper, L. A., Cotter, P. D., Hill, C. & Ross, R. P. (2015). *Microbiol. Mol. Biol. Rev.* **79**, 171-191.

Dubois, A. (1995). *Emerg. Infect. Dis.* **1**, 79.

Dyballa, N. & Metzger, S. (2009). *Journal of visualized experiments: JoVE*.

Falord, M., Karimova, G., Hiron, A. & Msadek, T. (2012). *Antimicrob. Agents Chemother.* **56**, 1047-1058.

Falord, M., Mäder, U., Hiron, A., Debarbouille, M. & Msadek, T. (2011). *PLoS One* **6**, e21323.

Fernández, L., Delgado, S., Herrero, H., Maldonado, A. & Rodríguez, J. M. (2008). *J. Hum. Lact.* **24**, 311-316.

Gasteiger, E., Hoogland, C., Gattiker, A., Wilkins, M. R., Appel, R. D. & Bairoch, A. (2005). *The proteomics protocols handbook*, pp. 571-607: Springer.

Gebhard, S. (2012). *Mol. Microbiol.* **86**, 1295-1317.

Gebhard, S., Fang, C., Shaaly, A., Leslie, D. J., Weimar, M. R., Kalamorz, F., Carne, A. & Cook, G. M. (2014). *Antimicrob. Agents Chemother.* **58**, 1425-1433.

Guder, A., Wiedemann, I. & Sahl, H. G. (2000). *Peptide Science* **55**, 62-73.

Hacker, C., Christ, N. A., Duchardt-Ferner, E., Korn, S., Göbl, C., Berninger, L., Düsterhus, S., Hellmich, U. A., Madl, T. & Kötter, P. (2015). *J. Biol. Chem.*, jbc. M115. 679969.

Hasper, H. E., de Kruijff, B. & Breukink, E. (2004). *Biochemistry* **43**, 11567-11575.

Hiron, A., Falord, M., Valle, J., Débarbouillé, M. & Msadek, T. (2011). *Mol. Microbiol.* **81**, 602-622.

Hsu, S.-T. D., Breukink, E., Tischenko, E., Lutters, M. A., de Kruijff, B., Kaptein, R., Bonvin, A. M. & van Nuland, N. A. (2004). *Nat. Struct. Mol. Biol.* **11**, 963-967.

Johns, S. & Speth, R. (2010). TOPO2, Transmembrane protein display software.

Jung, G. & Sahl, H.-G. (1991). *Nisin and novel lantibiotics*. Springer Science & Business Media.

Kallenberg, F., Dintner, S., Schmitz, R. & Gebhard, S. (2013). *J. Bacteriol.* **195**, 3287-3297.

Kawada-Matsuo, M., Yoshida, Y., Zendo, T., Nagao, J., Oogai, Y., Nakamura, Y., Sonomoto, K., Nakamura, N. & Komatsuzawa, H. (2013). *PLoS One* **8**, e69455.

Khosa, S., Alkhatib, Z. & Smits, S. H. (2013). *Biol. Chem.* **394**, 1543-1549.

Kim, T.-S., Hur, J.-W., Yu, M., Cheigh, C.-I., Kim, K.-N., Hwang, J.-K. & Pyun, Y.-R. (2003). *Journal of Food Protection®* **66**, 3-12.

Li, B., Yu, J. P. J., Brunzelle, J. S., Moll, G. N., Van der Donk, W. A. & Nair, S. K. (2006). *Sci* **311**, 1464-1467.

Linton, A. (1958). *J. Bacteriol.* **76**, 94.

Majchrzykiewicz, J. A., Kuipers, O. P. & Bijlsma, J. J. (2010). *Antimicrob. Agents Chemother.* **54**, 440-451.

Mascher, T. (2006). *FEMS Microbiol. Lett.* **264**, 133-144.

McBride, S. M. & Sonenshein, A. L. (2011). *Infect. Immun.* **79**, 167-176.

Meehl, M., Herbert, S., Götz, F. & Cheung, A. (2007). *Antimicrob. Agents Chemother.* **51**, 2679-2689.

Mota-Meira, M., Lapointe, G., Lacroix, C. & Lavoie, M. C. (2000). *Antimicrob. Agents Chemother.* **44**, 24-29.

Nawrocki, K. L., Crispell, E. K. & McBride, S. M. (2014). *Antibiotics* **3**, 461-492.

Ohki, R., Giyanto, Tateno, K., Masuyama, W., Moriya, S., Kobayashi, K. & Ogasawara, N. (2003). *Mol. Microbiol.* **49**, 1135-1144.

Ouyang, J., Tian, X.-L., Versey, J., Wishart, A. & Li, Y.-H. (2010). *Antimicrob. Agents Chemother.* **54**, 3895-3906.

Pierce, B. G., Wiehe, K., Hwang, H., Kim, B.-H., Vreven, T. & Weng, Z. (2014). *Bioinformatics* **30**, 1771-1773.

Revilla‐Guarinos, A., Gebhard, S., Mascher, T. & Zúñiga, M. (2014). *Environ. Microbiol.* **16**, 1225-1237.

Rietkötter, E., Hoyer, D. & Mascher, T. (2008). *Mol. Microbiol.* **68**, 768-785.

Rogers, A. M. & Montville, T. J. (1991). *Food Biotechnol.* **5**, 161-168.

Sahl, H.-G. & Bierbaum, G. (1998). *Annual Reviews in Microbiology* **52**, 41-79.

Sahl, H. G., Jack, R. W. & Bierbaum, G. (1995). *Eur. J. Biochem.* **230**, 827-853.

Šali, A. & Blundell, T. L. (1993). *J. Mol. Biol.* **234**, 779-815.

Schultz, J., Milpetz, F., Bork, P. & Ponting, C. P. (1998). *Proceedings of the National Academy of Sciences* **95**, 5857-5864.

Sennhauser, G., Amstutz, P., Briand, C., Storchenegger, O. & Grutter, M. (2007). *PLoS Biol.* **5**, e7.

Staroń, A., Finkeisen, D. E. & Mascher, T. (2011). *Antimicrob. Agents Chemother.* **55**, 515-525.

Stein, T., Heinzmann, S., Solovieva, I. & Entian, K.-D. (2003). *J. Biol. Chem.* **278**, 89-94.

Suárez, J. M., Edwards, A. N. & McBride, S. M. (2013). *J. Bacteriol.* **195**, 2621-2631.

Sun, Z., Zhong, J., Liang, X., Liu, J., Chen, X. & Huan, L. (2009). *Antimicrob. Agents Chemother.* **53**, 1964-1973.

Takala, T. M., Koponen, O., Qiao, M. & Saris, P. E. (2004). *FEMS Microbiol. Lett.* **237**, 171-177.

Tsuda, H., Yamashita, Y., Shibata, Y., Nakano, Y. & Koga, T. (2002). *Antimicrob. Agents Chemother.* **46**, 3756-3764.

Valenta, C., Bernkop‐SchnüRch, A. & Rigler, H. P. (1996). *J. Pharm. Pharmacol.* **48**, 988-991.

Vos, W. M., Kuipers, O. P., Meer, J. R. & Siezen, R. J. (1995). *Mol. Microbiol.* **17**, 427-437.

Wiedemann, I., Breukink, E., Van Kraaij, C., Kuipers, O. P., Bierbaum, G., De Kruijff, B. & Sahl, H.-G. (2001). *J. Biol. Chem.* **276**, 1772-1779.

Xu, Y., Sim, S.-H., Nam, K. H., Jin, X. L., Kim, H.-M., Hwang, K. Y., Lee, K. & Ha, N.-C. (2009). *Biochemistry* **48**, 5218-5225.Yang, S.-C., Lin, C.-H., Sung, C. T. & Fang, J.-Y. (2014). *Front. Microbiol.* **5**.

Yoshida, Y., Matsuo, M., Oogai, Y., Kato, F., Nakamura, N., Sugai, M. & Komatsuzawa, H. (2011). *FEMS Microbiol. Lett.* **320**, 33-39.

4. Discussion

In this thesis, an operon responsible for conferring nisin resistance in *Streptococcus agalactiae* was discovered. Furthermore, the corresponding proteins were studied on a molecular level elucidating the involved mechanism of resistance through structural characterization.

4.1 Nisin resistance

Of all the lantibiotics known so far, nisin remains the most extensively studied lantibiotic [35, 59]. Nisin has been commercially used in the food industry for a long time [225] and displays antimicrobial activity against various Gram-positive bacteria including human pathogenic strains such as *S. epidermis* and *S. aureus* [226].

However, some bacteria like *L. monocytogenes* [146, 178] are inherently resistant to nisin [121]. Interestingly, a unique nisin degrading mechanism has been identified that involves the presence of a nisin resistance protein (NSR) [198]. NSR is present in lantibiotic non-producing strains [206, 198] and proteolytically degrades nisin by cleaving the six amino acids from the carboxyl tail of nisin [198]. The resulting nisin fragment ($nisin^{1-28}$) displays 100-fold lower bactericidal activity and reduced affinity for cell membrane [198].

By genomic data and comparative sequence analysis, *nsr* gene was identified in various bacterial strains of corynebacterium, leuconostoc, enterococcus, staphylococcus and streptococcus genera (chapter I). Furthermore, *nsr* gene is localized on a specific operon within the genome, termed here as *nsr* operon encoding six different proteins (Figure 13). The *nsr* operon resembles the immunity operon of the nisin producing strains [64] as it consists of a membrane associated *nsr*, and an ABC transporter, termed here as *nsrFP* (NsrF is named after *lanF* found in the producer strains and P stands for the permease). Furthermore, a two-component system is also present, consisting of the response regulator and the histidine kinase (designated as *nsrR* and *nsrK*, respectively). Additionally, the *nsr* operons identified could be categorized in four different groups based on the orientation and the order of the genes (chapter I).

Although a few similar resistance operons against lantibiotics are known such as *cpr*ABCK-R in *C. difficile* provides resistance against lantibiotics such as nisin, gallidermin, subtilin [182]. A multicomponent operon *lia*IHGFSR in *Bacillus* spp. confers resistance towards bacitracin, ramoplanin, vancomycin and nisin [177, 175]. *lct*GEF*lcr*XRS and *nsr*XRS form

two distinct gene systems in *S. mutans* which confer resistance against nisin, nukacin ISK-1 and lacticin 481 [163]. However, other than determination of the genes involved in resistance, there is nothing known about these proteins on a molecular level. Furthermore, the molecular and structural characterizations of these proteins involved in lantibiotic resistance are still missing.

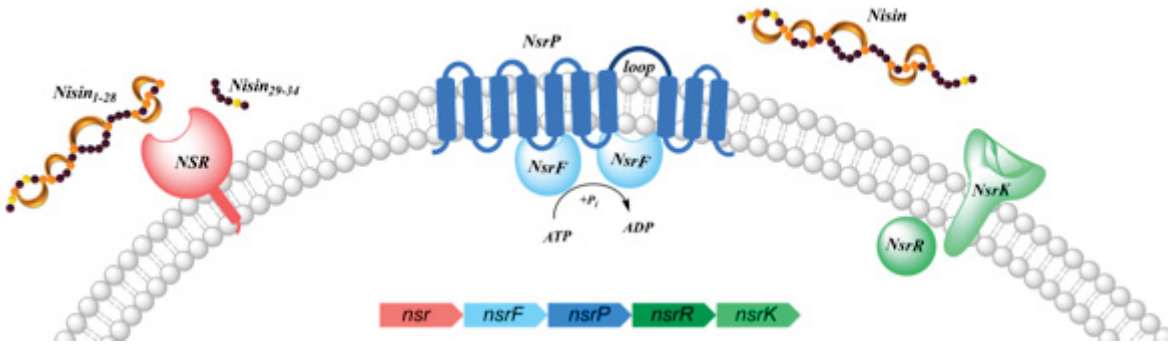

Figure 13: The nisin resistance system. The nisin resistance protein (NSR) is shown in shade of pink. The two-component system regulatory proteins: NsrR (dark green) and NsrK (light green) and the ABC transporter proteins: NsrF (sky blue) NsrP (blue) are also shown with the extracellular domain (loop) highlighted in dark blue. Adapted from chapter I and created with Chem BioDraw 13.0

Thereby, to compare the results obtained within this thesis, the well characterized nisin immunity system from the nisin producing strains serves as a model. Additionally, the distinct proteins involved in immunity and regulation of nisin in lantibiotic producer strains are extensively studied and various studies involving these proteins are available including functional and structural information.

4.2 Differentiating innate immunity of producers and intrinsic resistance of non-producers

The focus within this section is on the innate immunity present in the producer strains towards lantibiotics, specifically nisin and the intrinsic resistance of the non-producers against nisin through a comparison of the known biochemical and structural data in the literature published and the data obtained within this thesis.

Lantibiotics have a broad spectrum of activity including various Gram-positive bacteria, where low nanomolar concentrations of lantibiotics are already enough to permeabilize the bacterial membrane. Thus, the lantibiotic producer strains have an inbuilt self-protection

mechanism (immunity) to prevent cell death caused due to the action of its cognate lantibiotic [93]. This immunity system consists of a membrane–associated lipoprotein (usually referred to as LanI), and/or an ABC transporter (termed as LanFEG and comprising of three subunits) [91]. Although, some lantibiotic immunity systems such as Pep5, epicidin, epilancin and lactocin S only require LanI for immunity, other lantibiotics with a dual mode of action involving pore formation and lipid II binding such as nisin, subtilin, epidermin, gallidermin and lacticin 3147 require additionally the presence of LanFEG also [227, 59, 64]. Some examples are NisI and NisFEG of the nisin system, SpaI and SpaFEG confer immunity towards subtilin, PepI constitutes the immunity system of Pep5 producing strains [228].

On the contrary, an intrinsic resistance mechanism is present in some lantibiotic non-producer strains including human pathogenic strains to combat the effect of the lantibiotic present in the environment. This resistance is mediated by the expression of several genes localized on a specific operon, which resembles the genetic architecture of the lantibiotic immunity genes found in producing strains. However, it lacks the structural gene and the genes for modification and transportation of the lantibiotic outside the cell. Furthermore, the upregulation of these genes is mediated by a specific two-component system similar to the one found in lantibiotic producing strains [93, 184]. Some examples for such lantibiotic-resistance operons are *gra*XSR-*vra*FG in *S. aureus* conferring resistance against nisin A and nukacin ISK-1; the *cpr* operon in *C. difficile* conferring resistance against multiple lantibiotics such as nisin, gallidermin, subtilin, and mutacin 1140; *lct*GEF*lcr*XRS in *S. mutans* conferring resistance against nisin, nukacin ISK-1 and lacticin 481 [163]. The resistance system comprises of an ABC transporter (usually comprising of two subunits) and/or a resistance protein (in case of nisin – proteolytically cleaves nisin).

The most extensively studied lantibiotic till date is nisin, which is produced by some strains of *L. lactis* and *S. uberis* strains [4, 78, 229]. Active nisin consists of 34 amino acids and contains five (methyl-)lanthionine rings where the first three rings (ring A-C) are separated from the last two intertwined rings (ring D-E) by a flexible hinge region [230]. Rings A and B are able to bind lipid II, a essential component in Gram-positive bacteria for cell wall synthesis which thereby is inhibited [231], whereas the hinge region and ring D and E, are able to flip into the membrane and create pores [85, 232, 89], which lead to an efflux of nutrients and small compounds out of the cell, subsequently leading to cell death [233].

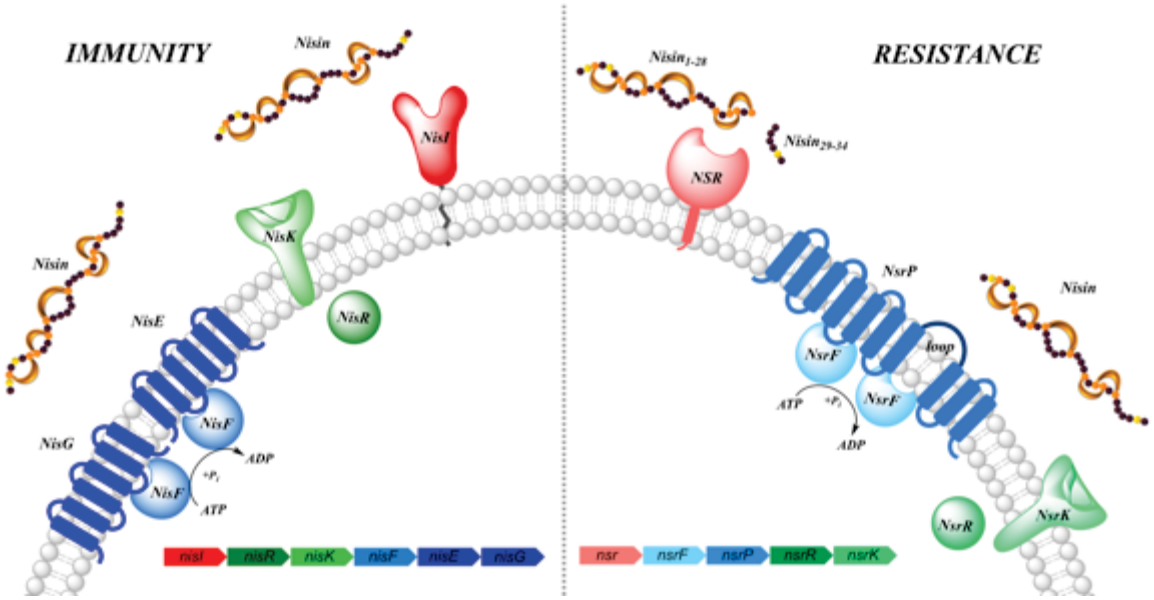

Figure 14: The nisin immunity and resistant system. Both the systems comprise of a lipoprotein (colored in red), an ABC transporter (depicted in blue) and a two-component system (shown in green). Six genes comprise the immunity system while there are five genes in the resistant system. Functionally similar genes are colour coded identically with the exception of NisI and NSR.

The nisin producer *L. lactis* strains protect themselves from the suicidal activity of nisin by expressing two protein comprising the immunity system: the lipoprotein NisI and the ABC transporter NisFEG [94] (Figure 14).

On the contrary, in non-nisin producer strains such as *S. agalactiae*, a similar operon confers resistance against nisin [184]. This operon is characterized by the presence of a nisin resistance protein (NSR) and an ABC transporter NsrFP which are auto-regulated by a two-component system comprising of NsrR and NsrK (chapter I) (Figure 14).

4.3 The first line of defense: NisI and NSR

The following section compares the immunity protein of the nisin producing strains with its counterpart resistance protein in the nisin resistant strains, which forms the first line of defense against the killing mechanism of the lantibiotics.

Since low amounts of lantibiotics are already enough to permeabilize the cell membrane and kill the bacteria, the producer strain regulates the expression of its immunity genes to combat this self-suicidal action. One of the primarily components of this self-immunity is the so-called LanI family of proteins. Although, some lantibiotic immunity systems such as

Pep5, epicidin, epilancin and lactocin S only require LanI for immunity, other lantibiotics with a dual mode of action involving pore formation and lipid II binding such as nisin, subtilin, epidermin, gallidermin and lacticin 3147 require additionally the presence of LanFEG also [227, 59, 64].

4.3.1 The nisin immunity protein NisI

In nisin producing strains, the immunity protein NisI is 27.8 kDa comprising of 245 amino acid residues [94, 234]. It carries a 19 residues long lipoprotein signal peptide, and a site for lipid modification (Cys1 in mature NisI) [91, 234]. NisI is secreted through the cytoplasmic membrane where cleavage of the signal peptide occurs, and the mature NisI (226 amino acid residues and 25.8 kDa in size) is anchored to the outside of the cytoplasmic membrane by its N-terminal lipid [224]. However, approximately one-third of NisI escapes this modification machinery and is released into the extracellular environment in a lipid-free form that forms an additional mechanism of immunity [102, 235].

The main function of NisI is to provide immunity by directly interacting with nisin to prevent its attachment to the membrane, inhibiting pore formation [103, 236], thereby protecting the nisin-producing bacteria. Important here is the fact that NisI is not involved any modification or degradation of nisin [93, 101, 224, 237, 103, 102, 238].

When expressed in the nisin sensitive *L. lactis* strain NZ900, which does not carry the immunity genes *nisI* and *nisFEG* within its genome, NisI confers 8-10 fold immunity. This was measured by comparing the IC_{50} values against nisin with and without expressing NisI [238].

Various studies have indicated the importance of the C-terminus of NisI, especially the last 22 amino acids, in binding to nisin and inhibition of nisin mediated pore formation [239, 238]. A deletion of the last 5 residues decreases the immunity conferred by NisI to approximately 78% [239]. Furthermore, a longer deletion of the last 22 residues, reduces the capability of NisI to inhibit the activity of nisin by a factor of one-third [238].

Recently, in addition to the binding capability of NisI, a second mechanism of conferring immunity by NisI was also identified. Upon addition of nisin to *L. lactis* cells, expressing solely NisI, the cells cluster and form large chains of up to 30 cells [238]. This clustering appears to reduce the possibility of nisin to reach lipid II. This effect has been called a "shielding mechanism" and is reversible [238]. This way when the concentration of nisin

increases to a certain threshold (in the reported study around 60-70 nM), which coincides with the measured IC_{50} values, the cells are immune to nisin [238]. Interestingly, this phenomenon does not occur with the NisI variant lacking the C-terminal 22 amino acids, leading to the assumption that the observed cell clustering is initiated by the C-terminus [238]. This suggests that the inhibition observed when nisin was added to NisI expressing *L. lactis* cells is not due to cell death rather the cell clustering prevents the cells from further growing.

Similarly, the pore formation is also observed when adding low amounts of nisin (10 nM) to nisin sensitive *L. lactis* strains as measured by Sytox Assay [238]. However, when expressing NisI even upto concentration of 1000 nM, this pore formation is not observed, clearly suggesting that the cell clustering is also a way of shielding *L. lactis* membrane and prevent nisin mediated pore formation [238]. Furthermore, pore formation was observed with the C-terminus deletion mutant of NisI reiterating the importance of the C-terminus of NisI (last 21 amino acid fragment) in interaction with nisin and provides specificity to NisI-nisin interaction [239].

The substrate specificity of NisI lies in the N-terminus of nisin, presumably the first two rings. *In vivo* growth experiments have showed that variations at the C-terminus of nisin had no major effect on the *L. lactis* sensitive strain as the IC_{50} values still remain the same [240]. Since the first two rings of nisin (N-terminal region) are crucial for its initial binding to lipid II [85] which eventually leads to pore formation, it could be that NisI shares the same specificity.

Since NisI conferred immunity is a result of its binding to nisin, it is surprising that nisin binds to NisI with a weak affinity as determined by its K_D in low micromolar range (approximately 0.6–2 μM) [235, 236]. However, this high value might be the result of the in vitro measurement being performed without the membrane environment.

Although NisI doesn't show any sequence homology with other LanI immunity proteins [241], the cellular function of NisI is similar to the subtilin immunity protein SpaI in *B. subtilis*, involving binding to subtilin, thereby protecting the producer membrane [242]. Interestingly, despite the high sequence homology of 60% between nisin and subtilin, no cross immunity has been observed so far [223] indicating towards the specificity of the immunity protein towards its respective lantibiotic.

4.3.2 Nisin Resistance Protein NSR

The counter part of NisI in the nisin resistance system is, the nisin resistance protein termed NSR. NSR of *S. agalactiae* contains 320 amino acids and has a theoretical molecular weight of 36.2 kDa [206]. NSR has a N-terminus hydrophobic region encoding a transmembrane sequence of 21 residues [206] and is localized in the membrane.

NSR is proteolytic degrading nisin [198]. This nisin degradation mechanism is quite unique since the lanthionine rings cause steric hindrance, inhibiting the protease cleavage [85]. NSR cleaves of the last six amino acids of nisin, yielding two fragments of nisin and the major product is called nisin$^{1-28}$. This nisin variant displays 100-fold less bactericidal activity and has less affinity for the bacterial membrane [198]. So by reducing the effectiveness of nisin, the non-producing strains become more resistant. When expressed in a nisin sensitive *L. lactis* strain, NSR confers 18-20 fold resistance (chapter I) as determined by the IC_{50} assay.

Furthermore, for the nisin variants CCCCA and CCCAA (last or the last two C-terminally located rings are missing), the resistance mediated by NSR in nisin sensitive *L. lactis* strain dropped to mere 1.4-1.7 fold (chapter III). Additionally, removing the last six or twelve amino acids of nisin ($nisin_{1-28}$ and $nisin_{1-22}$, respectively) completely abolished the resistance, clearly indicating the importance of the last ring as well as the C-terminal tail of nisin for recognition by NSR (chapter III).

Although, nisin shares a high sequence similarity of around 63% with subtilin; and various lantibiotics such as subtilin, subtilomycin which also harbour five lanthionine rings in their structures [243]. However, the specificity of NSR towards other lantibiotics is still unknown and is possible that NSR exhibits broader substrate specificity.

4.3.3 Structural comparison of NSR and NisI

Recently, the structure of NisI (in two domains) from *L. lactis* was solved using NMR spectroscopy (PDB codes: 2N32 and 2N2E) [236]. NisI is a two-domain predominantly β-sheet protein (Figure 15).

The N-terminal part (1-111 residues) is connected to the C-terminal domain (120-226) via a flexible linker (112-119) (Figure 15). Interestingly, both the domains of NisI adopt a similar fold which has been previously been observed in the structure of SpaI the immunity protein of the lantibiotic subtilin from *Bacillus subtilis* [236]. However, in contrast to two domains

NisI, SpaI is a single domain protein. A seven-stranded antiparallel twisted β-sheet forms the core of the N- and C- terminal domain of NisI with the strand order β1-β2-β3-β8-β7-β6b-β4a. An extended β-hairpin is formed by strands β4b and β6a and is stabilized by hydrophobic packing interactions with residues from β1 and β2. In addition, the β-hairpin is flanked by a short 3_{10} helix. However, NisI lacks the N-terminus unstructured region, which is present in SpaI and supposedly allows interaction with the host membrane [242, 236].

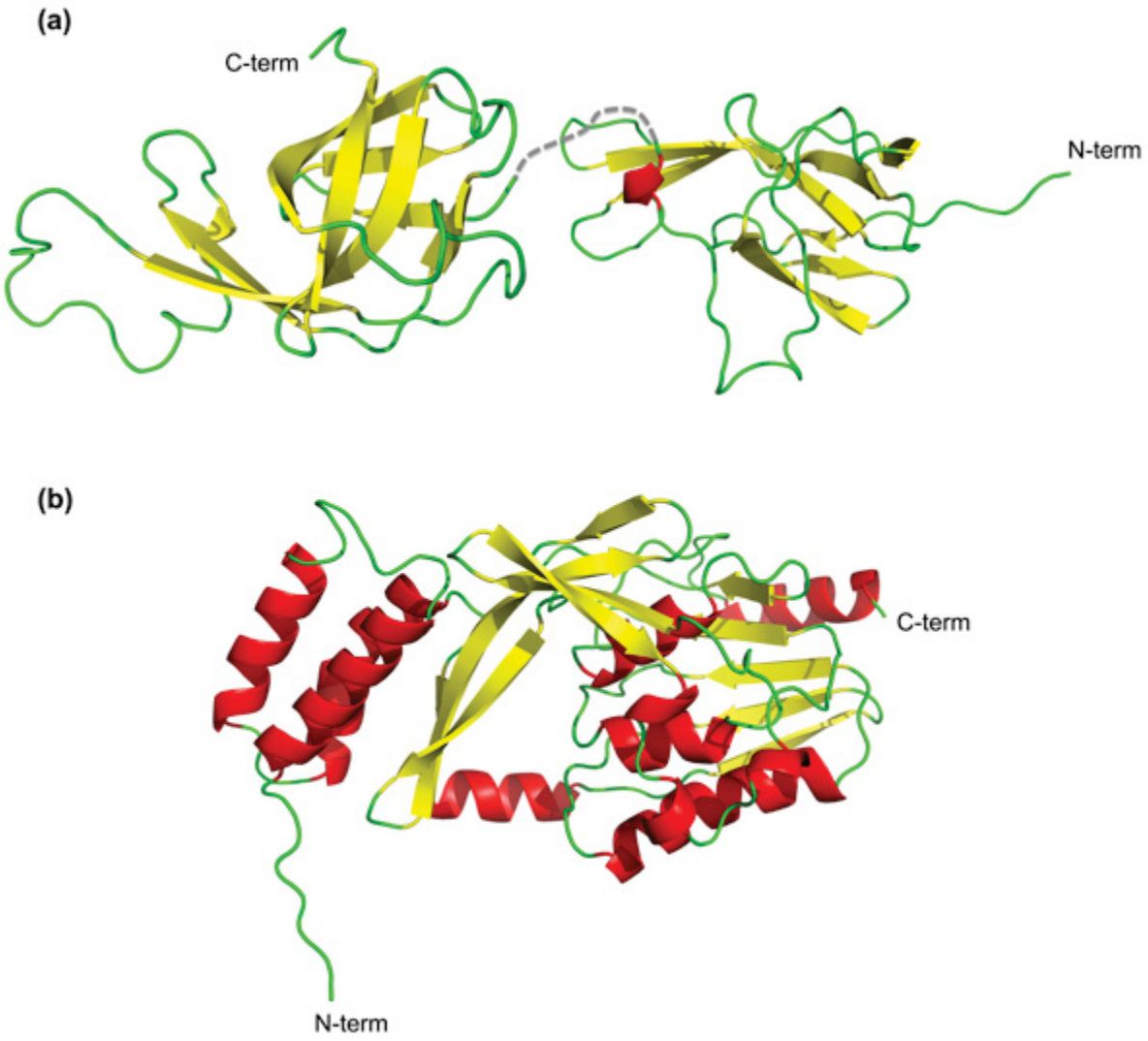

Figure 15: Cartoon representation of the structures of NisI and NSR. The structures of (a) NisI (PDB codes: 2N32 and 2N2E) [236] and (b) NSR (chapter III) are shown with the secondary elements colour coded as red for helices, yellow for sheets and green for the loops. The figure was prepared with Pymol.

Although, an interaction of NisI with the membrane was previously postulated, NMR experiments were performed to confirm the same. These revealed that only the N-terminal domain has affinity towards membrane environment, possibly localized at the membrane while the C-terminal domain does not bind to lipids. Instead, the C-terminal domain specifically binds nisin [236]. This further supports the previous observation about the importance of the C-terminal 22 amino acids for the functioning of NisI *in vivo* [239, 238].
Although structurally similar (Figure 16), both the domains of NisI differ in their surface properties (Figure 17). While the surface of the N-terminal domain is highly positively charged and interacts with membranes, the C-terminal domain has highly negatively charged surface with hydrophobic patches and is able to bind nisin (Figure 17). Thereby modulating the membrane affinity of the N-terminal domain by shielding its membrane binding surface [236].

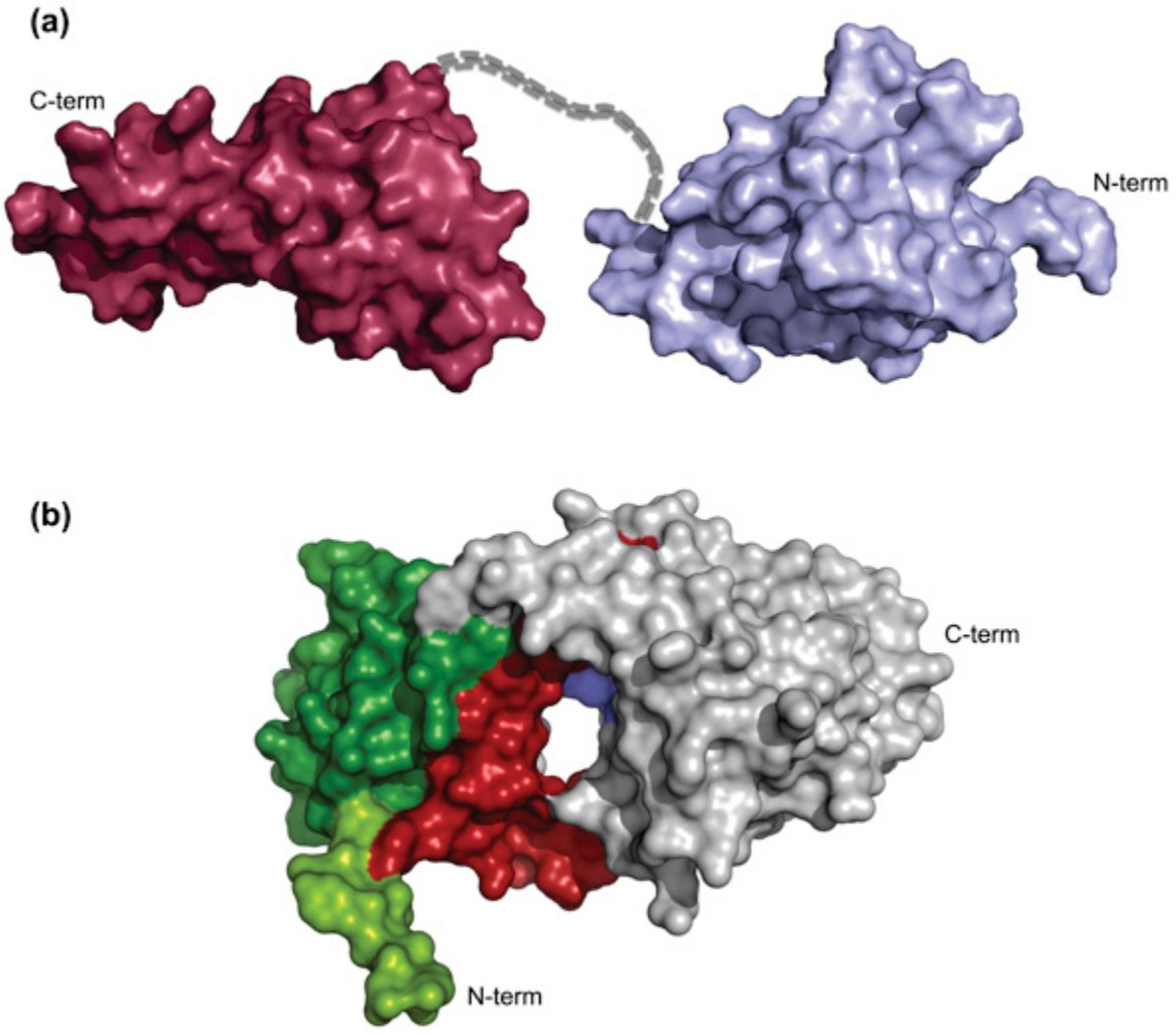

Figure 16: Surface representation of the structures of NisI and NSR. The different domains of (a) NisI (PDB codes: 2N32 and 2N2E) [236] and (b) NSR (chapter III) are colored differently.

On the contrary, the crystal structure of nisin resistance protein from *S. agalactiae* (*Sa*NSR; without the signal peptide) presented within this thesis (chapter III) was solved using X-ray crystallography and comprises of an equal ratio of α-helices and β-strands (eleven each) (chapter III) (Figure 15) and is composed of three domains (Figure 16). An N-terminal helical bundle, the protease cap and core domains, together form a hydrophobic tunnel of ~10 Å width (Figure 16-17). Although the overall fold of NSR does not resemble any specific protein of which the structure is resolved, however the domains alone have some homologous structures. An interaction of NSR with the membrane has not been observed yet. The hydrophobic negatively charged tunnel (Figure 16) is responsible for binding to nisin by 'roping in' the peptide.

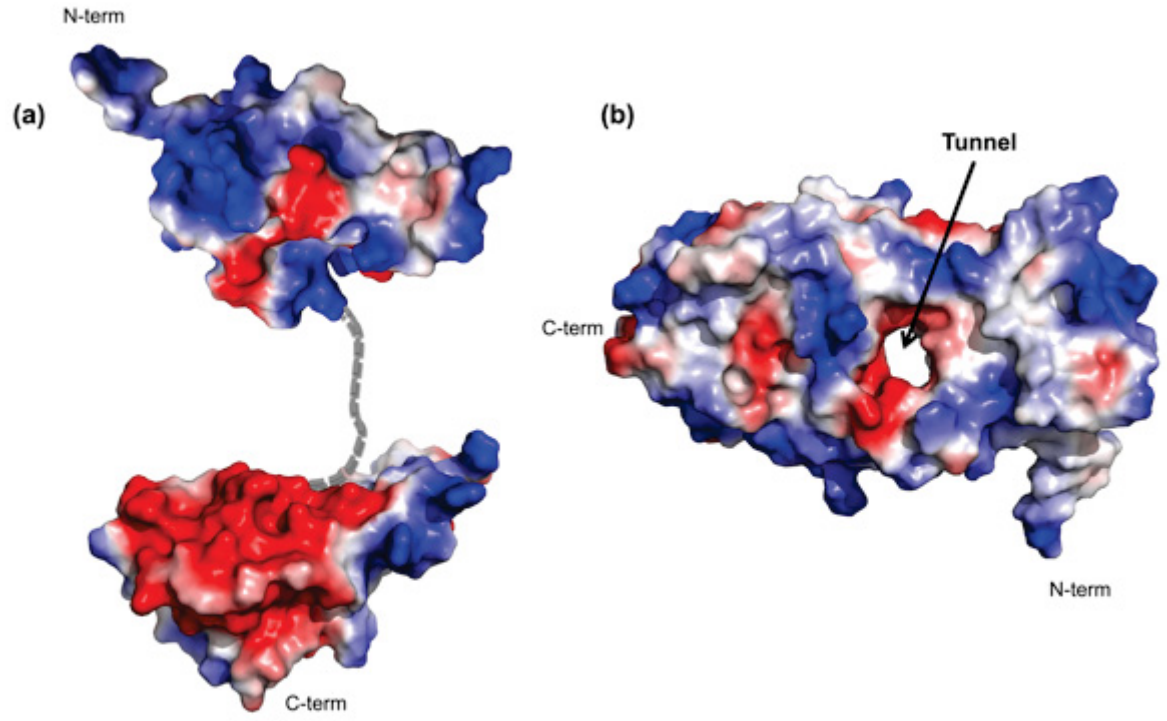

Figure 17: Electrostatic surface potential of the structures of NisI and NSR. The electrostatic surface potential of (a) NisI (PDB codes: 2N32 and 2N2E) [236] and (b) NSR (chapter III) structures is shown. Negatively charged surface areas are colored in red, positively charged areas colored in blue and white areas correspond to hydrophobic surfaces. The figure was prepared with Pymol.

The structure of NSR highlights the importance of the highly conserved TASSAEM region that harbours the catalytically active serine (chapter III). Additionally, the residues forming the hydrophobic interactions for proper orientation of rings D and E of nisin are embedded in the protease core domain that is situated in the middle of NSR protein (chapter III). Although the structure of NSR lacks its substrate nisin, instead a peptide named 'N-pep' was bound in the active site. This information was further used for modeling and molecular dynamic simulations where the N-pep molecule was replaced by the nisin molecule which showed that nisin is stably bound in the tunnel created by the distinct domains of NSR (chapter III).

Table 1: Summary of the comparison between NisI from nisin producing strains and NSR from nisin resistant strains.

	NisI	*NSR*
Sequence length (amino acids)	**245**	**320**
Molecular weight	**27.8 kDa (full-length) / 25.8 kDa (processed)**	**36.2 kDa**
Localization	**Membrane attached / lipid-free**	**Membrane spanning**
Sequence motif	**N-terminal signal peptide**	**N-terminal transmembrane helix / conserved TASSEAM region**
Modification	**Cys linked lipid**	**-**
Function	**Nisin Binding**	**Nisin cleavage at Ser 29**
Observed mechanism	**Reversible cell clustering**	**Lowering activity of nisin**
Substrate specificity	**N-terminus of nisin (rings A and B)**	**C-terminus (rings D and E plus C-terminal located six amino acids)**
Conferred Immunity/ Resistance (sensitive *L. lactis* strain NZ9000 4-6 nM)	**8-10-fold**	**20-fold**
Important residues	**Tyr152, Asp155**	**His98, Ser236**
Binding site	**C-terminus (last 21 amino acids)**	**TASSEAM region**
Binding affinity	**1 µM**	**Not determined**

Structure determined	**NMR**	**X-ray crystallography**
Structure	**β-sheet (two domains)**	**Three domains**
Binding site determined	**NMR / Mutational studies**	**Molecular dynamic simulations/ Mutational studies**

NSR provides resistance against nisin by proteolytically cleaving the peptide bond between MeLan28 and Ser29 of nisin, resulting in two fragments that display less antimicrobial activity and low affinity for membrane [198]. The model of *Sa*NSR/nisin complex certainly demonstrates the significance of C-terminally located last lanthionine ring of nisin for substrate specificity (chapter III). Additionally, mutagenesis analyses support the fact that NSR recognizes the last ring of nisin as it functions as a plug onto the tunnel, properly placing the nisin cleavage site (chapter III).

4.4 Second line of defence: NisFEG and NsrFP

In addition to the membrane anchored immunity/ resistance protein, both the nisin immunity and resistance systems have the presence of an ABC transporter, NisFEG and NsrFP, respectively (Figure 18). They are build up of an soluble ATP binding domain NisF and NsrF which need to dimerize to hydrolyse ATP which consequently is the energy needed by the ABC transporter. The transmembrane domains are NisE and NisG for the immunity system and NsrP of the resistance system.

4.4.1 NisFEG of nisin producers

In the nisin immunity system of nisin producing strains, the cytoplasmic NisF is composed of 225 amino acids and is 24.6 kDa in size. It has ATP-binding sites within the N-terminal end of the protein [94]. Additionally, NisE and NisG are predominantly hydrophobic proteins that together form the integral membrane part of the ABC transporter and are composed of six transmembrane helices each [94]. NisE comprises of 242 amino acids and is 27.6 kDa whereas NisG is 24.1 kDa in size with 214 amino acids. Using sequence similarity searches likely NisFEG exhibits a 2:1:1 stoichiometry to form a functional lantibiotic immunity LanABC transporter [94] (Figure 18). Various gene knockout studies

have shown that out of all the three genes encoding the ABC transporter, deletion of *nisE* gene has the most detrimental effect on the nisin production and immunity [94].

The primarily function of NisFEG in providing immunity to the producer strains is to efflux nisin molecules from the membrane before they can form pores [103, 244]. A similar function has been identified for the subtilin immunity ABC transporter SpaFEG which expulses subtilin molecules from the cytoplasmic membrane into the extracellular medium [223].

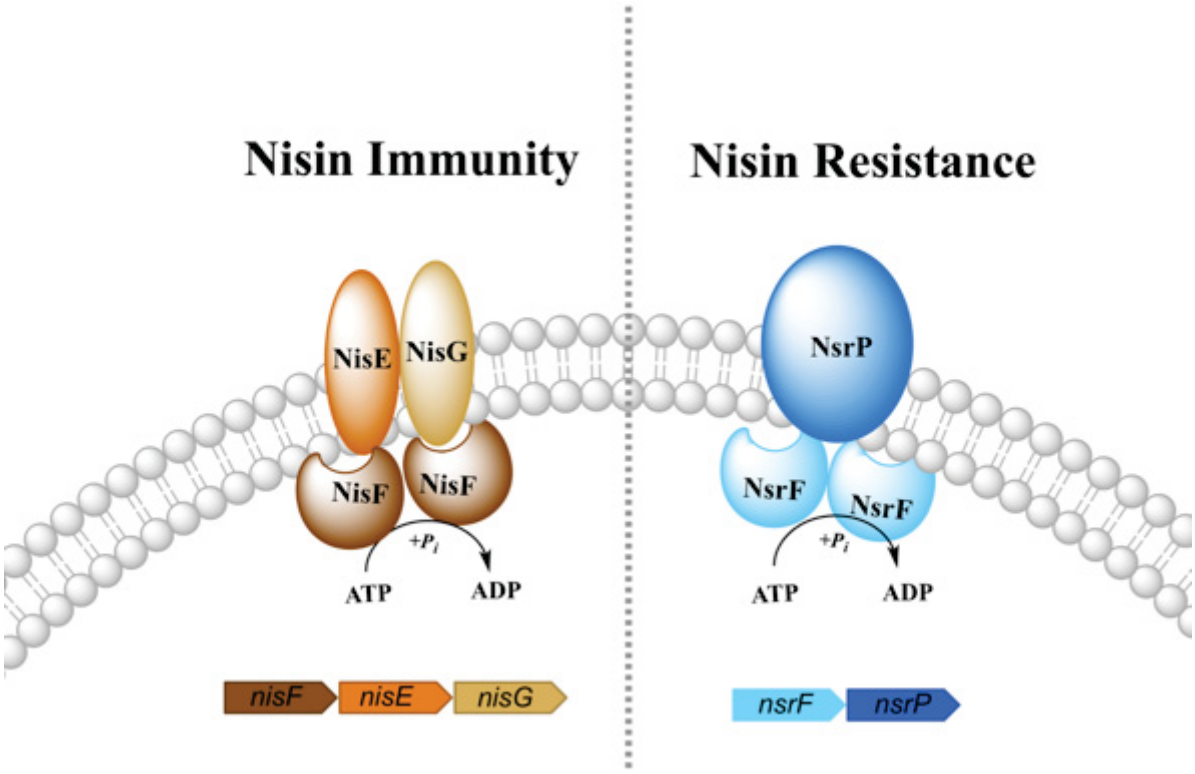

Figure 18: Schematic representation of the ABC transporters involved in nisin immunity and resistance. The ABC transporter involved in nisin immunity (colored in brown and orange) represents a stoichiometry of $NisF_2$:NisE:NisG while the resistance associated ABC transporter (shown in blue) exists in a $NsrF_2$:NsrP ratio.

When expressed in the nisin sensitive *L. lactis* strain NZ9000, which does not carry the immunity genes *nisI* and *nisFEG* within its genome, NisFEG confers seven-eight fold of immunity when expressed alone. [244].

The substrate specificity of NisFEG has been extensively studied. It has been shown that NisFEG recognizes the last C-terminally located lanthionine ring and the last six amino acids of nisin as a reduction of 50% in the immunity provided by NisFEG was seen upon deletion of either of them [244].

4.4.2 NsrFP of nisin non-producers

In contrast, the nucleotide-binding domain of the nisin resistance system is NsrF, which is 28.3 kDa in size and comprises of 250 amino acids residues [245]. Although NisF and NsrF both belong to the P-loop NTPase superfamily and have the presence of the signature motifs of ABC transporters [246], they are just 28% identical [247].

The lantibiotic resistance ABC transporters usually comprise of a single membrane subunit and in comparison to the lantibiotic immunity system, the transmembrane domains NisE and NisG are apparently fused as one into NsrP. Furthermore, NsrP is composed of 612 amino acids and is 69.4 kDa with ten transmembrane helices [248]. It forms the complete transmembrane domain of the ABC transporter NsrFP of the nisin resistance system, leading to a 2:1 stoichiometry for NsrFP (chapter I and VI) (Figure 18). Additionally, NisEG and NsrP share an identity of 21% [247]. The only known exception of a three-component lantibiotic resistance transporter is CprABC in *C. difficile* [182]. A noteworthy point worth mentioning is that unlike NsrFP, CprABC is not specific for a particular lantibiotic and instead recognizes various lantibiotics including nisin, subtilin and cinnamycin [169]. Although a part of NsrFP recognizes nisin (chapter VI), whether it also recognizes various substrates is yet to be determined.

Contrarily, to the immunity ABC transporters that efflux out the lantibiotic, a binding function to the lantibiotic is postulated for lantibiotic resistance ABC transporter systems [121] as also confirmed in chapter VI where a part of the resistance NsrFP transporter binds to nisin. However, the knockout studies and substrate specificity is yet to be determined for NsrFP.

4.4.3 The cytoplasmic loop

The most remarkable difference between the ABC transporters involved in immunity of lantibiotic producing strains and the resistance-associated transporters in non-nisin producing strains is the presence of a large extracellular loop approximately 200-250 amino acids in between helices VII and VIII of the permease (Figure 19) (chapter VI) [174, 181,

184]. This feature is not present in lantibiotic immunity-providing ABC transporters and is a characteristic for the two-component ABC transporters involved in lantibiotic resistance [121] such as BceAB in *B. subtilis* [186], BraAB [167] and NsrFP in *S. agalactiae* (chapter I and VI).

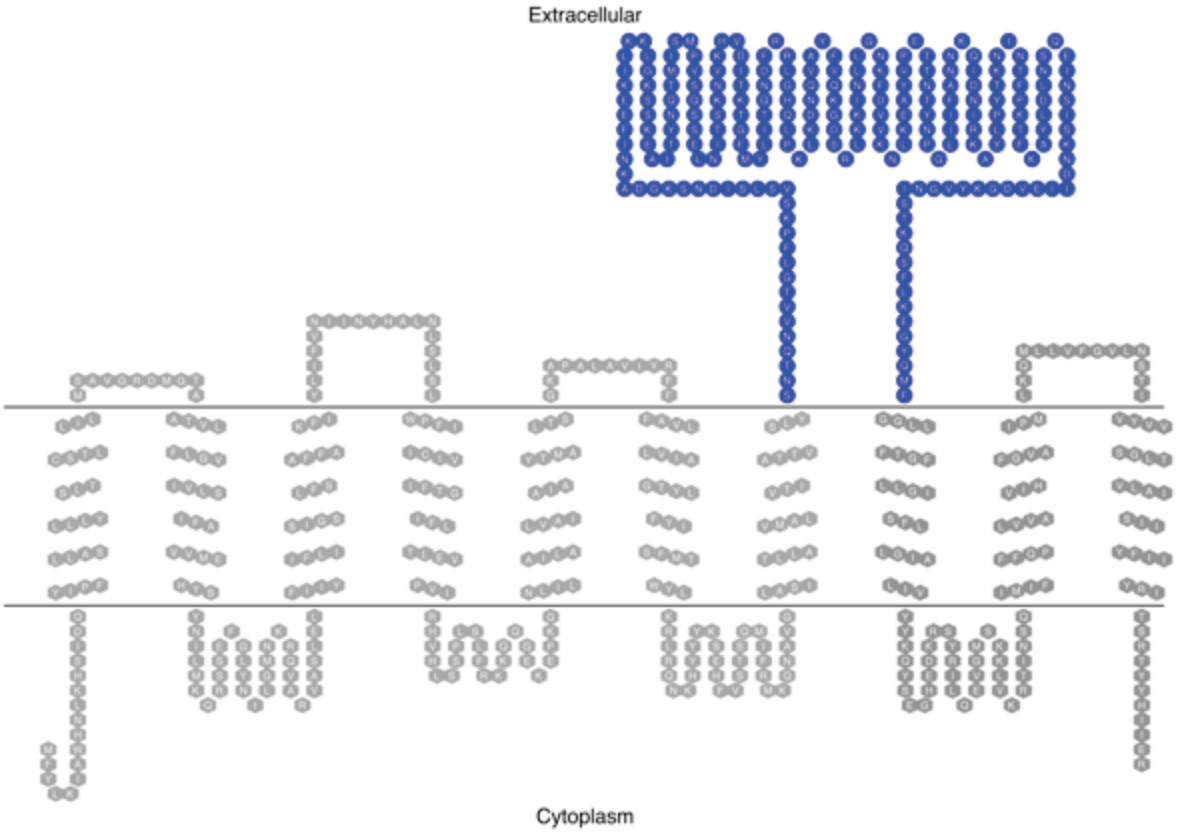

Figure 19: Schematic representation of NsrP loop. The amino acid sequence of NsrP is shown. 221 residues comprising NsrP loop are highlighted in blue while the rest residues are colored in grey. The figure is the output of TOPO2 server [249]. Taken from chapter VI.

Although the loop is the least conserved domain among resistance associated ABC transporters, these loops are known to be specific for their own ABC transporters [250]. A hybrid of the permease BceB from *B. subtilis* and the extracellular domain from another related Bce-AB type transporter did not restore bacitracin resistance in the BceAB transporter [250].

Since the histidine kinases of the associated TCSs lack the sensory domain, these loops function as an additional co-sensor for the regulation of the transcription of the associated genes [186, 250] which includes binding to the AMP/lantibiotic and somehow passing on the signal to the TCSs for upregulation and sensing.

Chapter VI focussed on the possible interaction between NsrP loop and nisin and it was seen that "NsrP loop" indeed interacts with nisin. NsrP loop is 221 amino acids (25.1 kDa) and is present in between helices VII and VIII (Chapters I and VI) (Figure 19).

Furthermore, NsrP loop exhibits a weak affinity for nisin as indicated from the obtained value for the equilibrium dissociation constant K_D for NsrP loop: nisin interaction in the micromolar range (around 1 μM). This rather low affinity of NsrP loop for nisin is unexpected since nanomolar concentrations of nisin are already enough to affect cell growth. Thus, if NsrP loop provides resistance against nisin through binding, it should have a higher affinity towards nisin. However, this high value is further supported by the weak affinity for nisin displayed by nisin immunity protein NisI of nisin producing strains [235, 236] which also functions primarily by specific binding to nisin [103, 235]. It could be possible that this high value is a result of the absence of the membrane environment in *in vitro* experiments.

Table 2: Summary of the differences between the ABC transporters from the nisin producing strains and the nisin resistant strains.

	NisFEG	*NsrFP*
Sequence length (amino acids)	**225 + 242 + 214**	**250 + 612**
Molecular weight	**24.6 kDa + 27.6 kDa + 24.1 kDa**	**28.3 kDa + 69.4 kDa**
Localization	**Membrane spanning**	**Membrane spanning**
Genes encoding ABC transporters	**Three**	**Two**
Extracytoplasmic loop	**Absent**	**Present**
Transmembrane helices	**6 + 6**	**10**
Stoichiometry	**2:1:1**	**2:1**
Function	**Expelling nisin**	**Not known**
Observed mechanism	**Preventing pore formation**	**Binds nisin and additional function not determined yet**
Structure	**Not determined**	**Not determined**
Substrate specificity	**C-terminus (last ring and the last 6 amino acids of nisin)**	**Not determined**
Conferred Immunity/	**6-8-fold**	**Not determined**

Resistance (sensitive *L. lactis* strain NZ9000)		
Structure determined	**Not determined**	**Not determined**

In addition to binding to the substrate, various additional roles have been identified for these extracellular domains. In *B. subtilis*, the "BceB-loop" is required for bacitracin induced expression of *bce*AB genes and for proper folding of BceAB [250]. Further extensive studies of NsrP loop are required to elucidate these additional functions.

4.5 Cooperativity amongst the immunity and resistance proteins?

It is well known that both the nisin immunity proteins act cooperatively [237, 103] as full immunity up to ~ 750 nM nisin (1000 IU/ml) against nisin is only achieved when both *nisI* and *nisFEG* are expressed [224]. Gene knockout studies have shown that NisI and NisFEG alone provide only 4-20% of the full immunity [237, 103]. Furthermore, NisIFEG together confers a 100-fold immunity against nisin in the nisin sensitive *L. lactis* strain [240]. Similarly, in the subtilin immunity system, SpaI and SpaFEG cooperatively provide immunity to *B. subtilis* against the produced subtilin [223].

Additionally, NisI is known to be more effective in providing immunity than NisFEG, thus, playing a larger role than NisFEG [94].

Previous studies have shown that the immunity system is specific for its cognate lantibiotic and no cross- immunity has been observed [103]. Although, nisin and subtilin share high sequence homology [223], no cross- immunity has been observed.

However, it is still unknown whether in the resistance system, NSR and NsrFP act cooperatively or provide a higher resistance against nisin when both are expressed. Additionally, the exact contribution of NSR and NsrFP in providing resistance is still unidentified.

4.6 Regulation of immunity and resistance

The transcription of the immunity genes in the lantibiotic producing strains is activated via the two-component system comprising of a receptor histidine kinase and a transcriptional

response regulator. Similarly, the two-component system present in the lantibiotic non-producing strains is also responsible for the upregulation of the corresponding genes in the operon.

Similar to lantibiotic systems [158, 251], the RR and HK genes of the resistance systems are genetically linked and cotranscribed, leading to increased protein production [121].

4.6.1 NisK and NsrK

In nisin producing strains, external nisin acts as a signal, which is taken up by the histidine kinase NisK, inducing an autophosphorylation of its conserved histidine residue. NisK comprises of 447 amino acid residues and contains all the standard features: N-terminal sensory domain with cytoplasmic signalling modules and the transmitter domain comprising of HisKA and HATPase_c for kinase activity [217] (Figure 20). NisK belongs to the EnvZ (belonging to the TCS EnvZ-OmpR) subfamily of histidine kinases. Although the first ring A of nisin is important for auto inducing activity of NisK [252], the first three rings of nisin are required for activating NisK itself [253].

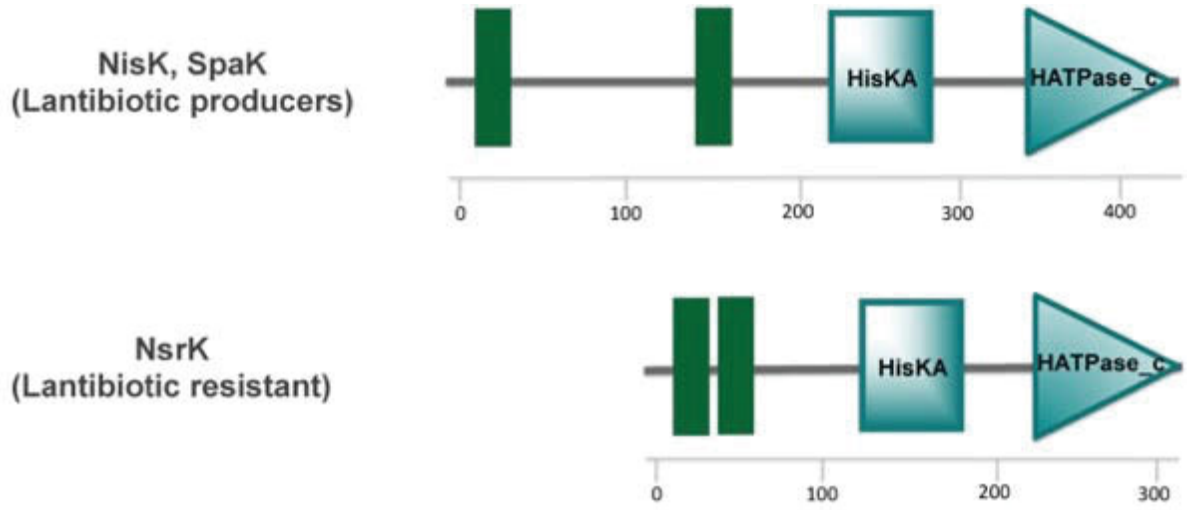

Figure 20: Domain organization of the histidine kinases present in lantibiotic producing and resistant strains. The figure is based on the graphical output of the SMART web server Schultz, Milpetz [217]. Scale bar represents the number of amino acids and a grey line represents the proteins. The conserved domains are labelled in cyan.

On the other hand, NsrK belongs to the class of intramembrane-sensing histidine kinases (IM-HKs) which are characterized by an N-terminal sensing domain consisting of two

deduced transmembrane helices and the absence of signalling modules in the cytoplasmic part [173] as depicted from the smaller size (312 amino acids) (Figure 20). Some other notable members of this family of kinases are BceS, YvcQ and LiaS from resistance systems [162, 177, 175]. Although the exact functioning of NsrK has not been elucidated, it is suggested that these kinases detect their stimuli from within or at the membrane interface (Mascher, 2006; Mascher *et al.*, 2006), with the aid of an ABC transporter that is usually cotranscribed and contains a sensory domain [181].

Table 3: Summary of the differences between the histidine kinases NisK and NsrK from the immunity and resistant systems, respectively.

	NisK	*NsrK*
Sequence length (amino acids)	**447**	**312**
Molecular weight	**51.3 kDa**	**36.5 kDa**
Localization	**Membrane spanning**	**Membrane spanning**
Histidine Kinase Family	**EnvZ-like histidine kinases**	**Intramembrane-sensing histidine kinases (IM-HKs)**
Cytoplasmic signalling modules	**Present**	**Absent**
Sequence motif	**HisKA and HATPase_c**	**HisKA and HATPase_c**
Function	**Nisin-mediated signal transduction**	**Not determined**
Observed mechanism	**Quorum sensing**	**Not determined**
Substrate specificity	**Ring A of nisin**	**Not determined**
Activation of kinase	**Rings A-C of nisin**	**Not determined**
Structure determined	**Not determined**	**Not determined**

4.6.1 NisR versus NsrR

NisR (from nisin producing system) is composed of 229 amino acid residues and is 26.7 kDa in size (Figure 20). Upon phosphorylation NisR binds to various promoters such as *nisA* and *nisF* of the nisin operon, thereby activating the transcription of the structural, modification and immunity genes of the nisin operon [104, 105]. Although, the NisR-NisK

induced NICE (nisin controlled gene expression) system has been used for a long time [254], detailed studies of NisR on a structural level are still missing.

On the contrary, NsrR (nisin resistant system of non-producers) is 25.4 kDa and comprises of 222 amino acid residues (Figure 21). The structure of NsrR was solved using X-ray crystallography (chapter V) and reveals that it is a DNA-binding response regulator possessing all the characteristic structural features of the OmpR subfamily that are characterized with a typical helix-turn-helix motif (chapter V).

Additionally, dimerization of NsrR occurs through α4-β5-α5 interface and putative residues involved in DNA-binding could be identified (chapter V). However, the distinct promoters for the *nsr* operon are yet to be identified.

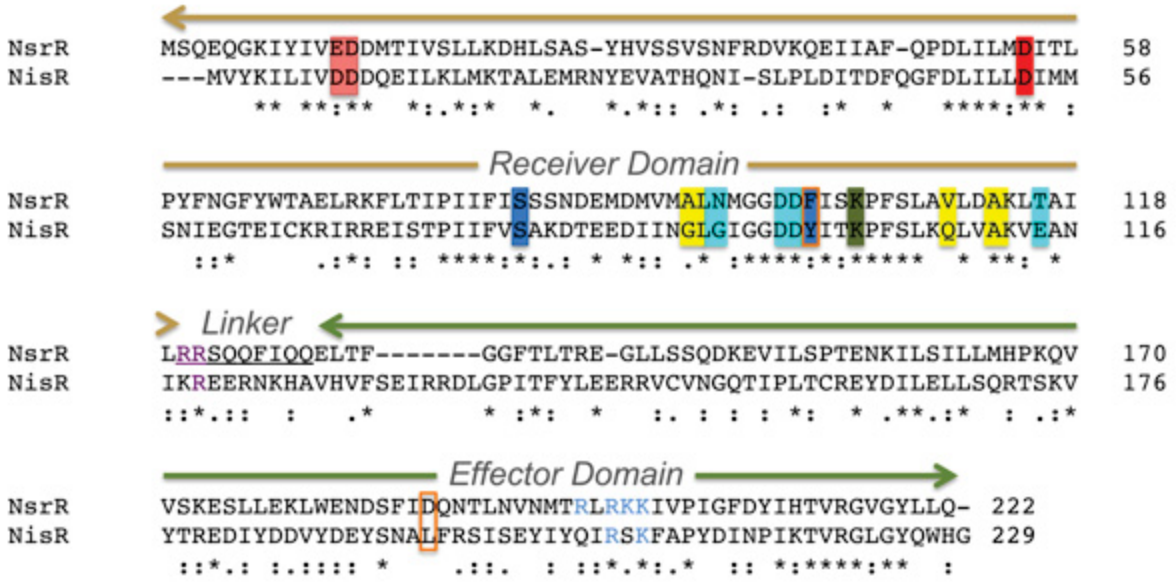

Figure 21: Sequence alignment of NsrR and NisR. A sequence alignment of NsrR with NisR is shown. The active site aspartate residue (highlighted in red), the residues forming the acidic pocket surrounding it (highlighted in pink), the switch residues (highlighted in blue), the conserved lysine residue (highlighted in green), the highly conserved residue of the linker region (colored in purple), the residues involved in dimer interface of receiver domain (highlighted in yellow), residues involved in interdomain interactions (shown in orange boxes and in cyan) and the residues involved in interaction with DNA (colored in blue) are shown. The linker region of NsrR is underlined within the sequence. Based on Figure 3 of chapter IV and [247].

Although both the response regulators NisR and NsrR are quite dissimilar with a sequence identity of 33% (Figure 21), both belong to the OmpR/PhoB subfamily of response regulators [255, 256]. Additionally, the residues forming the dimer interface as well as the interdomain interactions are different indicating towards distinct mode of interactions (Figure 21).

Table 4: Summary of the differences between the response regulators NisR and NsrR from the immunity and resistant systems.

	NisR	*NsrR*
Sequence length (amino acids)	**229**	**222**
Molecular weight	**26.7 kDa**	**25.4 kDa**
Localization	**Cytosol**	**Cytosol**
Response Regulator Family	**OmpR/PhoB**	**OmpR/PhoB**
Sequence motif	**Not determined**	**Active aspartate and switch residues**
Function	**Activation of the transcription of genes of nisin operon**	**Not determined**
Observed mechanism	**Binding to *nisA* and *nisF* promoter**	**Not determined**
Important residues	**Not determined**	**Asp55, Ser82, Phe101, Lys104, Asp188**
Binding site	**Not determined**	**Effector domain**
Structure determined	**Not determined**	**X-ray crystallography**
Binding site determined	**Not determined**	**Structural comparison**

4.7 Model for the mechanism of nisin resistance in *S. agalactiae*

This section summarizes the results obtained in the preceding chapters. Considering lantibiotic immunity system as a paradigm, a model is proposed for nisin resistance in *S. agalactiae* as represented in Figure 22.

1. The active nisin comes in contact with the membrane of the resistant strains such as *S. agalactiae*.
2. The initial resistance process involves the binding of nisin to the serine protease NSR. In detail, NSR harbours a hydrophobic tunnel that 'ropes in' the nisin peptide through hydrophobic interactions. These interactions are highly relevant for the molecular

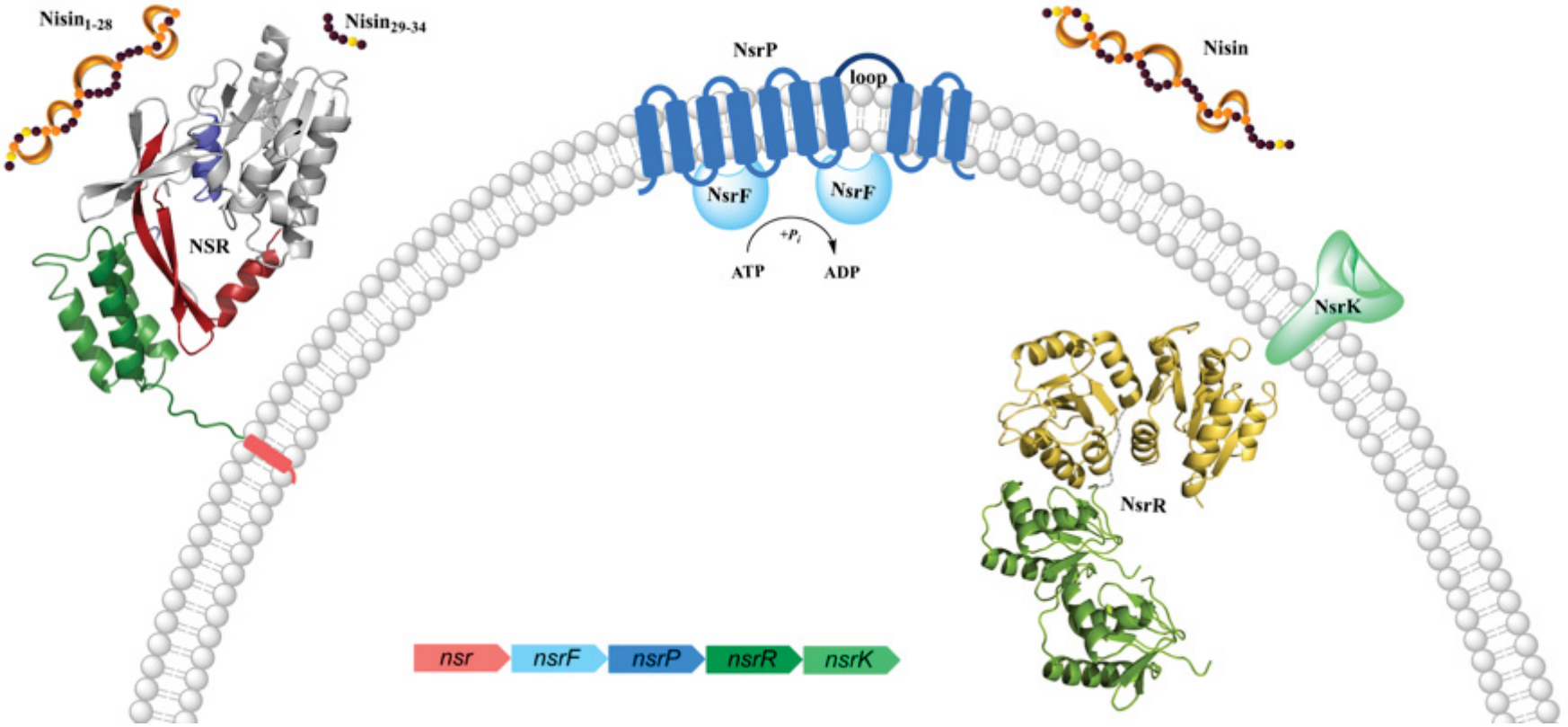

Figure 22: Structural representation of the nisin resistance operon in *S. agalactiae*. The structures of *Sa*NSR and NsrR are shown in a cartoon representation. NsrFP (ABC transporter) and NsrK (histidine kinase) are schematically shown in blue and green, respectively.

recognition of nisin and the substrate specificity of *Sa*NSR. Furthermore, upon interaction of the C-terminally located lanthionine ring E with NSR, this 'roping in' is stopped, thereby acting as plug.

3. Binding of the lanthionine ring E at one end of the hydrophobic tunnel of NSR ensures the exact coordination of the nisin cleavage site at the highly conserved TASSAEM region. This leads to the cleavage of nisin at MeLan position 28 and Ser29, yielding two fragments of nisin (nisin$^{1-28}$ and nisin$^{29-34}$). The nisin$^{1-28}$ has 100-fold less antimicrobial activity and displays less affinity for the membrane, thereby providing resistant to *S. agalactiae* against nisin.

4. Simultaneously, upon increasing concentrations of nisin in the environment, the ABC transporter NsrFP is activated through ATP hydrolysis. The NsrP loop recognises and binds nisin and induces a signal transfer to the two-component system.

5. Upon receiving signal from the loop, the histidine kinase NsrK is phosphorylated at a conserved histidine residue. And the high energetic potential of this phosphoryl group is transferred to the response regulator NsrR.

6. Subsequently, the receiver domain of NsrR is phosphorylated at the active aspartate residue, which leads to various conformational changes including the formation of dimer using α4-β5-α5 as an interface.

7. Additionally, this activation signal reaches the effector domain of NsrR through the linker region. The effector domain is also dimerized and thereby binds DNA through various conserved residues, initiating the transcription of the genes of the *nsr* operon.

8. Thus, the genes express more proteins making the process of resistance more efficient, so that the *S. agalactiae* is able to degrade/expel nisin out of the environment. When the nisin molecules are absent, the resistance system diverts back to its initial position.

5. Literature

1. Hancock, R.E. and R. Lehrer, *Cationic peptides: a new source of antibiotics.* Trends in biotechnology, 1998. **16**(2): p. 82-88.

2. Malmsten, M., *Antimicrobial peptides.* Upsala journal of medical sciences, 2014. **119**(2): p. 199-204.

3. Rogers, L., *The inhibiting effect of Streptococcus lactis on Lactobacillus bulgaricus.* Journal of bacteriology, 1928. **16**(5): p. 321.

4. Rogers, L. and E. Whittier, *Limiting factors in the lactic fermentation.* Journal of bacteriology, 1928. **16**(4): p. 211.

5. Chopra, L., et al., *Sonorensin: an antimicrobial peptide, belonging to the heterocycloanthracin subfamily of bacteriocins, from a new marine isolate, Bacillus sonorensis MT93.* Applied and environmental microbiology, 2014. **80**(10): p. 2981-2990.

6. Martin, E., T. Ganz, and R.I. Lehrer, *Defensins and other endogenous peptide antibiotics of vertebrates.* Journal of Leukocyte Biology, 1995. **58**(2): p. 128-136.

7. Wang, Z. and G. Wang, *APD: the antimicrobial peptide database.* Nucleic acids research, 2004. **32**(suppl 1): p. D590-D592.

8. Pasupuleti, M., A. Schmidtchen, and M. Malmsten, *Antimicrobial peptides: key components of the innate immune system.* Critical reviews in biotechnology, 2012. **32**(2): p. 143-171.

9. Nawrocki, K.L., E.K. Crispell, and S.M. McBride, *Antimicrobial peptide resistance mechanisms of gram-positive bacteria.* Antibiotics, 2014. **3**(4): p. 461-492.

10. Hancock, R.E. and H.-G. Sahl, *Antimicrobial and host-defense peptides as new anti-infective therapeutic strategies.* Nature biotechnology, 2006. **24**(12): p. 1551-1557.

11. Hale, J.D. and R.E. Hancock, *Alternative mechanisms of action of cationic antimicrobial peptides on bacteria.* 2007.

12. Zasloff, M., *Antimicrobial peptides of multicellular organisms.* nature, 2002. **415**(6870): p. 389-395.

13. Brogden, K.A., *Antimicrobial peptides: pore formers or metabolic inhibitors in bacteria?* Nature Reviews Microbiology, 2005. **3**(3): p. 238-250.

14. Marr, A.K., W.J. Gooderham, and R.E. Hancock, *Antibacterial peptides for therapeutic use: obstacles and realistic outlook.* Current opinion in pharmacology, 2006. **6**(5): p. 468-472.

15. Bradshaw, J.P., *Cationic antimicrobial peptides.* BioDrugs, 2003. **17**(4): p. 233-240.

16. Peschel, A. and H.-G. Sahl, *The co-evolution of host cationic antimicrobial peptides and microbial resistance.* Nature Reviews Microbiology, 2006. **4**(7): p. 529-536.

17. Harris, M., et al., *Loss of mannosylphosphate from Candida albicans cell wall proteins results in enhanced resistance to the inhibitory effect of a cationic antimicrobial peptide via reduced peptide binding to the cell surface.* Microbiology, 2009. **155**(4): p. 1058-1070.

18. Brown, K.L. and R.E. Hancock, *Cationic host defense (antimicrobial) peptides.* Current opinion in immunology, 2006. **18**(1): p. 24-30.

19. Mader, J.S. and D.W. Hoskin, *Cationic antimicrobial peptides as novel cytotoxic agents for cancer treatment.* 2006.

20. Mookherjee, N. and R. Hancock, *Cationic host defence peptides: innate immune regulatory peptides as a novel approach for treating infections.* Cellular and molecular life sciences, 2007. **64**(7-8): p. 922-933.

21. Steinstraesser, L., et al., *Host defense peptides in wound healing.* Molecular medicine, 2008. **14**(7-8): p. 528.

22. Diamond, G., et al., *The roles of antimicrobial peptides in innate host defense.* Current pharmaceutical design, 2009. **15**(21): p. 2377.

23. Wang, G., *Improved methods for classification, prediction, and design of antimicrobial peptides*, in *Computational Peptidology*. 2015, Springer. p. 43-66.

24. Chen, H., et al., *Recent advances in the research and development of human defensins.* Peptides, 2006. **27**(4): p. 931-940.

25. Hancock, R.E., *Cationic peptides: effectors in innate immunity and novel antimicrobials.* The Lancet infectious diseases, 2001. **1**(3): p. 156-164.

26. Boman, H.G., *Peptide antibiotics and their role in innate immunity.* Annual review of immunology, 1995. **13**(1): p. 61-92.

27. Hancock, R.E., *Peptide antibiotics.* The Lancet, 1997. **349**(9049): p. 418-422.

28. Stciner, H., et al., *Séquence and spe-cificity of two antibacterial proteins involved in insect immunity.* Nature, 1981. **292**: p. 246-8.

29. Zasloff, M., *Magainins, a class of antimicrobial peptides from Xenopus skin: isolation, characterization of two active forms, and partial cDNA sequence of a precursor.* Proceedings of the National Academy of Sciences, 1987. **84**(15): p. 5449-5453.

30. Selsted, M., et al., *Primary structures of three human neutrophil defensins.* Journal of Clinical Investigation, 1985. **76**(4): p. 1436.

31. Selsted, M.E., et al., *Indolicidin, a novel bactericidal tridecapeptide amide from neutrophils.* Journal of Biological Chemistry, 1992. **267**(7): p. 4292-4295.

32. Casteels, P., et al., *Apidaecins: antibacterial peptides from honeybees.* The EMBO journal, 1989. **8**(8): p. 2387.

33. Xu, F., et al., *Eukaryotic expression and antimicrobial spectrum determination of the peptide tachyplesin II.* Protein expression and purification, 2008. **58**(2): p. 175-183.

34. McAnulty, J.F., et al., *Suppression of cold ischemic injury in stored kidneys by the antimicrobial peptide bactenecin.* Cryobiology, 2004. **49**(3): p. 230-240.

35. Mattick, A., A. Hirsch, and N. Berridge, *Further observations on an inhibitory substance (nisin) from lactic streptococci.* The Lancet, 1947. **250**(6462): p. 5-8.

36. Klaenhammer, T.R., *Bacteriocins of lactic acid bacteria.* Biochimie, 1988. **70**(3): p. 337-349.

37. Riley, M.A., *Molecular mechanisms of bacteriocin evolution.* Annual review of genetics, 1998. **32**(1): p. 255-278.

38. Gratia, A., *Sur un remarquable exemple d'antagonisme entre deux souches de colibacille.* CR Soc Biol, 1925. **93**: p. 1040-1041.

39. Galesloot, T.E., *Lactic Acid Bacteria Which Destroy The Antibioticum (Nisin) Of S-Lactis.* Nederlands Melk-En Zuiveltijdschrift, 1956. **10**(2): p. 143-155.

40. Delves-Brougthon, J., *Nisin and its uses as a food preservative.* Food Technology, 1990. **44**(11): p. 100-117.

41. Chatterjee, S., et al., *Mersacidin, a new antibiotic from Bacillus Fermentation, isolation, purification and chemical characterization.* The Journal of antibiotics, 1992. **45**(6): p. 832-838.

42. Cotter, P.D., C. Hill, and R.P. Ross, *Bacteriocins: developing innate immunity for food.* Nature Reviews Microbiology, 2005. **3**(10): p. 777-788.

43. Jarvis, B., J. Jeffcoat, and G. Cheeseman, *Molecular weight distribution of nisin.* Biochimica et Biophysica Acta (BBA)-Protein Structure, 1968. **168**(1): p. 153-155.

44. Bierbaum, G., et al., *Engineering of a novel thioether bridge and role of modified residues in the lantibiotic Pep5.* Applied and environmental microbiology, 1996. **62**(2): p. 385-392.

45. Sahl, H.-G. and G. Bierbaum, *Lantibiotics: biosynthesis and biological activities of uniquely modified peptides from gram-positive bacteria.* Annual Reviews in Microbiology, 1998. **52**(1): p. 41-79.

46. Lai, A.-Y., S. Tran, and R. Simmonds, *Functional characterization of domains found within a lytic enzyme produced by Streptococcus equi subsp. zooepidemicus.* FEMS microbiology letters, 2002. **215**(1): p. 133-138.

47. Chumchalová, J. and J. Šmarda, *Human tumor cells are selectively inhibited by colicins.* Folia microbiologica, 2003. **48**(1): p. 111-115.

48. Farías, M., et al., *Purification and N‐terminal amino acid sequence of Enterocin CRL 35, a 'pediocin‐like' bacteriocin produced by Enterococcus faecium CRL 35.* Letters in applied microbiology, 1996. **22**(6): p. 417-419.

49. Farkas-Himsley, H., et al., *The bacterial colicin active against tumor cells in vitro and in vivo is verotoxin 1.* Proceedings of the National Academy of Sciences, 1995. **92**(15): p. 6996-7000.

50. Chen, H. and D. Hoover, *Bacteriocins and their food applications.* Comprehensive reviews in food science and food safety, 2003. **2**(3): p. 82-100.

51. Schnell, N., et al., *Prepeptide sequence of epidermin, a ribosomally synthesized antibiotic with four sulphide-rings.* 1988.

52. Sahl, H.G., R.W. Jack, and G. Bierbaum, *Biosynthesis and biological activities of lantibiotics with unique post‐translational modifications.* European Journal of Biochemistry, 1995. **230**(3): p. 827-853.

53. Vos, W.M., et al., *Maturation pathway of nisin and other lantibiotics: post‐translationally modified antimicrobial peptides exported by Gram‐positive bacteria.* Molecular microbiology, 1995. **17**(3): p. 427-437.

54. Guder, A., I. Wiedemann, and H.G. Sahl, *Posttranslationally modified bacteriocins—the lantibiotics.* Peptide Science, 2000. **55**(1): p. 62-73.

55. Ingram, L.C., *Synthesis of the antibiotic nisin: Formation of lanthionine and β-methyl-lanthione.* Biochimica et Biophysica Acta (BBA)-General Subjects, 1969. **184**(1): p. 216-219.

56. Jack, R.W. and H.-G. Sahl, *Unique peptide modifications involved in the biosynthesis of lantibiotics.* Trends in biotechnology, 1995. **13**(7): p. 269-278.

57. Willey, J.M. and W.A. van der Donk, *Lantibiotics: peptides of diverse structure and function.* Annu. Rev. Microbiol., 2007. **61**: p. 477-501.

58. Xie, L. and W.A. Van Der Donk, *Post-translational modifications during lantibiotic biosynthesis.* Current opinion in chemical biology, 2004. **8**(5): p. 498-507.

59. Chatterjee, C., et al., *Biosynthesis and mode of action of lantibiotics.* Chemical Reviews, 2005. **105**(2): p. 633-684.

60. Knerr, P.J. and W.A. van der Donk, *Discovery, biosynthesis, and engineering of lantipeptides.* Annual review of biochemistry, 2012. **81**: p. 479-505.

61. Pag, U. and H.-G. Sahl, *Multiple activities in lantibiotics-models for the design of novel antibiotics?* Current pharmaceutical design, 2002. **8**(9): p. 815-833.

62. Kodani, S., et al., *The SapB morphogen is a lantibiotic-like peptide derived from the product of the developmental gene ramS in Streptomyces coelicolor.* Proceedings of the National Academy of Sciences of the United States of America, 2004. **101**(31): p. 11448-11453.

63. Siezen, R.J., O.P. Kuipers, and W.M. de Vos, *Comparison of lantibiotic gene clusters and encoded proteins.* Antonie van Leeuwenhoek, 1996. **69**(2): p. 171-184.

64. Alkhatib, Z., et al., *Lantibiotics: how do producers become self-protected?* Journal of biotechnology, 2012. **159**(3): p. 145-154.

65. Boakes, S. and S. Wadman, *The therapeutic potential of lantibiotics.* Innov Pharm Technol, 2008. **27**: p. 22-25.

66. Dischinger, J., S.B. Chipalu, and G. Bierbaum, *Lantibiotics: promising candidates for future applications in health care.* International Journal of Medical Microbiology, 2014. **304**(1): p. 51-62.

67. Mota-Meira, M., et al., *MICs of mutacin B-Ny266, nisin A, vancomycin, and oxacillin against bacterial pathogens.* Antimicrobial agents and chemotherapy, 2000. **44**(1): p. 24-29.

68. Barnby-Smith, F.M., *Bacteriocins: applications in food preservation.* Trends in Food Science & Technology, 1992. **3**: p. 133-137.

69. Abee, T., L. Krockel, and C. Hill, *Bacteriocins: modes of action and potentials in food preservation and control of food poisoning.* International journal of food microbiology, 1995. **28**(2): p. 169-185.

70. Cleveland, J., et al., *Bacteriocins: safe, natural antimicrobials for food preservation.* International journal of food microbiology, 2001. **71**(1): p. 1-20.

71. Yang, S.-C., et al., *Antibacterial activities of bacteriocins: application in foods and pharmaceuticals.* Frontiers in microbiology, 2014. **5**.

72. Li, P., et al., *Antimicrobial macromolecules: synthesis methods and future applications.* Rsc Advances, 2012. **2**(10): p. 4031-4044.

73. Fernández, L., et al., *The bacteriocin nisin, an effective agent for the treatment of staphylococcal mastitis during lactation.* Journal of Human Lactation, 2008. **24**(3): p. 311-316.

74. Delves-Broughton, J., et al., *Applications of the bacteriocin, nisin.* Antonie van Leeuwenhoek, 1996. **69**(2): p. 193-202.

75. Lawton, E.M., et al., *Two-peptide lantibiotics: a medical perspective.* Mini reviews in medicinal chemistry, 2007. **7**(12): p. 1236-1247.

76. Hossain, M.S. and I. Biswas, *Mutacins from Streptococcus mutans UA159 are active against multiple streptococcal species.* Applied and environmental microbiology, 2011. **77**(7): p. 2428-2434.

77. Oliynyk, I., et al., *Effect of duramycin on chloride transport and intracellular calcium concentration in cystic fibrosis and non‐cystic fibrosis epithelia.* Apmis, 2010. **118**(12): p. 982-990.

78. Jung, G. and H.-G. Sahl, *Nisin and novel lantibiotics*. 1991: Springer Science & Business Media.

79. Cotter, P.D., C. Hill, and R.P. Ross, *Bacterial lantibiotics: strategies to improve therapeutic potential.* Current Protein and Peptide Science, 2005. **6**(1): p. 61-75.

80. Van de Ven, F., et al., *The spatial structure of nisin in aqueous solution.* Nisin and novel lantibiotics. Escom Publishers, Leiden, The Netherlands, 1991: p. 35-42.

81. Gross, E. and J.L. Morell, *Nisin. The assignment of sulfide bridges of. beta.-methyllanthionine to a novel bicyclic structure of identical ring size.* Journal of the American Chemical Society, 1970. **92**(9): p. 2919-2920.

82. Gross, E. and J.L. Morell, *Structure of nisin.* Journal of the American Chemical Society, 1971. **93**(18): p. 4634-4635.

83. Breukink, E., et al., *The C-terminal region of nisin is responsible for the initial interaction of nisin with the target membrane.* Biochemistry, 1997. **36**(23): p. 6968-6976.

84. Breukink, E., et al., *Use of the cell wall precursor lipid II by a pore-forming peptide antibiotic.* Science, 1999. **286**(5448): p. 2361-2364.

85. Wiedemann, I., et al., *Specific Binding of Nisin to the Peptidoglycan Precursor Lipid II Combines Pore Formation and Inhibition of Cell Wall Biosynthesis for Potent Antibiotic Activity.* Journal of Biological Chemistry, 2001. **276**(3): p. 1772-1779.

86. Hsu, S.-T.D., et al., *The nisin–lipid II complex reveals a pyrophosphate cage that provides a blueprint for novel antibiotics.* Nature structural & molecular biology, 2004. **11**(10): p. 963-967.

87. Breukink, E. and B. de Kruijff, *Lipid II as a target for antibiotics.* Nature Reviews Drug Discovery, 2006. **5**(4): p. 321-323.

88. de Kruijff, B., V. van Dam, and E. Breukink, *Lipid II: a central component in bacterial cell wall synthesis and a target for antibiotics.* Prostaglandins, leukotrienes and essential fatty acids, 2008. **79**(3): p. 117-121.

89. Hasper, H.E., B. de Kruijff, and E. Breukink, *Assembly and stability of nisin-lipid II pores.* Biochemistry, 2004. **43**(36): p. 11567-11575.

90. Abts, A., et al., *Easy and rapid purification of highly active nisin.* International journal of peptides, 2011. **2011**.

91. Kuipers, O.P., et al., *Characterization of the nisin gene cluster nisABTCIPR of Lactococcus lactis.* European Journal of Biochemistry, 1993. **216**(1): p. 281-291.

92. Van der Meer, J., et al., *Characterization of the Lactococcus lactis nisin A operon genes nisP, encoding a subtilisin-like serine protease involved in precursor processing, and nisR, encoding a regulatory protein involved in nisin biosynthesis.* Journal of bacteriology, 1993. **175**(9): p. 2578-2588.

93. Engelke, G., et al., *Regulation of nisin biosynthesis and immunity in Lactococcus lactis 6F3.* Applied and environmental microbiology, 1994. **60**(3): p. 814-825.

94. Siegers, K. and K. Entian, *Genes involved in immunity to the lantibiotic nisin produced by Lactococcus lactis 6F3.* Applied and Environmental Microbiology, 1995. **61**(3): p. 1082-1089.

95. van den Hooven, H.W., et al., *Structural features of the final intermediate in the biosynthesis of the lantibiotic nisin. Influence of the leader peptide.* Biochemistry, 1997. **36**(46): p. 14137-14145.

96. Koponen, O., et al., *NisB is required for the dehydration and NisC for the lanthionine formation in the post-translational modification of nisin.* Microbiology, 2002. **148**(11): p. 3561-3568.

97. Qiao, M. and P.E. Saris, *Evidence for a role of NisT in transport of the lantibiotic nisin produced by Lactococcus lactis N8.* FEMS microbiology letters, 1996. **144**(1): p. 89-93.

98. Kuipers, A., et al., *NisT, the transporter of the lantibiotic nisin, can transport fully modified, dehydrated, and unmodified prenisin and fusions of the leader peptide with non-lantibiotic peptides.* Journal of Biological Chemistry, 2004. **279**(21): p. 22176-22182.

99. Qiao, M., et al., *Regulation of the nisin operons in Lactococcus lactis N8.* Journal of applied bacteriology, 1996. **80**(6): p. 626-634.

100. Abts, A., *The Nisin ABC-Investigating the maturation process of the lanthipeptide nisin.* 2014.

101. Qiao, M., et al., *The cellular location and effect on nisin immunity of the NisI protein from Lactococcus lactis N8 expressed in Escherichia coli and L. lactis.* FEMS microbiology letters, 1995. **131**(1): p. 75-80.

102. Koponen, O., et al., *Distribution of the NisI immunity protein and enhancement of nisin activity by the lipid-free NisI.* FEMS microbiology letters, 2004. **231**(1): p. 85-90.

103. Stein, T., et al., *Function of Lactococcus lactis nisin immunity genes nisI and nisFEG after coordinated expression in the surrogate host Bacillus subtilis.* Journal of Biological Chemistry, 2003. **278**(1): p. 89-94.

104. Kuipers, O.P., et al., *Autoregulation of nisin biosynthesis in Lactococcus lactis by signal transduction.* Journal of Biological Chemistry, 1995. **270**(45): p. 27299-27304.

105. De Ruyter, P., et al., *Functional analysis of promoters in the nisin gene cluster of Lactococcus lactis.* Journal of bacteriology, 1996. **178**(12): p. 3434-3439.

106. Chan, W.C., et al., *Isolation and characterisation of two degradation products derived from the peptide antibiotic nisin.* Febs Letters, 1989. **252**(1): p. 29-36.

107. Jenson, I., L. Baird, and J. Delves-Broughton, *The use of nisin as a preservative in crumpets.* Journal of Food Protection®, 1994. **57**(10): p. 874-877.

108. Rayman, M.K., B. Aris, and A. Hurst, *Nisin: a possible alternative or adjunct to nitrite in the preservation of meats.* Applied and Environmental Microbiology, 1981. **41**(2): p. 375-380.

109. Ogden, K. and R. Tubb, *Inhibition of Beer-Spoilage Lactic Acid Bacteria By Nisin.* Journal of the Institute of Brewing, 1985. **91**(6): p. 390-392.

110. Ogden, K., *Nisin: a bacteriocin with a potential use in brewing.* Journal of the Institute of Brewing, 1986. **92**(4): p. 379-383.

111. Valenta, C., A. Bernkop‐SchnüRch, and H.P. Rigler, *The antistaphylococcal effect of nisin in a suitable vehicle: a potential therapy for atopic dermatitis in man.* Journal of pharmacy and pharmacology, 1996. **48**(9): p. 988-991.

112. Dubois, A., *Spiral bacteria in the human stomach: the gastric helicobacters.* Emerging infectious diseases, 1995. **1**(3): p. 79.

113. Kim, T.-S., et al., *Antagonism of Helicobacter pylori by bacteriocins of lactic acid bacteria.* Journal of Food Protection®, 2003. **66**(1): p. 3-12.

114. De Kwaadsteniet, M., K. Doeschate, and L. Dicks, *Nisin F in the treatment of respiratory tract infections caused by Staphylococcus aureus.* Letters in applied microbiology, 2009. **48**(1): p. 65-70.

115. Aranha, C., S. Gupta, and K. Reddy, *Contraceptive efficacy of antimicrobial peptide Nisin: in vitro and in vivo studies.* Contraception, 2004. **69**(4): p. 333-338.

116. Cao, L., et al., *Efficacy of nisin in treatment of clinical mastitis in lactating dairy cows.* Journal of dairy science, 2007. **90**(8): p. 3980-3985.

117. Wu, J., S. Hu, and L. Cao, *Therapeutic effect of nisin Z on subclinical mastitis in lactating cows.* Antimicrobial agents and chemotherapy, 2007. **51**(9): p. 3131-3135.

118. Hancock, R.E. and A. Rozek, *Role of membranes in the activities of antimicrobial cationic peptides.* FEMS microbiology letters, 2002. **206**(2): p. 143-149.

119. Nizet, V., *Antimicrobial peptide resistance mechanisms of human bacterial pathogens.* Current issues in molecular biology, 2006. **8**(1): p. 11.

120. de Freire Bastos, M.d.C., M.L.V. Coelho, and O.C. da Silva Santos, *Resistance to bacteriocins produced by Gram-positive bacteria.* Microbiology, 2015. **161**(Pt 4): p. 683-700.

121. Draper, L.A., et al., *Lantibiotic Resistance.* Microbiology and Molecular Biology Reviews, 2015. **79**(2): p. 171-191.

122. Weidenmaier, C. and A. Peschel, *Teichoic acids and related cell-wall glycopolymers in Gram-positive physiology and host interactions.* Nature Reviews Microbiology, 2008. **6**(4): p. 276-287.

123. Neuhaus, F.C.H., Michael P Debabov, Dmitri V Zhang, Qunying *The dlt operon in the biosynthesis of D-alanyl-lipoteichoic acid in Lactobacillus casei.* Microbial Drug Resistance, 1996. **2**(1): p. 77-84.

124. Peschel, A., et al., *Inactivation of the dlt Operon inStaphylococcus aureus Confers Sensitivity to Defensins, Protegrins, and Other Antimicrobial Peptides.* Journal of Biological Chemistry, 1999. **274**(13): p. 8405-8410.

125. Fabretti, F., et al., *Alanine esters of enterococcal lipoteichoic acid play a role in biofilm formation and resistance to antimicrobial peptides.* Infection and immunity, 2006. **74**(7): p. 4164-4171.

126. Kovács, M., et al., *A functional dlt operon, encoding proteins required for incorporation of d-alanine in teichoic acids in gram-positive bacteria, confers resistance to cationic antimicrobial peptides in Streptococcus pneumoniae.* Journal of bacteriology, 2006. **188**(16): p. 5797-5805.

127. Giaouris, E., et al., *Variations in the degree of D-alanylation of teichoic acids in Lactococcus lactis alter resistance to cationic antimicrobials but have no effect on bacterial surface hydrophobicity and charge.* Applied and environmental microbiology, 2008. **74**(15): p. 4764-4767.

128. McBride, S.M. and A.L. Sonenshein, *The dlt operon confers resistance to cationic antimicrobial peptides in Clostridium difficile.* Microbiology, 2011. **157**(5): p. 1457-1465.

129. Schwartz, B., J.A. Markwalder, and Y. Wang, *Lipid II: Total Synthesis of the Bacterial Cell Wall Precursor and Utilization as a Substrate for Glycosyltransfer and Transpeptidation by Penicillin Binding Protein (PBP) 1b of Eschericia coli.* Journal of the American Chemical Society, 2001. **123**(47): p. 11638-11643.

130. Gravesen, A., et al., *Spontaneous nisin-resistant Listeria monocytogenes mutants with increased expression of a putative penicillin-binding protein and their sensitivity to various antibiotics.* Microbial Drug Resistance, 2001. **7**(2): p. 127-135.

131. Kramer, N.E., et al., *Transcriptome analysis reveals mechanisms by which Lactococcus lactis acquires nisin resistance.* Antimicrobial agents and chemotherapy, 2006. **50**(5): p. 1753-1761.

132. Xuanyuan, Z., et al., *Loss of IrpT function in Lactococcus lactis subsp. lactis N8 results in increased nisin resistance.* Current microbiology, 2010. **61**(4): p. 329-334.

133. Storm, D.R. and J.L. Strominger, *Binding of bacitracin to cells and protoplasts of Micrococcus lysodeikticus.* Journal of Biological Chemistry, 1974. **249**(6): p. 1823-1827.

134. Labischinski, H., et al., *Direct proof of a" more-than-single-layered" peptidoglycan architecture of Escherichia coli W7: a neutron small-angle scattering study.* Journal of bacteriology, 1991. **173**(2): p. 751-756.

135. Schved, F., Y. Henis, and B. Juven, *Response of spheroplasts and chelator-permeabilized cells of Gram-negative bacteria to the action of the bacteriocins pediocin SJ-1 and nisin.* International journal of food microbiology, 1994. **21**(4): p. 305-314.

136. Stevens, K., et al., *Nisin treatment for inactivation of Salmonella species and other gram-negative bacteria.* Applied and Environmental Microbiology, 1991. **57**(12): p. 3613-3615.

137. Delves-Broughton, J., *The use of EDTA to enhance the efficacy of nisin towards Gram-negative bacteria.* International Biodeterioration & Biodegradation, 1993. **32**(1): p. 87-97.

138. Stevens, K., et al., *Nisin treatment for inactivation of Salmonella species and other gram-negative bacteria.* Applied and Environmental Microbiology, 1991. **57**(12): p. 3613-3615.

139. Kalchayanand, N., M. Hanlin, and B. Ray, *Sublethal injury makes Gram‐negative and resistant Gram‐positive bacteria sensitive to the bacteriocins, pediocin AcH and nisin.* Letters in Applied Microbiology, 1992. **15**(6): p. 239-243.

140. Boziaris, I. and M. Adams, *Transient sensitivity to nisin in cold‐shocked Gram negatives.* Letters in applied microbiology, 2000. **31**(3): p. 233-237.

141. Verheul, A., et al., *Modifications of membrane phospholipid composition in nisin-resistant Listeria monocytogenes Scott A.* Applied and Environmental Microbiology, 1997. **63**(9): p. 3451-3457.

142. Crandall, A.D. and T.J. Montville, *Nisin resistance in Listeria monocytogenes ATCC 700302 is a complex phenotype.* Applied and Environmental Microbiology, 1998. **64**(1): p. 231-237.

143. Mantovani, H.C. and J.B. Russell, *Nisin resistance of Streptococcus bovis.* Applied and environmental microbiology, 2001. **67**(2): p. 808-813.

144. Ming, X. and M.A. Daeschel, *Nisin resistance of foodborne bacteria and the specific resistance responses of Listeria monocytogenes Scott A.* Journal of Food Protection®, 1993. **56**(11): p. 944-948.

145. Ming, X. and M.A. Daeschel, *Correlation of cellular phospholipid content with nisin resistance of Listeria monocytogenes Scott A.* Journal of Food Protection®, 1995. **58**(4): p. 416-420.

146. Mazzotta, A. and T. Montville, *Nisin induces changes in membrane fatty acid composition of Listeria monocytogenes nisin‐resistant strains at 10° C and 30° C.* Journal of Applied Microbiology, 1997. **82**(1): p. 32-38.

147. Ernst, C.M., et al., *The bacterial defensin resistance protein MprF consists of separable domains for lipid lysinylation and antimicrobial peptide repulsion.* PLoS Pathog, 2009. **5**(11): p. e1000660.

148. Ernst, C.M. and A. Peschel, *Broad‐spectrum antimicrobial peptide resistance by MprF‐mediated aminoacylation and flipping of phospholipids.* Molecular microbiology, 2011. **80**(2): p. 290-299.

149. Nahaie, M., et al., *Polar lipid and isoprenoid quinone composition in the classification of Staphylococcus.* Journal of general microbiology, 1984. **130**(9): p. 2427-2437.

150. Fischer, W. and K. Leopold, *Polar lipids of four Listeria species containing L-lysylcardiolipin, a novel lipid structure, and other unique phospholipids.* International journal of systematic bacteriology, 1999. **49**(2): p. 653-662.

151. Staubitz, P. and A. Peschel, *MprF-mediated lysinylation of phospholipids in Bacillus subtilis–protection against bacteriocins in terrestrial habitats?* Microbiology, 2002. **148**(11): p. 3331-3332.

152. Bao, Y., et al., *Role of mprF1 and mprF2 in the pathogenicity of Enterococcus faecalis.* PloS one, 2012. **7**(6): p. e38458.

153. Mishra, N.N., et al., *Daptomycin resistance in enterococci is associated with distinct alterations of cell membrane phospholipid content.* PLoS One, 2012. **7**(8): p. e43958.

154. Samant, S., et al., *The Bacillus anthracis protein MprF is required for synthesis of lysylphosphatidylglycerols and for resistance to cationic antimicrobial peptides.* Journal of bacteriology, 2009. **191**(4): p. 1311-1319.

155. Maloney, E., et al., *The two-domain LysX protein of Mycobacterium tuberculosis is required for production of lysinylated phosphatidylglycerol and resistance to cationic antimicrobial peptides.* PLoS Pathog, 2009. **5**(7): p. e1000534-e1000534.

156. Heath, R.J. and C.O. Rock, *Enoyl-acyl carrier protein reductase (fabI) plays a determinant role in completing cycles of fatty acid elongation in Escherichia coli.* Journal of Biological Chemistry, 1995. **270**(44): p. 26538-26542.

157. Anaya-López, J.L., J.E. López-Meza, and A. Ochoa-Zarzosa, *Bacterial resistance to cationic antimicrobial peptides.* Critical reviews in microbiology, 2013. **39**(2): p. 180-195.

158. Kleerebezem, M., et al., *Quorum sensing by peptide pheromones and two‐component signal‐transduction systems in Gram‐positive bacteria.* Molecular microbiology, 1997. **24**(5): p. 895-904.

159. Bourret, R.B., K.A. Borkovich, and M.I. Simon, *Signal transduction pathways involving protein phosphorylation in prokaryotes.* Annual review of biochemistry, 1991. **60**(1): p. 401-441.

160. Stock, A.M., V.L. Robinson, and P.N. Goudreau, *Two-component signal transduction.* Annual review of biochemistry, 2000. **69**(1): p. 183-215.

161. West, A.H. and A.M. Stock, *Histidine kinases and response regulator proteins in two-component signaling systems.* Trends in biochemical sciences, 2001. **26**(6): p. 369-376.

162. Ohki, R., et al., *The BceRS two-component regulatory system induces expression of the bacitracin transporter, BceAB, in Bacillus subtilis.* Molecular Microbiology, 2003. **49**(4): p. 1135-1144.

163. Kawada-Matsuo, M., et al., *Involvement of the Novel Two-Component NsrRS and LcrRS Systems in Distinct Resistance Pathways against Nisin A and Nukacin ISK-1 in Streptococcus mutans.* Applied and Environmental Microbiology, 2013. **79**(15): p. 4751-4755.

164. Cotter, P.D., et al., *Identification and disruption of lisRK, a genetic locus encoding a two-component signal transduction system involved in stress tolerance and virulence in Listeria monocytogenes.* Journal of bacteriology, 1999. **181**(21): p. 6840-6843.

165. Meehl, M., et al., *Interaction of the GraRS two-component system with the VraFG ABC transporter to support vancomycin-intermediate resistance in Staphylococcus aureus.* Antimicrobial agents and chemotherapy, 2007. **51**(8): p. 2679-2689.

166. Kraus, D., et al., *The GraRS regulatory system controls Staphylococcus aureus susceptibility to antimicrobial host defenses.* BMC microbiology, 2008. **8**(1): p. 85.

167. Kawada-Matsuo, M., et al., *Three distinct two-component systems are involved in resistance to the class I bacteriocins, nukacin ISK-1 and nisin A, in Staphylococcus aureus.* PloS one, 2013. **8**(7): p. e69455.

168. Hiron, A., et al., *Bacitracin and nisin resistance in Staphylococcus aureus: a novel pathway involving the BraS/BraR two‐component system (SA2417/SA2418) and both the BraD/BraE and VraD/VraE ABC transporters.* Molecular microbiology, 2011. **81**(3): p. 602-622.

169. Suárez, J.M., A.N. Edwards, and S.M. McBride, *The Clostridium difficile cpr locus is regulated by a noncontiguous two-component system in response to type A and B lantibiotics.* Journal of bacteriology, 2013. **195**(11): p. 2621-2631.

170. Falord, M., et al., *GraXSR proteins interact with the VraFG ABC transporter to form a five-component system required for cationic antimicrobial peptide sensing and*

resistance in Staphylococcus aureus. Antimicrobial agents and chemotherapy, 2012. **56**(2): p. 1047-1058.

171. Ouyang, J., et al., *The BceABRS four-component system regulates the bacitracin-induced cell envelope stress response in Streptococcus mutans.* Antimicrobial agents and chemotherapy, 2010. **54**(9): p. 3895-3906.

172. Gebhard, S., et al., *Identification and characterization of a bacitracin resistance network in Enterococcus faecalis.* Antimicrobial agents and chemotherapy, 2014. **58**(3): p. 1425-1433.

173. Mascher, T., *Intramembrane-sensing histidine kinases: a new family of cell envelope stress sensors in Firmicutes bacteria.* FEMS microbiology letters, 2006. **264**(2): p. 133-144.

174. Dintner, S., et al., *Coevolution of ABC transporters and two-component regulatory systems as resistance modules against antimicrobial peptides in Firmicutes bacteria.* Journal of bacteriology, 2011. **193**(15): p. 3851-3862.

175. Jordan, S., et al., *Regulation of LiaRS-dependent gene expression in Bacillus subtilis: identification of inhibitor proteins, regulator binding sites, and target genes of a conserved cell envelope stress-sensing two-component system.* Journal of bacteriology, 2006. **188**(14): p. 5153-5166.

176. O'Connell-Motherway, M., et al., *Six putative two-component regulatory systems isolated from Lactococcus lactis subsp. cremoris MG1363.* Microbiology, 2000. **146**(4): p. 935-947.

177. Mascher, T., et al., *Antibiotic-inducible promoter regulated by the cell envelope stress-sensing two-component system LiaRS of Bacillus subtilis.* Antimicrobial agents and chemotherapy, 2004. **48**(8): p. 2888-2896.

178. Bergholz, T.M., et al., *Nisin resistance of Listeria monocytogenes is increased by exposure to salt stress and is mediated via LiaR.* Applied and environmental microbiology, 2013. **79**(18): p. 5682-5688.

179. Schmitt, L. and R. Tampé, *Structure and mechanism of ABC transporters.* Current Opinion in Structural Biology, 2002. **12**(6): p. 754-760.

180. Klein, C. and K. Entian, *Genes involved in self-protection against the lantibiotic subtilin produced by Bacillus subtilis ATCC 6633.* Applied and Environmental Microbiology, 1994. **60**(8): p. 2793-2801.

181. Gebhard, S., *ABC transporters of antimicrobial peptides in Firmicutes bacteria–phylogeny, function and regulation.* Molecular microbiology, 2012. **86**(6): p. 1295-1317.

182. McBride, S.M. and A.L. Sonenshein, *Identification of a genetic locus responsible for antimicrobial peptide resistance in Clostridium difficile.* Infection and immunity, 2011. **79**(1): p. 167-176.

183. Bernard, R., et al., *Resistance to bacitracin in Bacillus subtilis: unexpected requirement of the BceAB ABC transporter in the control of expression of its own structural genes.* Journal of bacteriology, 2007. **189**(23): p. 8636-8642.

184. Khosa, S., Z. Alkhatib, and S.H. Smits, *NSR from Streptococcus agalactiae confers resistance against nisin and is encoded by a conserved nsr operon.* Biological chemistry, 2013. **394**(11): p. 1543-1549.

185. Revilla‐Guarinos, A., et al., *Defence against antimicrobial peptides: different strategies in Firmicutes.* Environmental microbiology, 2014. **16**(5): p. 1225-1237.

186. Rietkötter, E., D. Hoyer, and T. Mascher, *Bacitracin sensing in Bacillus subtilis.* Molecular microbiology, 2008. **68**(3): p. 768-785.

187. Yoshida, Y., et al., *Bacitracin sensing and resistance in Staphylococcus aureus.* FEMS microbiology letters, 2011. **320**(1): p. 33-39.

188. Staroń, A., D.E. Finkeisen, and T. Mascher, *Peptide antibiotic sensing and detoxification modules of Bacillus subtilis.* Antimicrobial agents and chemotherapy, 2011. **55**(2): p. 515-525.

189. Tsuda, H., et al., *Genes involved in bacitracin resistance in Streptococcus mutans.* Antimicrobial agents and chemotherapy, 2002. **46**(12): p. 3756-3764.

190. Becker, P., R. Hakenbeck, and B. Henrich, *An ABC transporter of Streptococcus pneumoniae involved in susceptibility to vancoresmycin and bacitracin.* Antimicrobial agents and chemotherapy, 2009. **53**(5): p. 2034-2041.

191. Majchrzykiewicz, J.A., O.P. Kuipers, and J.J. Bijlsma, *Generic and specific adaptive responses of Streptococcus pneumoniae to challenge with three distinct antimicrobial peptides, bacitracin, LL-37, and nisin.* Antimicrobial agents and chemotherapy, 2010. **54**(1): p. 440-451.

192. Jarvis, B., *Resistance to nisin and production of nisin-inactivating enzymes by several Bacillus species.* Journal of general microbiology, 1967. **47**(1): p. 33-48.

193. Jarvis, B., *Enzymic reduction of the C-terminal dehydroalanyl-lysine sequence in nisin.* Biochem. J, 1970. **119**(56P).

194. Kooy, J., *Strains of Lactobacillus plantarum which inhibit the activity of the antibiotics produced by Streptococcus lactis.* Ned Melk Zuiveltijdschr, 1952. **6**: p. 323-330.

195. Alifax, P.R. and R. Chevalier, *Etude de la nisinase produite par Streptococcus thermophilus.* Journal of Dairy Research, 1962. **29**(03): p. 233-240.

196. Carlson, S. and H. Bauer, *A study of problems associated with resistance to nisin.* Arch. Hyg. Bakteriol, 1957. **141**: p. 445-460.

197. Jarvis, B. and J. Farr, *Partial purification, specificity and mechanism of action of the nisin-inactivating enzyme from Bacillus cereus.* Biochimica et Biophysica Acta (BBA)-Enzymology, 1971. **227**(2): p. 232-240.

198. Sun, Z., et al., *Novel mechanism for nisin resistance via proteolytic degradation of nisin by the nisin resistance protein NSR.* Antimicrobial agents and chemotherapy, 2009. **53**(5): p. 1964-1973.

199. Butcher, B.G. and J.D. Helmann, *Identification of Bacillus subtilis σ W ‐ dependent genes that provide intrinsic resistance to antimicrobial compounds produced by Bacilli.* Molecular microbiology, 2006. **60**(3): p. 765-782.

200. Falord, M., et al., *Investigation of the Staphylococcus aureus GraSR regulon reveals novel links to virulence, stress response and cell wall signal transduction pathways.* PLoS One, 2011. **6**(7): p. e21323.

201. Arthur, M., et al., *The vanZ gene of Tn1546 from Enterococcus faecium BM4147 confers resistance to teicoplanin.* Gene, 1995. **154**(1): p. 87-92.

202. McKay, L.L. and K.A. Baldwin, *Conjugative 40-megadalton plasmid in Streptococcus lactis subsp. diacetylactis DRC3 is associated with resistance to nisin and bacteriophage.* Applied and Environmental Microbiology, 1984. **47**(1): p. 68-74.

203. Klaenhammer, T.R. and R.B. Sanozky, *Conjugal transfer from Streptococcus lactis ME2 of plasmids encoding phage resistance, nisin resistance and lactose-fermenting ability: evidence for a high-frequency conjugative plasmid responsible for abortive infection of virulent bacteriophage.* Journal of general microbiology, 1985. **131**(6): p. 1531-1541.

204. Duan, K., et al., *Identification and characterization of a mobilizing plasmid, pND300, in Lactococcus lactis M189 and its encoded nisin resistance determinant.* Journal of applied bacteriology, 1996. **81**(5): p. 493-500.

205. Tang, S., et al., *[Isolation and characterization of a plasmid pTS50, which encodes nisin resistance determinant in Lactococcus lactis TS1640].* Wei sheng wu xue bao= Acta microbiologica Sinica, 2001. **41**(5): p. 536-541.

206. Froseth, B.R. and L.L. Mckay, *Molecular characterization of the nisin resistance region of Lactococcus lactis subsp. lactis biovar diacetylactis DRC3.* Applied and environmental microbiology, 1991. **57**(3): p. 804-811.

207. Liang, X., et al., *Adverse effect of nisin resistance protein on nisin-induced expression system in Lactococcus lactis.* Microbiological Research, 2010. **165**(6): p. 458-465.

208. Silber, K.R., K.C. Keiler, and R.T. Sauer, *Tsp: a tail-specific protease that selectively degrades proteins with nonpolar C termini.* Proceedings of the National Academy of Sciences, 1992. **89**(1): p. 295-299.

209. Keiler, K.C. and R.T. Sauer, *Sequence determinants of C-terminal substrate recognition by the Tsp protease.* Journal of Biological Chemistry, 1996. **271**(5): p. 2589-2593.

210. Beebe, K.D., et al., *Substrate recognition through a PDZ domain in tail-specific protease.* Biochemistry, 2000. **39**(11): p. 3149-3155.

211. Rawlings, N.D., et al., *MEROPS: the database of proteolytic enzymes, their substrates and inhibitors.* Nucleic acids research, 2013: p. gkt953.

212. Oman, T.J., et al., *Sublancin is not a lantibiotic but an S-linked glycopeptide.* Nature chemical biology, 2011. **7**(2): p. 78-80.

213. Paik, S.H., A. Chakicherla, and J.N. Hansen, *Identification and characterization of the structural and transporter genes for, and the chemical and biological properties of, sublancin 168, a novel lantibiotic produced by Bacillus subtilis 168.* Journal of Biological Chemistry, 1998. **273**(36): p. 23134-23142.

214. Kunst, F., et al., *The complete genome sequence of the gram-positive bacterium Bacillus subtilis.* Nature, 1997. **390**(6657): p. 249-256.

215. Yokoyama, H. and I. Matsui, *A novel thermostable membrane protease forming an operon with a stomatin homolog from the hyperthermophilic archaebacterium Pyrococcus horikoshii.* Journal of Biological Chemistry, 2005. **280**(8): p. 6588-6594.

216. Jordan, S., M.I. Hutchings, and T. Mascher, *Cell envelope stress response in Gram-positive bacteria.* FEMS microbiology reviews, 2008. **32**(1): p. 107-146.

217. Schultz, J., et al., *SMART, a simple modular architecture research tool: identification of signaling domains.* Proceedings of the National Academy of Sciences, 1998. **95**(11): p. 5857-5864.

218. Lukat, G.S. and J.B. Stock, *Response regulation in bacterial chemotaxis.* Journal of cellular biochemistry, 1993. **51**(1): p. 41-46.

219. Revilla-Guarinos, A., et al., *Characterization of a regulatory network of peptide antibiotic detoxification modules in Lactobacillus casei BL23.* Applied and environmental microbiology, 2013. **79**(10): p. 3160-3170.

220. Collins, B., et al., *The ABC transporter AnrAB contributes to the innate resistance of Listeria monocytogenes to nisin, bacitracin, and various β -lactam antibiotics.* Antimicrobial agents and chemotherapy, 2010. **54**(10): p. 4416-4423.

221. Kallenberg, F., et al., *Identification of regions important for resistance and signalling within the antimicrobial peptide transporter BceAB of Bacillus subtilis.* Journal of bacteriology, 2013. **195**(14): p. 3287-3297.

222. Dintner, S., et al., *A Sensory Complex Consisting of an ATP-binding Cassette Transporter and a Two-component Regulatory System Controls Bacitracin Resistance in Bacillus subtilis.* Journal of Biological Chemistry, 2014. **289**(40): p. 27899-27910.

223. Stein, T., et al., *Expression and functional analysis of the subtilin immunity genes spaIFEG in the subtilin-sensitive host Bacillus subtilis MO1099.* Journal of bacteriology, 2005. **187**(3): p. 822-828.

224. Ra, S.R., et al., *Genes responsible for nisin synthesis, regulation and immunity form a regulon of two operons and are induced by nisin in Lactoccocus lactis N8.* Microbiology, 1996. **142**(5): p. 1281-1288.

225. Delves‐Broughton, J., *Nisin and its application as a food preservative.* International Journal of Dairy Technology, 1990. **43**(3): p. 73-76.

226. Hurst, A., *Nisin.* Advances in applied microbiology, 1981. **27**: p. 85-123.

227. Guder, A., et al., *Role of the single regulator MrsR1 and the two-component system MrsR2/K2 in the regulation of mersacidin production and immunity.* Applied and environmental microbiology, 2002. **68**(1): p. 106-113.

228. Saris, P.E.J., et al., *Immunity to lantibiotics.* Antonie van Leeuwenhoek, 1996. **69**(2): p. 151-159.

229. Piper, C., et al., *Bioengineering of a Nisin A-producing Lactococcus lactis to create isogenic strains producing the natural variants Nisin F, Q and Z.* Microb Biotechnol, 2011. **4**(3): p. 375-82.

230. Van de Ven, F.J., et al., *NMR studies of lantibiotics. The structure of nisin in aqueous solution.* Eur J Biochem, 1991. **202**(3): p. 1181-8.

231. Hsu, S.T., et al., *The nisin-lipid II complex reveals a pyrophosphate cage that provides a blueprint for novel antibiotics.* Nat Struct Mol Biol, 2004. **11**(10): p. 963-7.

232. van Heusden, H.E., B. de Kruijff, and E. Breukink, *Lipid II induces a transmembrane orientation of the pore-forming peptide lantibiotic nisin.* Biochemistry, 2002. **41**(40): p. 12171-8.

233. Ruhr, E. and H.-G. Sahl, *Mode of action of the peptide antibiotic nisin and influence on the membrane potential of whole cells and on cytoplasmic and artificial membrane vesicles.* Antimicrobial Agents and Chemotherapy, 1985. **27**(5): p. 841-845.

234. Sutcliffe, I.C. and R. Russell, *Lipoproteins of gram-positive bacteria.* Journal of bacteriology, 1995. **177**(5): p. 1123.

235. Takala, T.M., et al., *Lipid-free NisI: interaction with nisin and contribution to nisin immunity via secretion.* FEMS microbiology letters, 2004. **237**(1): p. 171-177.

236. Hacker, C., et al., *The solution structure of the lantibiotic immunity protein NisI and its interactions with nisin.* Journal of Biological Chemistry, 2015: p. jbc. M115. 679969.

237. Ra, R., et al., *Effects of gene disruptions in the nisin gene cluster of Lactococcus lactis on nisin production and producer immunity.* Microbiology, 1999. **145**(5): p. 1227-1233.

238. AlKhatib, Z., et al., *Lantibiotic immunity: Inhibition of nisin mediated pore formation by NisI.* PloS one, 2014. **9**(7): p. e102246.

239. Takala, T.M. and P.E. Saris, *C terminus of NisI provides specificity to nisin.* Microbiology, 2006. **152**(12): p. 3543-3549.

240. Alkhatib, Z., *Charakterisierung der Nisin immunität System NisI und NisFEG von Lactococcus lactis*. 2014.

241. Twomey, D., et al., *Lantibiotics produced by lactic acid bacteria: structure, function and applications.* Antonie Van Leeuwenhoek, 2002. **82**(1-4): p. 165-185.

242. Christ, N.A., et al., *The First structure of a lantibiotic immunity protein, SpaI from Bacillus subtilis, reveals a novel fold.* Journal of Biological Chemistry, 2012. **287**(42): p. 35286-35298.

243. Barbosa, J., T.n. Caetano, and S.n. Mendo, *Class I and Class II Lanthipeptides Produced by Bacillus spp.* Journal of natural products, 2015.

244. Alkhatib, Z., et al., *The C‐terminus of nisin is important for the ABC transporter NisFEG to confer immunity in Lactococcus lactis.* MicrobiologyOpen, 2014. **3**(5): p. 752-763.

245. Consortium, T.U., *UniProt: a hub for protein information.* Nucleic Acids Research, 2015. **43**(D1): p. D204-D212.

246. Altschul, S.F., et al., *Basic local alignment search tool.* Journal of molecular biology, 1990. **215**(3): p. 403-410.

247. Larkin, M.A., et al., *Clustal W and Clustal X version 2.0.* Bioinformatics, 2007. **23**(21): p. 2947-2948.

248. Gasteiger, E., et al., *Protein identification and analysis tools on the ExPASy server*. 2005: Springer.

249. Johns, S. and R. Speth, *TOPO2, Transmembrane protein display software*. 2010.

250. Coumes-Florens, S., et al., *A new highly conserved antibiotic sensing/resistance pathway in firmicutes involves an ABC transporter interplaying with a signal transduction system.* PloS one, 2011. **6**(1).

251. Kuipers, O.P., et al., *Quorum sensing-controlled gene expression in lactic acid bacteria.* Journal of Biotechnology, 1998. **64**(1): p. 15-21.

252. Rink, R., et al., *Dissection and modulation of the four distinct activities of nisin by mutagenesis of rings A and B and by C-terminal truncation.* Applied and environmental microbiology, 2007. **73**(18): p. 5809-5816.

253. Dodd, H., et al., *Molecular analysis of the regulation of nisin immunity.* Microbiology, 1996. **142**(9): p. 2385-2392.

254. Mierau, I. and M. Kleerebezem, *10 years of the nisin-controlled gene expression system (NICE) in Lactococcus lactis.* Applied microbiology and biotechnology, 2005. **68**(6): p. 705-717.

255. Martínez-Hackert, E. and A.M. Stock, *Structural relationships in the OmpR family of winged-helix transcription factors.* Journal of molecular biology, 1997. **269**(3): p. 301-312.

256. Kleerebezem, M., W. De Vos, and O. Kuipers, *The lantibiotics nisin in subtilin act as extracellular regulators of their own biosynthesis.* 1998.

6. Curriculum vitae

Personal Data

Date of Birth	**April 30, 1988**
Nationality	**Indian**

Research Experience

Since Sep 2012	*Ph.D. student* at the Institute of Biochemistry, **Heinrich Heine University**, *Duesseldorf, Germany* with **Prof. Dr. Lutz Schmitt** and **Dr. Sander Smits**
Jan - Sept 2012	*Master's Research at the* Lab of **Prof. Brian Sutton**, Randall Division, **King's College London**, London, UK
Mar 2010 - Jun 2011	*Summer Undergraduate Research* Internship at the Lab of **Dr. Samudrala Gourinath**, School of Life Sciences, **Jawaharlal Nehru University**, *New Delhi, India*
Jun - Jul 2009	*Summer Training* at **Clonegen Biotechnology Pvt. Ltd**., Noida, *India*
Jun - Jul 2008	*Summer Internship* - **Institute of Genomics and Integrative Biology (IGIB)**, *Structural Biology Lab, New Delhi, India* in the lab of **Dr. Bhupesh Taneja**

Academic Education

Sep 2011- Sep 2012	*Masters studies* at ***King's College London*****,** London, United Kingdom. Degree: MRes. in Molecular Biophysics **(*passed with distinction)***
Aug 2006 - Jul 2010	*Bachelor studies* at ***Amity University Uttar Pradesh*** Noida, India. Degree: B.Tech in Biotechnology **(*CGPA 7.79/10)***

School Education

Apr 1992 - May 2006	**Cambridge School Noida, U.P., India**

Stipends and Awards

Sep 2015	**Poster Prize:** *Poster* 'Structural basis of lantibiotic recognition by the nisin resistance protein from *Streptococcus agalactiae'* at IMAP2015

	***'International Meeting on Antimicrobial Peptides'*, London.**
Sep 2012 - May 2015	***iGRASPseed scholarship for doctoral research, Heinrich Heine University, Duesseldorf.***
Apr 2004 - Mar 2006	**Academic s*cholarship for studies*** at ***Cambridge School Noida,*.**
May 2006	**A*cademic excellence award, Cambridge School Noida*.**

Professional Memberships

2012 - present	***Member,*** *Interdisciplinary Graduate and Research Academy Duesseldorf***.**
2012 - present	***Member,*** *Heinrich Heine International Graduate School of Protein Science and Technology (iGRASPseed)***.**
2012 - 2013	***Member,*** *British Crystallographic Association.*

Workshops and Conferences

Sep 2015	Annual Meeting of the German Pharmaceutical Society – DPHG 2015 ***'I3 – Interactions, Integrations and Innovations'* at Heinrich Heine University Duesseldorf.** ***Poster:*** Structural basis of lantibiotic recognition by the nisin resistance protein from *Streptococcus agalactiae.*
Sep 2015	IMAP2015 ***'International Meeting on Antimicrobial Peptides'* at Burlington House, London.** ***Poster:*** Structural basis of lantibiotic recognition by the nisin resistance protein from *Streptococcus agalactiae.*
Aug 2015	CLIB-GC and iGRASPseed Symposium **'*From Gene to Protein and Beyond'* at Heinrich Heine University Duesseldorf.**
Mar 2015	Sigma-Aldrich Workshop ***'Seminar for Sample Preparation and HPLC'* at Heinrich Heine University Duesseldorf.**
Sep 2014	BioCrys2014 Course ***'Fundamental of Modern Methods of BioCrystallography'* at Oeiras, Portugal.** ***Poster:*** Purification and Structural studies of Nisin Resistance Protein (NSR).
Sep 2014	CLIB-GC and iGRASPseed Symposium **'*From Gene to Protein and Beyond'* at Heinrich Heine University Duesseldorf.**
Nov 2013	BioStruct Symposium 2013 **'*Biological Structures in Molecular Medicine and Biotechnology*' at Haus der Universitaet, Duesseldorf.** ***Poster:*** Purification and Structural studies of Nisin Resistance Protein (NSR).

Sep 2013	CLIB-GC and iGRASPseed Symposium **'*From Gene to Protein and Beyond'* at Heinrich Heine University Duesseldorf.**
Apr 2012	***'30th** Annual Spring Meeting'* **of** British Crystallographic Association **at University of Warwick, Coventry.**

List of Publications

Khosa, S., AlKhatib, Z., & Smits, S. H. (2013). NSR from *Streptococcus agalactiae* confers resistance against nisin and is encoded by a conserved nsr operon. *Biological chemistry*, *394*(11), 1543-1549.

Khosa, S., Hoeppner, A., Kleinschrodt, D., & Smits, S. H. J. (2015). Overexpression, purification, crystallization and preliminary X-ray diffraction of the nisin resistance protein from *Streptococcus agalactiae*. *Acta Crystallographica Section F: Structural Biology Communications*, *71*(6), 671-675.

Khosa, S., Hoeppner, A., Kleinschrodt, D., & Smits, S. H. J. (2015). Overexpression, purification and crystallization of the response regulator NsrR involved in nisin resistance. *Acta Crystallographica Section F: Structural Biology Communications*, *71*(10), 1322-1326.

Khosa, S.[#], Frieg, B.[#], Mulnaes, D., Kleinschrodt, D., Hoeppner, A., Gohlke, H., & Smits, S. H. J. (2015). Structural basis of lantibiotic recognition by the nisin resistance protein from *Streptococcus agalactiae*. *Scientific Reports. Accepted.*

[#]equally contributed

Khosa, S., Hoeppner, A., Gohlke, H., Schmitt, L., & Smits, S. H. J. (2015). Structure of the response regulator NsrR from *Streptococcus agalactiae*, which is involved in lantibiotic resistance. *PlosOne. Under review.*

7. Acknowledgements

With a great sense of gratitude, I would like to specially thank Prof. Dr. Lutz Schmitt, for giving me this great opportunity to carry out research work in his institute. With great reverence, I sincerely thank him for his guidance, encouragement, extremely positive attitude and 'awesomely-working' advices on both research as well as on my career which have been invaluable.

I wish to express my profound gratitude to Dr. Sander Smits and am truly indebted for his scholarly advice, expert guidance, encouragement, motivation, suggestions as well as inspiration throughout the course of this study. I would also thank him for all the faith and confidence he reposed in me & special thanks for his extreme patience and the invaluable time spent in open & honest discussions. He has been very supportive, generous, enthusiastic, detail oriented and the list goes on. I would also like to thank him for giving me the working freedom to choose between various 'to-be working' proteins, the great opportunities (including a permanent membership at my favourite place: ESRF) and all the learning experiences. I am indeed privileged to have him share his expert knowledge of crystallography and sharing with me the art of solving structures. I am extremely grateful for his great care, be it accompanying to the student centre or showing around the institute. It has been truly an honour & privilege to work under Dr. Sander Smith and his diligent efforts in improving the overall quality of this study are invaluable.

I express my special thanks to Dr. Ulrich Schulte for his precious comments and discussions especially throughout our course of Wednesday seminars. I would also thank him for his guidance and support. I am also grateful to him for always lending his pointer.

I would also like to thank Prof. Dr. Holger Gohlke, my second supervisor, for his guidance and fruitful discussions. Special thanks for all the modelling collaborations.

I take this privilege to express my gracious thanks and regards to Dr. Astrid Hoeppner for all her 'magic', guidance, care and support. I am also grateful to her for all the ESRF trips, being the best company ever. I am extremely thankful to her for sharing her knowledge of crystallization with me and teaching me the correct way of data collection, all the late–night-synchrotron chats (also in crystallization lab) and all the positive energy during synchrotron

breakdowns. I would also thank her for providing me the freedom to use everything available (and also the unavailable ones). Special thanks for ordering crystallography books for me and lending them to me on a 'never-ending expiry' basis.

I would like to mention my deep-hearted thanks to Dr. Diana Kleinschrodt for her extreme care. I would also thank her for the cloning and especially for her help, suggestions and for teaching me the art of cloning. I am also grateful for all her efforts and extreme patience with me especially during primer designing. She has always been there not only as a guide but also as a friend who is always ready to talk about anything, help solve problems and a stress- buster.

I would also like to thank André for his invaluable advices and ready-to help attitude. Since the very start of my PhD till the end of his PhD, it was really a great pleasure to work with him and am really thankful for all the amazing times. I am really grateful to him for introducing me all the techniques, especially the Aktas and columns. I would also thank him for answering all my (stupid) never-ending list of questions, solving all my Akta/SEC column problems and thankfully never getting annoyed for that. I am also grateful to him for being the best neighbour. I would also thank him for his valuable suggestions, excellent guidance, care, and support and for being a great mentor. I owe him a lot (especially the success of this project). I would also thank him for all the faith he had in me and for inculcating all the confidence and being the 'problem-solver'.

I express my special thanks to my '*Lactis* and IC_{50} queen' Zainab, for being my best friend. I am extremely grateful to her for making me always feel at home. I would also thank her for her precious comments, and advices. Special thanks for introducing me to the world of never-ending IC_{50}s. I am also grateful to her for creating our very own international corner in the lab, all the great outings and ice-cream sessions. I am also thankful for her great care and support throughout our time together. It was a real fun and pleasure to work beside her.

I would also express my deepest gratitude to our very own 'crystal queen' Stefanie, for all her (always-working, superb) 'magic' and her 'magic hands'. I wish I could forever keep her magic with me. I am extremely thankful to her for our extremely successful (although unexpected) synchrotron trip where everything went well without any breakdown or problems, yielding three structures. Special thanks for the luckiest 13^{th}: sustaining my

extremely nervous time there and having all the faith and bringing the positive energy and good luck with her. I would also thank her for her always-happy attitude and am extremely grateful to her for preparing the plates at short notices, taking great care of the plates and all the support throughout the course of my study.

I am extremely grateful to Kalpana for being the awesome ‘plant lady’. Special thanks for being my support system and a very good friend with whom I could share everything. I am also grateful to her for her extreme care and advices. I would like to thank her for all the delicious home-cooked food she brought me, the tea breaks, nice lunches, dinners and outings. I would like to mention my deep-hearted thanks for always accompanying me to the visa office, thereby making my life a lot lot easier and stress-free. I am extremely grateful to her for making the working weekends always fun! I wish you great luck with the plant ABCs.

I am extremely lucky to have joined the nisin group and would sincerely thank all the ‘NICE’ members for all the great discussions, advices and collaborations.

I would like to mention my deep-hearted thanks to Eleanor for taking over the awesome gift of NisR, which had been on going since generations at our institute (I think Sander being the first one to work on it). All the best and hope you are surely the one to end this project! I am also grateful to her for giving me company in the small room: our own ‘kabuff’ and all the nice time. Special thanks for showing me the Chinese side of Duesseldorf, great lunches, dinners, stress relieving activities, shopping sprees, ‘Keep calm’ thingie, outdoor travels and especially for sharing the liking of Harry Potter. I hope she keeps the international spirit alive in the institute.

I would also like to mention my deep-hearted thanks to the ‘Nisin King’ Jens for his great support, invaluable advices and help. I am also extremely grateful to him for lending the Akta systems, providing the nisin rings, cryos and for creating the much-needed program on the Explorer. I would also thank him for all the discussions and extreme help with all the ordering, especially the rabbit. Special thanks for his unforgettable cooperation with the HPLC, ‘always possible’ attitude and answering all my crazy questions. It was a great pleasure to collaborate with him in the last few months and am really indebted to all his valuable inputs, enormous help and suggestions. I am also extremely privileged by his

ability to give me frequent heart attacks throughout! I wish him good luck and success and really hope that he is either able to get a new HPLC soon or finds someone who is capable enough to complete our secret side project.

I am also grateful to the 'Lactis King' Marcel for all the awesome advices, tips and discussions. I would also thank him for his extreme support with columns during my crazy synchrotron trips and especially for showing me membrane preparation. I am also grateful to him for sharing his expert knowledge of nisin with me. Special thanks for providing the cryos, often needed nisin and competent cells. I also express my gratitude for being a great company to the conference in London and thanks for all the enjoyment and fun there! Special special thanks for translating the abstract in German.

I would also express my gracious thanks and regards to superman Sven, my first neighbour. I am extremely grateful for all his translations and consider myself lucky to have joined around his time. I am also grateful to him for making me extremely comfortable in the new environment. I would also like to thank him for being extremely generous in his help, be it getting the Internet password or the keys for the institute. Special thanks for his great support during the practical courses and for teaching me ATPases. I could not have managed to do that alone and really owe him that. I wish him good luck with his PhD. Do remember always 'thingie is my word'.
I would like to express my gratitude to Michael for being a great sport throughout and for his extreme support. I would also thank him for all the stimulus discussions, advices and help. Special thanks for the Hogwarts Express to Harry Potter Exhibition, chats during our bus travels, cooking tips and all travelling guides. I am extremely grateful for his great help and advices with all the official stuff. And am still amused with his great skill of scaring people, especially me.
Here I have to say that in the starting I had the feeling that they both fight a lot, however, it took me a lot of time to understand their fights are like a typical husband-wife! They are a perfect 'working' couple!

I would also like to express my thanks to Kerstin Ma'am for completing our newly joined PhD students' corner downstairs. I am also grateful for all her advices, support and English translations throughout my stint there. I would also thank her for being a great and constant neighbour in lab as well as in office. Special thanks for all the Indian dinners, the late-night

working sessions and rides home. I would also thank her for all the practice presentation sessions we had and for sharing my problems. I hope she keeps the Indian spirit alive in the institute, as she is the only European I have seen so far who can not only eat typical (too hot) Indian food but also possesses the art of cooking it. I wish her good luck with HlyB and great success!

I would like to mention my thanks to 'Miss Weasley' (Rebecca) for being a great support. I am also grateful to her for comments, suggestions and tea sessions. It was a pleasure to guide her through the purifications and hope that I was of some help. I wish her great luck with Vif. P.S.: Sander's personal proteins are really crazy at the start, but work beautifully later, especially for crystallizations. Thus, I would be looking forward to the structure of Vif soon.

I would also thank the 'Green plant lady' Katharina for all the nice time, frequent chats in office and great cooking sessions. It was always a real fun to call her name while entering. I am also grateful to her for great lunches, outings and shopping trips. I wish her all the best with her project! And I would always remember that she was and will always be the queen!

I would also like to express my great thanks to Sandra for her support, from my first synchrotron trip to solving the structures in the kabuff. I am also thankful to her for readily exchanging Aktas, our frequent chats and for being a great company in lab as well as in office!

I am really grateful to Martina for always bearing with my super expensive research by providing numerous columns, concentrators and ordering all the stuff. I am extremely thankful for her friendly and extremely warm nature. Be it my first lunch at the Mensa or the first Betriebsausflug, she has always been so friendly. Special thanks for the all the lovely gifts she brought me from various places. It was always a pleasure to talk with her and see the live photos!

I would also like to express my thanks to Katja for her help with the practical course. It was a real pleasure to share the course with her. Special thanks for sharing her great yeast and membrane skills with me! It was always nice to talk with her and also refreshing to see her always smiling! Keep smiling always and good luck.

I am really thankful (and relieved) to Manuel for taking over our extremely crazy practical course and hope that he gets accustomed to it soon. I am also grateful for all the talks and discussions. I wish him good luck with the crystallization of Pdr5.

I would also express my deep-hearted thanks to Iris for her great help with cloning. Special thanks for help with designing primers and for showing how to do cloning. I would also thank her for providing me the vectors and bringing all the chemicals. I am really sorry for always increasing her work!

I am also thankful to Susanne for receiving all the phone calls in the office downstairs (otherwise, I would have to attend the German calls). Special thanks for answering my questions and being a company on weekends!

I would like to wish Romy all the best! I wish her great success with our most crazy Haemolysin secretion system.
I would also welcome the new comers: Tobias, Andreas, Hilke, Jose and Janpeter, and wish them all the luck and great success with their research.

I am also thankful to all my students. Betty: for always believing in me. Even though the project didn't went well, she always had the confidence in the project. Nina for her assistance with the mutant studies.
Tim: for taking over the most difficult protein on earth. It was really great to work with him and I think we made a good team. I would always remember our crazy MST days that ran more than 24 hrs. Special thanks for bringing the sun to our lab. And always remember: Tim, faster, faster, faster!!!! I wish him luck with all his future endeavours especially his PhD.

I am extremely grateful to Frau Blum for arranging all the official work and the flight tickets. Special thanks for managing all the paper work. Without her help, it would have been impossible.

I would also like to thank Frau Rasid for all the autoclaving and cleaning. My extremely weak German skills never stopped her from conversing with me.

I am also grateful to Christian for guiding me in my early start days of lab work and advices. I am also thankful to him for fruitful discussions that helped me think about my project and take it in the right direction.

I express my express my deepest gratitude to Philipp for initiating this great, always working, super successful project. He always had great ideas! I am also grateful to him for his guidance and tips. Special thanks for his nice window desk and immensely useful pair of scissors!

I am also grateful to Nils for his extreme patience and guidance. Special thanks for all the stimulating discussion sessions and introducing the practical course to me. I am also thankful to him for his great support with all the computer programs and for his diligent efforts in getting me a laptop. I would also never forget his special 'Nil's minutes'.

I am also thankful to Marianne for being a great company in office as well as in lab. I am also grateful to her for being a great support and tutor in the practical course. Special thanks for all the English translations of the manuscript.

I would also like to thank: Ricarda – for her extreme help with Akta systems; Rakesh – for introducing the flurolog to me and being a great company in the office; Miro – for great discussions. I would also like to mention my thanks to Isa, Iris G. and Sabrina.

I am extremely thankful to Christoph Müller (ESRF) for his extreme patience and diligent efforts with my difficult project. I am extremely grateful for his help; always happy and calm attitude (even in times of synchrotron crisis). Special thanks for arranging all the extra beam time and sharing his expert knowledge (all the basics as well as the complicated stuff, ways of collecting precise diffraction data) with me. Thanks to him, I can literally collect dataset (including MAD) with my eyes shut. I also owe him my weeklong learning trip at ESRF where I had the opportunity to work under his guidance and supervision and of course in his lab too. Special thanks for showing and arranging the extremely cool and fancy stuff with krypton soaks with Philip. I have really gained a lot of knowledge from all the synchrotron experiences, which I would always carry, till eternity.

I am also grateful to Martina (iGrasp*seed*) for her constant support, cooperation and help throughout the course of my PhD. Special thanks for simplifying all the official work, readily changing dates of progress meetings and for always accommodating even latecomers like me. I would also like to thank Jessica, Jennifer and all the iGrasp*seed* fellows for all the nice time, stimulating discussions and great presentations.

Last but not the least, I would like to thank my family for all the love & support that they have provided throughout my research and life in general. My parents and my sister Vasundra have always been incredibly supportive with everything I have done finally leading to this PhD thesis and I am very proud to be a member of their family. Their blessings, unconditional love and endless faith in me have been the most driving inspiration in my life. I truly cannot thank them enough for their great support without which I would not have been here and could not have made this far without all of them. A special thanks for instilling in me all the self-confidence. Although many countries apart, you all were always there to cheer me up! As Dad always says 'So what! That's really very simple! Believe in yourself and you can do it. Remember always whatever happens, happens for the best'. Well, I took his advice, and now I would soon have a doctoral degree. Words cannot describe my sincere appreciation for them all. I owe all my success to them.
I am also thankful to my grandparents for all their blessings! I love you all a lot.

I would also like to thank the Almighty God for his grace. I hope his gracious blessings will continue to shower on me in the future also.

8. Declaration

The dissertation presented here has been made independently and without unauthorized assistance. The dissertation has not been submitted in this or any similar form to any other institution. I have not taken any unsuccessful promotion exams so far.

(Sakshi Khosa)